ZooKeys 1057: 1–21 (2021)
doi: 10.3897/zookeys.1057.67433
https://zookeys.pensoft.net

RESEARCH ARTICLE

A peer-reviewed open-access journal
ZooKeys
Launched to accelerate biodiversity research

A review of *Madagopsina* Feijen, Feijen & Feijen (Diptera, Diopsidae) with description of a new species, key to the species, and discussion of intrageneric relationships

Hans R. Feijen[1], Frida A. A. Feijen[2], Cobi Feijen[1], Benoît Gilles[3]

1 *Naturalis Biodiversity Center, P. O. Box 9517, 2300 RA Leiden, Netherlands* **2** *ETH Zürich, Institute of Integrative Biology (IBZ), 8092 Zürich, Switzerland* **3** *Passion-Entomologie Association, 327 rue de Périgueux, 16000 Angoulême, France*

Corresponding author: Hans R. Feijen (hans.feijen@naturalis.nl)

Academic editor: Rudolf Meier | Received 16 April 2021 | Accepted 6 August 2021 | Published 24 August 2021

http://zoobank.org/7363A758-7D55-4532-9A08-0A02B5A8B15F

Citation: Feijen HR, Feijen FAA, Feijen C, Gilles B (2021) A review of *Madagopsina* Feijen, Feijen & Feijen (Diptera, Diopsidae) with description of a new species, key to the species, and discussion of intrageneric relationships. ZooKeys 1057: 1–21. https://doi.org/10.3897/zookeys.1057.67433

Abstract

For the recently established genus *Madagopsina* (Diopsidae, stalk-eyed flies), *Madagopsina makayensis* Feijen, Feijen & Feijen, **sp. nov.** is described from Madagascar. A concise catalogue is given for the genus and an identification key is presented for its six species. The differential character states are listed for the two species groups of the genus: the *Madagopsina apollo* species group and the *Madagopsina apographica* species group. The intrageneric relations are discussed based on morphology, geometric morphometrics analysis of wing shape, and allometric data for eye span against body length. Each of these three procedures places the new species in the *M. apollo* species group with *Madagopsina parvapollina* as its closest relative. New records are presented for *M. apographica* and *M. parvapollina*.

Keywords

Allometry, catalogue, Madagascar, stalk-eyed flies, wing morphometry

Introduction

In 2018, Feijen et al. erected *Madagopsina* Feijen, Feijen & Feijen and *Gracilopsina* Feijen, Feijen & Feijen as endemic genera for Madagascar. These new genera were

placed in a Diopsidae clade with irrorated wings, named the *Teleopsis* genus group. In *Madagopsina*, two earlier described species were placed: *Diopsis apollo* Brunetti and *Diopsis* (*Eurydiopsis*) *apographica* Séguy. In addition, three new species were described for *Madagopsina*: *M. freidbergi*, *M. parvapollina*, and *M. tschirnhausi*. Shortly after the 2018 publication, a single specimen of *Madagopsina* was received which turned out to be an undescribed species. This species is described herein. In *Madagopsina*, two species groups were distinguished by Feijen et al. (2018), the *Madagopsina apollo* species group and the *Madagopsina apographica* species group. Based on morphology, allometric data and geometric morphometrics analysis of wing shape, the new species is placed in the *M. apollo* species group. Because of the description of the new species, the sets of character states for the two species groups need to be adapted. A concise catalogue for *Madagopsina* is presented, as well as a new identification key to the six species of the genus. Some new *Madagopsina* records are included in the catalogue. The first live photographs of *M. parvapollina* are presented as these high-resolution pictures nicely show differential characters for the species group. In Feijen and Feijen (2021 in press), a key to the Afrotropical genera of Diopsidae is presented along with a synopsis of the Afrotropical Diopsidae fauna, including the genus *Madagopsina*.

Materials and methods

The description of *M. makayensis* Feijen, Feijen & Feijen, sp. nov. is based on a single male specimen that was preserved in alcohol. The holotype is now pinned with the genitalia placed in a genitalia tube attached to the pin. Some additional records for *Madagopsina* became known via photographs placed on www.iNaturalist.org. For the rate of dimorphism *D*, the difference between males and females in allometric slope for eye span on body length is used in the Diopsidae (Baker and Wilkinson 2001). Details on procedures for preparing genitalia slides, and procedures for taking measurements are given in Feijen et al. (2018). For information on morphological terminology and on photographic equipment used, the reader is referred to the same source. Some changes have been made to the terminology used: the aedeagus is now referred to as phallus, while the apodeme of the surstylus is now called the apophysis. The procedures for the wing geometric morphometrics analysis are described in Feijen et al. (2018). The following institutional codens and abbreviations are used:

RMNH Naturalis Biodiversity Center (formerly Rijksmuseum van Natuurlijke Historie), Leiden, The Netherlands,
AU Approximately Unbiased *p*-value,
BP Bootstrap Probability values,
D Rate of Dimorphism,
SE Standard Error.

Taxonomy

Family Diopsidae Billberg, 1820

Diopsidae Billberg, 1820: 115 (as Natio Diopsides). Type genus: *Diopsis* Linnaeus, 1775: 5.

Genus *Madagopsina* Feijen, Feijen & Feijen, 2018

Figures 1–31

Madagopsina Feijen, Feijen & Feijen, 2018:145. Type species *Diopsis apollo* Brunetti, 1928.
Eurydiopsis sensu Séguy & Vanschuytbroeck (nec Frey) - in part; Shillito 1971: 287; Feijen 1981: 482; Feijen 1989: 63; Feijen and Feijen 2013: 182, 185.

Remarks. A concise catalogue for the genus is given below. For details on the type series, records, and combinations to various other genera of the earlier described species can be referred to Feijen et al. (2018). Reference is now made to new records which appeared after this publication. The new species *Madagopsina makayensis* Feijen, Feijen & Feijen, sp. nov. is added.

Madagopsina apographica (Séguy, 1949)

Figures 12, 26

Diopsis (*Eurydiopsis*) *apographicus* Séguy, 1949: 69.
Eurydiopsis anjahanaribei Vanschuytbroeck, 1965: 336.
Madagopsina apographica; Feijen et al. 2018: 151.

New records. Madagascar, 1 ♀, Fianarantsoa, Vatovavy, Fitovinany, Ifanadiana, 21°15'34"S, 47°24'55"E, 977 m, 7.xi.2014, lemurtaquin, (ref. www.inaturalist.org/observations/36199753); 1 ?sex (probably ♀), Antsiranana, Sava, Sambava, rainforest, 14°26'60"S, 49°43'10"E, 1310 m, 30.x.2016, Éric Mathieu (ref. www.inaturalist.org/observations/69807405). The new records fall well within the eastern forests distribution as indicated in Feijen et al. (2018).

Madagopsina apollo (Brunetti, 1928)

Figures 9, 23

Diopsis apollo Brunetti, 1928: 280.
Madagopsina apollo; Feijen et al. 2018: 160.

Figures 1–2. *Madagopsina parvapollina*, live photographs by Gernot Kunz, Mahajanga, Boeny (www.inaturalist.org/observations/20766277) **1** anterior view **2** dorsal view.

Madagopsina freidbergi **Feijen, Feijen & Feijen, 2018**

Figures 13, 27

Madagopsina freidbergi Feijen et al., 2018: 165.

Figures 3–4. *Madagopsina makayensis* Feijen, Feijen & Feijen, sp. nov., ♂, holotype, Makay **3** habitus, dorsolateral view **4** thorax, dorsolateral view. Scale bars: 1 mm.

***Madagopsina parvapollina* Feijen, Feijen & Feijen, 2018**
Figures 1, 2, 11, 25

Madagopsina parvapollina Feijen et al. 2018: 172.

New records. Madagascar, 1 ♂, Mahajanga, Boeny, 16°24'44"S, 45°18'48"E, 123 m, 23.x.2016, Gernot Kunz (ref. www.inaturalist.org/observations/20766277); 1 ?sex (probably ♂), Mahajanga, Boeny, Soalala, 16°26'4"S, 45°21'20"E, 138 m, Josiane Lips,

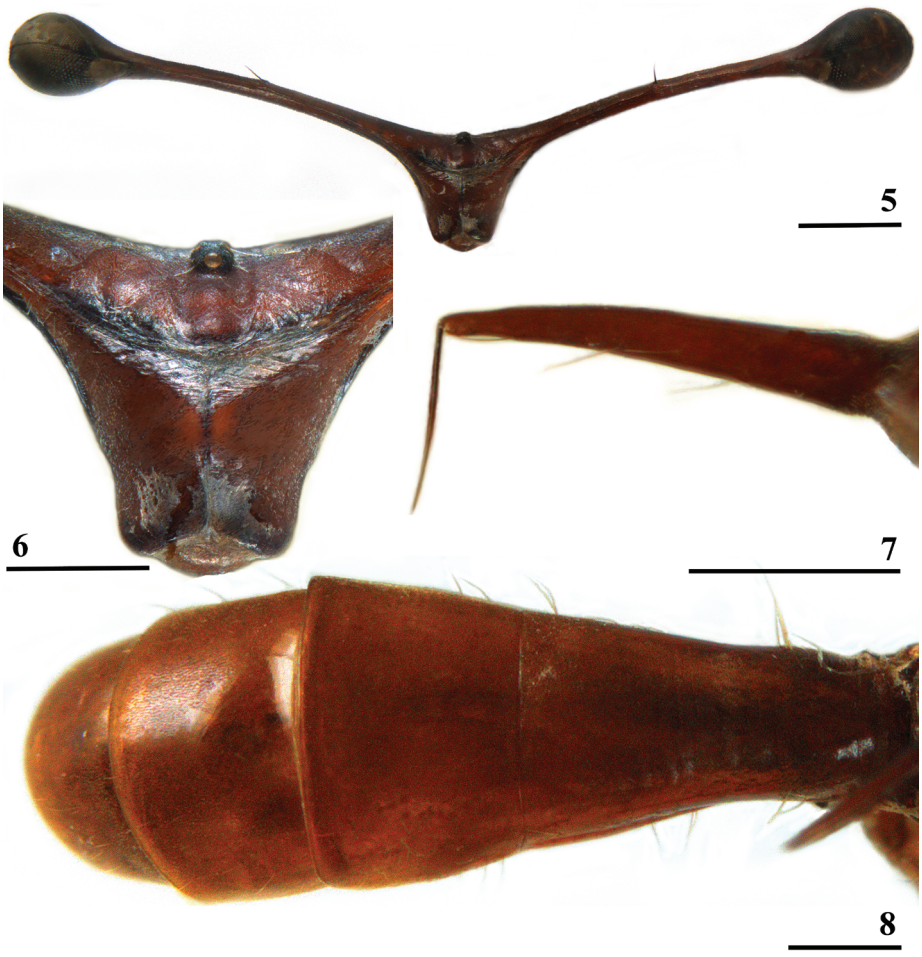

Figures 5–8. *Madagopsina makayensis* Feijen, Feijen & Feijen, sp. nov., ♂, holotype, Makay **5** head, anterior view **6** central head, anterior view **7** scutellar spine and apical seta, inner view (seta not in natural position in line with spine) **8** abdomen, dorsal view. Scale bars: 1 mm (**5**); 0.5 mm (**6–8**).

Olivier Testa (ref. www.inaturalist.org/observations/37503778 and www.inaturalist.org/observations/37503777), the photograph formed part of a batch made during a caving expedition in Namoroka caves, while all pictures were taken in caves or at the entrance; 1 ♂ Makay, canyon, sous-bois, rive d'une rivière [undergrowth, riverbank], 21°10'11"S, 45°22'15"E, 528 m, 30.vii–3.viii.2017, leg. Benoît Gilles. The new records fall well within the western forests distribution as indicated in Feijen et al. (2018).

Madagopsina tschirnhausi Feijen, Feijen & Feijen, 2018

Figures 14, 28

Madagopsina tschirnhausi Feijen et al. 2018: 178.

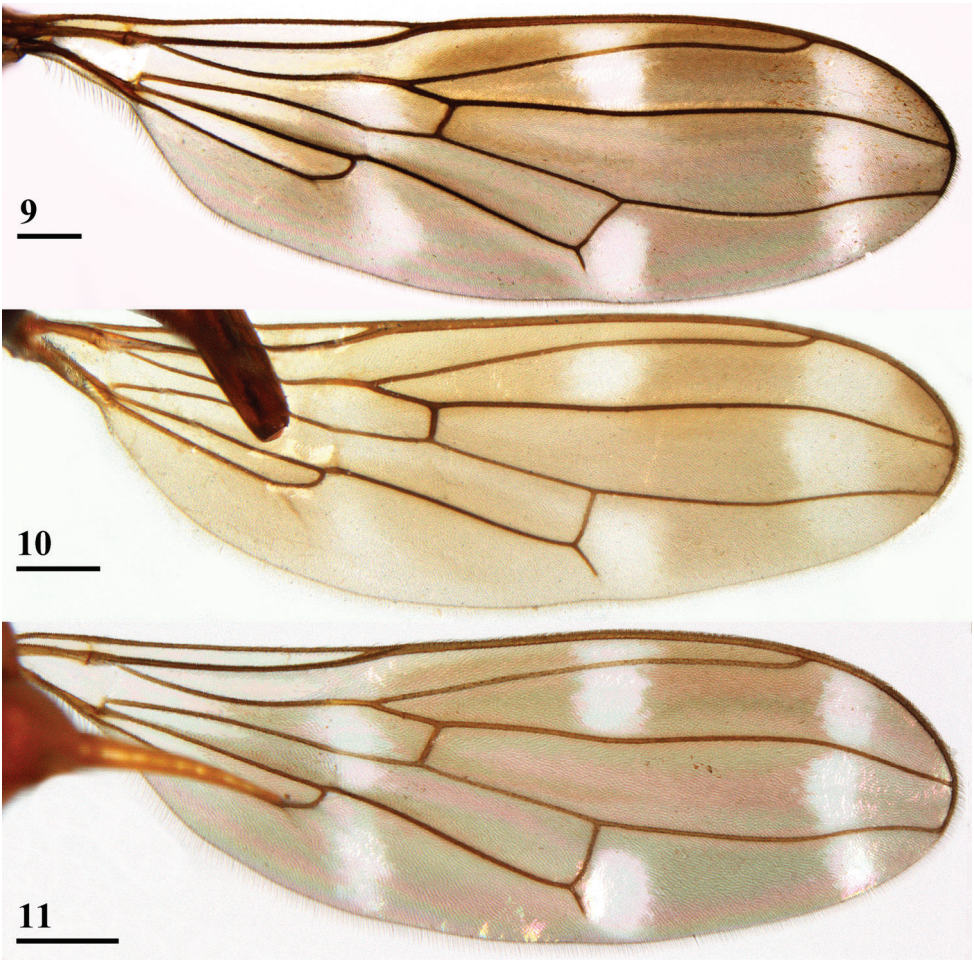

Figures 9–11. *Madagopsina apollo* species group, dorsal view of wings **9** *M. apollo*, ♂, Ambohitra **10** *M. makayensis* Feijen, Feijen & Feijen, sp. nov., ♂, holotype, Makay **11** *M. parvapollina*, ♀, paratype, Ankarana. Scale bars: 0.5 mm. Figures **9, 11** (Feijen et al. 2018, figures 6, 7).

***Madagopsina makayensis* Feijen, Feijen & Feijen, sp. nov.**
http://zoobank.org/A6766D1D-FCB3-49B6-A640-278DDE98BB4A
Figs 3–8, 10, 15–22, 24, 29–31

Type material. ***Holotype*,** ♂ (RMNH), Madagascar, Makay, canyon, sous-bois, rive d'une rivière [undergrowth, riverbank], 21°10'11"S, 45°22'15"E, 528 m, 30.vii–3.viii.2017, leg. Benoît Gilles.

Diagnosis. *Madagopsina makayensis* Feijen, Feijen & Feijen, sp. nov. can be recognised by its medium size (body length ♂ 7.3 mm), brown colour (however, due to conservation in alcohol it is likely that all the brown colours would be more yellowish in a live specimen, like in the other *Madagopsina* species), body mainly thinly pruinose (pollinose) with few small setulae, only katepisternum and katepimeron glossy,

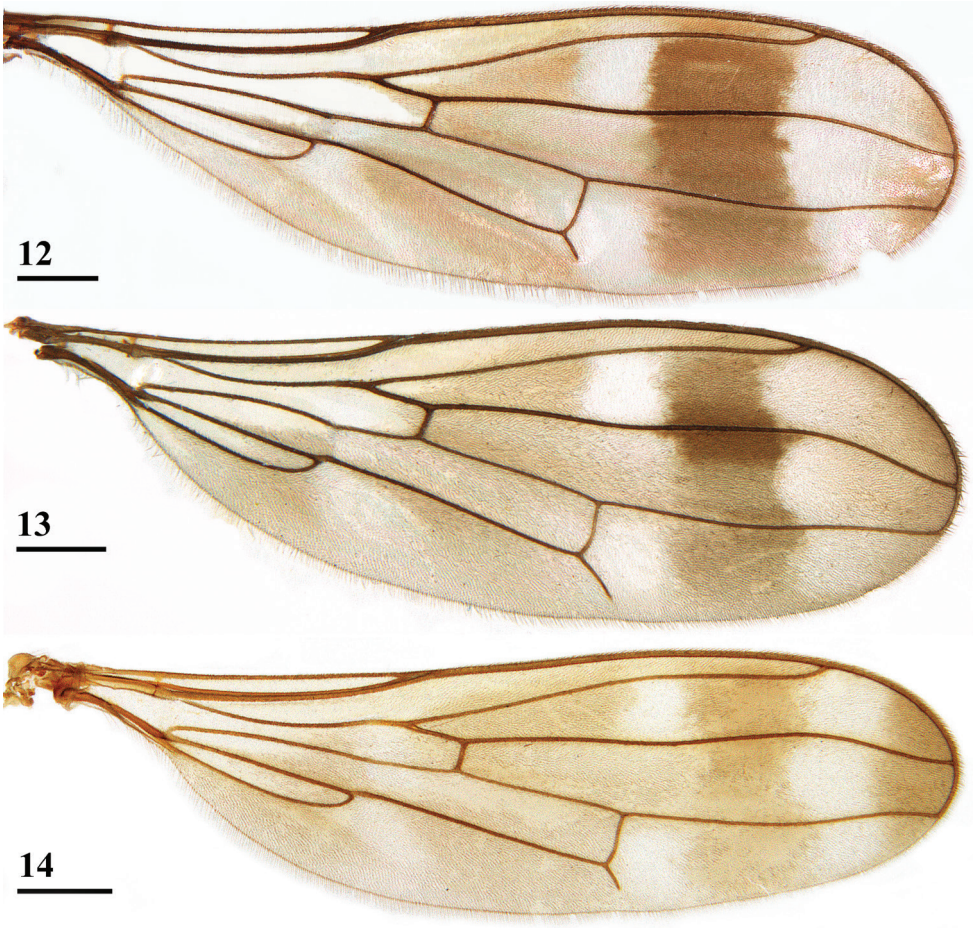

Figures 12–14. *Madagopsina apographica* species group, dorsal view of wings **12** *M. apographica*, ♀, Fianarantsoa **13** *M. freidbergi*, ♀, paratype, Vohimana **14** *M. tschirnhausi*, ♂, holotype, Mount Ambre. Scale bars 0.5 mm. Figures **12–14** (Feijen et al. 2018, figures 8–10).

absence of facial teeth, medium-sized inner vertical seta (1.7 × stalk diameter), scutellar spines 2.0 × as long as scutellum, quite large apical seta (45% of scutellar spine length), incrassate fore femora with around 48 tubercles, irrorated wings with three vague crossbands including an H-shaped configuration with central and preapical crossbands, wing apex infuscated, central band slightly broader than preapical band, pale wing spots in cell r2+3 and cell m1, a vague pale spot in cell m4, abdomen club-shaped, no pruinose spots on tergites, ♂ spiracles 7 in slit of synsternite 7+8, surstyli rounded and bulbous with an apically rounded apophysis, microtrichia on posterior apical third, phallapodeme with ratio posterior arm/anterior arm 1.05, straight ejaculatory apodeme with only a slight sickle-shape apically, phallus remarkably broad and sclerotised, assumed moderate sexual dimorphism with regards to eye span ($D \approx 1.0$),

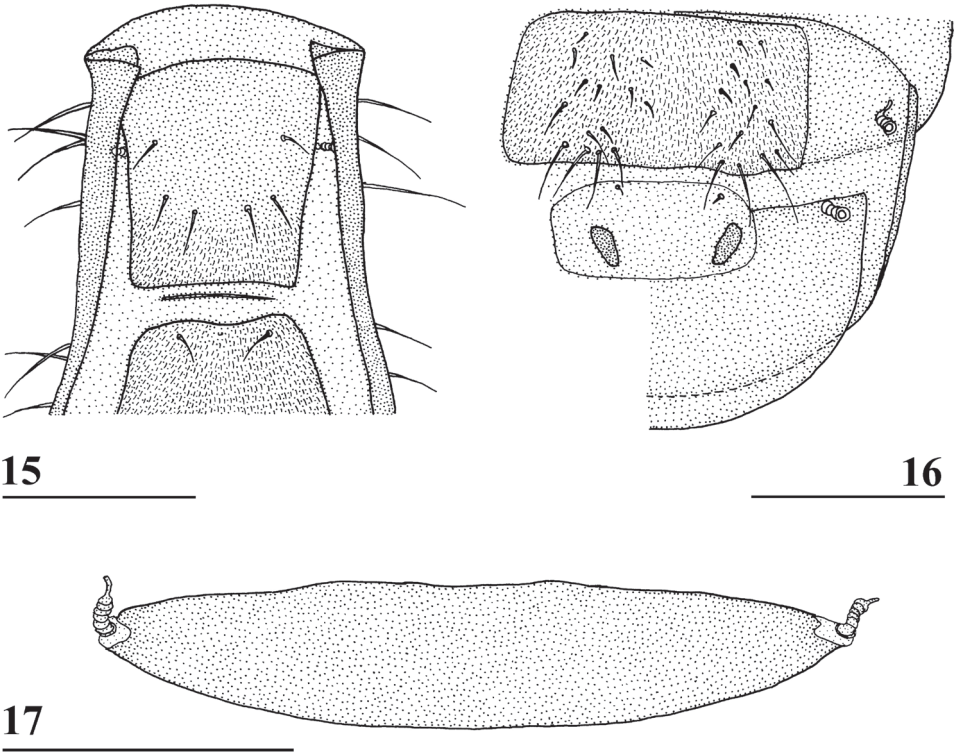

Figures 15–17. *Madagopsina makayensis* Feijen, Feijen & Feijen, sp. nov., ♂, holotype, Makay **15** basal section of abdomen with intersternite 1–2, ventral view **16** sternites 5 and 6, ventral view **17** synsternite 7+8, ventral view. Scale bars: 0.5 mm.

ratio eye span/body length ~ 1.20 in ♂. *Madagopsina makayensis* Feijen, Feijen & Feijen, sp. nov. belongs to the *M. apollo* species group, which furthermore includes *M. apollo* and *M. parvapollina*.

Description. ***Measurements***. Body length ♂ 7.3 mm; eye span 8.8 mm; wing length 5.9 mm; length of scutellar spine 1.01 mm.

Head. Central part brown, ocellar tubercle and arcuate groove dark brown; central head thinly pruinose (Figs 3–6); an elongate bulbous medial ridge in front of ocellar tubercle, parallel grooves on both sides of this ridge, lateral areas of frons flat; medial occiput flat; face convex in profile, facial corners square, no facial teeth (Figs 5, 6); clypeus small, not protruding; arista finely microtrichose on less than basal half; the rate of dimorphism cannot be calculated, but in the graph (Fig. 31) with the allometric lines for the three species of the *M. apollo* species group it can be seen that the single data point is located in line with the allometric line for *M. parvapollina* males, while given that the slopes for the females for the species must be almost identical, it follows that *D* for the new species must be almost identical to the D = 0.98 for *M. parvapollina* or slightly higher (see also the section "Allometric aspects with regard to

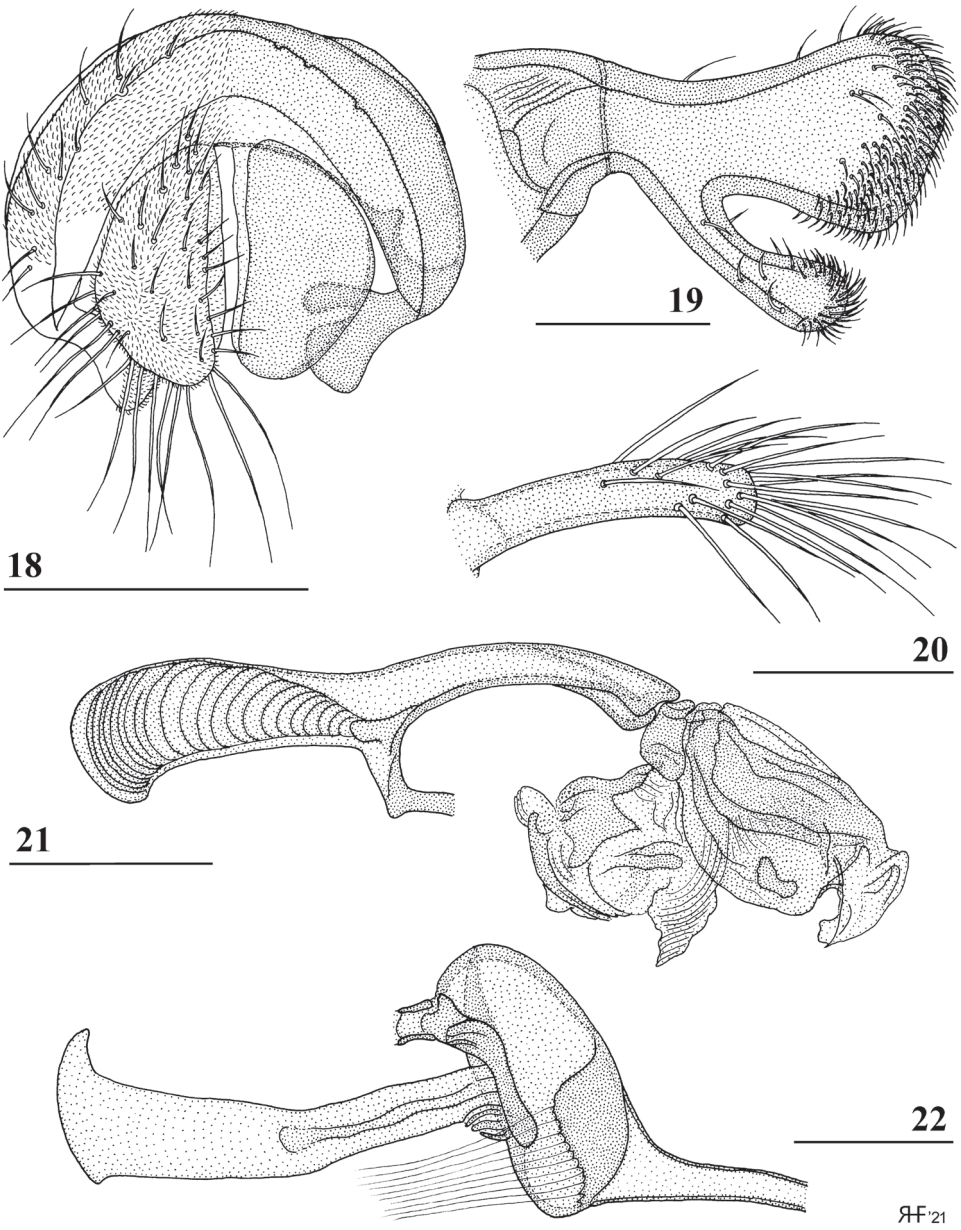

Figures 18–22. *Madagopsina makayensis* Feijen, Feijen & Feijen, sp. nov., ♂, holotype, Makay **18** epandrium with surstyli and cerci, posterior view **19** surstylus, inner view **20** hypandrial clasper, lateral view **21** phallapodeme and phallus, lateral view **22** ejaculatory apodeme and sac. Scale bars: 0.5 mm (**18, 21**); 0.1 mm (**19, 20, 22**).

eye span" below); eye span large in male (119.6% of body length), also a comparison of this ratio eye span/body length of the single male with the mean ratio eye span/body length of the other *Madagopsina* species (Feijen et al. 2018) supports the view that

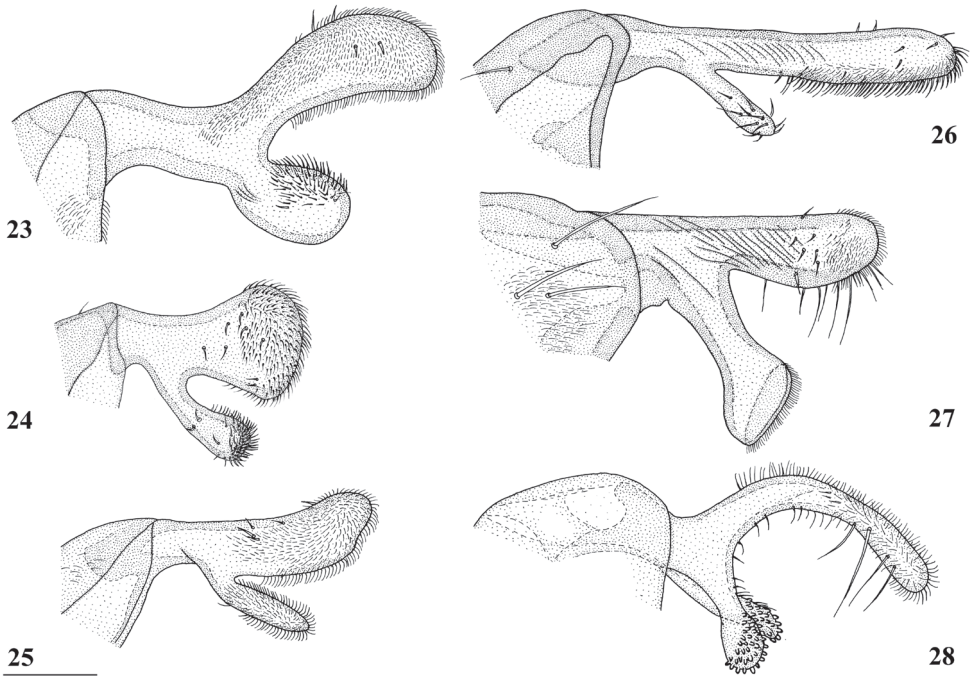

Figures 23–28. Posterior view of *Madagopsina* surstyli **23–25** *M. apollo* species group **26–28** *M. apographica* species group **23** *M. apollo* **24** *M. makayensis* Feijen, Feijen & Feijen, sp. nov. **25** *M. parvapollina* **26** *M. apographica* **27** *M. freidbergi* **28** *M. tschirnhausi*. Scale bar 0.1 mm (all drawn to the same scale). Figures **25–28** (Feijen et al. 2018, figures 187, 184, 186, 188).

this is a dimorphic species with a moderate rate of dimorphism $D \approx 1.0$; stalks thinly pruinose, brown, broad apical parts dark, funiculus brown, pruinose; inner vertical seta medium-sized, 1.7 × diameter of eye stalk (Figs 3, 5), base of inner vertical seta a minor elevation, one-eighth diameter of the stalk; outer vertical seta broken off; central head and stalks with a few tiny white setulae.

Thorax. Collar, scutum, scutellum and postscutellum pruinose, brown (Figs 3, 4), spines glossy; pleura dorsally brownish pruinose, katepisternum and katepimeron largely glossy; ratio scutal length/scutal width ~ 0.80; scutellar spines almost straight, diverging under an angle of ~ 65°, ratio scutellar spine/scutellum in ♂, 2.00, ratio scutellar spine/body length in ♂, 0.14; metapleural spines well developed, pointing almost laterally (Fig. 3); apical seta quite large, 45% of length of scutellar spine, posteriorly directed (Figs 4, 7, in Fig. 7 the seta is not in its natural, posteriorly directed, position); scutum almost devoid of setulae, scutellar spines with each ~ 10 small setulae, not on warts.

Wing. Irrorated with a rather vague, brownish, H-shaped configuration; apex (8% of wing length) with brownish infuscation (convex on proximal side); 3 crossbands, the basal and central band hardly separated, a pale preapical band and three pale spots (Figs 3, 10); preapical crossband (distal leg of H) broad, marginally darker than other bands and with slightly irregular edges; preapical band connected to central band in cell r1, in cell r4+5 and around veins R2+3 and R4+5; central band slightly broader

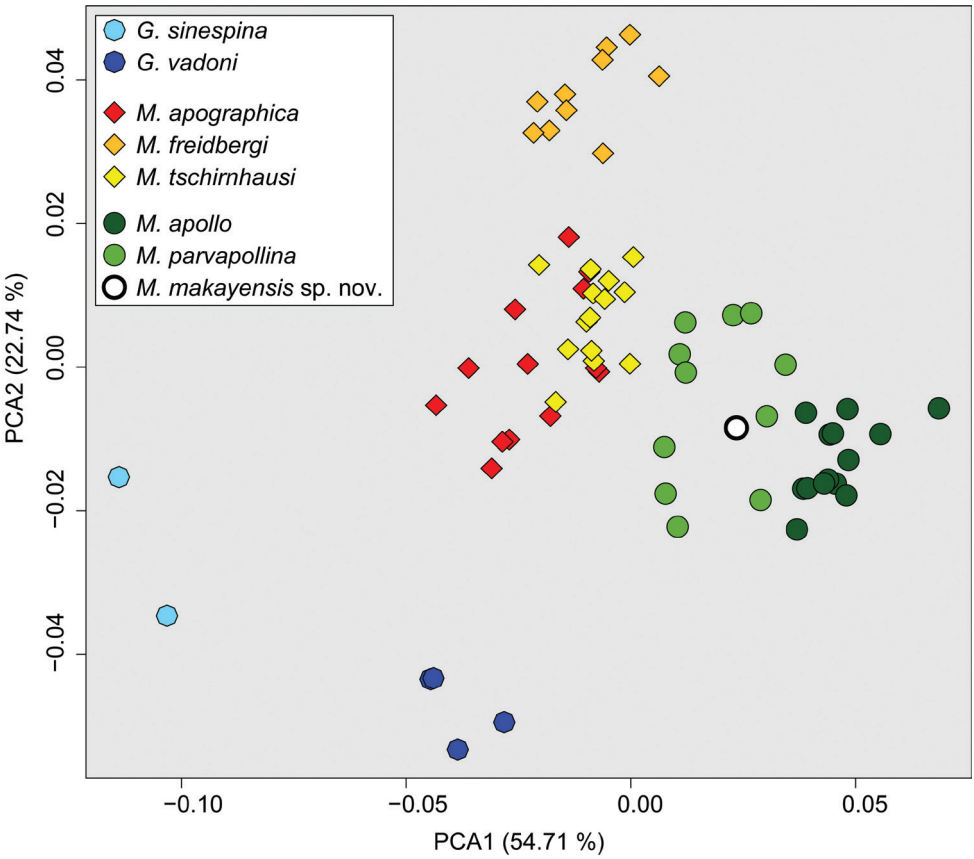

Figure 29. Principal component analysis of wing venation morphometry for the two species of *Gracilopsina* and six species of *Madagopsina*: biplot of the first two PCA axes.

than preapical band and with ill-defined proximal edge, only in cell m4 vaguely separated from basal band; basal band running from cell c to posterior wing margin, widening posteriorly; this infuscation pattern creates a pale (but not hyaline) preapical band between dark preapical band and infuscated wing apex, two pale spots between central and dark preapical bands (one in cell r2+3 and one in cell m1), and one vague pale spot centrally in cell m4 between basal and central band (Figs 3, 10); glabrous basal areas include basal apices of cell c and cell r1, basal half of cell br, basal quarter of cell bm+dm except for posterior margin and basal third of cell cua; vein M4 reaching to just beyond halfway the wing margin.

Legs. Coxa 1 pale yellowish, glossy but with dense white pruinescence on anterior side, trochanter 1 pale, pruinose; fore femur yellowish brown but dorsally darker, glossy but dorsally and apically pruinose; fore tibia and metatarsus darker brown, other fore tarsi pale and covered with whitish pruinescence; mid- and hind legs more uniformly yellowish, femora pruinose dorsally and with dark brown spot on apical fifth; femur 1 (Figs 3, 4) incrassate in ♂ (ratio of length/width 3.2), two rows of tubercles on distal

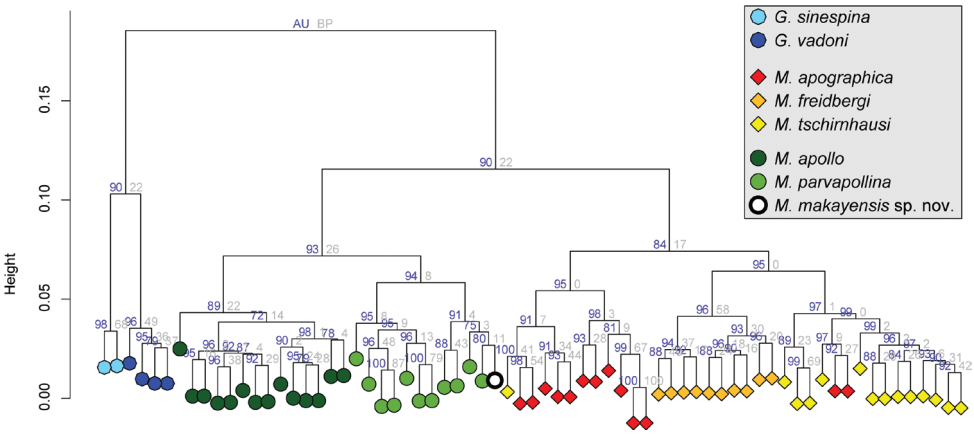

Figure 30. Cluster dendrogram for the Euclidian distance in wing morphometry PCA for the *Gracilopsina* and *Madagopsina* species using the complete clustering method. Branch labels give the approximately unbiased *p*-value (AU) and bootstrap probability (BP) values (%).

two-thirds, inner row in ♂ with 25 and 28 tubercles (mean 26.5, *n* = 2), outer row in ♂ with 21 and 22 tubercles (mean 21.5, *n* = 2); femur 1 with whitish setulae ventrally.

Preabdomen. Abdomen club-shaped (ratio length/broadest width 2.8); syntergite gradually widening posteriorly, seam between tergites 1 and 2 not visible, suture between tergites 2 and 3 distinct (Fig. 8); tergites uniformly yellowish brown (Figs 3, 8), thinly pruinose; syntergite basally with white setulae laterally, otherwise tergites with a few whitish setulae; anterior line-like section (intersternite 1–2) of sternite 2 not linked to main sternite 2 (Fig. 15); ratio length sternites 1+2+3/width posterior sternite 2 2.8 in ♂, ratio length/width of sternite 2 1.2 in ♂; sternites very pale, pruinose (except for basal two-thirds of sternite 1); spiracle 1 in tergite (Fig. 15).

Postabdomen male. Sternite 4 a rectangular plate; sternite 5 (Fig. 16) a rectangular plate, slightly more sclerotised laterally; sternite 6 vague with a pair of small sclerotised sections (Fig. 16); synsternite 7+8 quite large, symmetrical, narrowing laterally, lateral slits enclosing hardly sclerotised areas (Fig. 17); both spiracles located in the lateral slits of the synsternite (Fig. 17); epandrium (Fig. 18) rounded, with ~ 11 pairs of setulae, ventrally bare, otherwise clothed in microtrichia; surstyli (Figs 19, 24) articulated, apically broadening, apex rounded and bulbous, with a long, apically broadening and rounded, apophysis; in posterior view (Fig. 24) a few small setulae on apical halves of surstylus and apophysis with the apical third of the surstylus and only the apex of the apophysis clothed in microtrichia, on inner side only microtrichia on the apices of surstylus and its apophysis with a few small setulae on apophysis and apical third of surstylus (Fig. 19); surstyli interconnected via thin, rod-like processus longi (Fig. 18); cerci rather broad, ratio of length/width 1.9, basally and apically tapering, apex rounded, clothed in microtrichia and a set of setulae, some of the apical setulae almost as long as the cerci (Fig. 18); hypandrial clasper (Fig. 20) straight and rod-like with relatively long setulae on distal half; phallapodeme solidly built and rather straight (Fig. 21), anterior arm rounded api-

cally, posterior arm slightly longer than anterior arm (ratio posterior arm/anterior arm 1.05) and strongly bifurcated to accommodate the very broad phallus; phallus (Fig. 21) a rather short complex of lobes and sclerites, remarkably broad and heavily sclerotised, intromittent organ very short; ejaculatory apodeme straight, hardly broadening apically except for a small sickle-shape of apex (Fig. 22), ejaculatory sac rounded.

Distribution and habitat. The new species is only known from the Makay massif in Toliara province. The Makay is a mountain range of almost 4000 km^2 in south-western Madagascar. The altitude varies from 200 m at the bottom of canyons to 1000 m for the plateaus. The Makay with its exceptional biodiversity (see Wendenbaum 2011) is considered to be one of the least studied areas in Madagascar. Its forests belong to the deciduous, seasonally dry, western forests of low altitude (Du Puy and Moat 1999). In the dry season, wet areas remain near the rivers. Many Diopsidae, including aggregations, were observed on vegetation in wet, shady places. The single specimen of this new species was collected in undergrowth along a riverbank at an altitude of 527 m. On the same location the following Diopsidae were collected: 5 ♀ and 5 ♂ *Sphyracephala beccarii* (Rondani), 5 ♀ and 2 ♂ *Diopsis nigrosicus* Séguy, and 1 ♂ *M. parvapollina*.

Etymology. This species is named *M. makayensis* Feijen, Feijen & Feijen, sp. nov., referring to the place of origin of the holotype.

Key to the species of *Madagopsina*

This key is a revised version of the *Madagopsina* section of the key in Feijen et al. (2018). It now also includes *M. makayensis* Feijen, Feijen & Feijen, sp. nov. for which only the male is known. The couplet separating the two species groups has been changed to accommodate the new species. In the 2018 key also an error occurred: in the couplet separating *M. apollo* and *M. parvapollina*, the character states for the apical seta should have been reversed.

1 Fore femur incrassate in females (ratio length/width 3.4–3.5) and males (ratio length/width 3.2–3.7) (Figs 2, 4), pleurotergal spines laterally directed (Fig. 2), dark preapical wing band (width 18–20% of wing length) as broad as central band and equal in colour (Figs 9–11), abdomen club-shaped (ratio length/broadest width ≤ 3) (Fig. 8), tergites glossy, ratio length sternites 1+2+3/width posterior sternite 2 2.8–3.1, posterior arm of phallapodeme longer than anterior arm (ratio ~ 1.05–1.40) (Fig. 21)..... **2 (*Madagopsina apollo* species group)**

– Fore femur moderately incrassate to slender in females (ratio length/width 4.6–6.0) and males (ratio length/width 4.6–6.3), pleurotergal spines posterolaterally directed, dark preapical wing band (width 13–14% of wing length) distinctly narrower than central band and darker (Figs 12–14), abdomen slender (ratio length/broadest width ~ 4), tergites thinly pollinose with a pair of pollinose lateral spots on tergite 3, ratio length sternites 1+2+3/width posterior sternite 2 4.1–4.8, posterior arm of phallapodeme shorter than anterior arm (ratio ~ 0.71–0.93)..... ..... **4 (*Madagopsina apographica* species group)**

2 Large – females on average 9.6 mm (range 8.3–10.2), males on average 9.5 mm (range 8.0–10.1), inner vertical seta 0.8 × stalk diameter, small apical seta (23% of length of scutellar spine), male sternite 5 without combs, apophysis of surstylus short (~ 30% of length of surstylus) and bulbous (Fig. 23), subanal plate heart-shaped with bulbous lateral areas..... ***Madagopsina apollo***

– Medium-sized – females on average 6.1 mm (range 5.4–6.8), males on average 6.3 mm (range 5.6–7.0) or just larger to 7.3 mm (*M. makayensis* Feijen, Feijen & Feijen, sp. nov.), inner vertical seta 1.6–1.7 × stalk diameter (Figs 1, 3), medium-sized apical seta (37–43% of length of scutellar spine) (Fig. 2, 7), male sternite 5 with or without posterior combs of spine-like setulae, apophysis of surstylus long (> 55% of length of surstylus) and slender (Figs 24, 25), subanal plate triangular (not yet known for *M. makayensis* Feijen, Feijen & Feijen, sp. nov.) **3**

3 Body length of male 7.3 mm, apical seta 45% of length of scutellar spine, anterior central hyaline wing spot in cell r2+3 and not extending into cell r1 (Fig. 10), fore femora with ~ 48 tubercles, male sternite 5 without combs, surstylus and its apophysis both apically broadening and rounded (Fig. 24)..... ..... ***Madagopsina makayensis*** **Feijen, Feijen & Feijen, sp. nov.**

– Body length males on average 6.3 mm (range 5.6–7.0), apical seta on average 37% of length of scutellar spine, anterior central hyaline wing spot in cells r1 and r2+3 (Fig. 11), fore femora with ~ 36 tubercles, male sternite 5 with posterior combs of spine-like setulae, surstylus and its apophysis both straight, slender and not apically broadening (Fig. 25) ..... ***Madagopsina parvapollina***

4 Inner vertical seta 2.3 × stalk diameter, femur 1 moderately incrassate in females and males (ratio length/width in both sexes 4.6), ratio scutellar spine/scutellum 2.1–2.3, dark preapical wing band rather vague but slightly darker than central band (Fig. 14), basal wing band extending through cell br (Fig. 14), cell br with microtrichia on apical half, tergite 3 with a pair of tiny posterolateral pollinose spots, surstylus strongly curved (Fig. 28)..... ***Madagopsina tschirnhausi***

– Inner vertical seta 1.1–1.4 × stalk diameter, femur 1 slender in females (ratio length/width 5.3–5.9) and males (ratio length/width 5.3–6.3), ratio scutellar spine/scutellum 2.5–3.1, dark preapical wing band distinct and much darker than central band (Figs 12, 13), basal wing band not extending anteriorly of vein M1 (Figs 12, 13), cell br with microtrichia only on apical 10%, tergite 3 with laterally a pair of large pollinose spots, surstylus straight (Figs 26, 27)..... **5**

5 Inner vertical seta 1.4 × stalk diameter, femur 1 slender in females and males (ratio length/width 5.3), ratio scutellar spine/scutellum 2.9–3.1, preapical dark band uniformly dark, only paler in cell r1 (Fig. 12), pollinose spots on tergite 3 posterolaterally located, ♀ sternite 8 divided in two sclerites, apophysis of surstylus less than half the size of central surstylus (Fig. 26)..... ***Madagopsina apographica***

– Inner vertical seta 1.1× diameter of stalk, femur 1 very slender in females (ratio length/width 6.0) and males (ratio length/width 6.3), ratio scutellar spine/scutellum 2.5, preapical dark band with distinctly darker spot around vein R4+5 (Fig. 13), pollinose spots on tergite 3 mediolaterally located, ♀ sternite 8 a single sclerite, apophysis of surstylus equal in size to central surstylus (Fig. 27) ..... ***Madagopsina freidbergi***

Discussion

Geometric morphometrics analysis of wing shape

Feijen et al. (2018) proved that principal component analysis (PCA) of wing morphometry was powerful enough to recover the *Madagopsina* and *Gracilopsina* taxa previously delimited by adult morphology. Their biplot of the first two PCA axes showed clear distinction between the two genera and seven species while these two axes explained 54.8% and 22.9% of variation. Only specimens from *M. tschirnhausi* and *M. apographica* overlapped slightly. The *M. apographica* species group and the *M. apollo* species group were also delimited. Feijen et al. (2018) stated that the limited intraspecific variation in the PCA plot could, to some extent, be explained by the fact that the wings in the, mostly, pinned flies are often not perfectly flat. So, the PCA leads to a cluster pattern that is in accordance with morphological characters. The same pattern was seen in the hierarchical clustering analysis of PCA scores. Only three of 68 specimens were assigned to the wrong species cluster using the 'complete' cluster method. Both analyses were now repeated with inclusion of the wing data for the single specimen of the new species. The biplot of the first two PCA axes (Fig. 29) shows the distinction between the two genera and eight species, while the two axes explained 54.7% and 22.7% of variation. *M. makayensis* Feijen, Feijen & Feijen, sp. nov. is placed squarely in the cluster for the *M. apollo* species group, while within this group it is more closely related to *M. parvapollina* than to *M. apollo*. This same pattern is seen in the hierarchical clustering analysis of PCA scores using the complete cluster method (Fig. 30). This method showed that within *Madagopsina* the three species *M. apollo*, *M. parvapollina* and *M. makayensis* Feijen, Feijen & Feijen, sp. nov. form one cluster (the *M. apollo* species group, - AU = 93, BP = 26), while *M. freidbergi*, *M. tschirnhausi*, and *M. apographica* form a distinct second cluster (the *M. apographica* group – AU = 84, BP = 17). *M. makayensis* Feijen, Feijen & Feijen, sp. nov. is placed within the cluster for *M. parvapollina*.

Allometric aspects with regard to eye span

For all five *Madagopsina* species included in Feijen et al. (2018), graphs were presented for eye span plotted against body length for both sexes. The differences in allometric slopes for males and females indicated the rate of sexual dimorphism *D* for the species. Between the species the allometric slopes for males varied from 1.64–2.13 and for females from 0.85–1.21. Of special interest were the allometric lines for the two species then forming the *M. apollo* species group: *M. apollo* and *M. parvapollina* (Fig. 31). According to Feijen et al. (2018) the two species are externally very similar. They can in the first place be distinguished by the well-separated size ranges (see also Fig. 31). Comparison of the allometric lines for the two species, showed that the female lines are collinear, but given the size difference well separated. In fact, the female lines for the *M. apographica* species group also do not differ much from those of the *M. apollo* group. The slopes of the male lines for *M. apollo* and *M. parvapollina* were almost similar with 1.87 and 1.89, respectively, but the intercepts are distinct. This leads to two parallel lines (Fig. 31). Now that *M. makayensis* Feijen, Feijen & Feijen, sp. nov.

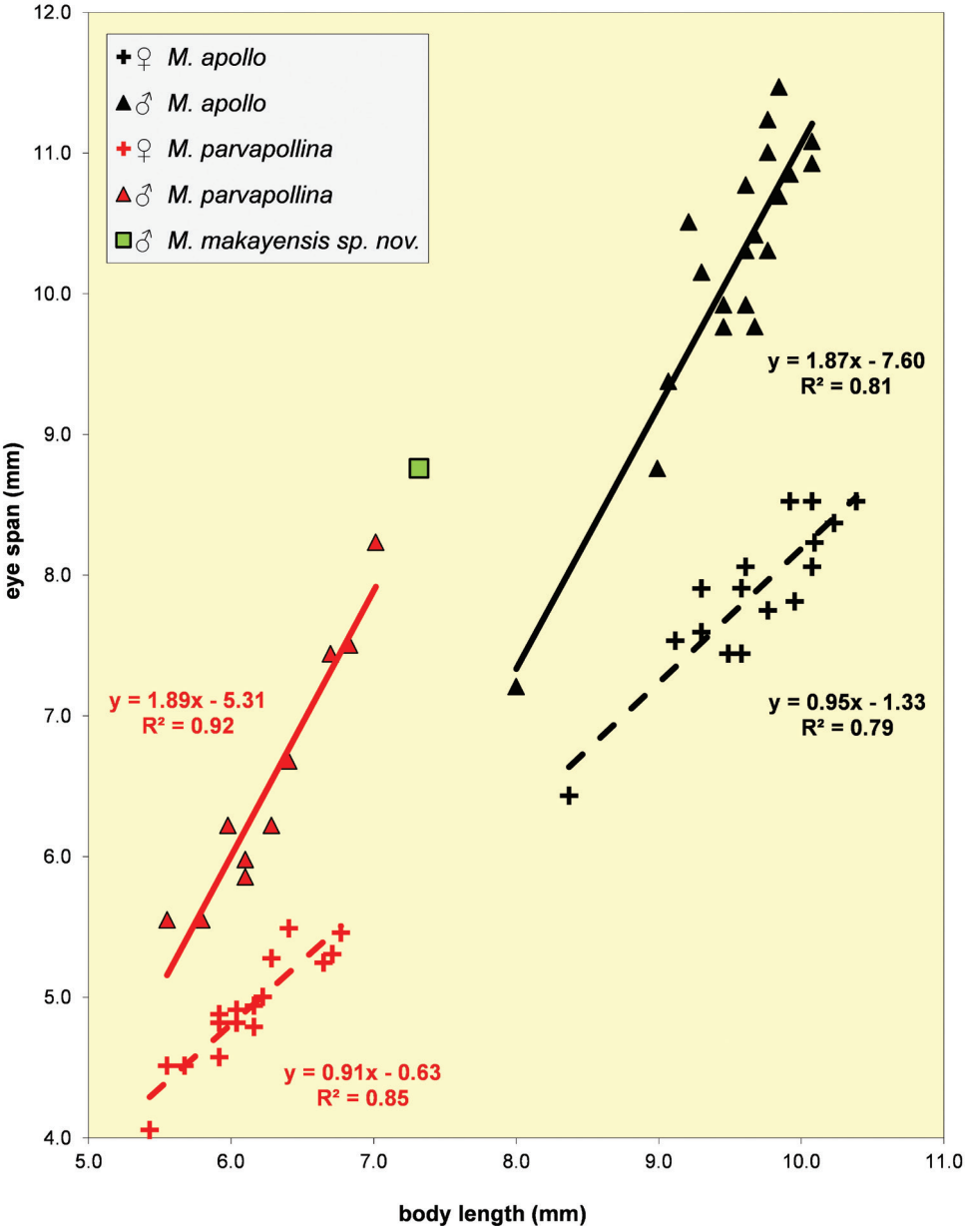

Figure 31. Eye span plotted against body length for the three species in the *Madagopsina apollo* species group: *M. apollo*, *M. parvapollina* and *M. makayensis* Feijen, Feijen & Feijen, sp. nov. Note the position of the single data point for the ♂ of the latter species, in line with the ♂ data points for *M. parvapollina*.

has become the third species in the *M. apollo* group, its place can be considered in the graph with the allometric lines for the other two species. Only one male specimen is available for *M. makayensis* Feijen, Feijen & Feijen, sp. nov., so a single data point is available in the graph (Fig. 31). The single male data point is in line with the allometric

line for *M. parvapollina* males, which forms an indication that the new species has a closer relationship to *M. parvapollina*. The new species is probably also slightly larger than *M. parvapollina*. Although no females were available for *M. makayensis* Feijen, Feijen & Feijen, sp. nov. it can be assumed that the allometric line for these females will be collinear with those for *M. apollo* and *M. parvapollina*. Given also that $D = 0.98$ for *M. parvapollina*, it can safely be predicted that *M. makayensis* Feijen, Feijen & Feijen, sp. nov. is a clear dimorphic species with a low rate of dimorphism $D \approx 1.0$. Another indication that *D* for the new species must be quite similar to those for the other two species rests on the similarity in the ratio eye span / body length. For the male *M. makayensis* Feijen, Feijen & Feijen, sp. nov. this comes to 1.20, while for males of *M. apollo* and *M. parvapollina* this ratio was 1.07 ± SE 0.01 and 1.04 ± SE 0.02, respectively.

Male genitalia

According to Feijen et al. (2018), preliminary results from divergence dating analysis suggest a minimum age estimate of around 10 million years for the divergence of *M. freidbergi* and *M. tschirnhausi*. However, reaching convergence in divergence dating analysis proved difficult and longer runs will later be required. Feijen et al (2018) considered the large differences in postabdominal structures in *Madagopsina* as additional support that its species diverged long ago. In *M. makayensis* Feijen, Feijen & Feijen, sp. nov., the male genitalia are also quite distinct from the other *Madagopsina* species. The major differences in surstyli for the six species are illustrated (Figs 23–28). In other Diopsidae genera and species groups, the differences in surstyli are often much smaller, as can, for instance, be seen in *Eurydiopsis* (Feijen 1999: figs 1–9), the sister genus of *Madagopsina*. The differences in hypandrial claspers are also large in *Madagopsina*, as can be noted by comparing these claspers in the new species (Fig. 20) with those of the other five species (Feijen et al. 2018: figs 178–182). For the closely related Syringogastridae, Marshall et al. (2009) referred to the hypandrial claspers as the "large, setulose ventral lobe" of the hypandrial arms. The short, broad, and heavily sclerotised phallus (Fig. 21) in *M. makayensis* Feijen, Feijen & Feijen, sp. nov. is not only unusual for *Madagopsina*, but for the whole Diopsidae family.

Morphological differences between the two species groups of *Madagopsina*

Due to the description of a new species in the *M. apollo* species group, the list of differences with the *M. apographica* group has to be somewhat revised. A major difference between the two groups, according to Feijen et al. (2018) concerns the anterior central hyaline wing spot. In the *M. apollo* group this spot was located in cells r1 and r2+3, while in the *M. apographica* group this spot only occurred in cell r2+3 and did not extend into cell r1. However, in *M. makayensis* Feijen, Feijen & Feijen, sp. nov. this spot also does not extend into cell r1, so this character can no longer be used to separate the two groups (compare Figs 9–11 with Figs 12–14). The slight difference in pruinescence of the tergites is now also removed from

Table 1. Differential character states for the *Madagopsina apollo* species group and *Madagopsina apographica* species group.

Character		*Madagopsina*	
		***apollo* species group**	***apographica* species group**
head	arista	basal half finely microtrichose	almost bare
thorax	scutum length/width	0.80–0.88	0.93–0.95
	pleurotergal spines	laterally directed	posterolaterally directed
wing	width dark preapical band/wing length	0.18–0.20	0.13–0.14
	dark preapical band	as broad as central band and equal in colour	distinctly narrower than central band and darker
femur 1	ratio length/width ♀	3.4–3.5	4.6–6.0
	ratio length/width ♂	3.2–3.7	4.6–6.3
abdomen	shape	club-shaped	slender
	ratio length/broadest width	≤3	~4
	tergite 3	no spots	one pair of lateral spots
	sternite 2 length/width	1.2–1.6	1.9–2.8
	length St1+St2+St3/ width posterior St2	2.8–3.1	4.1–4.8
genitalia	ratio posterior/anterior arm of phallapodeme	1.1–1.4	0.7–0.9

the list of differences. In the *M. apollo* group the tergites were glossy, while in the *M. apographica* group they were slightly pruinose. In *M. makayensis* Feijen, Feijen & Feijen, sp. nov. the tergites are also slightly pruinose, so this character is now also removed from the list of differences. In Table 1, the new list of differences is presented. Compared with Feijen et al. (2018), the range of some ratios is slightly adapted. In the wing pattern another major difference is now introduced: the width of the dark preapical wing band as compared with the wing length and also as compared with the central wing band. Within the *M. apollo* species group, *M. parvapollina* and *M. makayensis* Feijen, Feijen & Feijen, sp. nov. are more closely related to each other than to *M. apollo*. The latter species stands out by its much larger body size, much shorter inner vertical seta and apical seta, much shorter and bulbous apophysis of the surstylus, and its peculiar subanal plate (heart-shaped with bulbous lateral areas).

Conclusions

The division of *Madagopsina* into the *M. apollo* species group and the *M. apographica* species group is consolidated by the inclusion of the morphological data for *M. makayensis* Feijen, Feijen & Feijen, sp. nov. Within the *M. apollo* group, the new species is more closely related to *M. parvapollina*. The division into two species groups and the closer relationship of *M. makayensis* Feijen, Feijen & Feijen, sp. nov. to *M. parvapollina* is fully supported by the geometric morphometrics analysis of wing shape and the analysis of the allometric data with regard to eye span.

Acknowledgements

The many live Diopsidae photographs made available via www.iNaturalist.org are greatly appreciated. Via this website, photographs and/or records supplied by "lemurtaquin", Éric Mathieu, Gernot Kunz, Josiane Lips, and Olivier Testa could be examined. The permission to use two photographs by Gernot Kunz is gratefully acknowledged. We are grateful to the editor-in-chief of Tijdschrift voor Entomologie, Herman de Jong, for permission to reuse figures earlier published in that journal. The comments by Steve Gaimari and an anonymous reviewer were greatly appreciated.

References

Baker RH, Wilkinson GS (2001) Phylogenetic analysis of sexual dimorphism and eyespan allometry in stalk-eyed flies (Diopsidae). Evolution 55: 1373–1385. https://doi.org/10.1111/j.0014-3820.2001.tb00659.x

Billberg GJ (1820) Enumeratio insectorum in Museo Gust. Joh. Billberg. Gadelianis, Stockholm, 138 pp. https://doi.org/10.5962/bhl.title.49763

Brunetti E (1928) XXXIII. – New Species of Diopsidae (Diptera). Annals and Magazine of Natural History (Series 10) 2(9): 275–285. https://doi.org/10.1080/00222932808672878

Du Puy DJ, Moat J (1999) Vegetation mapping and biodiversity conservation in Madagascar using geographical information systems. In: Timberlake J, Kativu S (Eds) African plants: biodiversity, taxonomy and uses - Proceedings of the 1997 AETFAT Congress, Harare, Zimbabwe. Royal Botanic Gardens, Kew, 245–251.

Feijen HR (1981) A review of *Diopsina* Curran, 1928 (Diptera: Diopsidae), with a note on *Cyrtodiopsis*. Annals of the Natal Museum 24: 465–482. https://journals.co.za/content/annals/24/2/AJA03040798_549

Feijen HR (1989) Diopsidae. Volume IX, Cyclorrhapha III (Schizophora other than Calyptratae), Part 12. In: Griffiths GCD (Ed.) Flies of the Nearctic Region. Schweizerbart, Stuttgart, 1–122.

Feijen HR (1999) A revision of *Eurydiopsis* Frey (Diptera, Diopsidae) with description of four new Oriental species. Tijdschrift voor Entomologie 141(2): 221–240. https://doi.org/10.1163/22119434-99900012

Feijen HR, Feijen C (2013) A revision of the genus *Diopsina* Curran (Diptera, Diopsidae) with description of a new species from Guinea-Bissau. Tijdschrift voor Entomologie 156: 161–189. https://doi.org/10.1163/22119434-00002029

Feijen HR, Feijen C (2021 in press) Diopsidae (Stalk-eyed Flies and Afromontane Forest Flies), chapter 64. In: Kirk-Spriggs AH, Sinclair BJ (Eds) Manual of Afrotropical Diptera. Volume 3. Brachycera: Cyclorrhapha, excluding Calyptratae. Suricata 6. South African National Biodiversity Institute, Pretoria.

Feijen HR, Feijen FAA, Feijen C (2018) *Madagopsina* gen. n. and *Gracilopsina* gen. n. (Diptera: Diopsidae) from Madagascar with description of four new species. Tijdschrift voor Entomologie 160(3): 141–215. https://doi.org/10.1163/22119434-00002069

Linnaeus C [and Dahl A] (1775) Dissertatio Entomologica, Bigas Insectorum Sistens, Quam Divinis Auspiciis, etc. Thesis, Upsala University. Typis Edmannianis, Upsaliæ, [iv +] 7 pp. https://doi.org/10.5962/bhl.title.12431

Marshall SA, Buck M, Skevington JH, Grimaldi D (2009) A revision of the family Syringogastridae (Diptera: Diopsoidea). Zootaxa 1996: 1–80. https://doi.org/10.11646/zootaxa.1996.1.1

Séguy E (1949) Diopsides de Madagascar. Mémoires de l'Institut Scientifique de Madagascar A 3(1): 65–76.

Shillito JF (1971) The genera of Diopsidae (Insecta: Diptera). Zoological Journal of the Linnean Society 50(3): 287–295. https://doi.org/10.1111/j.1096-3642.1971.tb00763.x

Vanschuytbroek P (1965) Description de deux Diptères Diopsidae nouveaux de Madagascar. Revue de Zoologie et de Botanique Africaines 71(3/4): 336–338.

Wendenbaum E (2011) Makay, À la découverte du dernier Éden. Éditions de la Martinière, Paris, 178 pp.

ZooKeys 1057: 23–36 (2021)
doi: 10.3897/zookeys.1057.65877
https://zookeys.pensoft.net

RESEARCH ARTICLE

A peer-reviewed open-access journal
ZooKeys
Launched to accelerate biodiversity research

Rugitermes ursulae (Isoptera, Kalotermitidae), a new drywood termite from the Caribbean coast of Colombia

Robin Casalla[1], Rudolf H. Scheffrahn[2], Judith Korb[3]

1 *Universidad del Norte, Departamento de Química y Biología. Kilómetro 5 Antigua vía Puerto Colombia, Barranquilla Colombia* **2** *Fort Lauderdale Research and Education Center, University of Florida, 3205 College Avenue Davie, Florida 33314, USA* **3** *Universität Freiburg, Evolutionary Biology & Ecology. Hauptstrasse 1, Freiburg 79104, Germany*

Corresponding author: Robin Casalla (casallar@uninorte.edu.co)

Academic editor: Eliana Cancello | Received 12 March 2021 | Accepted 12 July 2021 | Published 25 August 2021

http://zoobank.org/64412433-2263-4CEF-85DA-9E08F06C4C1B

Citation: Casalla R, Scheffrahn RH, Korb J (2021) *Rugitermes ursulae* (Isoptera, Kalotermitidae), a new drywood termite from the Caribbean coast of Colombia. ZooKeys 1057: 23–36. https://doi.org/10.3897/zookeys.1057.65877

Abstract

Rugitermes ursulae **sp. nov.** is described from a sample collected inside a dead branch in a tropical dry forest of Colombia's Caribbean coast using molecular information and external morphological characters of the imago and soldier castes. *Rugitermes ursulae* **sp. nov.** soldiers and imagoes are the smallest among all described *Rugitermes* species. The imago's head capsule coloration is dark castaneous, while the pronotum is contrastingly pale yellow. Our description includes soldier characters, such as subflangular elevation and shape of the antennal sockets, that can help in identification of samples lacking imagoes.

Keywords

DNA barcoding, imago, northern Colombian coast, soldier, taxonomy, tropical dry forest

Introduction

Records of termites from Colombia have increased in recent years (Scheffrahn 2010; Casalla et al. 2016a, b; Postle and Scheffrahn 2016; Castro et al. 2018; Pinzón and Castro 2018; Casalla and Korb 2019; Castro and Scheffrahn 2019; Scheffrahn 2019; Pinzón et al. 2020). The "Los Primates" area in the mountains of the municipality of Colosó, Sucre, is one of the best-preserved areas of tropical dry forest on the Colombian Caribbean coast (Pizano and García 2014) (Fig. 1).

Figure 1. Type localities of *Rugitermes* species described from Colombia. *Rugitermes ursulae* sp. nov. (red square) and *R. tinto* (green squares).

Rugitermes Holmgren, 1911, is a genus from the family Kalotermitidae, mainly found in the Neotropics (Krishna et al. 2013; Scheffrahn 2015; Scheffrahn and Carrijo 2020). Twelve *Rugitermes* species are currently known from South America, including the most recently described *Rugitermes tinto* Scheffrahn & Pinzón, 2020, *Rugitermes aridus* Scheffrahn, 2020, *Rugitermes rufus* Scheffrahn, 2020 and *Rugitermes volcanensis* Scheffrahn, 2020 (Scheffrahn and Carrijo 2020; Scheffrahn and Pinzón 2020) from the Andean region (Table 1).

Table 1. Comparison of head measurements (mm) and coloration of soldiers and imagoes of different *Rugitermes* species.

No.	Species	Distribution*	Soldier		Imago				Reference
			Head width	Mean	Head width	Mean	Head color	Pronotum color	
1	*R. ursulae* sp. nov.	SA (Colombia)	1.12–1.22	1.17	1.10–1.20	1.15	Dark castaneous	Pale yellow	This publication
2	*R. flavicinctus*	SA (Guyana)	1.19–1.35	1.27	1.19	1.19	Black	Yellow	Emerson 1925
3	*R. rufus*	SA (Bolivia)	1.16–1.56	1.42	1.19–1.26	1.23	Reddish		Scheffrahn and Carrijo 2020
4	*R. magninotus*	SA (Guyana, Peru)	1.38–1.48	1.43	1.25	1.25	Black	Yellow	Emerson 1925
5	*R. volcanensis*	SA (Bolivia)	1.24–1.88	1.54	1.21	1.21	Black		Scheffrahn and Carrijo 2020
6	*R. athertoni*	OC (Polynesia)	1.47–1.73	1.60	1.26	1.26	Brown/Black		Light 1932
7	*R. aridus*	SA (Peru)	1.44–1.72	1.60	NA	NA	Black	Yellow	Scheffrahn and Carrijo 2020
8	*R. niger*	SA (Brazil)	1.50–1.80	1.65	1.26–1.34	1.30	Black		Oliveira 1979
9	*R. kirbyi*	CA (Costa Rica, Panama)	1.65	1.65	1.60	1.60	Black	Yellow	Snyder 1926
10	*R. tinto*	SA (Colombia)	1.52–1.90	1.72	1.31	1.31	Black	Yellow	Scheffrahn and Pinzón 2020
11	*R. unicolor*	CA (Honduras)	1.80	1.80	1.60	1.60	Yellow-brown	Yellow	Snyder 1952
12	*R. panamae*	CA (Panamá)	1.8–2.0	1.90	1.4	1.40	Black	Yellow	Snyder 1925
13	*R. bicolor*	SA (Guyana)	1.80–2.07	1.94	1.51	1.51	Black	Yellow	Emerson 1925
14	*R. occidentalis*	SA (Argentina)	2.00	2.00	1.35	1.35	Black	Brown	Silvestri 1901
15	*R. laticollis*	SA (Bolivia, Ecuador)	1.83–2.43	2.06	1.5–2.00	1.68	Black		Snyder 1957; Scheffrahn 2015
16	*R. costaricensis*	CA (Costa Rica)	2.10	2.10	1.80	1.80	Yellow-brown	Yellow	Snyder 1926
17	*R. nodulosus*	SA (Brazil)	NA	NA	NA	NA	Black	Yellow	Hagen 1858
18	*R. rugosus*	SA (Brazil)	1.21 (1.7?)	NA	NA	NA	Black		Hagen 1858

NA = Not available
* CA = Central America, OC = Oceania, SA = South America
Soldier's scale 1.1 1.2 1.3 1.4 1.5 1.6 1.7 1.8 1.9 2 2.1
Imago's scale 1.1 1.2 1.3 1.4 1.5 1.6 1.7 1.8

Rugitermes species have few species-specific diagnostic characters. The dorsal antennal ridge and the anterolateral corner of the frontal ridge of the soldier head, the size of the eyes of imagoes and soldiers as well as the imago's head shape can provide useful information to describe a new species (Krishna et al. 1961; Scheffrahn and Carrijo 2020).

Here, we describe the soldiers and imagoes of *Rugitermes ursulae* sp. nov. from a sample collected inside a dead branch in the tropical dry forest of Colombia's Caribbean coast. In addition, we performed molecular analyses based on the marker COII (cytochrome oxidase II) and including representatives of other genera of Kalotermitidae to support species description.

Materials and methods

Study sites and sampling

In July 2014, a survey was done in the tropical dry forest of Colombia's Caribbean coast (Casalla and Korb 2019). One sample of a new *Rugitermes* species was collected, which was preserved in 100% ethanol for molecular DNA analysis and in 80% ethanol for museum curation.

Identification and genetic analysis

Rugitermes ursulae sp. nov. was compared with *Rugitermes* samples from the University of Florida Termite Collection (UFTC), USA, and with descriptions and measurements from the literature (Hagen 1858; Silvestri 1901; Emerson 1925; Snyder 1925, 1926, 1952, 1957; Light 1932; Oliveira 1979; Scheffrahn 2015, 2020; Scheffrahn and Pinzón 2020). Specimens of *R. ursulae* were sequenced for a fragment of the molecular marker COII for genetic comparisons. Total DNA was extracted from the heads of pseudergates ('false workers') using the CTAB protocol (Fuchs et al. 2003). Due to limited availability of mitochondrial gene sequence data for species of Kalotermitidae at the National Center for Biotechnology Information (NCBI), we restricted our sequencing to the COII fragment (~740 bp), for which most data were available. We also sequenced a *Rugitermes* specimen from Colombia (*Rugitermes* ADD 2015-29), which lacks imagoes. PCRs and sequencing were performed following the protocol in Hausberger et al. (2011).

We considered COII sequences for 26 species of Kalotermitidae (if available three species per genus) and the woodroach, *Cryptocercus punctulatus*, as an outgroup (Suppl. material 1: Table S1). Thus, we covered 18 of the 22 known genera of Kalotermitidae worldwide. Sequences were aligned at the nucleotide level with the MUSCLE alignment algorithm as implemented in MEGA X v.10.1.8 with default settings (Kumar et al. 2018).

We inferred a phylogenetic tree based on the maximum likelihood (ML) approach. We selected the best fitting model using ModelFinder (Kalyaanamoorthy et al. 2017), which includes the free rate variation as implemented in IQ-TREE v. 1.6.12 (Nguyen et al. 2015). The selected model and parameter setting was TIM2+F+I+G4 according to the corrected Akaike Information Criterion (AICc, Kalyaanamoorthy et al. 2017). We performed 20 independent ML tree searches, 10 with a random starting tree and 10 with a parsimony starting tree, using the selected model, random seeds, and otherwise defaults settings. We compared the tree topologies among all inferred ML trees using Unique tree v. 1.9 (kindly provided by T. Wong and available upon request, Australian National University) as described in Misof et al. (2014), which resulted in one unique topology among the 20 inferred trees. We selected the ML tree with the best log likelihood value (including branch length). For statistical support, we performed 1000 non-parametric, slow bootstrap (BS) replicates with random starting trees and mapped statistical support onto the best ML tree using IQ-TREE. We ensured bootstrap convergence applying 'posteriori bootstrap criteria' (see Pattengale et al. 2010) using majority rule (MR) and 10,000 pseudo-replicates. Convergence was checked in five runs independently with different random seeds, all bootstrap convergence checks were performed with default settings in RaxML v.8.2.11 (Stamatakis 2014). Bootstrap convergence was achieved in each run after 5000 BS replicates. The best ML with statistical BS support tree was visualized using Seaview v.5.0.4 (Gouy et al. 2010).

We calculated *p*-distances between COII sequences with MEGA X v.10.1.8 (Kumar et al. 2018) using the following parameters: *p*-distance model, variance estimation model with 10,000 bootstrap replicates; the rate variation among sites (ASRV) was modeled with a gamma distribution (+G).

Imaging and measurements

Specimens were suspended in hand sanitizer and images were taken with a Leica M205 C stereomicroscope coupled to a Leica MC190 HD digital camera. Helicon Focus software was used to stack pictures. Measurements were done following Roonwal (1969).

Results

Taxonomy

Rugitermes ursulae **Casalla, Scheffrahn & Korb, sp. nov.**
http://zoobank.org/F5008BCF-2569-4654-81ED-B18815044CF9
Figs 2, 3; Tables 1–3

Material examined. ***Holotype*** soldier. Colombia: Colosó, Sucre (9.5435, -75.34884), 400 meters a.s.l., 11.JUL.2014, R. Casalla, ADD-2014-10A. ***Paratypes.*** One additional soldier, 12 pseudergates, a pair of reproductive, same colony sample as holotype ADD-2014-10B. Voucher specimen are held at the Universidad del Norte, Colombia. Holotype soldier (ADD-2014-10A) and one reproductive paratype of *Rugitermes ursulae* sp. nov. (ADD-2014-10B-1) will be deposited at the Natural History Museum of the Alexander von Humboldt Institute of Bogotá (MIAvH, Colombia) and a paratype soldier (ADD-2014-10B-2) and reproductive (ADD-2014-10B-3) at the collection of the American Museum of Natural History, New York. (AMNH, USA). Pseudergates ('false workers') of *R. ursulae* will be part of the collection of termites of the Department of Chemistry and Biology at the University del Norte.

Diagnosis. The soldier of *R. ursulae* sp. nov. is the smallest of all congeneric soldiers (Fig. 2). The size of the head is remarkably small (Tables 1, 2). The pronotum width is almost twice its length, for both imago and soldier. Antennal sockets are pronounced, protruded, and rectangular in the soldier. The soldier of *R. ursulae* sp. nov. can be distinguished by its small subflangular elevation.

The imago of *R. ursulae* sp. nov. is also the smallest of all *Rugitermes* species (Fig. 3; Tables 1, 3). The imago of *R. ursulae* sp. nov. has disproportionally large eyes and ocelli in relation to head dimensions, when compared with another small *Rugitermes* species, *R. flavicinctus*, which is known from Guyana (Table 1; Fig. 3). *Rugitermes ursulae* sp. nov. is the only *Rugitermes* imago with a dark-castaneous head capsule and pale-yellow coloration of the pronotum.

Type locality. "Los primates" Colosó, Sucre, Colombia (Fig. 1, Suppl. material 2: Fig. S1)

Description. ***Soldier*** (Fig. 2, Table 2). Head capsule, in dorsal view, light yellowish orange. Occiput and posterior vertex grading from pale orange to yellow orange towards frons. Postmentum concolorous with head capsule; narrowest at posterior third (Fig. 2C). Pronotum pale yellow, nearly transparent toward lateral margins. Mandibles dark reddish brown near base, grading to black from mid-length to tips. Third an-

Figure 2. *Rugitermes ursulae* sp. nov. soldier (holotype) head and pronotum **A** dorsal **B** lateral **C** ventral view **D** frontal view (black arrows mark inconspicuous subflangular elevation, red arrows mark margins of antennal carinae) **E** anterior dorsal (yellow arrow marks frontolateral ridge).

tennal article clavate, more pigmented than other articles; article formula 2<3>4=5. Pronotum twice as wide as long, anterior margin shallowly concave, anterolateral corners evenly rounded with a few bristles and scattered setae in posterolateral margins. Postmentum concolorous with head capsule; narrowest at posterior third (Fig. 2C). Eye spots barely discernable, forming pale blotches behind antennal carinae. In dorsal view, head capsule rectangular with lateral margins parallel. Frons angled ca 30° below plane of vertex (Fig. 2B); frons weakly concave with undulating rugosity in middle extending to postclypeus (Fig. 2E). In frontal view, shallow elevations on each side of frontal margin; about a dozen medium to long setae above and lateral to each eleva-

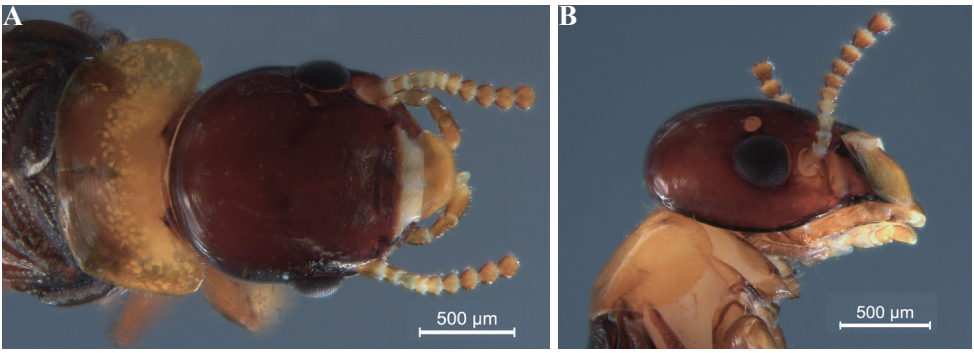

Figure 3. *Rugitermes ursulae* sp. nov**.** imago head and pronotum **A** dorsal **B** lateral view.

Table 2. Measurements (mm) of *Rugitermes ursulae* sp. nov. soldiers (*N* = 2).

Character	Holotype	Measurements
Head length with mandibles	2.81	2.81, 2.90
Head length to lateral base of mandibles	1.87	1.87, 1.99
Head width max.	1.12	1.12, 1.22
Head height with postmentum	1.06	1.06, 1.20
Postmentum width min.	0.22	0.22, 0.24
Postmentum length	1.34	1.34, 1.38
Pronotum width	1.27	1.27, 1.39
Pronotum length	0.63	0.63, 0.70
Third antennal article length	0.16	0.16, 0.17
Left mandible length (from dorsal condyle)	1.17	1.17, 1.22
Frontal angle (° degrees)	34	29, 34

Table 3. Measurements (mm) of *Rugitermes ursulae* sp. nov. dealated imagoes (*N* = 2).

Character	Measurements
Eye diameter max.	0.30, 032
Ocellus diameter max.	0.09, 0.10
Head width (max. with eyes)	1.10, 1.20
Head length to tip	1.44, 1.49
Head height	0.78, 0.87
Pronotum width max.	1.25, 1.27
Pronotum length min.	0.64, 0.70

tion (Fig. 2D). Frontolateral ridges about 85° in dorsal view; corners evenly rounded (Fig. 2E). Antennal carinae with projecting dorsal and posterior margins not exceeding head width; anterior margins below frontolateral ridges. Mandibles with weak basal humps; outer margins of blades straight from humps to distal fourth. First marginal tooth of left mandible three-fourths from tip; directed forward. First marginal tooth of right mandible at basal third.

Imago (Fig. 3, Table 3). Head capsule dark castaneous; pronotum pale yellowish, contrasting sharply with head capsule. Eyes small, ellipsoid. Ocellus hyaline, nearly circular, separated from eye by one-third its diameter. Antennae articles 2–4 pale yellow; first darker, fifth and beyond progressively darker. Antennae with at

least 10 articles (broken), formula 1>2=3>4. Head vertex and frons with few short setae. Pronotum twice as wide as long. Pronotum wider than head capsule; anterior margin straight, posterolateral corners evenly rounded with scattered bristles, posterior margin narrowly concave. Legs light brown grading to pale yellow toward tibia. Arolium present.

Distribution and biological observations. 'Los Primates' is located in the mountains of the municipality of Colosó, Sucre. It is a regional forest reserve created in 1983, containing primary and secondary tropical dry forest. The mean annual temperature is 26.7 °C (min: 25.8 °C; max: 27.8 °C) with an annual precipitation of around 1337 mm (INDERENA, 1983; Hijmans et al. 2005). The specimens of *Rugitermes ursulae* sp. nov. were collected from a small, dry branch (ca 12 mm in diameter) of a leafless bush (Suppl. material 2: Fig. S1).

Etymology. "Ursulae" derived from a diminutive of the Latin *ursa*, which means "little bear", in line with the small size of the species. Ursula is also the name of José Arcadio Buendía's wife in the novel "One hundred years of solitude" written by Gabriel García Márquez and represents an apology/symbolism for the spiritual engine, entrepreneurship, and hard and silent work of many women around the world.

Molecular analysis of the COII fragment. The topology and splits inferred from the multiple sequence alignment of the COII fragment for all Kalotermitidae genera available in NCBI, and including our new species, revealed a COII ML gene tree that clearly separated *R. ursulae* sp. nov. from the two other *Rugitermes* species with maximal BS support. Furthermore, it suggests that the genus *Rugitermes* is monophyletic (maximal BS support) and that it is the sister taxon of *Postelectrotermes*, however support values for the latter are low (19% BS; Fig. 4).

The *p*-distance analyses revealed that the barcode sequences most similar to *R. ursulae* (accession number: MW600961) belonged to *Rugitermes* sp. A TB-2014 (accession number: KP026284.1) and *Rugitermes* ADD 2015-29 (accession number: MW600962); they shared 87% and 86% sequence similarity (*p*-distance), respectively (Suppl. material 1: Table S2).

Key to *Rugitermes* from Colombia

1 Soldier with dark coloration of anterior head capsule. Anterolateral corners of frontal ridges project to form acute angles. Maximum soldier head width (mean) 1.72 mm; imago with a black head capsule; pronotum brownish orange, compound eye small, nearly circular. Ocellus very small; maximum head width (mean) 1.31 mm ..... ***Rugitermes tinto***

– Soldier with light yellowish orange of anterior head capsule. Anterolateral corners poorly developed. Maximum soldier head width (mean) 1.17 mm; imago with a dark-castaneous head capsule; pronotum pale yellowish, compound eye large, nearly circular. Ocellus small, oval shape; head width (mean) 1.15 mm.....***Rugitermes ursulae* sp. nov.**

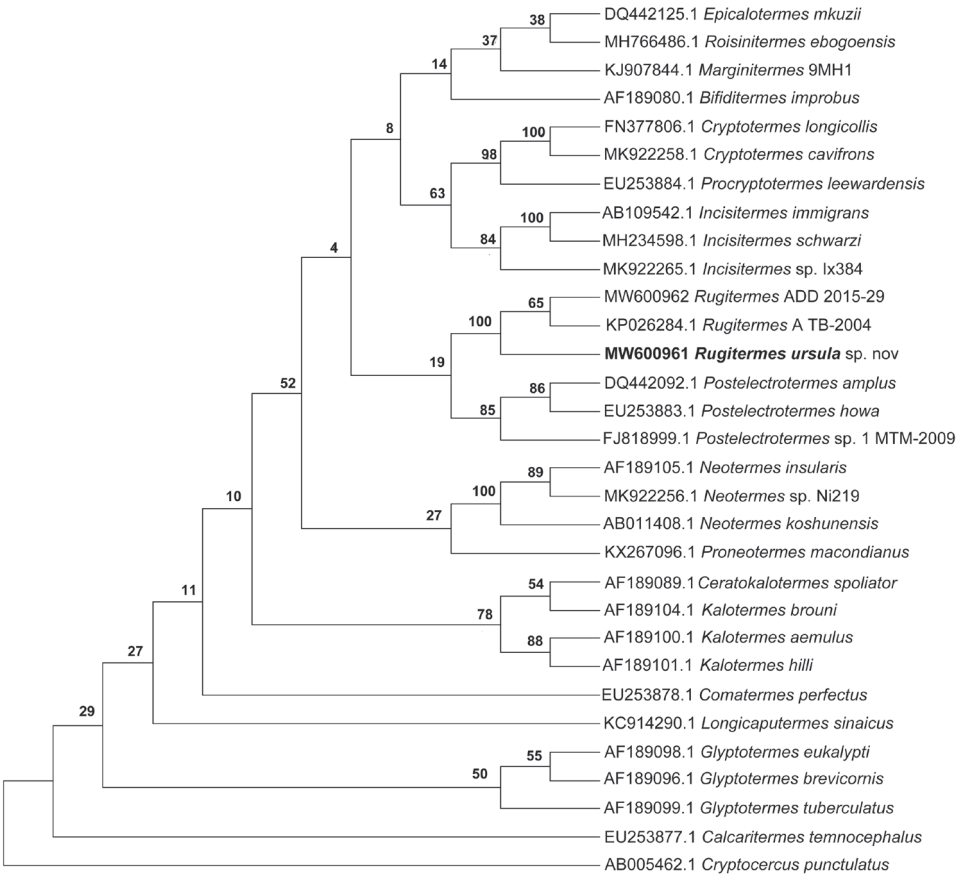

Figure 4. Maximum likelihood (ML) tree inferred from COII mtDNA gene sequences of 30 species of Kalotermitidae, including the woodroach, *Cryptocercus punctulatus*, as outgroup. Numbers before the splits show statistical bootstrap support (BS). Terminals are labeled with the respective NCBI access numbers and genus or species name. *Rugitermes ursulae* sp. nov. is shown in bold.

Discussion

The Caribbean Region of Colombia is rich in Kalotermitidae and the tropical dry forest supports a high species diversity for this family (Casalla et al. 2016a, b; Casalla and Korb 2019; Pinzón et al. 2020).

The phylogenetic relationships within the Kalotermitidae are not clearly resolved among the most recently discovered genera (Krishna 1961; Krishna et al. 2013). Molecular markers have helped to resolve the evolutionary relationships among termites (Bourguignon et al. 2015) but for some termite families such as the Kalotermitidae hurdles still persist. Thompson et al. (2000), using COII and cytochrome B sequences, inferred the phylogeny of Kalotermitidae of the Australian region. In addition to describing a new species, we used the generated COII sequences in an effort to obtain

better resolution of the phylogenetic relationships among the Kalotermitidae. We use representatives of 18 genera from all over the world (Table 1). However, the relationships among genera could not be clearly resolved (Fig. 4). Clearly, more integrative studies that combine additional molecular, morphological, and ecological data are needed. For our study, phylogenetic reconstruction was mainly applied to test whether *R. ursulae* differed genetically from other *Rugitermes* species.

Molecular markers often allow a clear separation between *Rugitermes* congeners (Scheffrahn and Carrijo 2020). In line with this, *R. ursulae* sp. nov. was clearly separated from the other *Rugitermes* species in our study (Fig. 4). However, it is generally difficult to describe new *Rugitermes* species when only a few specimens are available. However, the anterolateral ridges of the frons seem to be good diagnostic markers in *Rugitermes* (Scheffrahn and Carrijo 2020). This differed clearly in *Rugitermes ursulae* sp. nov. compared to described congeners. We identified the subflangular region (frontal head view) and the angle of the frontolateral ridge to be species-specific traits of soldiers. In addition, the coloration and the head of size of the imagoes, which are the smallest among all *Rugitermes* species (Table 1), support the description of a new species.

Our study shows the importance of further surveys at isolated sites in the tropics as they continue to reveal many new species. This is also essential for phylogenetic studies to infer the evolutionary history of the Kalotermitidae, and any taxonomic lineage in a broad way.

Acknowledgments

We thank the Universidad del Norte Barranquilla, Colombia, for a research grant to RC as part of its Strategic Research Area in Biodiversity, Ecosystem Services and Human Well-being, the University of Freiburg, and COLCIENCIAS-Colfuturo for financial support. We are also grateful to the National Agency of Environmental Licenses for research permit no. 739/ANLA/MADS (8 July 2014). We thanks to John Warner for English editing, Karen Meusemann for phylogenetic analyses and discussions, and two reviewers and the editor for helpful comments and careful review of the manuscript.

References

Bourguignon T, Lo N, Cameron SL, Šobotník J, Hayashi Y, Shigenobu S, Watanabe D, Roisin Y, Miura T, Evans TA (2015) The evolutionary history of termites as inferred from 66 mitochondrial genomes. Molecular Biology and Evolution 32: 40–621. https://doi.org/10.1093/molbev/msu308

Bucek A, Šobotník J, He S, Shi M, McMahon D, Holmes E, Roisin Y, Lo N, Bourguignon T (2019) Evolution of Termite Symbiosis Informed by Transcriptome-Based Phylogenies. Current Biology 29: 3728–3734. https://doi.org/10.1016/j.cub.2019.08.076

Casalla R, Scheffrahn RH, Korb J (2016a) *Cryptotermes colombianus* a new drywood termite and distribution record of *Cryptotermes* in Colombia. ZooKeys 596: 39–52. https://doi.org/10.3897/zookeys.596.9080

Casalla R, Scheffrahn RH, Korb J (2016b) *Proneotermes macondianus*, a new drywood termite from Colombia and expanded distribution of *Proneotermes* in the Neotropics (Isoptera, Kalotermitidae). ZooKeys 623: 43–60. https://doi.org/10.3897/zookeys.623.9677

Casalla R, Korb J (2019) Termite diversity in Neotropical dry forests of Colombia and the potential role of rainfall in structuring termite diversity. Biotropica 51: 165–177. https://doi.org/10.1111/btp.12626

Castro D, Scheffrahn RH, Carrijo T (2018) *Echinotermes biriba*, a new genus and species of soldierless termite from the Colombian and Peruvian Amazon (Termitidae, Apicotermitinae). ZooKeys 748: 21–30. https://doi.org/10.3897/zookeys.748.24253

Castro D, Scheffrahn RH (2019) A new species of *Acorhinotermes* Emerson, 1949 (Blattodea, Isoptera, Rhinotermitidae) from Colombia, with a key to Neotropical Rhinotermitinae species based on minor soldiers. ZooKeys 891: 61–70. https://doi.org/10.3897/zookeys.891.37523

Emerson AE (1925) The termites of Kartabo, Bartica District, British Guiana. Zoologica (New York) 6: 291–459.

Fuchs A, Heinze J, Reber-Funk C, Korb J (2003) Isolation and characterization of six microsatellite loci in the drywood termite *Cryptotermes secundus* (Kalotermitidae). Molecular Ecology Notes 3: 355–357. https://doi.org/10.1046/j.1471-8286.2003.00448.x

Gouy M, Guindon S, Gascuel O (2010) SeaView version 4: a multiplatform graphical user interface for sequence alignment and phylogenetic tree building. Molecular Biology and Evolution 27: 221–224. https://doi.org/10.1093/molbev/msp259

Hausberger B, Kimpel D, Neer A, Korb J (2011) Uncovering cryptic species diversity of a termite community in a West African savanna. Molecular Phylogenetics and Evolution 61: 964–969. https://doi.org/10.1016/j.ympev.2011.08.015

Hagen H (1858) Monographie der Termiten. Linnaea Entomologica 12: [i-iii +] 4–342. [+ 459.]

Hijmans R, Cameron S, Parra J, Jones P, Jarvis A (2005) Very high-resolution interpolated climate surfaces for global land areas. International Journal of Climatology 25: 1965–1978. https://doi.org/10.1002/joc.1276

Holmgren N (1911) Termitenstudien. 2. Systematik der Termiten. Die Familien Mastotermitidae, Protermitidae und Mesotermitidae. Kungliga Svenska Vetenskaps-Akademiens Handlingar 46: 1–86. [+ 6 pls]

INDERENA (1983) Acuerdo 0028 del 6 de julio 1983. Por el cual se declara área de reserva forestal protectora, la Serranía de Coraza y Montes de María (Serranía de San Jacinto), ubicada en jurisdicción de los Municipios de Toluviejo, Colosó y Chalán (Departamento de Sucre). Bogotá, Colombia, 6 pp.

Inward D, Vogler A, Eggleton P (2007) A comprehensive phylogenetic analysis of termites (Isoptera) illuminates key aspects of their evolutionary biology. Molecular Phylogenetic and Evolution 44: 953–967. https://doi.org/10.1016/j.ympev.2007.05.014

Kalyaanamoorthy S, Minh BQ, Wong TKF, von Haeseler A, Jermiin LS (2017) ModelFinder: fast model selection for accurate phylogenetic estimates. Nature Methods 14: 587–589. https://doi.org/10.1038/nmeth.4285

Krishna K (1961) A generic revision and phylogenetic study of the family Kalotermitidae (Isoptera). Bulletin of the American Museum of Natural History 122: 303–408.

Krishna K, Grimaldi DA, Krishna V, Engel MS (2013) Treatise on the Isoptera of the world. Vol. 2 Basal Families. American Museum of Natural History Bulletin 377: 201–623. https://doi.org/10.1206/377.2

Kumar S, Stecher G, Li M, Knyaz C, Tamura K (2018) MEGA X: Molecular Evolutionary Genetics Analysis across computing platforms. Molecular Biology and Evolution 35: 1547–1549. https://doi.org/10.1093/molbev/msy096

Light S (1932) Termites of the Marquesas Islands. Bulletin of the Bernice Pauahi Bishop Museum 98: 73–86.

Misof B, Liu S, Meusemann K, Peters RS, Donath A, Mayer C, Frandsen PB, Ware J, Flouri T, Beutel RG, Niehuis O, Petersen M, Izquierdo-Carrasco F, Wappler T, Rust J, Aberer AJ, Aspöck U, Aspöck H, Bartel D, Blanke A, Berger S, Böhm A, Buckley TR, Calcott B, Chen J, Friedrich F, Fukui M, Fujita M, Greve C, Grobe P, Gu S, Huang Y, Jermiin LS, Kawahara AY, Krogmann L, Kubiak M, Lanfear R, Letsch H, Li Y, Li Z, Li J, Lu H, Machida R, Mashimo Y, Kapli P, McKenna DD, Meng G, Nakagaki Y, Navarrete-Heredia JL, Ott M, Ou Y, Pass G, Podsiadlowski L, Pohl H, von Reumont BM, Schütte K, Sekiya K, Shimizu S, Slipinski A, Stamatakis A, Song W, Su X, Szucsich NU, Tan M, Tan X, Tang M, Tang J, Timelthaler G, Tomizuka S, Trautwein M, Tong X, Uchifune T, Walzl MG, Wiegmann BM, Wilbrandt J, Wipfler B, Wong TKF, Wu Q, Wu G, Xie Y, Yang S, Yang Q, Yeates DK, Yoshizawa K, Zhang Q, Zhang R, Zhang W, Zhang Y, Zhao J, Zhou C, Zhou L, Ziesmann T, Zou S, Li Y, Xu X, Zhang Y, Yang H, Wang J, Wang J, Kjer KM, Zhou X (2014) Phylogenomics resolves the timing and pattern of insect evolution. Science 346: 763–767. https://doi.org/10.1126/science.1257570

Nguyen L, Schmidt H, Haeseler A, Quang B (2015) IQ-TREE: A Fast and Effective Stochastic Algorithm for Estimating Maximum-Likelihood Phylogenies, Molecular Biology and Evolution 32: 268–274. https://doi.org/10.1093/molbev/msu300

Oliveira G (1979) *Rugitermes niger* (Isoptera, Kalotermitidae), nova espécie de térmita do sul do Brasil. Dusenia 11: 9–14.

Pattengale N, Alipour M, Bininda-Emonds O, Moret B, Stamatakis A (2009) How Many Bootstrap Replicates Are Necessary?. In: Batzoglou S. (eds) Research in Computational Molecular Biology. RECOMB 2009. Lecture Notes in Computer Science, vol 5541. Springer, Berlin. https://doi.org/10.1007/978-3-642-02008-7_13

Pinzón O, Castro D (2018) New records of termites (Blattodea: Termitidae: Syntermitinae) from Colombia. Journal of Threatened Taxa 10: 12218–12225. https://doi.org/10.11609/jott.3909.10.9.12218-12225

Pinzón O, Casalla, R, Castro D, Vargas-Niño A (in press) Termitas de Colombia, 35 pp.

Pizano C, García H (2014) El Bosque Seco Tropical en Colombia. Instituto de Investigación de Recursos Biológicos Alexander von Humboldt (IAvH). Bogotá, Colombia, 354 pp.

Postle A, Scheffrahn RH (2016) A new termite (Isoptera, Termitidae, Syntermitinae, *Macuxitermes*) from Colombia. ZooKeys 587: 21–35. https://doi.org/10.3897/zookeys.587.7557

Ronquist F, Huelsenbeck JP (2003) MrBayes 3: Bayesian phylogenetic inference under mixed models. Bioinformatics 19: 1572–1574. https://doi.org/10.1093/bioinformatics/btg180

Roonwal M (1969) Measurement of termites (Isoptera) for taxonomic purposes. Journal of the Zoological Society of India 21: 9–66.

Scheffrahn RH (2010) An extraordinary new termite (Isoptera: Termitidae: Syntermitinae: *Rhynchotermes*) from the pasturelands of northern Colombia. Zootaxa 2387: 63–68. https://doi.org/10.11646/zootaxa.2387.1.6

Scheffrahn RH (2015) Global elevational, latitudinal, and climatic limits for termites and the redescription of *Rugitermes laticollis* Snyder (Isoptera: Kalotermitidae) from the Andean Highlands. Sociobiology 62: 426–438. https://doi.org/10.13102/sociobiology.v62i3.793

Scheffrahn RH (2019) Expanded New World distributions of genera in the termite family Kalotermitidae. Sociobiology 66: 136–153. https://doi.org/10.13102/sociobiology.v66i1.3492

Scheffrahn RH (2019) *Rhynchotermes armatus*, a new mandibulate nasute termite (Isoptera, Termitidae, Syntermitinae) from Colombia. ZooKeys 892: 135–142. https://doi.org/10.3897/zookeys.892.38743

Scheffrahn RH, Carrijo TF (2020) Three new species of *Rugitermes* (Isoptera, Kalotermitidae) from Peru and Bolivia. ZooKeys 1000: 31–44. hhttps://doi.org/10.3897/zookeys.1000.59219

Scheffrahn RH, Pinzón OP (2020) *Rugitermes tinto*: A new termite (Isoptera, Kalotermitidae) from the Andean region of Colombia. ZooKeys 963: 37–44. https://doi.org/10.3897/zookeys.963.55843

Silvestri F (1901) Nota preliminare sui Termitidi sud-americani. Bollettino dei Musei di Zoologia ed Anatomia Comparata della Reale Università di Torino 16: 1–8. https://www.biodiversitylibrary.org/page/11675026

Snyder T (1925) A new *Rugitermes* from Panama. Journal of the Washington Academy of Sciences 15: 197–200.

Snyder T (1926) Five new termites from Panama and Costa Rica. Proceedings of the Entomological Society of Washington 28: 7–16.

Snyder T (1952) A new *Rugitermes* from Guatemala. Proceedings of the Entomological Society of Washington 54: 303–305.

Snyder T (1957) A new *Rugitermes* from Bolivia (Isoptera, Kalotermitidae). Proceedings of the Entomological Society of Washington 59: 81–82.

Stamatakis A (2014) RAxML version 8: a tool for phylogenetic analysis and post-analysis of large phylogenies. Bioinformatics 30:1312-3. https://doi.org/10.1093/bioinformatics/btu033

Thompson G, Miller L, Lenz M, Crozier R (2000) Phylogenetic analysis and trait evolution in Australian lineages of drywood termites (Isoptera, Kalotermitidae). Molecular Phylogenetics and Evolution 17: 419–429. https://doi.org/10.1006/mpev.2000.0852

Supplementary material 1

Tables S1, S2

Authors: Robin Casalla, Rudolf H. Scheffrahn, Judith Korb

Data type: Sequence accession identifier and Measures of genetic distance

Explanation note: **Table S1.** GenBank accession numbers for COII gene sequences of Kalotermitidae used in this study. **Table S2.** Nucleotide *p*-distances for COII sequences between *Rugitermes ursulae* sp. nov. (bold) and other species belonging to Kalotermitidae. *Cryptocercus punctulatus* used as outgroup.

Link: https://doi.org/10.3897/zookeys.1057.65877.suppl1

Supplementary material 2

Figure S1

Authors: Robin Casalla, Rudolf H. Scheffrahn, Judith Korb

Data type: Multimedia: Photo

Explanation note: Biome for *Rugitermes ursulae* sp. nov. (Tropical dry forest, Colosó, Colombia, July 2014).

Link: https://doi.org/10.3897/zookeys.1057.65877.suppl2

Supplementary material 3

Supplementary references

Authors: Robin Casalla, Rudolf H. Scheffrahn, Judith Korb

Data type: References

Link: https://doi.org/10.3897/zookeys.1057.65877.suppl3

ZooKeys 1057: 37–48 (2021)
doi: 10.3897/zookeys.1057.66434
https://zookeys.pensoft.net

RESEARCH ARTICLE

A peer-reviewed open-access journal
ZooKeys
Launched to accelerate biodiversity research

New mimarachnids (Hemiptera, Fulgoromorpha, Fulgoroidea) in mid-Cretaceous Burmese amber

Xiao Zhang[1], Yunzhi Yao[2], Dong Ren[2], Hong Pang[1], Huayan Chen[1]

1 *State Key Laboratory of Biocontrol, School of Life Sciences/School of Ecology, Sun Yat-sen University, Guangzhou 510275, China* **2** *College of Life Sciences and Academy for Multidisciplinary Studies, Capital Normal University, Xisanhuanbeilu 105, Haidian District, Beijing 100048, China*

Corresponding author: Huayan Chen (chenhuayan@mail.sysu.edu.cn)

Academic editor: Mike Wilson | Received 24 March 2021 | Accepted 30 July 2021 | Published 25 August 2021

http://zoobank.org/F7F330B5-4188-493D-A3D1-37800007EA7D

Citation: Zhang X, Yao Y, Ren D, Pang H, Chen H (2021) New mimarachnids (Hemiptera, Fulgoromorpha, Fulgoroidea) in mid-Cretaceous Burmese amber. ZooKeys 1057: 37–48. https://doi.org/10.3897/zookeys.1057.66434

Abstract

A new genus and species, *Multistria orthotropa* **gen. et sp. nov.**, and a new species, *Dachibangus hui* **sp. nov.**, of Mimarachnidae are described from the mid-Cretaceous Burmese amber. These new taxa display unique wing color patterns and extend the Mesozoic diversity of Mimarachnidae. The evolution of wing venation, phylogenetic placement of Mimarachnidae, and anti-predation defenses of this family in Burmese amber forest are briefly discussed.

Keywords

fossil, palaeodiversity, planthopper, taxonomy, wing pigmentation

Introduction

Mimarachnidae Shcherbakov, 2007 is a small, extinct family belonging to the diverse phytophagous superfamily Fulgoroidea. They are medium-sized to large planthoppers and are characterized by the following characters: mesonotum with double median carinae, remnants of sensory pits in the adults, tegmina and hind wings with simplified venation and irregular network of veinlets, and basal cell absent or weak (Brysz and Szwedo 2019). Historically, species of this family were considered as members of the "cixiidae-like" planthoppers (Bourgoin and Szwedo 2008), and some mimarachnids

are specialized insects with peculiar and striking forms (Shcherbakov 2007; Jiang et al. 2018, 2019; Zhang et al. 2018).

Fossil Mimarachnidae currently consist of 17 described species in 12 genera distributed from high latitude regions to tropical equatorial regions in the Cretaceous of Eurasia (Bourgoin 2021). Two monotypic genera, *Mimarachne* Shcherbakov, 2007 and *Saltissus* Shcherbakov, 2007 were first described from the Lower Cretaceous Baissa of Russia (145–125 Ma), then *Nipponoridium* (Fujiyama 1978; Szwedo 2008) were described from the Lower Cretaceous Kuwajima of Japan (140–120 Ma) (Szwedo 2008); and two genera, *Mimamontsecia* Szwedo & Ansorge, 2015 and *Chalicoridulum* Szwedo & Ansorge, 2015 were found from the Lower Cretaceous north-eastern Spain (130.0–125.5 Ma). Most other fossil Mimarachnidae were discovered from the mid-Cretaceous Burmese Kachin amber (98.79 ± 0.62 Ma), including the genera of *Burmissus* Shcherbakov, 2017, *Dachibangus* Jiang, Szwedo & Wang, 2018, *Jaculistilus* Zhang, Ren & Yao, 2018, *Mimaplax* Jiang, Szwedo & Wang, 2019, *Ayaimatum* Jiang & Szwedo, 2020, *Cretodorus* Fu & Huang, 2020, and *Mimaeurypterus* Fu & Huang, 2021. In addition, some specimens from the Cretaceous of Siberia, Mongolia, and Kazakhstan were mentioned by Shcherbakov (2007) but not formally described.

Herein, we describe a new genus with a new species, *Multistria orthotropa* gen. et sp. nov., and a new species, *Dachibangus hui* sp. nov., of Mimarachnidae from the mid-Cretaceous Myanmar. Both new species possess well-preserved wing venation and color pattern.

Materials and methods

The specimens (contributed by Mr Zhengkun Hu) described in this study are from the Burmese amber collected from Hukawng Valley of Kachin in northern Myanmar (Li et al. 2017). The age of the Burmese amber is estimated to be the earliest Cenomanian, ~98.79 ± 0.62 Ma (Shi et al. 2012). Burmese amber from this site contains diverse insects (Ross 2021). The type specimens are housed in the Key Lab of Insect Evolution and Environmental Changes, College of Life Sciences, Capital Normal University, Beijing, China (CNUB; Yunzhi Yao, Curator).

The amber specimens were examined and photographed using a Nikon SMZ 25 microscope with an attached Nikon DS-Ri 2 digital camera system. The line drawings were made with Adobe Illustrator 2020 and Adobe Photoshop 2020. The wing venational nomenclature follows that of Bourgoin et al. (2015).

Systematic palaeontology

Order Hemiptera Linnaeus, 1758
Suborder Fulgoromorpha Evans, 1946
Superfamily Fulgoroidea Latreille, 1807
Family Mimarachnidae Shcherbakov, 2007

Genus *Multistria* Zhang, Yao & Pang, gen. nov.
http://zoobank.org/50100984-8987-45C5-8429-DE636BEFB635
Figures 1, 2

Etymology. The generic name is a combination of Latin "*multi-*" meaning "many" and "*stria*" meaning "streak", referring to its wrinkled posterior pronotum. Gender feminine.

Type species. *Multistria orthotropa* Zhang, Yao & Pang, sp. nov.

Diagnosis. Pronotum with posterior area rugulose (not rugulose in *Dachibangus*). Tegmen costal area narrow, exceeding 2/3 length of the wing, ScP + RA and RP single, close to each other, subparallel, MP with three terminals (no fewer than five terminals in *Dachibangus*), CuA forked early, near wing basal 1/3, CuA_2 slightly curved mediad at level of tornus (more curved in *Dachibangus*). Without narrow marginal membrane. Hind wing CuA with two terminals.

***Multistria orthotropa* Zhang, Yao & Pang, sp. nov.**
http://zoobank.org/335C6C62-D3F0-440E-8CCE-036E63AC8F42
Figures 1, 2

Etymology. The specific name is from a Latin word "*orthotropus*" meaning "straight", referring to its median carinae of mesonotum straight.

Type material. ***Holotype***, CNU-HOM-MA2021001, gender unknown, a complete specimen but ventral view not visible.

Locality and horizon. Hukawng Valley, Kachin State, Myanmar; mid-Cretaceous, lowermost Cenomanian.

Diagnosis. Pronotum with anterior margin almost straight, posterior margin slightly concave, median carinae of mesonotum straight. Tegmen without spots, common stem ScP + R shorter than basal cell, Pcu almost straight, free part of Pcu distinctly shorter than common stem of Pcu + A_1. Metatibio-metatarsal formula 5: 5: 5.

Description. A well-preserved specimen, but ventral view not visible; total length of the holotype about 15.98 mm.

Head: head with compound eyes about 2.52 mm wide, wider than half of pronotum width. Vertex triangular, without median carina, lateral margins carinate, posterior margin sinuous, trigons visible in dorsal view.

Thorax: pronotum subhexagonal, length distinctly shorter than mesonotum, about 4.3 times as wide as long in midline, posterior area of pronotum rugulose, anterior margin almost straight, posterior margin arcuate and concave, median carinae double and parallel, present throughout, lateral carinae invisible. Mesonotum poorly preserved, wider than long in midline, median carinae parallel and paired, diverging laterad on scutellum, lateral carinae invisible, scutellum indistinct. Tegula subquadrate, large and distinctly carinate.

Leg: only part of hind leg visible, covered with short setae. Hind tibia widened apically, with five apical teeth; hind tarsi with three segments, basitarsomere 1.72 mm

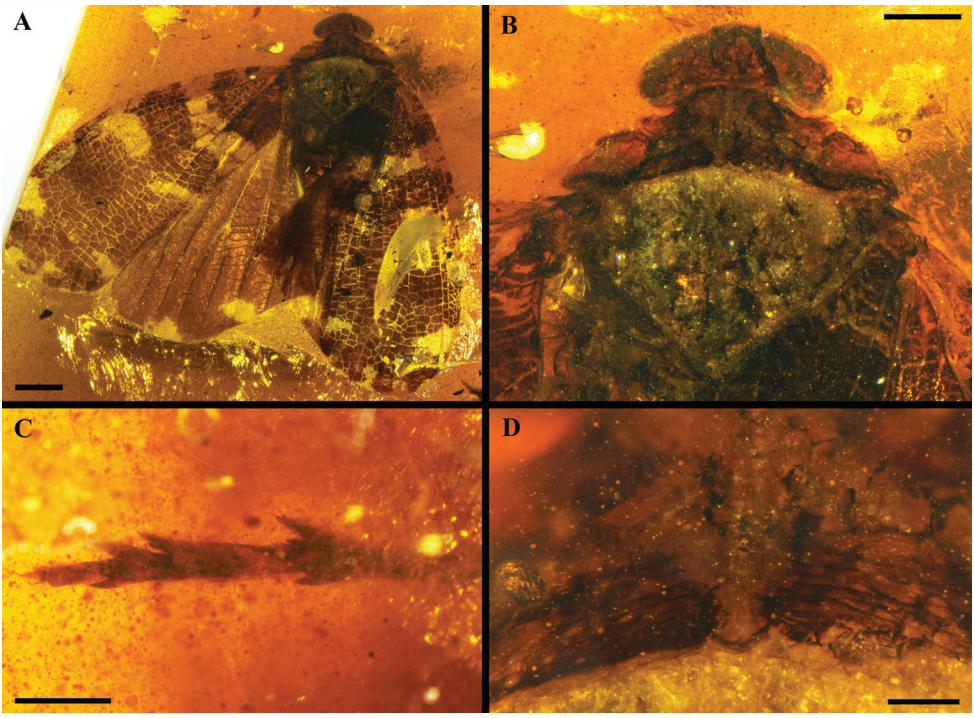

Figure 1. Holotype of *Multistria orthotropa* gen. et sp. nov. **A** habitus in dorsal view **B** head and thorax in dorsal view **C** hind tarsus **D** pronotum in dorsal view. Scale bars: 2 mm (**A**); 1 mm (**B, C**); 0.25 mm (**D**).

long, distinctly longer than combined length of midtarsomere and apical tarsomere, with five apical teeth, the external teeth longer than inner group; midtarsomere 0.89 mm long, with five apical teeth, the external teeth longer than inner group; subapical setae on all pectens invisible; apical tarsomere 0.67 mm long; tarsal claws developed, arolium wide.

Wings: membranous. Tegmen 14.03 mm long, 5.55 mm wide, about 2.5 times as long as wide, with distinct venation and irregular network veinlets, and also with irregular colour bands from base to apex, costal margin weakly arched at base, anteroapical and posteroapical angles broadly rounded, posterior margin straight, tornus present. Costal area narrow and long, with transverse veinlets, narrowing toward wing apex, basal cell weak, arculus indistinct, Pc + CP extends nearly to wing apex, apical portion invisible, common stem ScP + R + M longer than common stem ScP + R, branch ScP + RA and RP subparallel to costal margin, not forked, stem MP curved at base then almost straight, forked in wing apical half, with three terminals, branch MP_{1+2} forked, reaching margin with two terminals, branch MP_{3+4} simple, CuA forked near wing basal one-third, with two terminals, CuA_1 basally subparallel to CuA_2, CuA_2 slightly curved mediad at level of tornus, CuP present throughout wing, slightly sinuate, clavus open, Pcu and A_1 fused nearly at the same level of CuA forking, free part of Pcu distinctly shorter than common stem of Pcu + A_1, narrow marginal membrane absent.

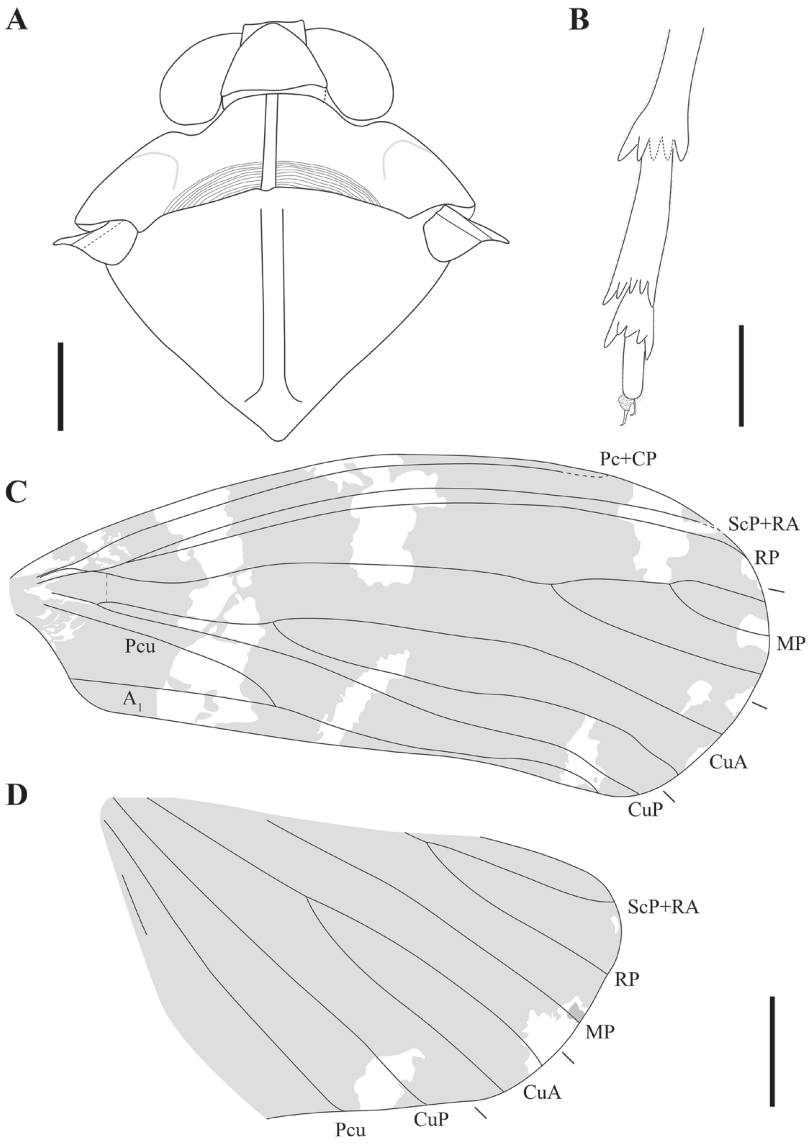

Figure 2. Line drawings of *Multistria orthotropa* gen. et sp. nov. **A** head and thorax **B** hind tarsus **C** forewing **D** hind wing. Scale bars: 1 mm (**A, B**); 2 mm (**C, D**).

Hind wing membranous, about 11.01 mm long, 6.60 mm wide, slightly shorter than tegmen, coloration of hind wing darker, two lighter irregular spots near posteroapical portion, irregular network veinlets present. Anteroapical angle round, ScP + R forked, with two terminals, ScP + RA curved in apical portion, stem MP single, CuA forked at wing midlength, reaching margin with two terminals, CuP almost straight, Pcu slightly sinuous.

Remarks. The new genus is assigned to Mimarachnidae based on the following characters: mesonotum with double median carinae, remnants of sensory pits at the adults, wings with simplified venation, and irregular network of veinlets, basal cell weak, hind wing MP simple. This new genus is distinguished from other genera by the following characters: posterior area of pronotum rugulose (vs no such character in the other known genera); tegmen costal area exceeding 2/3 length of the wing (vs less than ½ of wing length in *Chalicoridulum*, *Ayaimatum*, and *Mimaeurypterus*, costal area absent in *Mimaplax*); ScP + RA and RP single (vs ScP + RA and RP forked in *Mimarachne* and *Saltissus*, RP forked in *Mimamontsecia*); tegmen ScP + RA and RP close to each other, subparallel (vs ScP + RA diverging from RP in *Mimarachne*, *Saltissus*, *Chalicoridulum*, *Mimamontsecia*); MP with three terminals (vs single in *Cretodorus*, two terminals in *Saltissus*, *Chalicoridulum*, *Mimamontsecia*, *Burmissus*, and *Ayaimatum*, no fewer than four terminals in *Jaculistilus* and *Dachibangus*); CuA forked early, near wing basal 1/3 (forked late, near wing midpoint in *Mimaplax*, *Chalicoridulum*, *Saltissus*, *Burmissus*, *Ayaimatum*, *Cretodorus*); tegmen without narrow marginal membrane (vs with narrow marginal membrane in *Mimarachne*, *Chalicoridulum*, *Mimamontsecia*, *Burmissus*, *Cretodorus*, *Mimaeurypterus*); hind wing CuA with two terminals (vs three terminals in *Nipponoridium*).

Genus *Dachibangus* Jiang, Szwedo & Wang, 2018

Type species. *trimaculatus* Jiang, Szwedo & Wang, 2018; by original designation and monotype.

Dachibangus hui Zhang, Yao & Pang, sp. nov.

http://zoobank.org/24D479B0-EBB5-4C2F-95D3-3C1A41FF403A
Figures 3, 4

Etymology. The new specific name is dedicated to Mr Zhengkun Hu for his donation of the Burmese amber containing the holotype.

Type material. ***Holotype***, CNU-HOM-MA2021002, adult male, wings well preserved, but legs missing.

Locality and horizon. Hukawng Valley, Kachin State, Myanmar; mid-Cretaceous, lowermost Cenomanian.

Diagnosis. Median carinae of mesonotum straight, subparallel to each other, lateral carinae posterior portion nearly straight (median carinae slightly sinuate, lateral carinae posterior portion arcuate in *D. trimaculatus*); tegmen without spots (with spots in *D. trimaculatus* and *D. formosus*); common stem ScP + R as long as basal cell (ScP + R longer than basal cell in *D. formosus*, ScP + R about 1/2 of basal cell in *D. trimaculatus*); MP with five terminals (six terminals in *D. trimaculatus*); the bifurcation of MP_{1+2} slightly proximad of the bifurcation of MP_{3+4} (the bifurcation of MP_{1+2} slightly apicad of the bifurcation of MP_{3+4} in *D. formosus*); CuA_1 almost straight

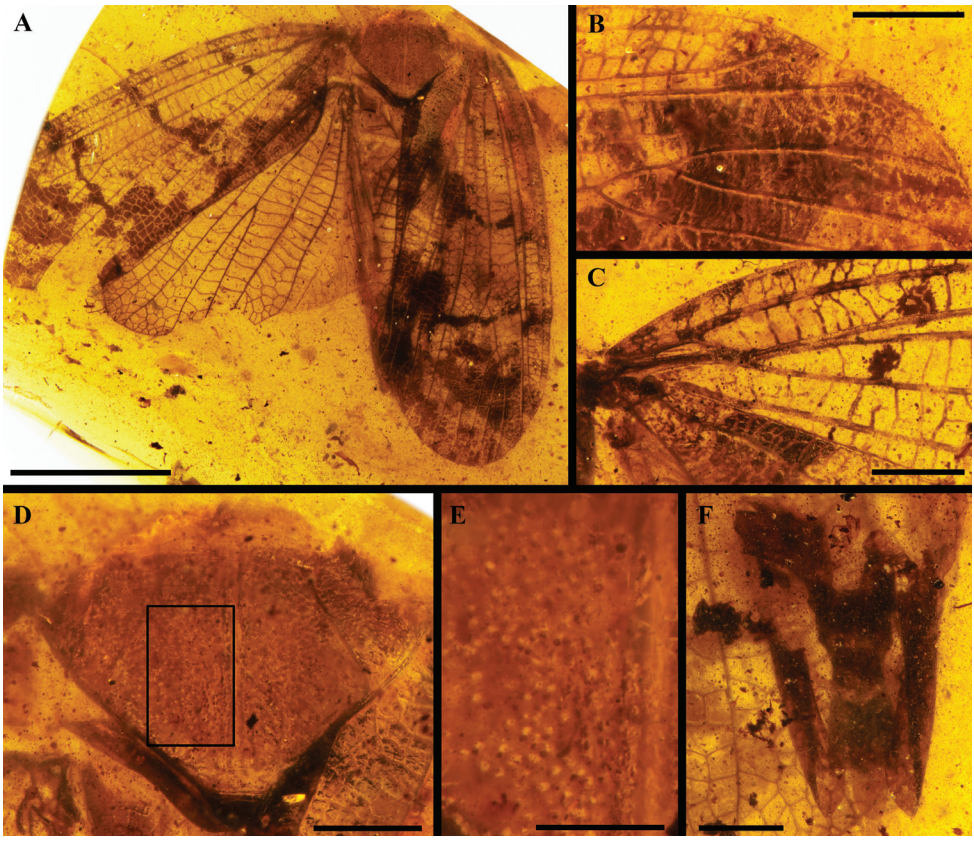

Figure 3. Holotype of *Dachibangus hui* sp. nov. **A** habitus in dorsal view **B** distal part of forewing **C** basal part of forewing **D** mesonotum **E** sensory pits on mesonotum **F** male terminalia in ventral view. Scale bars: 5 mm (**A**); 1 mm (**B, C, D, F**); 0.5 mm (**E**).

(arcuate in *D. trimaculatus*); CuA_2 slightly curved mediad at level of tornus (more curved in *D. formosus*, strongly curved in *D. trimaculatus*); CuP almost straight (sinuate in *D. trimaculatus* and *D. formosus*); free stem of Pcu nearly as long as common stem of Pcu + A_1 (Pcu longer than Pcu + A_1 in *D. trimaculatus*); CuP and Pcu + A_1 not close to each other (close to each other in *D. trimaculatus*); hind wing CuA forked at wing midlength (forked near wing base in *D. trimaculatus*).

Description. Total length of the preserved holotype about 14.21 mm, wings well-preserved.

Thorax: mesonotum wider than long in midline, densely punctate, median carinae paired, diverging laterad on scutellum, lateral carinae distinct, not reaching anterior margin, diverging posteriad, scutellum transversely wrinkled. Tegula large.

Wings: membranous. Tegmen 13.59 mm long, 5.06 mm wide, about 2.7 times as long as wide, with distinct venation and irregular network veinlets, and also with irregular colour bands from base to apex, costal margin weakly arched at base, apical margin

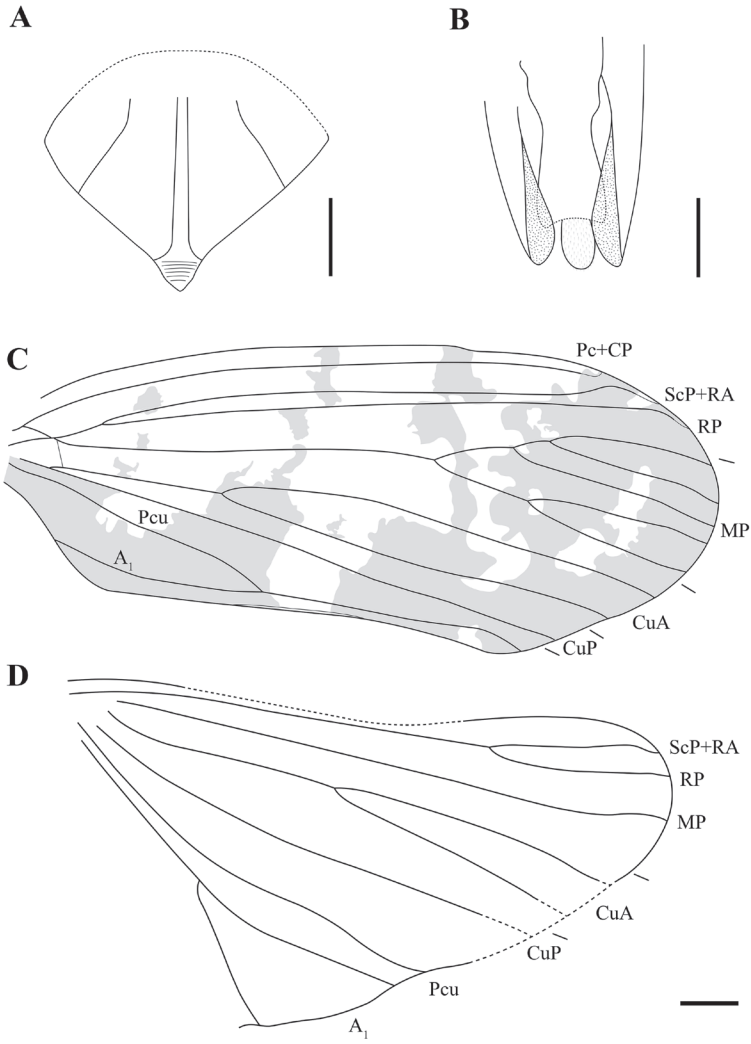

Figure 4. Line drawings of *Dachibangus hui* sp. nov. **A** mesonotum **B** male terminalia **C** forewing **D** hind wing. Scale bars: 1 mm (**A**–**D**).

round, posterior margin almost straight, tornus distinct. Costal area narrow and long, with transverse veinlets, narrowing toward tegmen apex, basal cell weak, arculus weak, Pc + CP parallel to costal margin, apical portion weakened, common stem ScP + R + M approximately as long as common stem ScP + R, ScP + RA not forked, posterior portion curved upward, then downward to apical margin, apical portion weakened, RP single, apical portion weakened, stem MP almost straight, forked in wing apical half, with five terminals, the bifurcation of MP_{1+2} slightly proximad of the bifurcation of MP_{3+4}, MP_{1+2} reaching margin with three terminals, MP_{3+4} with two terminals, CuA forked near wing basal one-third, with two terminals, CuP present throughout wing,

nearly straight, clavus open, Pcu and A_1 fused apicad of CuA forking, narrow marginal membrane absent, wing-coupling fore fold present.

Hind wing membranous, about 10.57 mm long, 5.63 mm wide, slightly shorter than tegmen, without distinct coloration, irregular network veinlets present. Anteroapical angle round, stem ScP + R straight, forked late, with two terminals, ScP + RA apical portion curved, MP single, CuA forked at wing midlength, with two terminals, CuP almost straight, apical portion absent, Pcu weakly sinuous, A_1 forked, giving off two branches.

Abdomen: male terminalia poorly preserved, with two symmetrical lobes, pygofer lobes carinate, anal tube elongate, anal styles protruding and ligulate.

Remarks. The new species is attributed to the genus *Dachibangus* due to mesonotum median carinae diverging laterad on scutellum, lateral carinae strongly diverging posteriad, tegmen with irregular colour bands, costal area narrow, ScP + RA curved downward in apical portion, MP at least with five terminals, CuA_2 curved mediad at level of tornus, tornus distinct.

Discussion

Including the new taxa described in this study, Mimarachnidae now comprise 13 genera and 19 species, all confined to the Cretaceous. Among them, five genera and five species have been described from the early Cretaceous of Russia, Spain, and Japan, and the rest were discovered from the mid-Cretaceous Burmese amber. During early Cretaceous period, tegmen ScP + RA and RP of mimarachnids were generally forked, with the MP having 2 or 3 terminals, such as in *Mimarachne*, *Saltissus*, and *Mimamontsecia*. However, by the mid-Cretaceous, tegmen ScP + RA, and RP were unbranched (all species) and the MP single (*Cretodorus*) or with 2 or 3 terminals (*Burmissus*, *Mimaplax*, *Ayaimatum*, and *Mimaeurypterus*) or with no fewer than 4 terminals (*Jaculistilus* and *Dachibangus*). Therefore, we speculate that the number of tegmen ScP + R terminals gradually reduced, and the number of MP terminals seems to have been diversified during the evolutionary process of Mimarachnidae.

The placement of Mimarachnidae in Fulgoroidea remains unclear. Shcherbakov (2007) placed Mimarachnidae in the "pre-cixioid section of Fulgoroidea" and related them to Perforissidae. Subsequently, this family was generally assigned into the "cixiidae-like" planthopper group (Bourgoin and Szwedo 2008; Szwedo and Ansorge 2015; Brysz and Szwedo 2019), which is an informal group comprises some extinct and extant families similar to Cixiidae. Mimarachnidae are unique planthoppers in the Mesozoic. Mimarachnidae and Perforissidae share many similar characters such as the simplified venation, remnants of sensory pits at the adults, destabilization of hind leg armature (Shcherbakov 2017). But, as Jiang et al. (2018) suggested, these similarities are also shared by various families of Fulgoroidea. These similarities cannot support a close relationship between Mimarachnidae and Perforissidae because they could also result from convergent or par-

allel evolution. Besides, Mimarachnidae and the "cixiidae-like" families show obvious differences in the morphology, such as venation patterns, shape of head and thorax, and number of carinae, which suggests that they do not form a lineage and share a common ancestor. A robust placement of Mimarachnidae in Fulgoroidea still needs further study.

Fulgoromorpha are phytophagous insects. These planthoppers stay on the host plants for a long time to suck fluids, with wings covering their bodies. Colour pattern of the wings might have become important for serving as a defensive strategy to disguise themselves from enemies. In *Multistria* gen. nov. and *Dachibangus*, the tegmina are covered with irregular color bands from the base to the apex, contrasting highly and extending to the tegmina edges. This disruptive coloration could effectively break up the shape and destroy the outline of the insects (Stevens and Merilaita 2009a, 2009b), and thereby make these larger planthoppers more difficult to be detected. Similarly, in *D. trimaculatus* Jiang, Szwedo & Wang, 2018, *D. formosus* Fu, Szwedo, Azar & Huang, 2019, and *Jaculistilus oligotrichus* Zhang, Ren & Yao, 2018, the dark wing spots are obvious and may also have anti-predation function (Théry and Gomez 2010). In addition, *Mimaplax ekrypsan* Jiang, Szwedo & Wang, 2019 used more complicate camouflaged configuration to avoid possible predation. It is possible that mimarachnids have evolved with a range of anti-predation defenses in Burmese amber forests, such as disruptive coloration, wing spots, and "flatoidinisation syndrome" (a specialized and complex camouflage, uniting shape, colour, and behaviour) (Jiang et al. 2019) to help them to avoid being attacked by predators.

Acknowledgements

We sincerely thank the editors and anonymous reviewers for their constructive criticism and valuable comments on this manuscript. This study was funded by Guangdong Basic and Applied Basic Research Foundation [2019A1515110610]; Beijing Municipal Natural Science Foundation and Beijing Municipal Education Commission [KZ201810028046]; the National Natural Science Foundation of China [no. 31970436]; Capacity Building for Sci-Tech Innovation-Fundamental Scientific Research Funds [no. 20530290051].

References

Bourgoin T (2021) FLOW (Fulgoromorpha Lists on The Web): a world knowledge base dedicated to Fulgoromorpha. Version 8, updated 2021-4-20. (http://hemiptera-databases.org/flow/)

Bourgoin T, Szwedo J (2008) The 'cixiid-like' fossil planthopper families. Bulletin of Insectology 61: 107–108.

Bourgoin T, Wang R, Asche M, Hoch H, Soulier-Perkins A, Stroinski A, Yap S, Szwedo J (2015) From micropterism to hyperpterism: recognition strategy and standardized homology-

driven terminology of the forewing venation patterns in planthoppers (Hemiptera: Fulgoromorpha). Zoomorphology 134: 63–77. https://doi.org/10.1007/s00435-014-0243-6

Brysz AM, Szwedo J (2019) Jeweled Achilidae - a new look at their systematics and relation to other Fulgoroidea (Hemiptera). Monographs of the Upper Silesian Museum 10: 93–130.

Evans JW (1946) External morphology and systematic position (Part 1). In: Evans JW (Ed) A natural classification of the leaf-hoppers (Jassoidea, Homoptera). Transactions of the Royal Entomological Society, London 96(3): 47–60.

Fu Y, Huang D (2020) New data on fossil mimarachnids (Hemiptera, Fulgoromorpha, Fulgoroidea) in mid-Cretaceous Burmese amber. Palaeoentomology 003(3): 317–331. https://doi.org/10.11646/palaeoentomology.3.3.12

Fu Y, Huang D (2021) New mimarachnids in mid-Cretaceous amber from northern Myanmar (Hemiptera, Fulgoromorpha). Cretaceous Research 119: 104682. https://doi.org/10.1016/j.cretres.2020.104682

Fujiyama I (1978) Some fossil insects from the Tedori Group (Upper Jurassic-Lower Cretaceous), Japan. Bulletin of the National Science Museum, Series C (Geology) 4: 181–191.

Jiang T, Szwedo J, Wang B (2018) A giant fossil Mimarachnidae planthopper from the mid-Cretaceous Burmese amber (Hemiptera, Fulgoromorpha). Cretaceous Research 89: 183–190. https://doi.org/10.1016/j.cretres.2018.03.020

Jiang T, Szwedo J, Wang B (2019) A unique camouflaged mimarachnid planthopper from mid-Cretaceous Burmese amber. Scientific Reports 9: 13112. https://doi.org/10.1038/s41598-019-49414-4

Jiang T, Szwedo J, Song Z, Chen J, Li Y, Jiang H (2020) *Ayaimatum trilobatum* gen. et sp. nov. of Mimarachnidae (Hemiptera: Fulgoromorpha) from mid-Cretaceous amber of Kachin (northern Myanmar). Acta Palaeontologica Sinica 59(1): 70–85.

Latreille PA (1807) Genera Crustaceorum et Insectorum secundum ordinem naturalem in familias disposita, iconibus exemplisque plurimis explicata. Armand Koenig, Paris & Argentorat 3: 1–258.

Li LF, Kopylov DS, Shih CK, Ren D (2017) The first record of Ichneumonidae (Insecta: Hymenoptera) from the Upper Cretaceous of Myanmar. Cretaceous Research 70: 152–162. https://doi.org/10.1016/j.cretres.2016.11.001

Linnaeus C (1758) Systema Naturae per regna tria naturae, secundum classes, ordines, genera, species, cum characteribus, differentiis, synonymis, locis. Tomus I. Editio Decima, Reformata. Cum Privilegio S:ae R:ae M:tis Sveciae. Impensis Direct. Laurentii Salvii, Holmiae, 823 pp.

Ross AJ (2021) Supplement to the Burmese (Myanmar) amber checklist and bibliography, 2020. Palaeoentomology 4(1): 57–76.

Shcherbakov DE (2007) Mesozoic spider mimics - Cretaceous Mimarachnidae fam. n. (Homoptera: Fulgoroidea). Russian Entomological Journal 16(3): 259–264.

Shcherbakov DE (2017) First record of the Cretaceous family Mimarachnidae (Homoptera: Fulgoroidea) in amber. Russian Entomological Journal 26(4): 389–392. https://doi.org/10.15298/rusentj.26.4.12

Shi G, Grimaldi DA, Harlow GE, Wang J, Yang M, Lei W, Li Q, Li X (2012) Age constraint on Burmese amber based on U-Pb dating of zircons. Cretaceous Research 37: 155–163. https://doi.org/10.1016/j.cretres.2012.03.014

Stevens M, Merilaita S (2009a) Animal camouflage: current issues and new perspectives. Philosophical Transactions of the Royal Society B: Biological Sciences 364: 423–427.

Stevens M, Merilaita S (2009b) Defining disruptive coloration and distinguishing its functions. Philosophical Transactions of the Royal Society B: Biological Sciences 364: 481–488.

Szwedo J (2008) Distributional and palaeoecological pattern of the Lower Cretaceous Mimarachnidae (Hemiptera: Fulgoromorpha). Entomologia Generalis 31(3): 231–242. https://doi.org/10.1127/entom.gen/31/2008/231

Szwedo J, Ansorge J (2015) The first Mimarachnidae (Hemiptera: Fulgoromorpha) from Lower Cretaceous lithographic limestones of the Sierra del Montsec in Spain. Cretaceous Research 52: 390–401. https://doi.org/10.1016/j.cretres.2014.03.001

Théry M, Gomez D (2010) Insect colours and visual appearance in the eyes of their predators. In: Casas J, Simpson SJ (Eds) Advances in Insect Physiology 38: 267–353. https://doi.org/10.1016/S0065-2806(10)38001-5

Zhang X, Ren D, Yao Y (2018) A new genus and species of Mimarachnidae (Hemiptera: Fulgoromorpha: Fulgoroidea) from mid-Cretaceous Burmese amber. Cretaceous Research 90: 168–173. https://doi.org/10.1016/j.cretres.2018.04.012

ZooKeys 1057: 49–103 (2021)
doi: 10.3897/zookeys.1057.68375
https://zookeys.pensoft.net

RESEARCH ARTICLE

A peer-reviewed open-access journal
ZooKeys
Launched to accelerate biodiversity research

Novel lures and COI sequences reveal cryptic new species of *Bactrocera* fruit flies in the Solomon Islands (Diptera, Tephritidae, Dacini)

Luc Leblanc[1], Francis Tsatsia[2], Camiel Doorenweerd[3]

1 *University of Idaho, Department of Entomology, Plant Pathology and Nematology, 875 Perimeter Drive, MS2329, Moscow, Idaho, 83844-2329, USA* **2** *Biosecurity Solomon Islands. Ministry of Agriculture and Livestock. P.O. Box G13, Honiara, Solomon Islands* **3** *University of Hawaii, Department of Plant and Environmental Protection Sciences, 3050 Maile Way, Honolulu, Hawaii, 96822-2231, USA*

Corresponding author: Luc Leblanc (leblancl@uidaho.edu)

Academic editor: Teresa Vera | Received 7 May 2021 | Accepted 11 August 2021 | Published 27 August 2021

http://zoobank.org/F3DC6F1E-2761-4534-836B-0058E835FEC0

Citation: Leblanc L, Tsatsia F, Doorenweerd C (2021) Novel lures and COI sequences reveal cryptic new species of Bactrocera fruit flies in the Solomon Islands (Diptera, Tephritidae, Dacini). ZooKeys 1057: 49–103. https://doi.org/10.3897/zookeys.1057.68375

Abstract

Results from a snap-shot survey of Dacine fruit flies carried out on three of the Solomon Islands in April 2018 are reported. Using traps baited with the male lures cue-lure, methyl eugenol, and zingerone, 30 of the 48 species previously known to occur in the Solomon Islands were collected. Six species are newly described here: *Bactrocera allodistincta* **sp. nov.**, *B. geminosimulata* **sp. nov.**, *B. kolombangarae* **sp. nov.**, *B. quasienochra* **sp. nov.**, *B. tsatsiai* **sp. nov.**, and *B. vargasi* **sp. nov.**, all authored by Leblanc & Doorenweerd. An illustrated key to the 54 species now known to be present in the country is provided.

Keywords

Dacus, Oceania, pest species, taxonomy, *Zeugodacus*

Introduction

Dacine fruit flies (Diptera: Tephritidae: Dacini), a species-rich Old World tropical group, is composed of 947 currently known species, including 83 crop pests (White and Elson-Harris 1992; Vargas et al. 2015; Doorenweerd et al. 2018). Diversity is particularly high in Australasia, with 332 species described and an imminent publication

of 65 new species from Papua New Guinea (R.A.I. Drew, pers. comm.). Many more new species are being discovered, especially cryptic species, with ever improving molecular diagnostic tools and the emergence of new generation male lures (De Meyer et al. 2015; Manrakhan et al. 2017; Royer et al. 2018, 2019; Doorenweerd et al. 2020).

The earliest Dacine fruit fly record in the Solomon Islands was the description of *Bactrocera longicornis* Macquart, in 1835. By 1939, eleven species were known (Malloch 1939), growing to 26 five decades later (Drew 1989). Extensive survey efforts through trapping and host fruit surveys during the Regional Fruit Fly Projects in the Pacific (Allwood and Drew 1997; Allwood 2000; Lidner and McLeod 2008) nearly doubled the number of species to 48 (Drew and Romig 2001). Two decades later, we carried out a snap-shot survey on three islands (Guadalcanal, Kolombangara, Gizo), with the inclusion of zingerone lure, to collect fresh material and develop molecular diagnostic tools to help further characterize the species found in the Solomon Islands. In just a couple of weeks, we discovered six new species, including cryptic species that would not have been detectable without molecular characterization. We herein describe these new species and provide a key to the 54 species now present in the Solomon Islands.

Materials and methods

Collecting and curation

We maintained 79 sets of three traps separately baited with male lures (cue-lure, methyl eugenol and zingerone) in the Solomon Islands in April 2018. We used commercially available cue-lure and methyl eugenol plugs (Scentry Biologicals, Billings, Montana). Zingerone (= vanillylacetone) lure was prepared by dipping dental cotton wicks in zingerone powder (Sigma-Aldrich) melted over a hot plate and allowed to solidify in the wicks. Small vertical bucket traps (Leblanc et al. 2015: fig. 1) were made of 5-oz urine sample cups (Stockwell Scientific, Scottsdale, Arizona) with two 20 mm wide lateral circular openings on opposite sides, 12 mm below the top, with a hole drilled in the lid center, through which a 30-cm-long, 15-gauge, aluminum tie wire was inserted, and bent into a hook below the lid. The male lure unit and a 10 × 10 mm piece of dichlorvos (DVVP) strip (Vaportape II; Hercon Environmental, Emingsville, PA) were attached to the hook below the lid. A 10-cm-wide black square plastic food plate (Waddington North America) was placed on top of the trap to prevent flooding by frequent rain. A solution of 25% propylene glycol (Better World Manufacturing, Fresno, CA) was used in the trap to preserve captured flies, until they were transferred to 95% ethanol during trap servicing. The 79 sets of traps in agricultural areas and endemic forest on the islands of Guadalcanal and Kolombangara, and agricultural areas on Gizo Island (Fig. 1) were maintained for 12, four, and six days, respectively. Forest trapping sites were ca. 50 meters apart along transects that followed trails. Sampled flies were stored in 95% ethanol in a -20 °C freezer to preserve DNA. All flies were identified to species using available keys (Drew 1989; Drew and Romig 2001). We pulled one or two legs from specimens

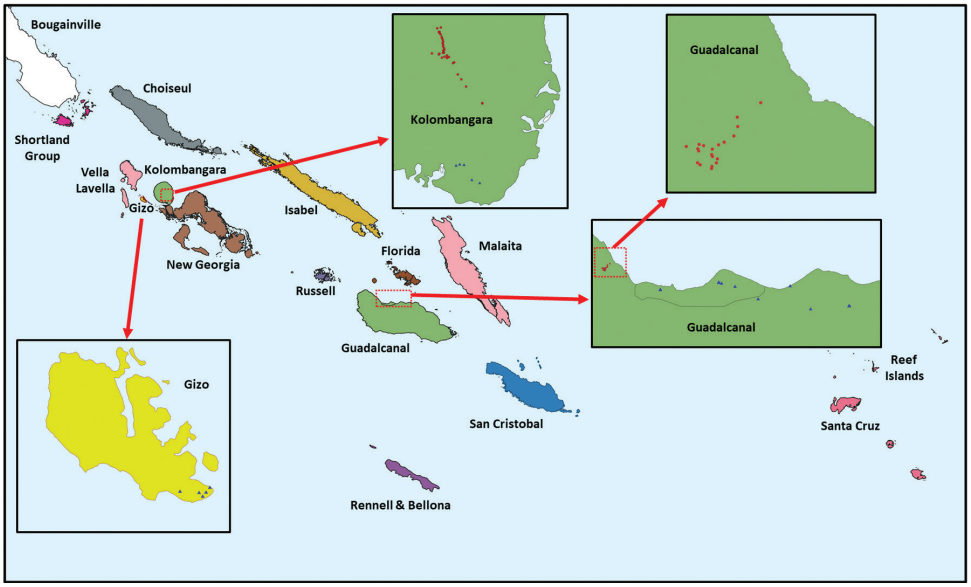

Figure 1. Map of the Solomon Islands, with groups of islands for distribution records, and trapping locations on Guadalcanal, Gizo and Kolombangara islands in the 2018 survey. Red circles are sites located in forest and blue triangles are sites in agricultural environments.

that were selected for DNA extraction (for further details on DNA extraction methods see Doorenweerd et al. 2020). All holotypes and all, or a subset of, the paratypes were double-mounted to be stored as dry specimens in collections for permanent future reference. Before drying flies for double-mounting (White and Elson-Harris 1992), we pinned them through the scutum with a minuten pin and soaked them in diethyl-ether for 3–12 hours to fix and preserve their natural coloration. We photographed specimens using a Nikon D7100 camera attached to an Olympus SZX10 microscope and used Helicon Focus pro v6.7.1 to merge pictures taken at a range of focal planes. To measure specimens (all available or up to 10 specimens measured per species), we used an ocular grid mounted on an Olympus SZ30 dissecting microscope.

Morphological terms and taxonomic assignment

Morphological terminology used in the descriptions follows White et al. (1999) and assignment of species to genera follows Doorenweerd et al. (2018). We treat *Zeugodacus* as a distinct genus from *Bactrocera* and *Dacus* (Krosch et al. 2012; Virgilio et al. 2015; Dupuis et al. 2017; San Jose et al. 2018). Subgenus assignment for each species follows reclassifications recently published by Hancock and Drew (Hancock 2015; Drew and Hancock 2016; Hancock and Drew 2015, 2018a, b). The host plant records included in the key follow the compilation published by Leblanc et al. (2012). For accurate taxonomic application of host plant records from the literature we used the World Flora Online (WFO 2021).

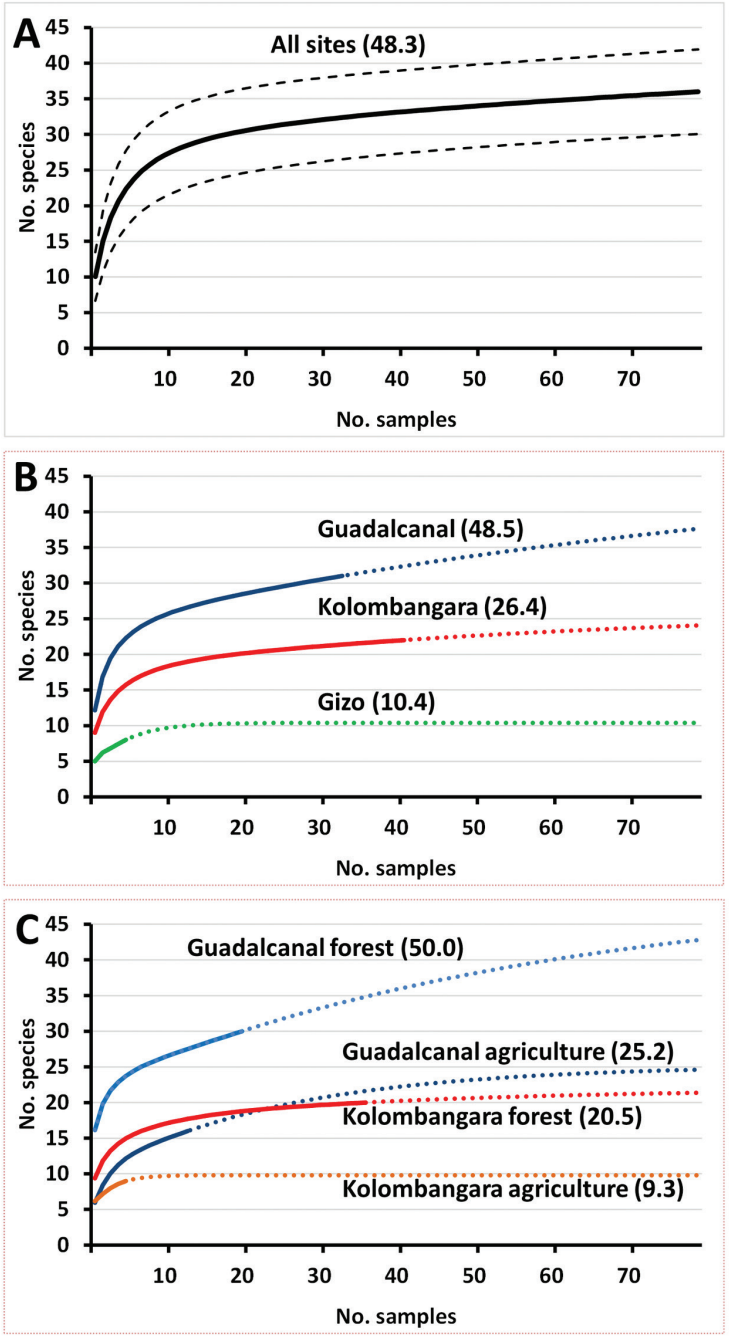

Figure 2. Species accumulation curves based on the 2018 survey of Solomon Islands **A** for all sampled sites with 95% confidence interval range **B** for the three individually sampled islands, and **C** comparing forest and agricultural sites separately on Guadalcanal and Kolombangara. Estimated species numbers for each curve (in brackets) based on the Chao 2 estimator.

COI sequence analysis

Representatives of all species newly described here were also included in the cytochrome c oxidase I (COI) study of Doorenweerd et al. (2020), under tentative species names. For that study, 1493 base pairs of the COI gene were sequenced and comparatively analyzed in a dataset that included 163 species of *Bactrocera*. We include here the maximum likelihood gene tree from that study and the summary *Bactrocera* species statistics as supplementary material (Suppl. material 1: Fig. S1, Suppl. material 2: Table S1). For the methods for DNA extraction, sequencing and analyses we refer to Doorenweerd et al. (2020). Collecting information as well as COI sequences are available on BOLD (Ratnasingham and Hebert 2007) dataset (DOI: http://dx.doi.org/10.5883/DS-DACCOI), as well as NCBI GenBank (accessions MZ196488–MZ196507). Each specimen for which DNA was extracted was assigned a unique code in the format "UHIM.ms00000", physically labelled as such, and this number forms the 'Sample ID' in BOLD.

Estimating biodiversity

We used EstimateS software (Colwell 2019) to generate species accumulation curves and estimate species diversity, using the incidence-based Chao 2 algorithm. We generated accumulation curves, with 100 randomizations without replacement for confidence intervals for all sites collectively, separately for each island, and comparing agricultural and forest sites in Guadalcanal and Kolombangara.

Abbreviations

BPBM Bernice Pauahi Bishop Museum, Honolulu, Hawaii, United States;
BSI Biosecurity Solomon Islands, Honiara, Solomon Islands;
WFBM William F. Barr Entomological Museum, Moscow, Idaho, United States;
UHIM University of Hawaii Insect Museum, Honolulu, Hawaii, United States;
USNM National Museum of Natural History, Smithsonian Institution, Washington DC, United States.

Results and taxonomy

***Bactrocera* (*Bactrocera*) *allodistincta* Leblanc & Doorenweerd, sp. nov.**
http://zoobank.org/6D929FD2-D802-42D1-B15D-B14C78CF4442
Fig. 3A–E

Type material. ***Holotype.*** Solomon Islands • ♂; Guadalcanal, forest; -9.4067, 159.8647; 167 m; 4–16 Apr. 2018; L. Leblanc, F. Tsatsia leg.; cue-lure baited trap FFSo015. Deposited in UHIM. ***Paratypes.*** 11 males. Solomon Islands • 1 ♂; Guadalcanal forest; -9.4041, 159.8628; 153 m; 4–16 Apr. 2018; L. Leblanc, F. Tsatsia leg.;

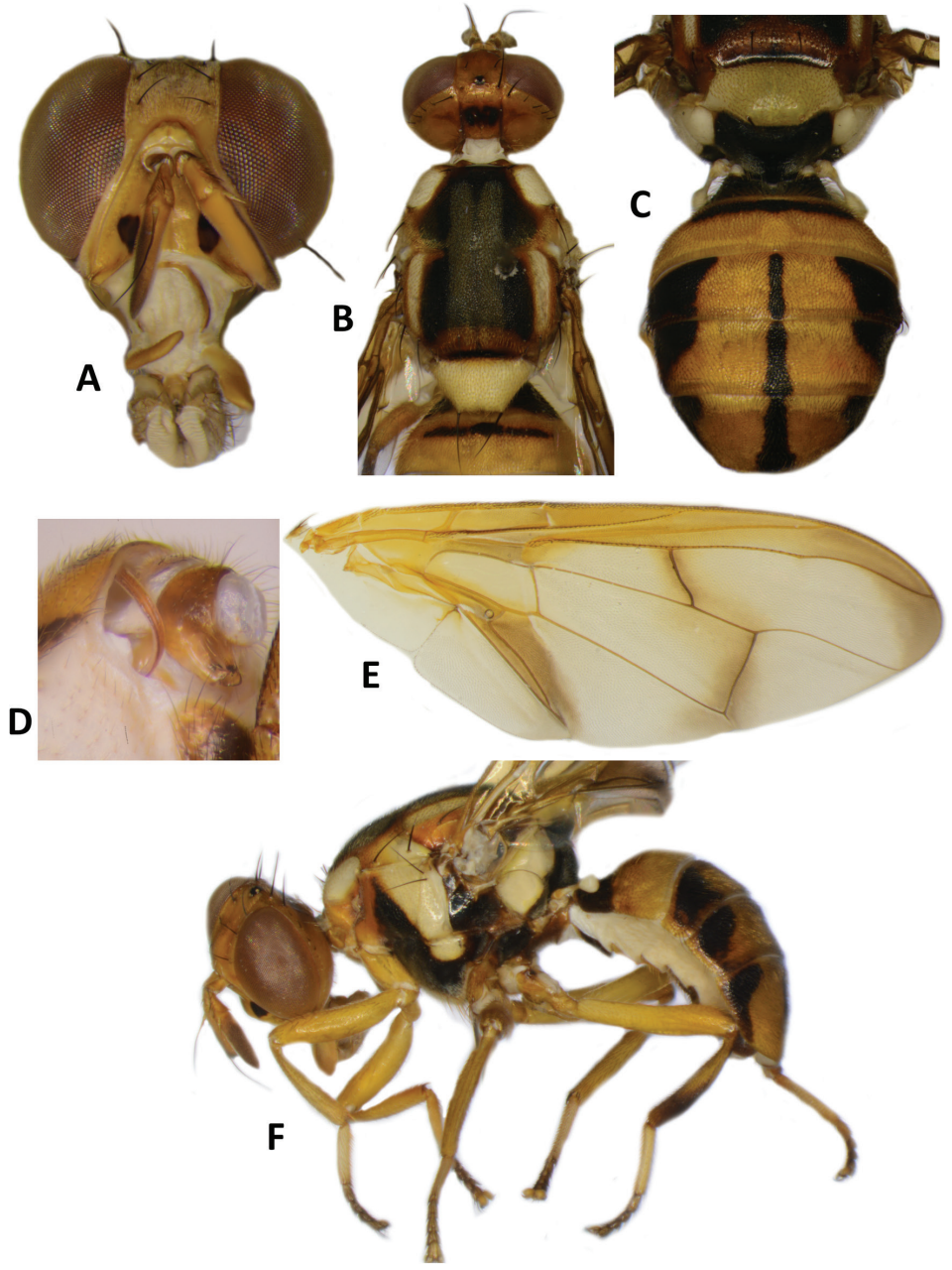

Figure 3. *Bactrocera allodistincta* sp. nov. **A** head **B** head and scutum **C** abdomen **D** male genitalia **E** wing **F** lateral view.

cue-lure baited trap FFSo011 • 1 ♂; same locality and date as for preceding; -9.4067, 159.8647; 167 m; trap FFSo015 • 1 ♂; same locality and date as for preceding; -9.4072, 159.8664; 153 m; trap FFSo016 • 2 ♂; same locality and date as for preced-

ing; -9.4064, 159.8671; 145 m; trap FFSo018; molecular voucher UHIM.ms08766 • 2 ♂; same locality and date as for preceding; -9.4059, 159.8672; 133 m; trap FFSo019 • 1 ♂; same locality and date as for preceding; -9.4055, 159.8665; 145 m; trap FFSo020 • 1 ♂; same locality and date as for preceding; -9.4040, 159.8652; 125 m; trap FFSo023 • 1 ♂; same locality and date as for preceding; -9.4026, 159.8695; 57 m; trap FFSo027 • 1 ♂; same locality and date as for preceding; -9.4000, 159.8700; 57 m; trap FFSo029. Seven of the paratypes are deposited at UHIM, three at WFBM, and one at USNM.

Differential diagnosis. *Bactrocera allodistincta* differs from *B. pseudodistincta* (Drew) (Fig. 4) in the presence of orange-brown lateral and posterior markings on the predominantly black scutum, abdominal tergites III–V with a narrower medial black stripe, the lateral black markings on tergite IV narrowed posteriorly, and the rather diffuse fuscous crossband on the wing. It differs from *B. distincta* (Malloch) in that the costal band is diffuse orange-brown and the crossband is sinuous, with a bend along vein M (Fig. 3E), whereas the entire costal band, including in the basicostal and costal cells, is dark fuscous and the crossband is broad and straight in *B. distincta* (Fig. 5E).

Molecular diagnosis. We obtained a single COI sequence (UHIM.ms08766) which matches closest to *Bactrocera pedestris* (Bezzi) [misidentified as *B. gombokensis* Drew & Hancock, 1994 in Doorenweerd et al. 2020], at 10.25% pairwise distance. *Bactrocera pseudodistincta* (Drew) [N = 2] is also represented in the dataset and does not appear as a close match, but *B. distincta* is not represented.

Description of adult. Male. ***Head*** (Fig. 3A). Height 1.56 ± 0.12 (SD) (1.37–1.67) mm. Frons of even width, 0.80 ± 0.03 (0.73–0.83) mm long and 1.40 ± 1.05 (1.33–1.50) times as long as broad; fulvous, sometimes fuscous around orbital seta and anteromedial hump; latter covered by short red-brown microtrichia; three pairs of dark fuscous frontal setae present; lunule fulvous. Ocellar triangle black. Vertex fulvous with two pairs of dark fuscous vertical setae. Face fulvous with a pair of moderately sized oval black spots in antennal furrows; length 0.49 ± 0.05 (0.43–0.60) mm. Gena fulvous, with a fuscous subocular spot and a dark fuscous seta. Occiput fulvous with a dark fuscous to black dorsomedial marking; a row of 4–6 dark fuscous postocular setae present behind eye. Antenna with scape and pedicel fulvous and first flagellomere fulvous with pale fuscous on lateral surface of flagellum; a strong red-brown dorsal seta on pedicel; arista fulvous basally and black distally; length of segments: 0.22 ± 0.04 (0.17–0.27) mm; 0.27 ± 0.03 (0.23–0.33) mm; 0.71 ± 0.04 (0.67–0.73) mm.

Thorax (Fig. 3B). Scutum black except orange-brown ventral to and narrowly medial to lateral postsutural vitta, around notopleural suture, along lateral margin between postpronotal lobe and notopleuron, medial to postpronotal lobe, and along posterior margin of scutum. Scutum with two broad parallel medial stripes of dense silvery microtrichia along entire scutum length. Pleural areas black except orange-brown anterior margin of anepisternum and proeipsternum. Yellow markings: postpronotal lobe; notopleuron; moderately broad paired parallel-sided lateral postsutural vitta reaching intra-alar seta posteriorly; broad anepisternal stripe with anterior margin straight, reaching to anterior notopleural seta dorsally; a large transverse spot on katepisternum

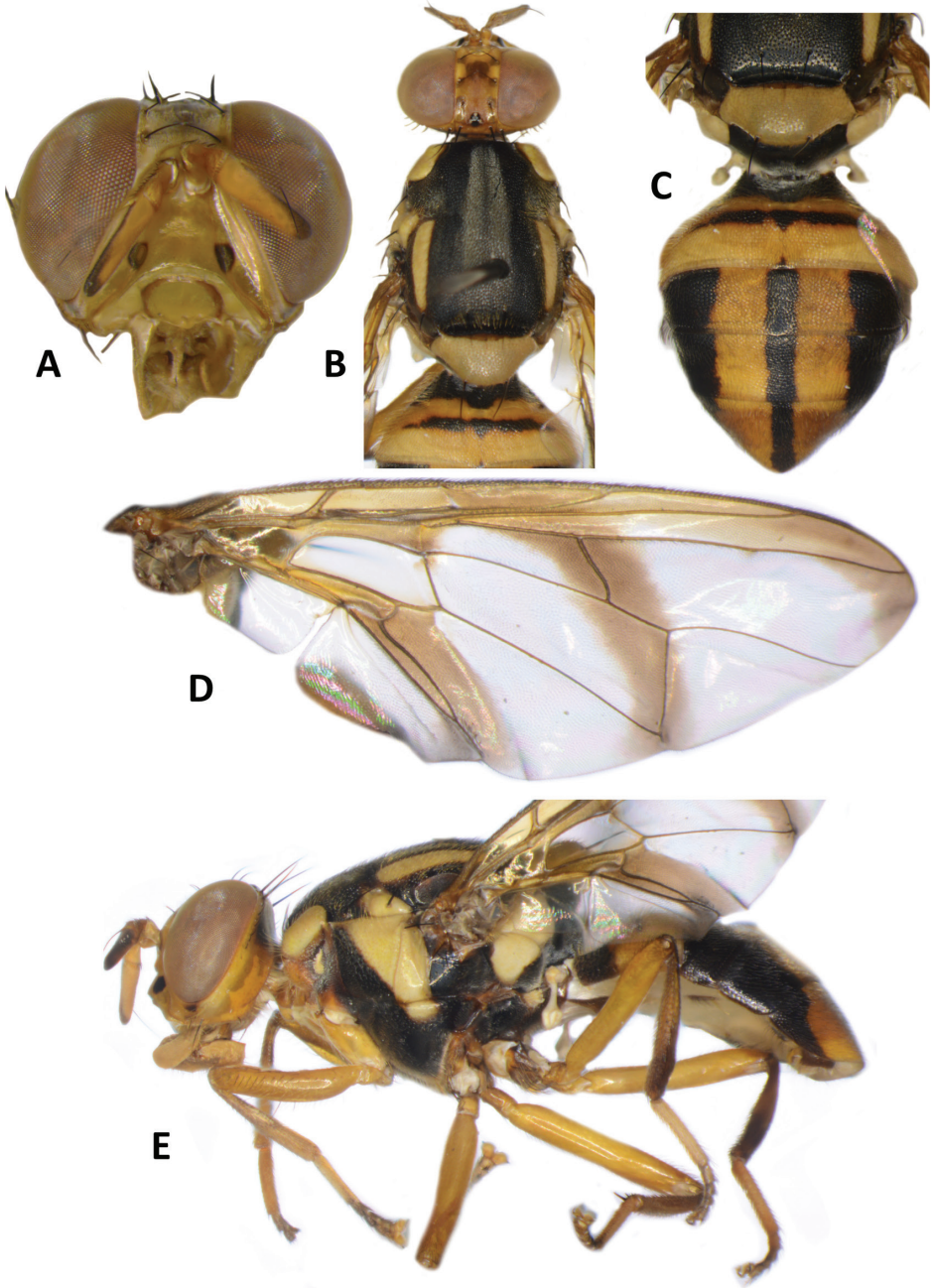

Figure 4. *Bactrocera pseudodistincta* (Drew) **A** head **B** head and scutum **C** abdomen **D** wing **E** lateral view.

below the anepisternal stripe; anterior ⅘ of anatergite and ¾ of katatergite (posteriorly black). Mediotergite black. Scutellum yellow except for very narrow black basal band. Setae: 1 pair scutellar; 1 pair prescutellar acrostichal; 1 pair intra-alar; 1 pair postalar;

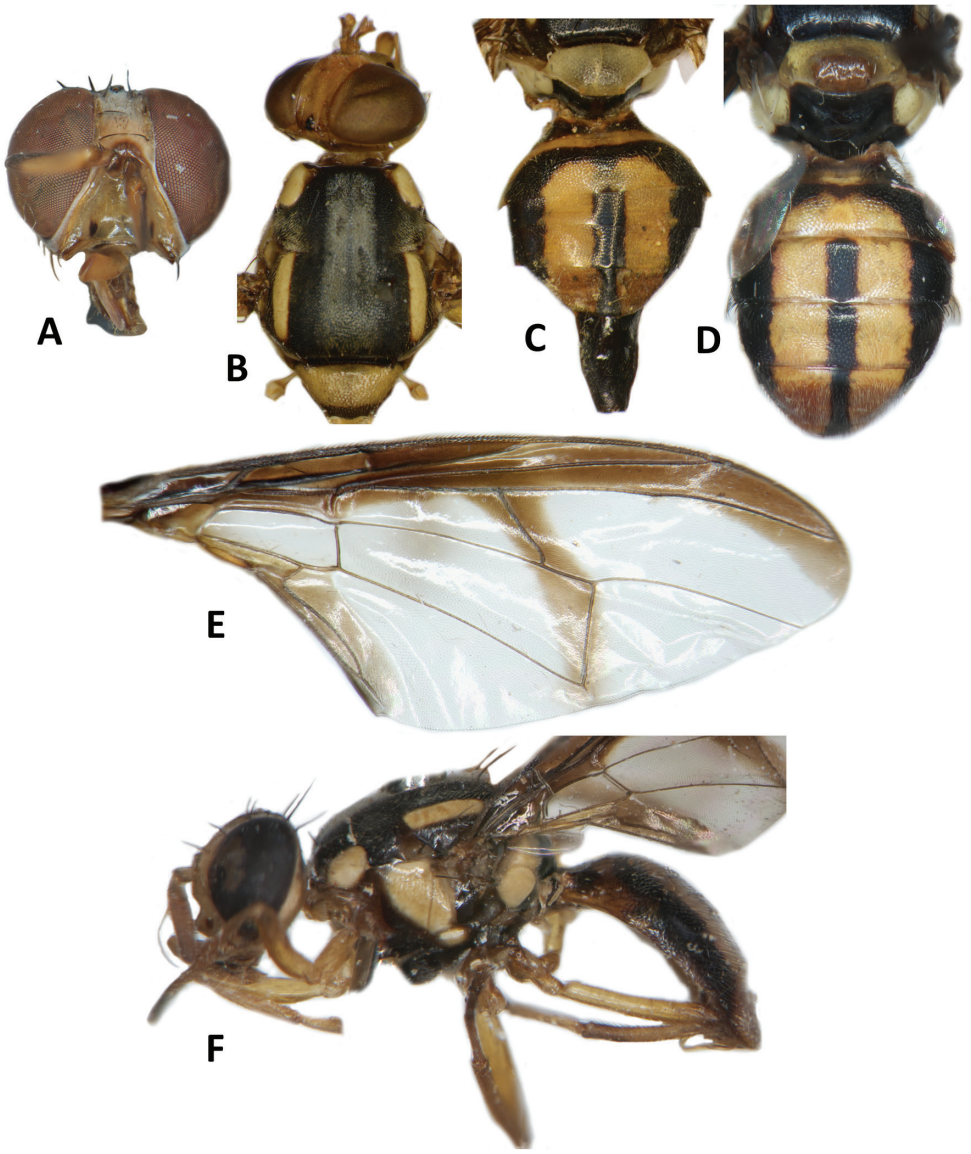

Figure 5. *Bactrocera distincta* (Malloch) **A** head **B** head and scutum **C** female abdomen **D** male abdomen **E** wing **F** lateral view.

1 pair postsutural supra-alar; 1 pair anepisternal; 2 pairs notopleural; 2 pairs scapular; all setae well developed and dark fuscous.

Legs (Fig. 3F). All legs entirely fulvous with apical ⅖ of hind tibia fuscous. Fore femur with a row of long pale dorsal setae. Mid-tibia with apical black spur.

Wing (Fig. 3E). Length 5.6 ± 0.2 (5.3–5.9) mm; basal costal and costal cells fuscous with microtrichia in posterodistal corner of costal cell; broad fuscous costal

band confluent with R_{4+5}, remaining broad at apex and ending at apex of medial vein; a diffuse orange-brown crossband along crossvein r-m, continuing along M and dm-cu to reach posterior wing margin, and a broad fuscous anal streak over cell bcu and basal margin of cu_1; remainder of wing light fuscous; dense aggregation of microtrichia around A_1 + CuA_2; supernumerary lobe weakly developed.

Abdomen (Fig. 3C, D). Oval with tergites not fused; pecten present on tergite III; posterior lobe of surstylus short; abdominal sternite V with a deep concavity on posterior margin. Base of syntergite I+II wider than long. Syntergite I+II orange-brown with base black and a narrow sub-basal transverse medial black band. Tergites III–V orange-brown with moderately broad medial black stripe reaching apex, and large lateral black markings on tergite III and anterolateral corners of tergites IV and V. Ceromata on tergite V indistinct from abdomen orange-brown color. Sternite I dark fuscous, sternite II fulvous, and sternites III–V fulvous tending fuscous medially.

Female. Unknown

Male attractant. Cue-lure.

Etymology. The specific name is a noun in apposition, derived from the Greek *allos* (another) and the species resembles *B. distincta* (Malloch). Previously, *B. pseudodistincta* (Drew) had been described as a species with similar appearance to *B. distincta*. All three are present in Oceania.

Notes. *Bactrocera allodistincta* was included as *B.* spnSol01 in Doorenweerd et al. (2020).

Bactrocera (*Bactrocera*) *geminosimulata* Leblanc & Doorenweerd, sp. nov.

http://zoobank.org/49835D53-30EE-47F9-9F64-DE320C2E046A
Fig. 6A–E, 9E–G

Type material. ***Holotype.*** Solomon Islands • ♂; Guadalcanal, forest; -9.4045, 159.8665; 120 m; 4–16 Apr. 2018; L. Leblanc, F. Tsatsia leg.; cue-lure baited trap FFSo022; molecular voucher UHIM.ms09156". Deposited in UHIM. ***Paratypes.*** 13 males. Solomon Islands • 4 ♂; Guadalcanal, forest; -9.4072, 159.8664; 153 m; 4–16 Apr. 2018; L. Leblanc, F. Tsatsia leg.; cue-lure baited trap FFSo016; molecular voucher UHIM.ms08673 • 2 ♂; same locality and date as for preceding; -9.4069, 159.8664; 153 m; trap FFSo017 • 2 ♂; same locality and date as for preceding; -9.4064, 159.8671; 145 m; trap FFSo018 • 1 ♂; same locality and date as for preceding; -9.4045, 159.8665; 139 m; trap FFSo022 • 2 ♂; same locality and date as for preceding; -9.4038, 159.8646; 103 m; trap FFSo024; molecular voucher UHIM.ms09155) • 2 ♂; same locality and date as for preceding; -9.4026, 159.8695; 57 m; trap FFSo027; molecular vouchers UHIM.ms09153, UHIM.ms09154. Nine of the paratypes are deposited at UHIM, three at WFBM, and one at USNM.

Differential diagnosis. *Bactrocera geminosimulata* is identical in all points to the sympatric *B. simulata* (Malloch), only distinguished by a subtle difference in wing infuscation in the presence of a light fuscous tinge as a broad, somewhat triangular

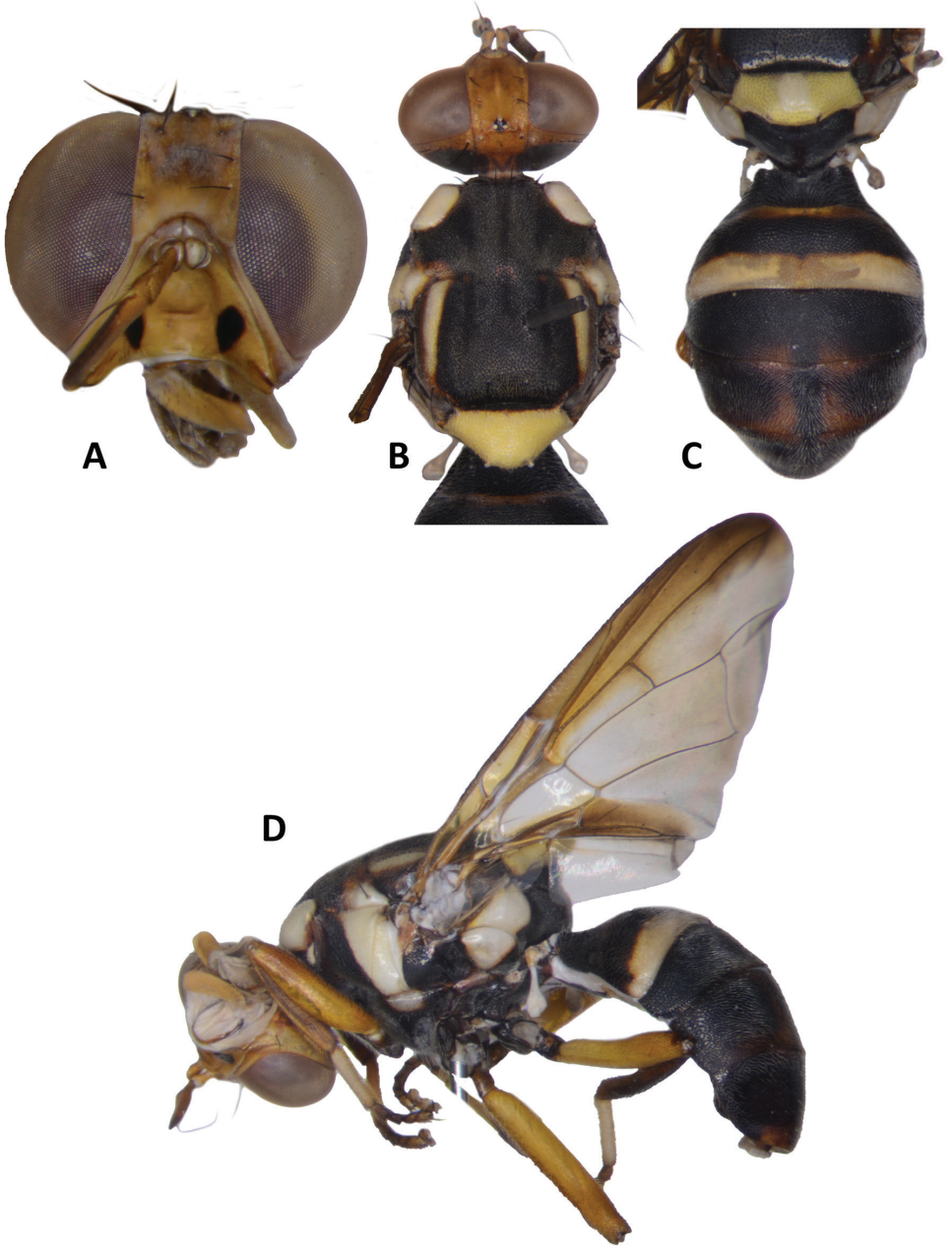

Figure 6. *Bactrocera geminosimulata* sp. nov. **A** head **B** head and scutum **C** abdomen **D** lateral view and wing.

area covering much of the middle of the wing, including the areas bordering r-m and dm-cu (Fig. 9E–G); the latter is absent in *B. simulata* (Fig. 9A–D). The new species can be distinguished from *B. bryoniae* (Tryon) by the lighter fuscous tinge of the costal band, a narrower anal streak and the largely to entirely black abdomen, whereas the

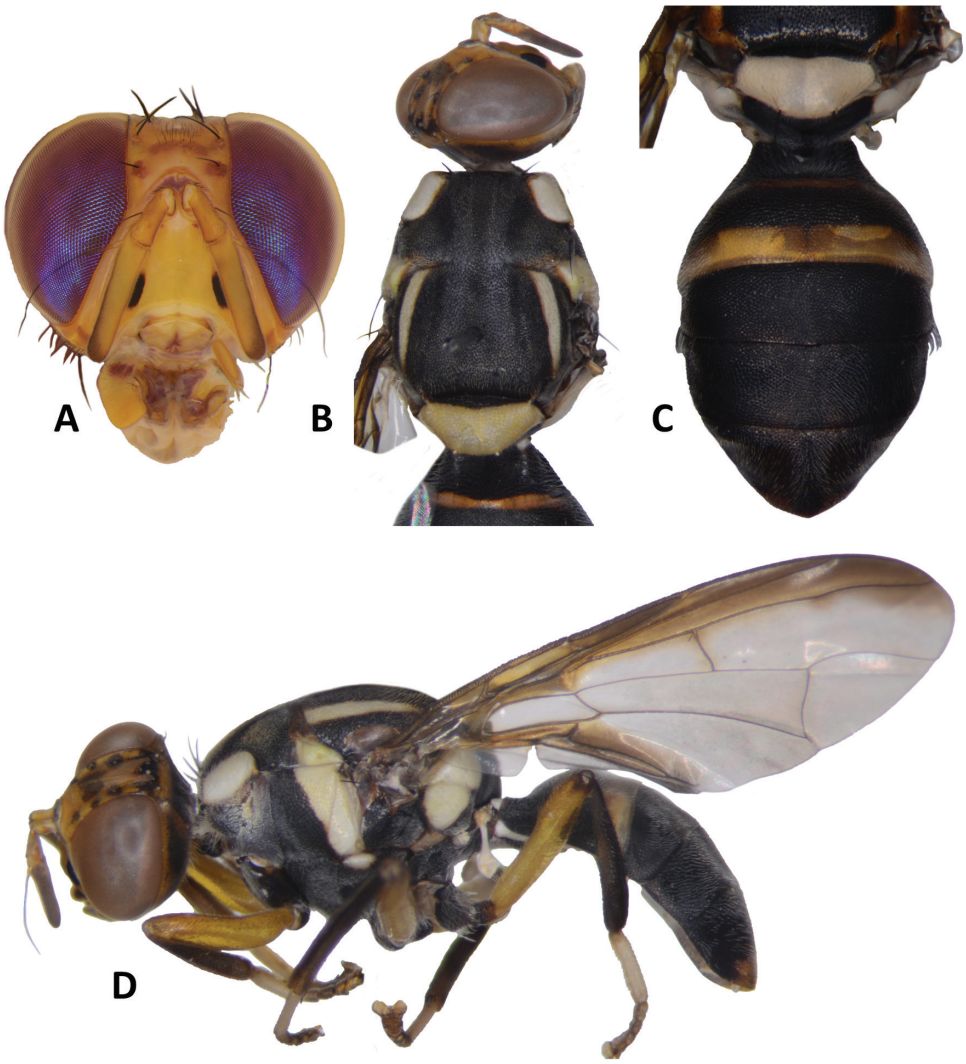

Figure 7. *Bactrocera simulata* (Malloch) **A** head **B** head and scutum **C** abdomen **D** lateral view and wing.

abdomen in *B. bryoniae* is orange-brown with a narrow black 'T'-shaped pattern (Fig. 8). *Bactrocera bryoniae* is widespread in Australia and New Guinea but is absent from the Solomon Islands.

Molecular diagnosis. The COI sequences of *B. geminosimulata* [N = 4] are similar to those of *B. bryoniae* [N = 5], but with a minimum of 1.47% pairwise distance. The reference COI dataset only includes *B. bryoniae* from Australia. The COI sequences suggest no close relationship with *B. simulata*, and can be used to reliably distinguish *B. geminosimulata* from *B. simulata*.

Description of adult. Male. ***Head*** (Fig. 6A). Height 2.02 ± 0.18 (SD) (1.77–2.17) mm. Frons, of even width, 0.98 ± 0.11 (0.83–1.07) mm long and 1.33 ± 0.08

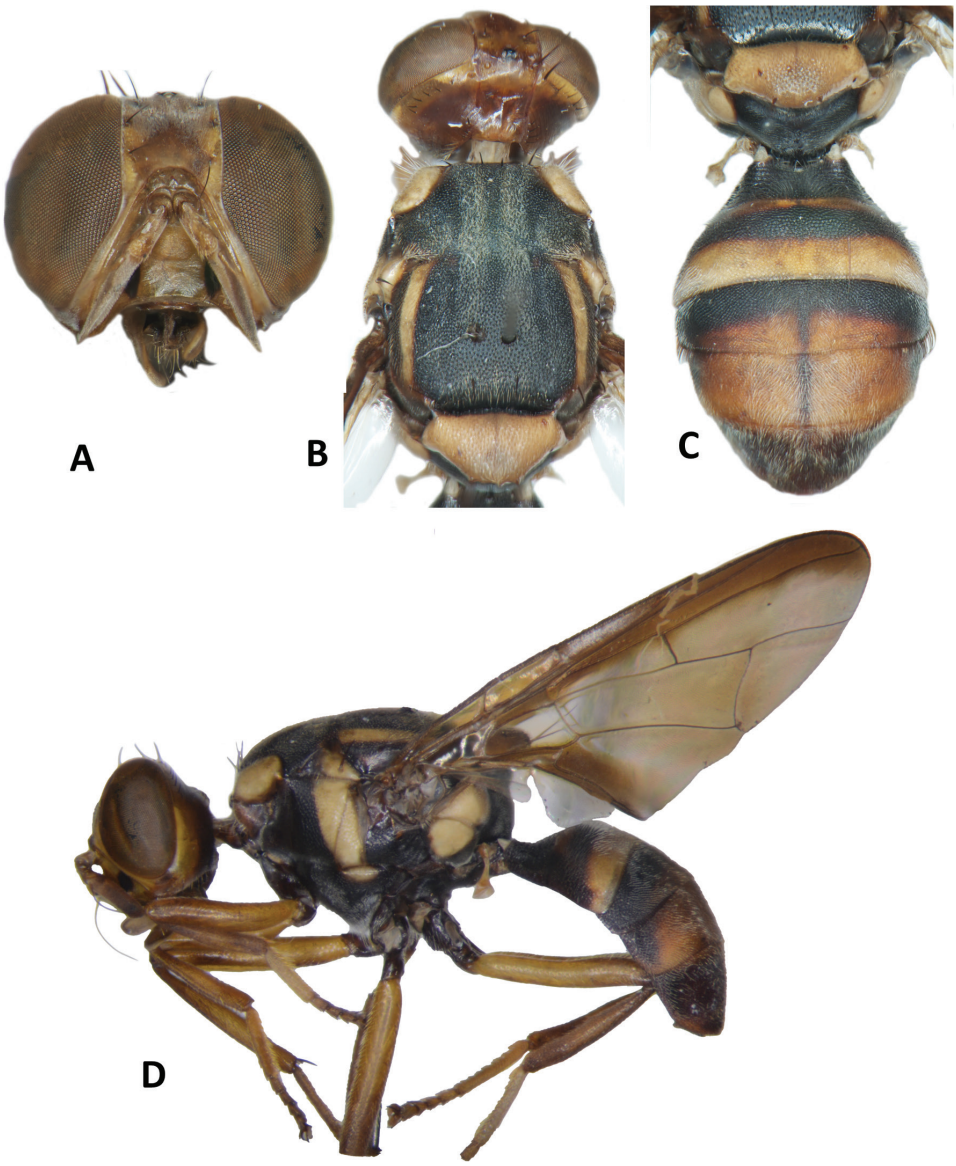

Figure 8. *Bactrocera bryoniae* (Tryon) **A** head **B** head and scutum **C** abdomen **D** lateral view and wing.

(1.24–1.43) times as long as broad; generally fulvous; anteromedial hump covered by short red-brown microtrichia; three pairs of black frontal setae present; lunule yellow. Ocellar triangle black. Vertex fulvous with two pairs of black vertical setae. Face fulvous with a pair of large circular black spots in antennal furrows; length 0.62 ± 0.07 (0.53–0.67) mm. Gena fulvous, with or without a faint dark fuscous subocular spot; red-brown seta present. Occiput dark fuscous and narrowly fulvous along eye margin; a row of 6–8 black postocular setae present behind eye. Antenna with scape and pedicel

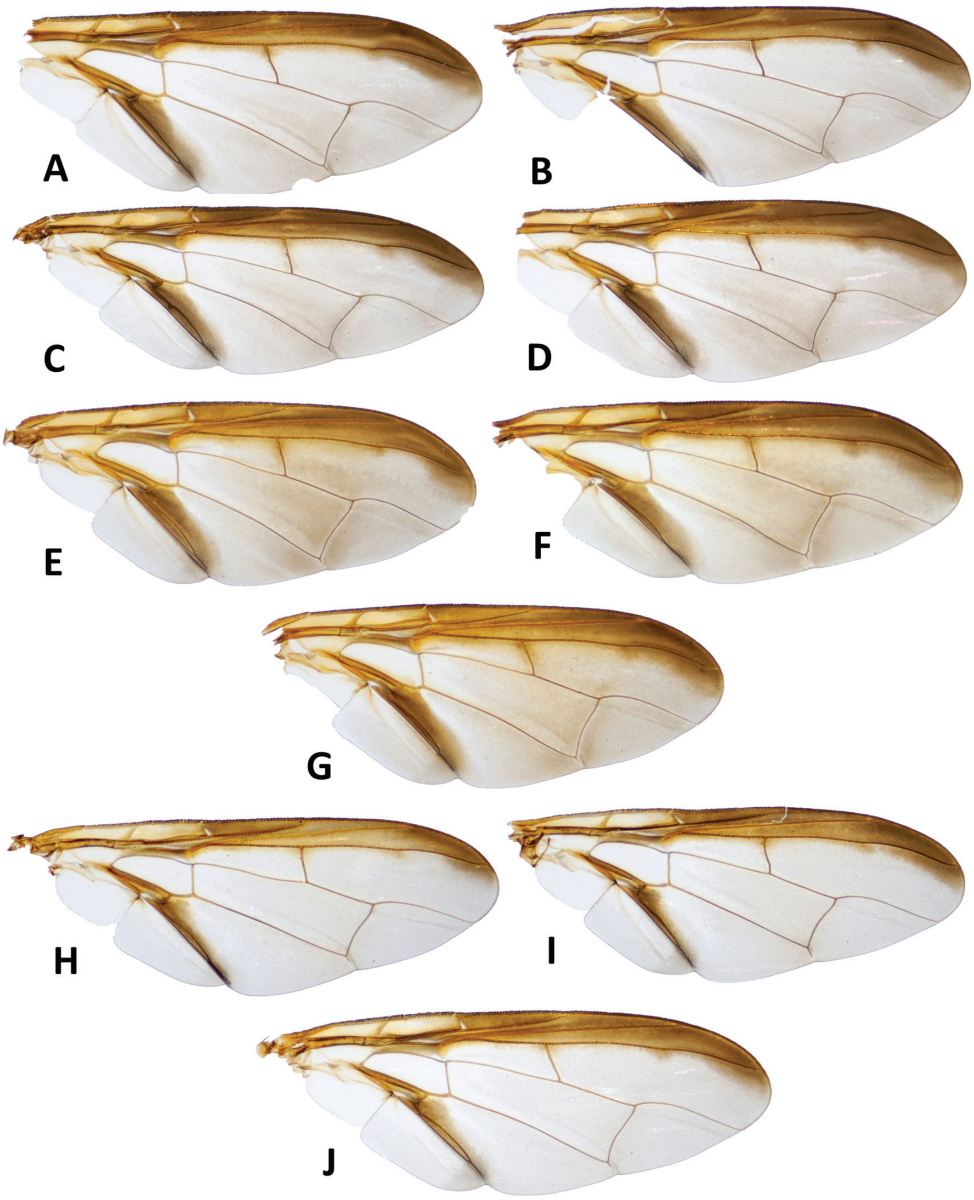

Figure 9. Wings of *Bactrocera simulata* (Malloch) **A** molecular voucher ms09146 **B** ms09147 **C** ms09148 **D** ms09151, *Bactrocera geminosimulata* sp. nov. **E** ms09153 **F** ms09154 **G** ms09155 *Bactrocera bryoniae* (Tryon) **H** ms01515 **I** ms01516 **J** ms07717.

fulvous and flagellum fulvous with light fuscous lateral surface; a strong red-brown dorsal seta on pedicel; arista fulvous basally and black distally; length of segments: 0.30 ± 0.03 (0.27–0.33) mm; 0.40 ± 0.05 (0.33–0.43) mm; 0.95 ± 0.07 (0.89–1.03) mm.

Thorax (Fig. 6B). Scutum black with small orange-brown markings anterior and posterior to lateral postsutural vitta. Pleural areas black. Yellow markings: postpronotal

lobe; notopleuron; moderately broad paired lateral postsutural vitta, tapering posteriorly and ending before intra-alar seta posteriorly; moderately broad anepisternal stripe with anterior margin straight, ending before anterior notopleural seta dorsally; a large transverse spot on katepisternum below the anepisternal stripe; anterior ¾ of anatergite and katatergite (posteriorly black). Mediotergite black. Scutellum yellow with narrow black basal band. Setae: 1 pair scutellar; 1 pair prescutellar acrostichal; 1 pair intra-alar; 1 pair postalar; 1 pair postsutural supra-alar; 1 pair anepisternal; 2 pairs notopleural; 2 pairs scapular; all setae well developed and black.

Legs (Fig. 6E). Coxae and trochanters black. Remainder of legs fulvous with hind tibia tending fuscous to dark fuscous. Fore femur with a row of long dark dorsal setae. Mid-tibia with an apical black spur.

Wing (Fig. 9E–G). Length 6.4 ± 0.4 (5.9–6.9) mm; basal costal and costal cells fulvous with microtrichia in posterodistal corner of costal cell; broad dark fuscous costal band confluent with R_{4+5}, ending between R_{4+5} and medial vein; light fuscous tinge as a broad, somewhat triangular area covering much of the middle of the wing, including the areas bordering r-m and dm-cu (absent in *B. simulata*); broad dark fuscous anal streak; dense aggregation of microtrichia around A_1 + CuA_2; supernumerary lobe moderately developed.

Abdomen (Fig. 6C, D). Oval with tergites not fused; pecten present on tergite III; posterior lobe of surstylus short; abdominal sternite V with a deep concavity on posterior margin. Base of syntergite I+II wider than long. Syntergite I+II black except for yellow along posterior half of and narrowly orange-brown along anterior margin of tergite II. Tergites III–V entirely black or with two broad longitudinal orange-brown areas running from center of tergite IV to posterior margin of tergite V, each side of a broad medial longitudinal dull black stripe. Ceromata on tergite V black. Abdominal sternites black.

Female. Unknown

Male attractant. Cue-lure.

Etymology. The specific name is a noun in apposition, derived from the Latin noun *geminus* (twins) and the epithet of the sympatric and morphologically nearly identical *B. simulata* (Malloch).

Notes. *Bactrocera geminosimulata* was included as *B.* spSol12 in Doorenweerd et al. (2020).

Bactrocera (*Parazeugodacus*) *kolombangarae* Leblanc & Doorenweerd, sp. nov.

http://zoobank.org/DEED6917-CAC4-4647-BB4F-4454B7F7AE3C
Fig. 10A–E

Type material. ***Holotype.*** Solomon Islands • ♂; Kolombangara, forest; -8.0252, 157.1159; 455 m; 9–13 Apr. 2018; L. Leblanc, F. Tsatsia leg.; zingerone baited trap FFSo059. Deposited in UHIM. ***Paratypes.*** 18 males. Solomon Islands • 1 ♂; Guadalcanal forest; -9.4048, 159.8645; 144 m; 4–16 Apr. 2018; L. Leblanc, F. Tsatsia leg.; zingerone baited trap FFSo013 • 1 ♂; Kolombangara, forest; -8.0680, 157.1434;

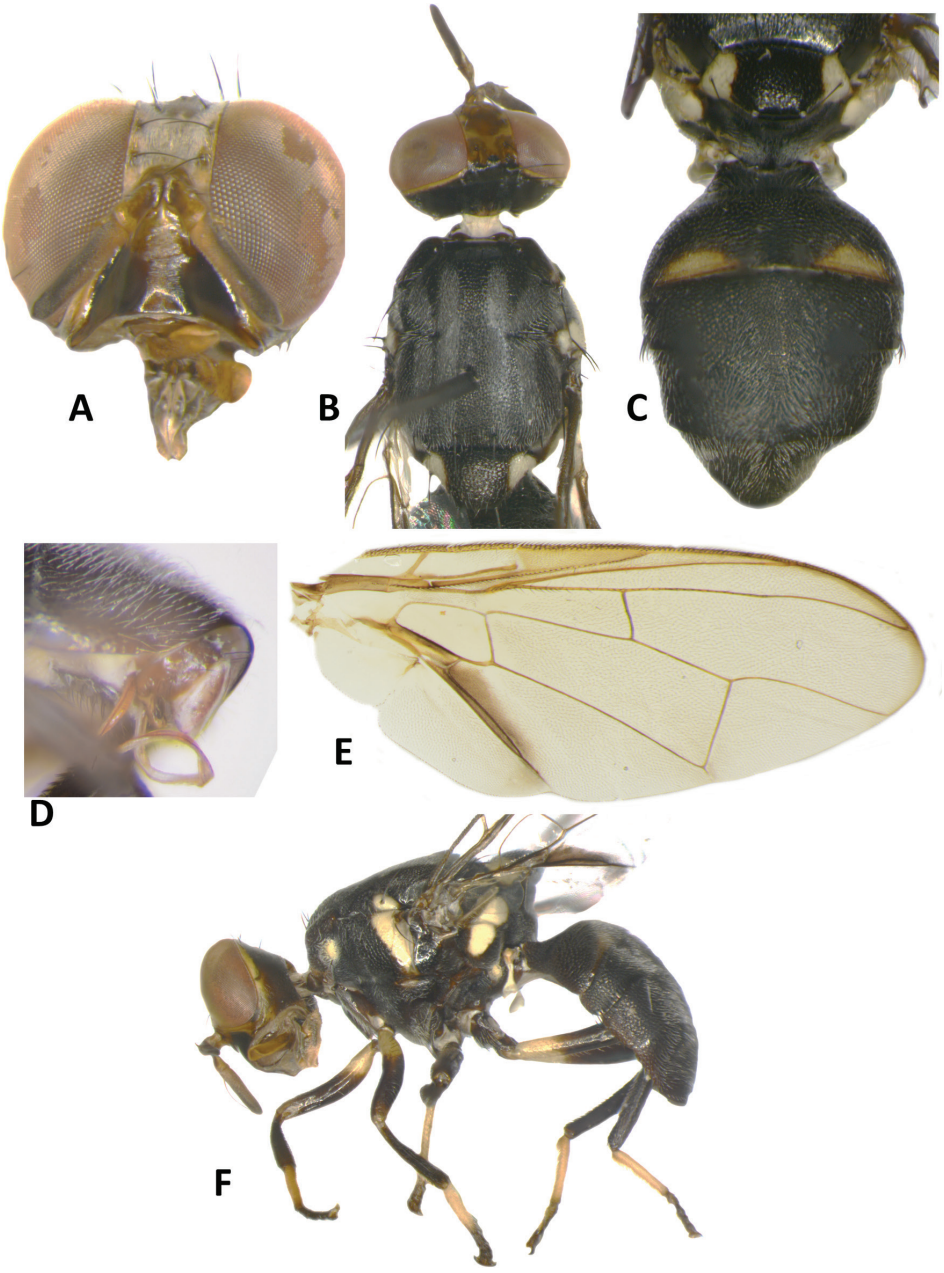

Figure 10. *Bactrocera kolombangarae* sp. nov. **A** head **B** head and scutum **C** abdomen **D** male genitalia **E** wing **F** lateral view.

156 m; 9–13 Apr. 2018; L. Leblanc, F. Tsatsia leg.; zingerone baited trap FFSo044 • 1 ♂; same locality and date as for preceding; -8.0563, 157.1320; 232 m; trap FFSo046 • 2 ♂; same locality and date as for preceding; -8.0512, 157.1287; 263 m; trap FFSo047;

molecular vouchers UHIM.ms08663, UHIM.ms08664 • 1 ♂; same locality and date as for preceding; -8.0479, 157.1262; 267 m; trap FFSo048 • 1 ♂; same locality and date as for preceding; -8.0364, 157.1186; 331 m; trap FFSo050 • 1 ♂; same locality and date as for preceding; -8.0297, 157.1166; 403 m; trap FFSo055 • 1 ♂; same locality and date as for preceding; -8.0273, 157.1160; 433 m; trap FFSo057 • 1 ♂; same locality and date as for preceding; -8.0260, 157.1156; 446 m; trap FFSo058 • 3 ♂; same locality and date as for preceding; -8.0238, 157.1157; 464 m; trap FFSo060 • 1 ♂; same locality and date as for preceding; -8.015, 157.1143; 523 m; trap FFSo068 • 1 ♂; same locality and date as for preceding; -8.0331, 157.1081; 325 m; trap FFSo071 • 1 ♂; same locality and date as for preceding; -8.0339, 157.1129; 245 m; trap FFSo073 • 2 ♂; same locality and date as for preceding; -8.0328, 157.1164; 356 m; trap FFSo075. Nine of the paratypes are deposited at UHIM, five at WFBM, three at USNM, and one at BSI.

Differential diagnosis. *Bactrocera kolombangarae* appears similar to *B. morula* (Fig. 11), but has two pairs of setae on the scutellum, a narrow anepisternal stripe, and the costal band very narrow and faint beyond the apex of R_{2+3} (Fig. 10). It is also similar to *B.* (*Parazeugodacus*) *abbreviata* (Hardy), a species from Southeast Asia. Unlike *B. kolombangarae*, *B. abbreviata* has yellow femora, very short lateral postsutural vitta, and orange-brown medially on abdomen tergites III–V.

Molecular diagnosis. We obtained two COI sequences (UHIM.ms08663, 4) that group with other members of subgenus *Parazeugodacus* in the maximum likelihood tree (Suppl. material 1: Fig. S1). The sequences are closest to *Bactrocera pendleburyi* (Perkins) [N = 11] but at a distance of 3.62%, *B. abbreviata* [N = 29] and *B. morula* [N = 3] are separated with larger distances.

Description of adult. Male. ***Head*** (Fig. 10A). Height 1.46 ± 0.11 (SD) (1.30–1.70) mm. Frons, of even width, 0.71 ± 0.06 (0.63–0.83) mm long and 1.57 ± 0.08 (1.46–1.77) times as long as broad; dark fulvous and frequently fuscous around orbital setae and on anteromedial hump; latter covered by short red-brown microtrichia; three pairs of black frontal setae present; lunule fulvous. Ocellar triangle black. Vertex dark fulvous with two pairs of black vertical setae. Face varying from mostly black, to lower ⅗ entirely black with or without traces of dark fulvous medially, and upper ⅖ dark fulvous, to a pair of very large spots in antennal furrows; length 0.47 ± 0.04 (0.43–0.53) mm. Gena fulvous, with fuscous subocular spot and a black seta. Occiput black and narrowly fulvous along eye margin; a row of 4–6 black postocular setae present behind eye. Antenna with scape dark fulvous, and pedicel and flagellum dark fuscous tending dark fulvous on inner surface; a strong red-brown dorsal seta on pedicel; arista fulvous basally and black apically; length of segments: 0.19 ± 0.02 (0.17–0.20) mm; 0.26 ± 0.03 (0.23–0.30) mm; 0.71 ± 0.06 (0.63–0.83) mm.

Thorax (Fig. 10B). Scutum entirely black with four parallel longitudinal rows of dense silvery microtrichia along entire length and two outer rows starting before notopleural sutures. Pleural areas black. Yellow markings: notopleuron; sometimes faint marking on posterior margin of postpronotal lobe; narrow anepisternal stripe with anterior margin straight, reaching to mid distance between anterior and posterior

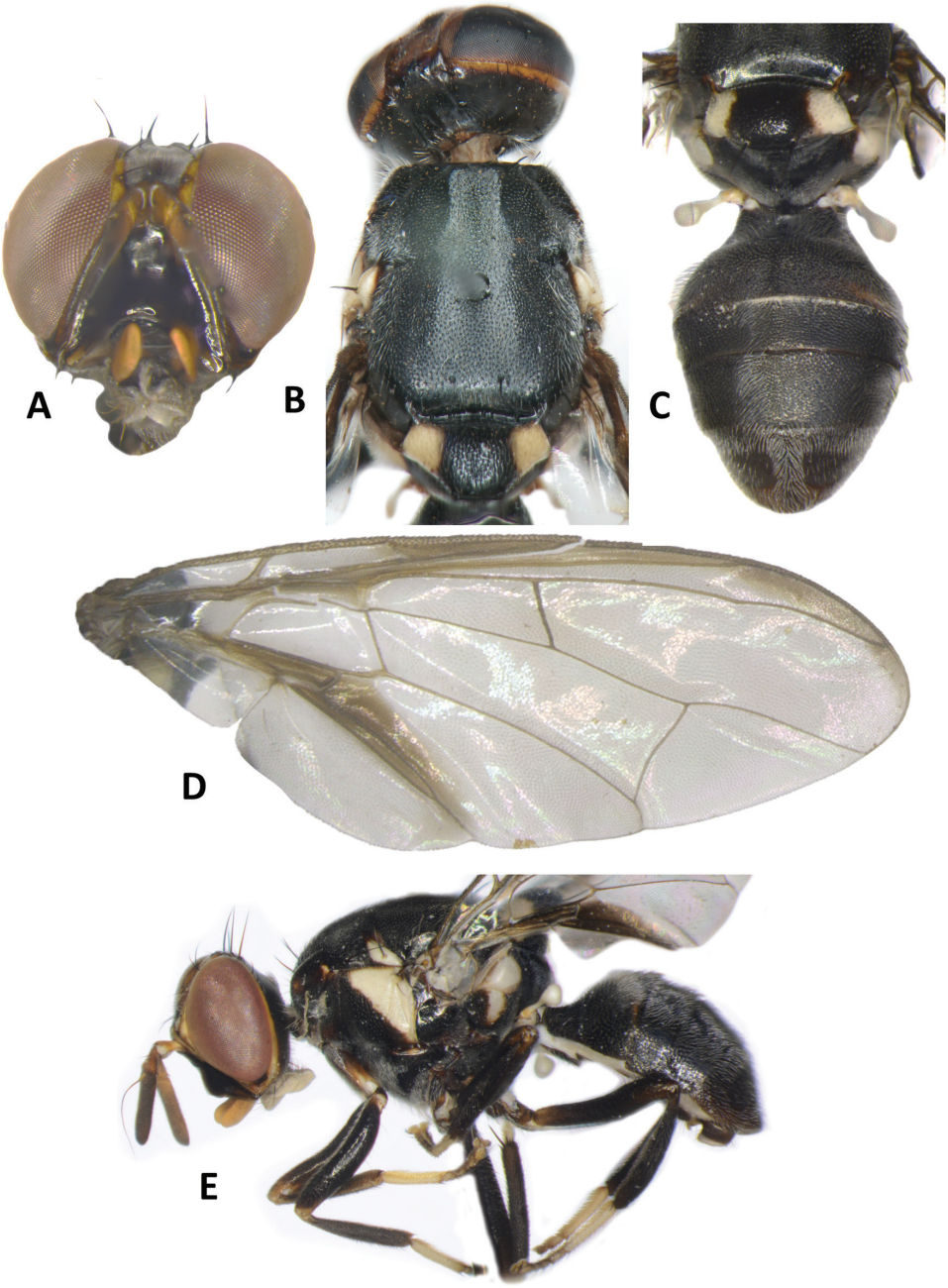

Figure 11. *Bactrocera morula* Drew **A** head **B** head and scutum **C** abdomen **D** wing **E** lateral view.

notopleural setae dorsally; a very small spot on katepisternum below the anepisternal stripe; anterior ¼ of anatergite and anterior half of katatergite (posteriorly black). Mediotergite black. Scutellum black and narrowly yellow anterolaterally. Setae: 2 pairs

scutellar; 1 pair prescutellar acrostichal; 1 pair intra-alar; 1 pair postalar; 1 pair postsutural supra-alar; 1 pair anepisternal; 2 pairs notopleural; 2 pairs scapular; all setae well developed and black.

Legs (Fig. 10F). Legs black with yellow at basal 2/5 of fore and hind femora and basal 1/6 of mid femur, and yellow fore basitarsus and mid and hind tarsi. Fore femur with a row of long pale dorsal setae. Mid-tibia with an apical black spur.

Wing (Fig. 10E). Length 4.9 ± 0.3 (4.5–5.6) mm; basal costal and costal cells hyaline with microtrichia in posterodistal corner of costal cell; narrow faint fuscous costal band confluent with R_{2+3}, remaining narrow and ending shortly past the apex of R_{2+3}; and moderately broad anal streak; remainder of wing hyaline; dense aggregation of microtrichia around A_1 + CuA_2; supernumerary lobe weakly developed.

Abdomen (Fig. 10C, D). Oval with tergites not fused; pecten present on tergite III; posterior lobe of surstylus short; abdominal sternite V with a shallow concavity on posterior margin. Base of syntergite I+II wider than long. Tergites entirely black except for elongate creamy yellow short sublateral bands along posterior margin of tergite II. Ceromata on tergite V black. Abdominal sternites dark except for yellow sternite II.

Female. Unknown

Male attractant. Zingerone.

Etymology. This species epithet is a noun in genitive case, derived from the locality where the majority of the specimens were collected; Kolombangara Island.

Notes. This species belongs to the subgenus *Parazeugodacus* as defined by Hancock and Drew (2015), based on morphological characters (shallow posterior concavity on male sternite V, posterior lobe of surstylus short, postpronotal seta absent, postsutural supra-alar, prescutellar acrostichal and two pairs of scutellar setae present, costal band very narrow and nearly indistinct). Its COI sequences also suggest closest affinity with other members of *Parazeugodacus* (Suppl. material 1: Fig. S1). *Bactrocera kolombangarae* was included as *B.* spnSol06 in Doorenweerd et al. (2020).

Bactrocera (*Bactrocera*) *quasienochra* Leblanc & Doorenweerd, sp. nov.

http://zoobank.org/3A13A2D0-6F79-4338-B501-887EEA24C356
Fig. 12A–E

Type material. ***Holotype.*** Solomon Islands • ♂; Guadalcanal, forest; -9.4064, 159.8671; 145 m; 4–16 Apr. 2018; L. Leblanc, F. Tsatsia leg.; cue-lure baited trap FFSo018; molecular voucher UHIM.ms08789. Deposited in UHIM.

Differential diagnosis. *Bactrocera quasienochra* (Fig. 12) is similar to *B. enochra* (Drew) (Fig. 13). It differs by the absence of broad black lateral markings on abdomen tergites III–V, and the narrower lateral postsutural vitta, ending before intra-alar seta.

Molecular diagnosis. We sequenced the holotype for COI, and its sequence is closest to an undescribed species from Malaysia (*B.* spMalaysia11 in Doorenweerd et al. (2020)) at 11.19% pairwise distance. The *B. quasienochra* sequence has an even greater distance to those of *B. enochra* [N = 6].

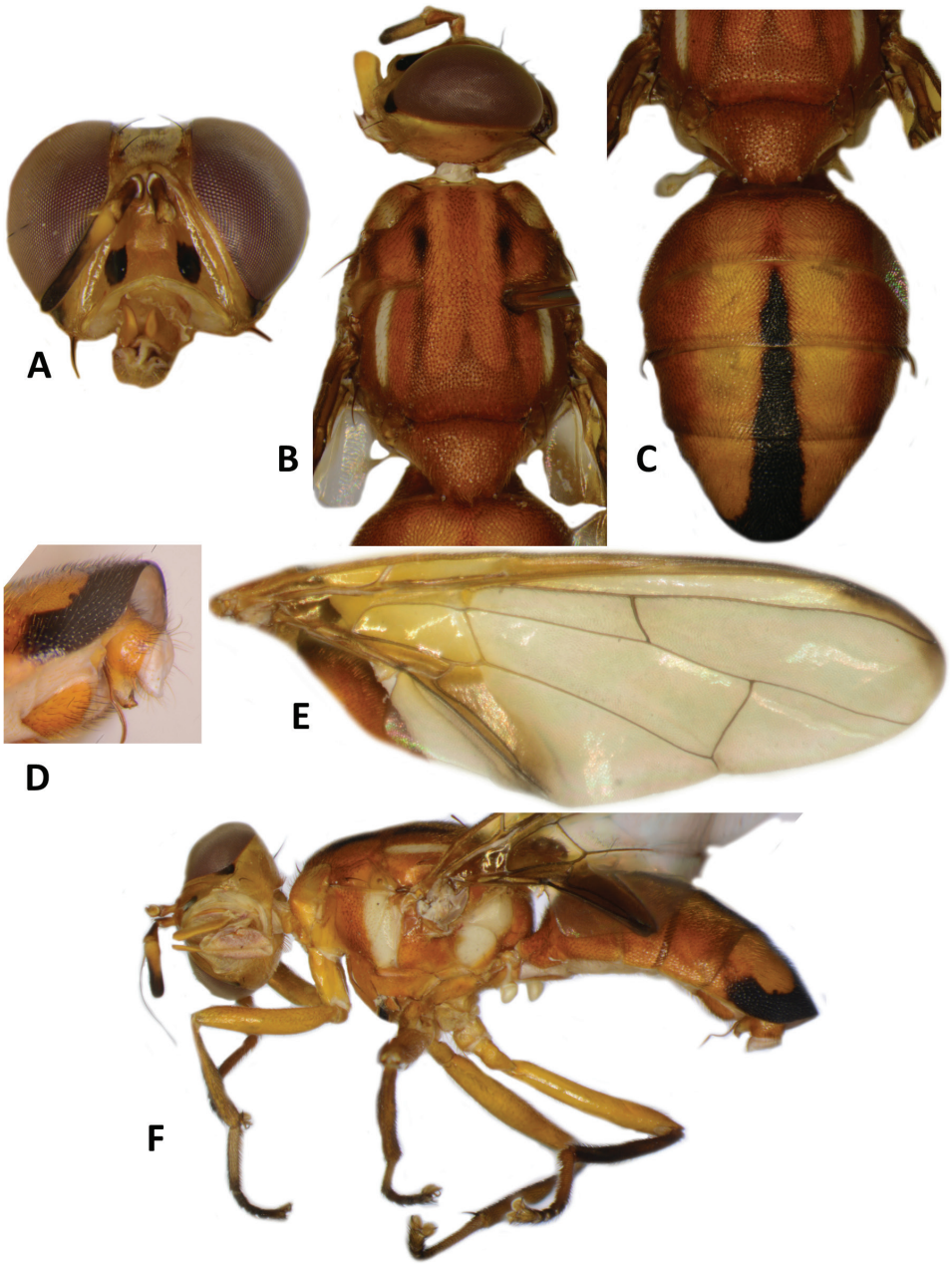

Figure 12. *Bactrocera quasienochra* sp. nov. **A** head **B** head and scutum **C** abdomen **D** male genitalia **E** wing **F** lateral view.

Description of adult. Male. ***Head*** (Fig. 12A). Height 1.83 mm. Frons, of even width, 0.93 mm long and 1.56 times as long as broad; dark fulvous and narrowly fulvous anterolaterally; anteromedial hump covered by short red-brown microtrichia; three pairs of dark fuscous frontal setae present; lunule fulvous. Ocellar triangle black.

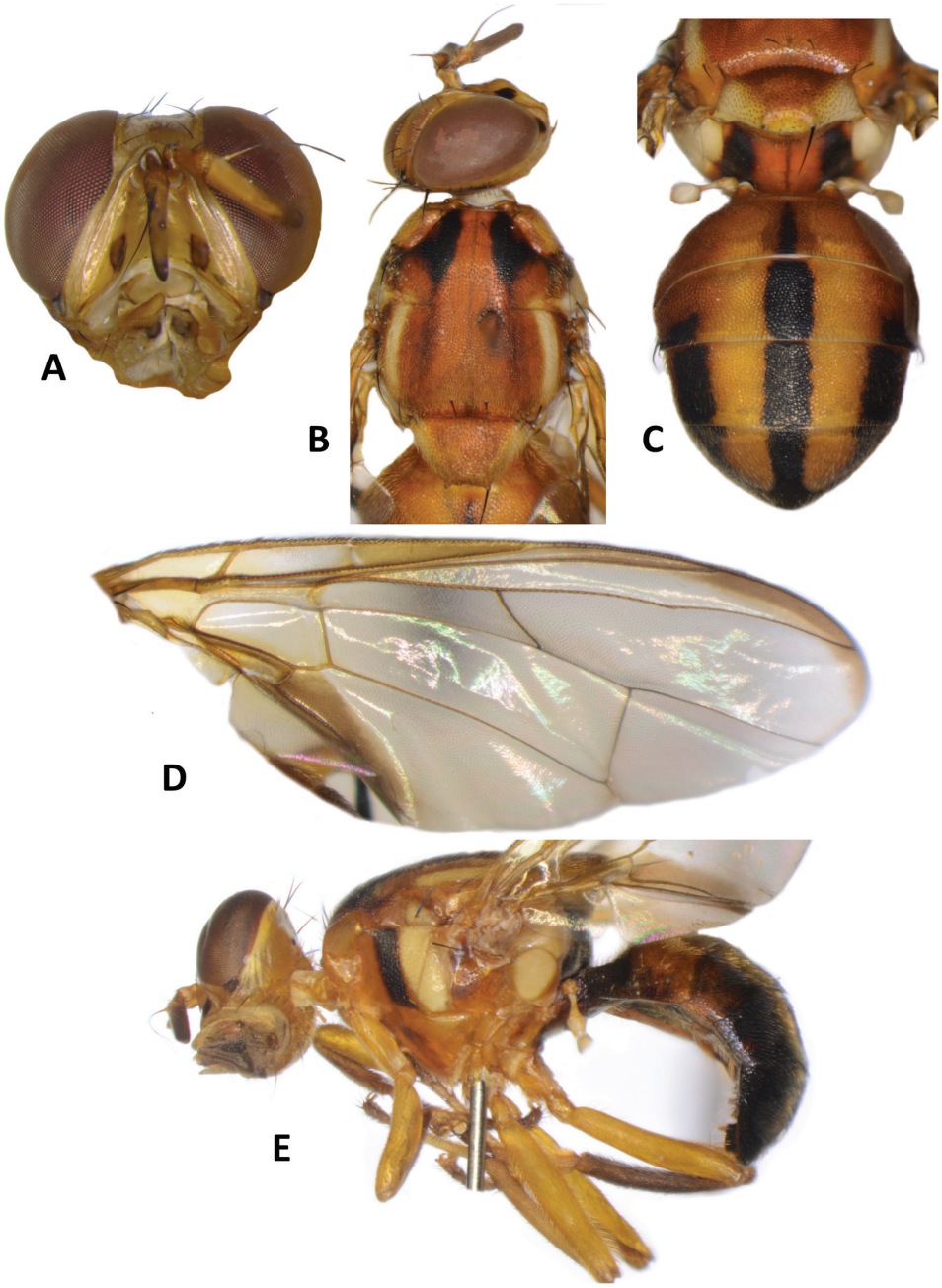

Figure 13. *Bactrocera enochra* (Drew) **A** head **B** head and scutum **C** abdomen **D** wing **E** lateral view.

Vertex fulvous with two pairs of dark fuscous vertical setae. Face fulvous with a pair of large oval black spots in antennal furrows; length 0.53 mm. Gena fulvous, with large dark fuscous subocular spot and a red-brown seta. Occiput fulvous and dark fulvous behind vertex; row of postocular setae weakly developed, with ca. four nearly indistinct

setae. Antenna with scape and pedicel dark fulvous and flagellum fulvous with lateral surface and inner apical half dark fuscous; a strong fulvous dorsal seta on pedicel; arista fulvous basally and black distally; length of segments: 0.27 mm; 0.30 mm; 0.87 mm.

Thorax (Fig. 12B). Scutum orange-brown with two short sublateral dark fuscous markings anterior to notopleural suture, and continued posteriorly as parallel lines formed by black microtrichia. Pleural areas orange-brown. Notopleuron light fulvous. Yellow markings: posterior half of postpronotal lobe (anteriorly orange-brown); narrow paired parallel-sided lateral postsutural vitta, slightly tapered posteriorly and ending before intra-alar seta; moderately broad anepisternal stripe with anterior margin straight, reaching to mid distance between anterior and posterior notopleural setae dorsally; anterior ⅔ anatergite and katatergite (posteriorly orange-brown). Mediotergite orange-brown. Scutellum orange-brown, and yellow on anterolateral surface and ventrally. Setae: 1 pair scutellar; prescutellar acrostichal absent; 1 pair intra-alar; 1 pair postalar; 1 pair postsutural supra-alar; 1 pair anepisternal; 2 pairs notopleural; 1 pair scapular (lateral position); all setae well developed and fuscous.

Legs (Fig. 12F). Legs entirely fulvous with hind tibia tending fuscous on dorsal surface. Fore femur with a row of long fulvous dorsal setae. Mid-tibia with an apical black spur.

Wing (Fig. 12E). Length 6.7 mm; basal costal and costal cells fuscous with microtrichia in posterodistal corner of costal cell; narrow fuscous costal band confluent with R_{2+3}, not expanded at apex, and ending mid distance between apex of R_{4+5} and medial vein, and broad fuscous anal streak; remainder of wing hyaline; dense aggregation of microtrichia around A_1 + CuA_2; supernumerary lobe weakly developed.

Abdomen (Fig. 12C, D). Elongate-oval with tergites not fused; pecten present on tergite III; posterior lobe of surstylus short; abdominal sternite V with a deep concavity on posterior margin. Base of syntergite I+II wider than long. All tergites orange-brown with a medial longitudinal black stripe gradually broadened from base of tergite III and extended apically along the entire lateral margins of tergite V except their bases. Ceromata on tergite V indistinct from abdomen orange-brown color. Abdominal sternites fulvous.

Female. Unknown

Male attractant. Cue-lure.

Etymology. The species name is a noun in apposition, derived from the Latin adverb *quasi* (just as if) used in conjunction with the epithet of the species it closely resembles; *B. enochra*.

Notes. *Bactrocera quasienochra* was included as *B.* spnSol03 in Doorenweerd et al. (2020).

Bactrocera (*Bactrocera*) *tsatsiai* Leblanc & Doorenweerd, sp. nov.

http://zoobank.org/8B4AC740-8648-44ED-87C8-84056641FEC4
Fig. 14A–I, 15

Type material. ***Holotype.*** Solomon Islands • ♂; Guadalcanal, forest; -9.4053, 159.8664; 139 m; 4–16 Apr. 2018; L. Leblanc, F. Tsatsia leg.; zingerone baited trap

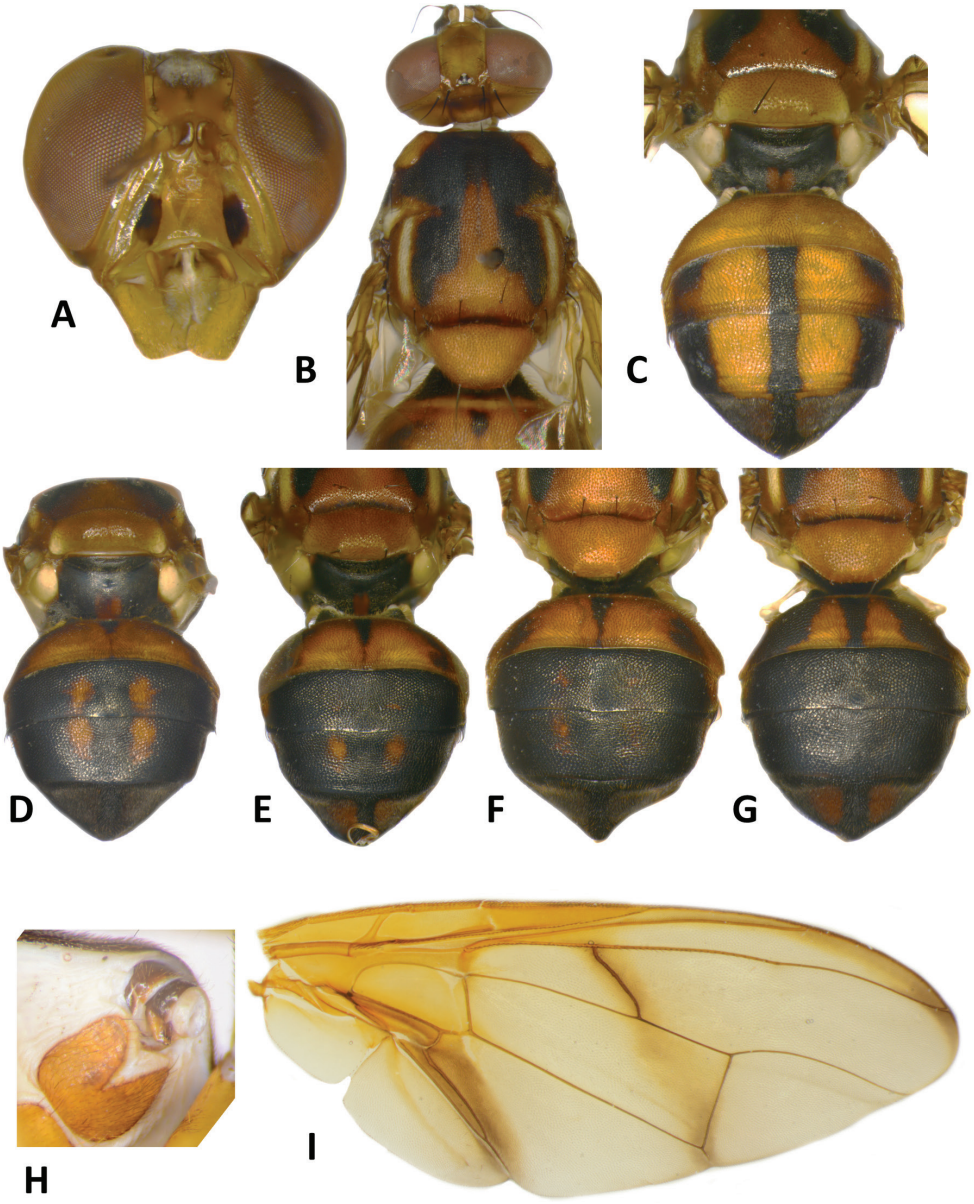

Figure 14. *Bactrocera tsatsiai* sp. nov. **A** head **B** head and scutum **C–G** abdomen variants **H** male genitalia **I** wing.

FFSo021. Deposited in UHIM. ***Paratypes.*** 28 males. Solomon Islands • 1 ♂ Guadalcanal, forest; -9.4041, 159.8628; 153 m; 4–16 Apr. 2018; L. Leblanc, F. Tsatsia leg.; zingerone baited trap FFSo011 • 2 ♂; same locality and date as for preceding; -9.4064, 159.8644; 167 m; trap FFSo14 • 1 ♂; same locality and date as for preceding; -9.4067, 159.8647; 167 m; trap FFSo015 • 1 ♂; same locality and date as for preceding;

-9.4069, 159.8664; 153 m; trap FFSo017 • 1 ♂; same locality and date as for preceding; -9.4059, 159.8672; 133 m; trap FFSo019 • 2 ♂; same locality and date as for preceding; -9.4035, 159.8681; 85 m; trap FFSo026; molecular voucher UHIM.ms08671 • 1 ♂; Kolombangara, forest; -8.0312, 157.1160; 348 m; 9–13 Apr. 2018; L. Leblanc, F. Tsatsia leg.; zingerone baited trap FFSo053 • 3 ♂; same locality and date as for preceding; -8.0297, 157.1166; 403 m; trap FFSo055 • 1 ♂; same locality and date as for preceding; -8.0283, 157.1159; 426 m; trap FFSo056 • 3 ♂; same locality and date as for preceding; -8.0218, 157.1150; 491 m; trap FFSo062 • 2 ♂; same locality and date as for preceding; -8.0200, 157.1143; 508 m; trap FFSo063 • 2 ♂; same locality and date as for preceding; -8.0190, 157.1133; 520 m; trap FFSo064 • 1 ♂; same locality and date as for preceding; -8.0181, 157.1129; 518 m; trap FFSo065 • 1 ♂; same locality and date as for preceding; -8.0181, 157.1134; 526 m; trap FFSo066 • 1 ♂; same locality and date as for preceding; -8.0157, 157.1118; 506 m; trap FFSo067 • 1 ♂; same locality and date as for preceding; -8.0150, 157.1143; 523 m; trap FFSo068 • 1 ♂; same locality and date as for preceding; -8.0327, 157.1159; 333 m; trap FFSo070 • 2 ♂; same locality and date as for preceding; -8.0356, 157.1193; 352 m; trap FFSo077 • 1 ♂; same locality and date as for preceding; -8.0357, 157.1200; 352 m; trap FFSo078. Fifteen of the paratypes are deposited at UHIM, seven at WFBM, four at USNM, and two at BSI.

Differential diagnosis. The broad orange-brown medial marking on the scutum uniquely defines *Bactrocera tsatsiai* within the genus, where all other species have either a yellow mark or no mark.

Molecular diagnosis. We obtained two COI sequences that are most similar to *Bactrocera hantanae* Tsuruta & White but at 10.79% pairwise distance.

Description of adult. Male. ***Head*** (Fig. 14A). Height 2.00 ± 0.09 (SD) (1.87–2.13) mm. Frons, of even width, 0.99 ± 0.04 (0.93–1.07) mm long and 1.56 ± 0.06 (1.47–1.63) times as long as broad; fulvous with red-brown microtrichia on anteromedial hump; three pairs of black frontal setae present; lunule yellow. Ocellar triangle black. Vertex fuscous with two pairs of black vertical setae. Face fulvous with a pair of large oval black spots in antennal furrows; length 0.60 ± 0.04 (0.53–0.67) mm. Gena fulvous, with small dark fuscous subocular spot and a black seta. Occiput fulvous; a row of 6–9 black postocular setae present behind eye. Antenna with scape and pedicel fulvous and flagellum fuscous with fulvous on inner surface; a strong black dorsal seta on pedicel; arista fulvous basally and black distally; length of segments: 0.25 ± 0.03 (0.20–0.30) mm; 0.32 ± 0.03 (0.27–0.37) mm; 0.87 ± 0.05 (0.80–0.93) mm.

Thorax (Fig. 14B). Scutum dark fuscous with orange-brown ventral to and narrowly anterior to lateral postsutural vitta, narrowly englobing notopleural suture, between postpronotal lobe and notopleuron, and as a medial band starting before notopleural suture and enlarged posteriorly to cover entire posterior margin region of scutum. Pleural areas black except orange-brown anepisternum and proepisternum. Yellow markings: postpronotal lobe (or may be anteriorly to entirely orange-brown), notopleuron; moderately broad paired parallel-sided lateral postsutural vitta ending at intra-alar seta posteriorly; moderately broad anepisternal stripe with anterior margin

Figure 15. *Bactrocera tsatsiai* sp. nov. lateral view.

slightly convex, reaching to mid distance between anterior and posterior notopleural setae dorsally; a small transverse spot on katepisternum below the anepisternal stripe; anterior ¾ of anatergite and katatergite (posteriorly black). Mediotergite black. Scutellum orange-brown, and yellow ventrally and narrowly on dorsolateral surface. Setae: 1 pair scutellar; 1 pair prescutellar acrostichal; 1 pair intra-alar; 1 pair postalar; 1 pair postsutural supra-alar; 1 pair anepisternal; 2 pairs notopleural; 2 pairs scapular; all setae well developed and black.

Legs (Fig. 15). All legs entirely fulvous with hind femur and fore tarsomeres II–IV fuscous. Fore femur with a row of long pale dorsal setae. Mid-tibia with an apical black spur.

Wing (Fig. 14I). Length 7.1 ± 0.3 (6.6–7.5) mm; basal costal and costal cells fuscous with microtrichia in posterodistal corner of costal cell; light fuscous costal band confluent with R_{2+3}, not expanded at apex and ending mid distance between apex of R_{4+5} and medial vein, a diffuse broad fuscous cross band along r-m crossvein, continuing in straight line through discal medial (dm) cell and reaching wing margin at level of CuA_1, and a broad fuscous anal streak; remainder of wing hyaline; dense aggregation of microtrichia around A_1 + CuA_2; supernumerary lobe moderately developed.

Abdomen (Fig. 14C–H). Oval with tergites not fused; pecten present on tergite III; posterior lobe of surstylus short; abdominal sternite V with a deep concavity on posterior margin. Base of syntergite I+II wider than long. Syntergite I+II with tergite I black and tergite II orange-brown with or without a small basal black triangular and two small sublateral black markings. Tergites III–V orange-brown with broad medial longitudinal black stripe reaching apex of tergite V and extended apically along entire lateral margins of tergite V, and two broad sublateral stripes covering tergite III (may be interrupted on that tergite) and continuing on tergite IV and along lateral margins on tergite V. Dark marking variable and may cover almost all of tergites III–V (Fig. 14C–G). Ceromata on tergite V dark fuscous. Abdominal sternites fulvous.

Female. Unknown

Male attractant. Zingerone.

Etymology. The epithet *tsatsiai* is a noun in genitive case, referring to the personal name Francis Tsatsia, a long-time colleague, friend, co-author of the present publication, and currently the director of Biosecurity Solomon Islands.

Notes. *Bactrocera tsatsiai* was included as *B.* spnSol05 in Doorenweerd et al. (2020).

Bactrocera (*Bactrocera*) *vargasi* Leblanc & Doorenweerd, sp. nov.

http://zoobank.org/BC8E46E7-1917-412C-AF67-7A487BDEFAFE
Fig. 16A–F

Type material. ***Holotype.*** Solomon Islands • ♂; Kolombangara, forest; -8.0563, 157.1320; 232 m; 9–13 Apr. 2018; L. Leblanc, F. Tsatsia leg.; zingerone baited trap FFSo046. Deposited in UHIM. ***Paratypes.*** 42 males. Solomon Islands • 2 ♂; Guadalcanal, forest; 4–16-iv-2018; L. Leblanc, F. Tsatsia leg.; -9.4041, 159.8628; 153 m; zingerone trap FFSo011 • 2 ♂; same locality and date as for preceding; -9.4045, 159.8644; 142 m; trap FFSo012 • 2 ♂; same locality and date as for preceding; -9.4048, 159.8645; 144 m; trap FFSo013 • 2 ♂; same locality and date as for preceding; -9.4064, 159.8644; 167 m; trap FFSo14 • 3 ♂; same locality and date as for preceding; -9.4067, 159.8647; 167 m; trap FFSo015; molecular vouchers UHIM.ms08665, UHIM.ms08666, UHIM.ms08667 • 2 ♂; same locality and date as for preceding; -9.4069, 159.8664; 153 m; trap FFSo017 • 4 ♂; same locality and date as for preceding; -9.4064, 159.8671; 145 m; trap FFSo018 • 2 ♂; same locality and date as for preceding; -9.4059, 159.8672; 133 m; trap FFSo019 • 2 ♂; same locality and date as for preceding; -9.4055, 159.8665; 145 m; trap FFSo020 • 1 ♂; same locality and date as for preceding; -9.4053, 159.8664; 139 m; trap FFSo021 • 3 ♂; same locality and date as for preceding; -9.4040, 159.8652; 125 m; trap FFSo023 • 3 ♂; same locality and date as for preceding; -9.4038, 159.8646; 103 m; trap FFSo024 • 1 ♂; same locality and date as for preceding; -9.4039, 159.8673; 103 m; trap FFSo025 • 2 ♂; same locality and date as for preceding; -9.4035, 159.8681; 85 m; trap FFSo026 • 2 ♂; same locality and date as for preceding; -9.4026, 159.8695; 57 m; trap FFSo027 • 1 ♂; same locality and date as for preceding; -9.400, 159.8700; 50 m; trap FFSo029 • 2 ♂; Kolombangara, forest; -8.0563, 157.1320; 232 m; 9–13 Apr. 2018; L. Leblanc,

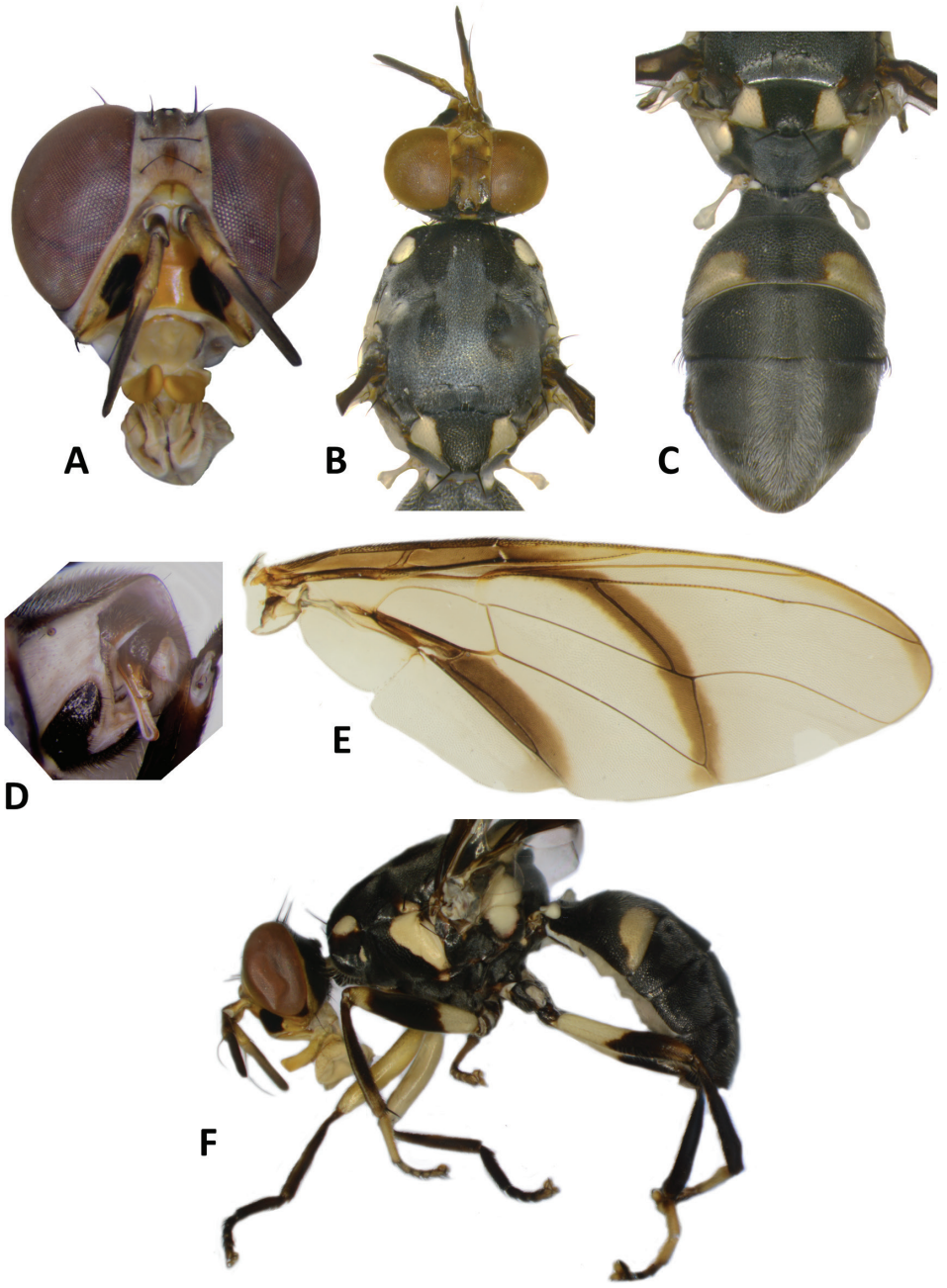

Figure 16. *Bactrocera vargasi* sp. nov. **A** head **B** head and scutum **C** abdomen **D** male genitalia **E** wing **F** lateral view.

F. Tsatsia leg.; zingerone baited trap FFSo046 • 2 ♂; same locality and date as for preceding; -8.0479, 157.1262; 267 m; trap FFSo048 • 1 ♂; same locality and date as for preceding; -8.0306, 157.1168; 389 m; trap FFSo054 • 1 ♂; same locality and date as

for preceding; -8.0252, 157.1159; 455 m; trap FFSo059 • 1 ♂; same locality and date as for preceding; -8.0328, 157.1164; 356 m; trap FFSo075 • 1 ♂; same locality and date as for preceding; -8.0395, 157.1237; 308 m; trap FFSo079. 29 of the paratypes are deposited at UHIM, seven at WFBM, four at USNM, and two at BSI.

Differential diagnosis. The overall appearance and specifically the wing of *B. vargasi* (Fig. 16E) is very similar to that of *B. frauenfeldi* (Schiner) (Fig. 17) [Solomon Island populations], *B. trilineola* Drew and *B. parafrauenfeldi* Drew [all three are members of the morphological *B. frauenfeldi* complex], but *B. vargasi* differs from *B. trilineola* and *B. parafrauenfeldi* in having a nearly entirely black abdomen (Fig. 16), and can be separated from *B. frauenfeldi* in lacking lateral postsutural yellow vitta.

Molecular diagnosis. We sequenced three specimens which have COI sequences closest to *B. quasiinfulata* Drew & Romig at 7.24% minimum pairwise distance. The maximum intraspecific distance is 1.2%. Sequences of the morphologically similar *B. frauenfeldi* and *B. trilineola* were also included in the reference dataset but are highly dissimilar to *B. vargasi* with >8% pairwise distance. *Bactrocera parafrauenfeldi* was not included in the reference set but is presumed to be closely related to *B. trilineola* (Drew 1989).

Description of adult. Male. ***Head*** (Fig. 16A). Height 1.61 ± 0.22 (SD) (1.33–1.93) mm. Frons, of even width, 0.83 ± 0.08 (0.67–0.93) mm long and 1.63 ± 0.11 (1.43–1.85) times as long as broad; fulvous and narrowly yellow along eye margin; anteromedial hump covered by short red-brown microtrichia; three pairs of black frontal setae present; lunule yellow. Ocellar triangle black. Vertex black with yellow spot behind ocellar triangle and two pairs of black vertical setae. Face fulvous with a pair of very large circular black spots in antennal furrows; length 0.51 ± 0.06 (0.43–0.63) mm. Gena fulvous, with small dark fuscous subocular spot and a red-brown seta. Occiput black and narrowly fulvous along eye margin; a row of 6–9 black postocular setae present behind eye. Antenna with scape and pedicel fulvous and flagellum dark fuscous tending dark fulvous on inner surface; a strong red-brown dorsal seta on pedicel; arista fulvous basally and black distally; length of segments: 0.31 ± 0.03 (0.27–0.33) mm; 0.36 ± 0.03 (0.33–0.40) mm; 0.88 ± 0.09 (0.73–1.00) mm.

Thorax (Fig. 16B). Scutum entirely black with dense silvery microtrichia on all scutum except two broad parallel longitudinal shining black areas interrupted at level of notopleural suture. Pleural areas black. Yellow markings: posterior half of postpronotal lobe (anteriorly fuscous); notopleuron; moderately broad anepisternal stripe with anterior margin convex, reaching to mid distance between anterior and posterior notopleural setae dorsally; a very small transverse spot on katepisternum below the anepisternal stripe; anterior ⅗ of anatergite and katatergite (posteriorly black). Mediotergite black. Scutellum broadly black medially and yellow laterally. Setae: 1 pair scutellar; 1 pair prescutellar acrostichal; 1 pair intra-alar; 1 pair postalar; 1 pair postsutural supra-alar; 1 pair anepisternal; 2 pairs notopleural; 2 pairs scapular; all setae well developed and black.

Legs (Fig. 16F). Legs black with yellow fore femur, basal ⅖ of mid and hind femur, and mid and hind tarsi. Fore femur with a row of long pale dorsal setae. Mid-tibia with an apical black spur.

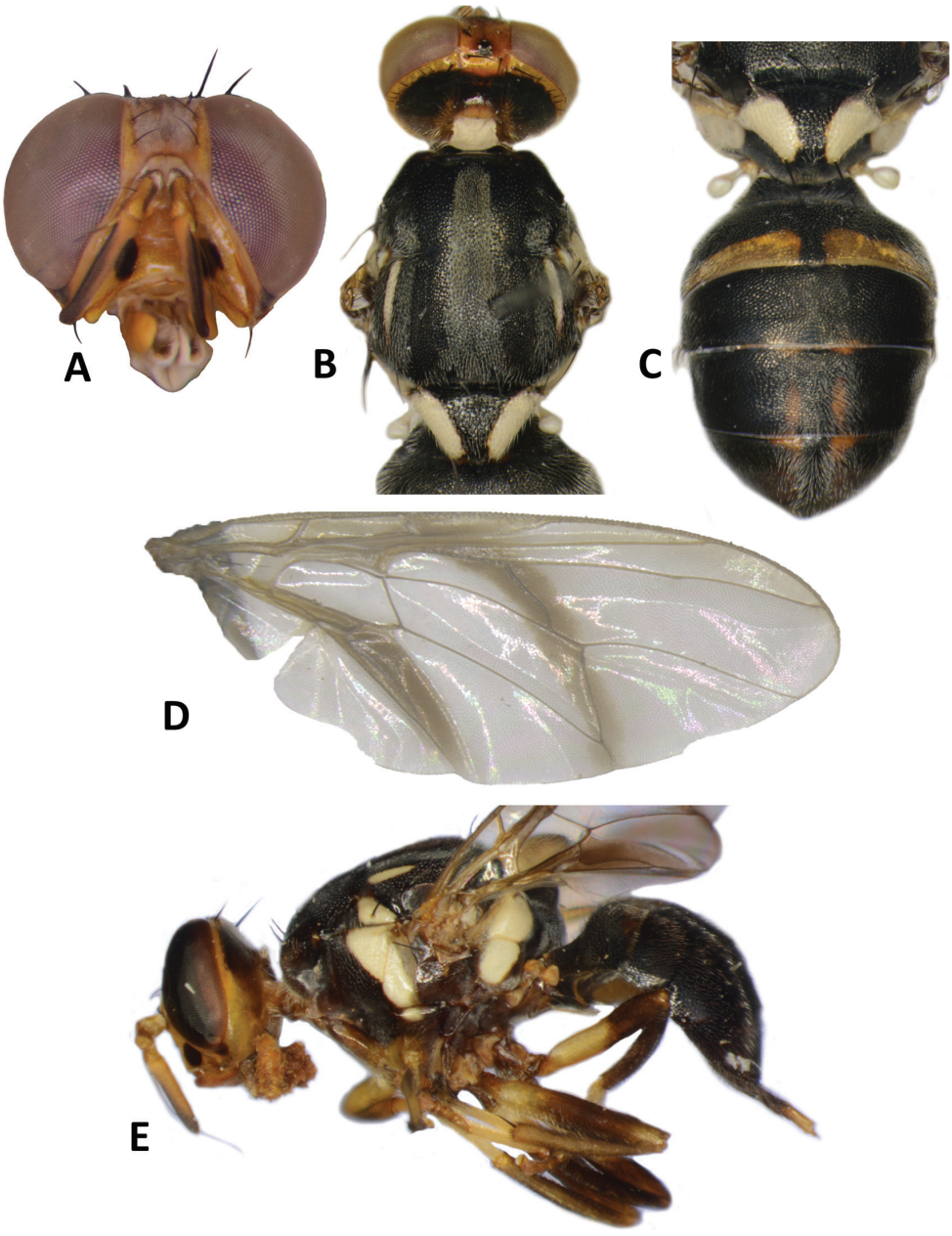

Figure 17. *Bactrocera frauenfeldi* (Schiner) **A** head **B** head and scutum **C** abdomen, male **D** wing **E** lateral view, female.

Wing (Fig. 16E). Length 6.2 ± 0.6 (5.3–6.9) mm; basal costal and costal cells dark fuscous with microtrichia covering both cells; faint narrow fuscous costal band confluent with R_{2+3}, remaining narrow to end shortly past the apex of R_{2+3}; dark fuscous

straight band across r-m and dm-cu veins and reaching wing margin; broad dark fuscous anal streak; remainder of wing hyaline; dense aggregation of microtrichia around A_1 + CuA_2; supernumerary lobe weakly developed.

Abdomen (Fig. 16C). Oval with tergites not fused; pecten present on tergite III; posterior lobe of surstylus short; abdominal sternum V with a deep concavity on posterior margin. Base of syntergite I+II wider than long. Tergites entirely black with yellow lateral bands along posterior margin of tergite II. Ceromata on tergite V black. Abdominal sternites black.

Female. Unknown.

Etymology. We proudly name this species to honor the famous fruit fly ecologist Roger I. Vargas (1947–2018) (Stark et al. 2018). The species name *vargasi* is a noun in genitive case. Roger and LL collaborated extensively on projects during years spent in the South Pacific Islands. Roger brought LL to Hawaii in 2003 to continue working on fruit flies, and he secured funding and provided guidance that allowed LL to obtain a PhD title in 2010.

Male attractant. Zingerone.

Notes. *Bactrocera vargasi* was included as *B.* spnSol07 in Doorenweerd et al. (2020).

Key to Dacine fruit fly species of Solomon Islands

This is a modified version of the key published by Drew and Romig (2001). We include for each species subgenus assignment and information on male lure attraction and host fruit (after Leblanc et al. 2012), whenever known.

1 Elongate large wasp-like fly; antenna longer than height of face; abdomen elongate and petiolate (base of syntergite I+II longer than wide), with a pronounced hump on tergite V in lateral view (unique to that species) (Fig. 18A–D) (cue-lure) (pest of cucurbit fruits) ..... ***Dacus* (*Mellesis*) *solomonensis* (Malloch)**

– More compact typical fly; antenna shorter than height of face; abdomen oval and not petiolate (base of syntergite I+II wider than long), and never with a hump on tergite V **2**

2 Wing without complete costal band, with large faint light fuscous spot covering apex, and a swelling (bulla) in CuA_2 cell; medial postsutural vitta large and triangular (Fig. 18 E–H) (bred from *Terminalia catappa* and *Gnetum gnemon*) .... **males of *B.* (*Bulladacus*) *penefurva* Drew**

– Wing with complete costal band, although sometimes noticeably paler beyond apex of R_1, with marking (when present) not as large spot at apex, and bulla absent (except in males of *B. pacificae*); medial postsutural vitta present or absent..... **3**

3 Wing membrane with infuscation in addition to costal band and anal streak (this may be narrow infuscation on one or both crossveins) (Figs 18K–24F) **4**

– Wing membrane colorless or lightly infuscated, except for costal band and anal streak (Figs 24I–28L) **31**

4 Scutum with medial postsutural vitta (Figs 18I–20A) **5**
– Scutum without medial postsutural vitta (Figs 20D–24D)..... **11**
5 Prescutellar acrostichal seta absent; postsutural supra-alar seta present or absent **6**
– Prescutellar acrostichal and postsutural supra-alar seta present **8**
6 Postsutural supra-alar seta absent; abdomen fulvous with broad dark fuscous lateral stripes on tergites III–V (Fig. 18I–K) (zingerone) .... ***B.* (*Tetradacus*) *pagdeni* (Malloch)**
– Postsutural supra-alar seta present; abdomen with black spot on tergite V (Fig. 18M) or with narrow medial and lateral stripes (Fig. 19B) **7**
7 Postpronotal lobe and notopleuron joined by lateral yellow band; wing with narrow pale infuscation along crossveins r-m and dm-cu; abdominal tergites entirely red-brown except for black spot in center of tergite V (Fig. 18L–N) (cue-lure) ... . ***Z.* (*Zeugodacus*) *univittatus* (Drew)**
– Postpronotal lobe and notopleuron not joined by yellow band; wing with fuscous tint throughout, broad fuscous costal band to R_{4+5}, narrow infuscation along r-m crossvein and broad infuscation along dm-cu crossvein; abdominal tergites III–V with narrow medial and lateral longitudinal black stripes (Fig. 19A–C) (cue-lure) ..... ***Z.* (*Javadacus*) *hamaceki* Drew & Romig**
8 Scutum glossy black; Z-shaped fuscous pattern across wing (Fig. 19D–F) (cue-lure) ..... ***Z.* (*Zeugodacus*) *amoenus* (Drew)**
– Scutum basically red-brown; wing with infuscation on one or both crossveins, but not a Z-shaped pattern **9**
9 Scutum red-brown with small dark markings and a very narrow medial postsutural vitta; scutellum with one or two pairs of setae (Fig. 19G–I) (cue-lure, zingerone) (pest of cucurbit flowers and fruits)..... ..... ***Z.* (*Javadacus*) *cucurbitae* (Coquillett)**
– Scutum entirely red-brown or red-brown with large dark markings and a broader medial postsutural vitta (Figs 19J, 20A); scutellum with two pairs of setae..... **10**
10 Wing with infuscation on dm-cu crossvein only; scutum entirely red-brown; abdominal tergites III–V red-brown without a distinct dark 'T'-shaped pattern (Fig. 19J–L) ..... ***Z.* (*Javadacus*) *fuscipennulus* (Drew & Romig)**
– Wing with infuscation on both crossveins; scutum red-brown with large black markings; abdominal tergites III–V red-brown with a black 'T'-shaped pattern (Fig. 20A–C) (cue-lure)..... ***Z.* (*Javadacus*) *abdoangustus* (Drew)**
11 Infuscation on wing on one crossvein only (Fig. 20F, J, N) **12**
– Infuscation on wing more extensive, as a very broad pattern across most of membrane, a recurved band, or one or more transverse bands..... **14**
12 Lateral postsutural vitta very short and narrowing posteriorly to end well before intra-alar seta (Fig. 20D–F) (methyl eugenol) .... ***B.* (*Bactrocera*) *melanogaster* (Drew)**
– Lateral postsutural vitta broad, parallel sided (or with only a slight narrowing posteriorly) and ending at intra-alar seta **13**

13 Anepisternal stripe reaching to postpronotal lobe dorsally; abdominal tergites III–V red-brown with a black 'T'-shaped and broad lateral black margins (Fig. 20G–I) (cue-lure) (bred from *Alpinia purpurata*)..... ***B.* (*Bactrocera*) *phaea* (Drew)**

– Anepisternal stripe reaching to anterior notopleural seta dorsally; abdominal tergites mostly black (Fig. 24K–N) (methyl eugenol) ..... ***B.* (*Bactrocera*) *neonigrita* Drew**

14 Scutellum with a black triangular dorsal marking or with an apical dark spot .**15**

– Scutellum yellow or orange-brown, except for a narrow dark basal band **20**

15 Costal band pale and indistinct beyond apex of R_1; a narrow transverse fuscous band across wing.....**16**

– Costal band distinct for entire length; infuscation across wing as a single band or a recurved band.....**17**

16 Lateral postsutural vitta present; abdomen orange-brown with a broad medial and two broad lateral black bands along tergites III–V (Fig. 17A–E) (cue-lure, zingerone) (polyphagous fruit pest bred from 28 host species in Solomon Islands)..... ***B.* (*Bactrocera*) *frauenfeldi* (Schiner)**

– Lateral postsutural vitta absent; abdomen entirely black except yellow lateral bands along posterior margin of tergite II (Fig. 16A–F) (zingerone)..... ***B.* (*Bactrocera*) *vargasi* sp. nov.**

17 Infuscation across wing as a recurved band (Fig. 21C, F) **18**

– Infuscation across wing as a single band (Figs 21I, 22C) **19**

18 Single U-shaped band across wing (Fig. 21A–C) (methyl eugenol) ..... ***B.* (*Bactrocera*) *reclinata* Drew**

– Broad recurved band across center of wing and a narrow transverse band across apex (Fig. 21D–F) (cue-lure).....***B.* (*Bactrocera*) *longicornis* Macquart**

19 Scutellum with a broad medial longitudinal black stripe; postpronotal lobe yellow except for anterior third dark fuscous to black; postpronotal lobe and notopleuron not joined by a yellow band; lateral postsutural vitta short and narrow; abdomen tergites III–V orange-brown with small irregularly shaped sublateral markings and a narrow medial longitudinal stripe (Fig. 21G–I) (cue-lure) ..... ***B.* (*Bactrocera*) *hollingsworthi* Drew & Romig**

– Scutellum yellow with at most an apical dark spot; postpronotal lobe yellow; postpronotal lobe and notopleuron joined by a narrow yellow band; lateral postsutural vitta well developed; abdomen tergites III–V orange-brown with a black medial longitudinal stripe and well defined black lateral markings (Fig. 22A–C) (cue-lure) ..... ***B.* (*Bactrocera*) *unitaeniola* Drew & Romig**

20 Wing with three broad transverse fuscous bands (Fig. 22D–F) (methyl eugenol) (pest of breadfruit and jackfruit) ..... ***B.* (*Bactrocera*) *umbrosa* (Fabricius)**

– Wing not so marked **21**

21 Postpronotal lobe and notopleuron joined by a broad yellow band (Fig. 22G–I) (cue-lure) .....***B.* (*Bactrocera*) *unifasciata* (Malloch)**

– Postpronotal lobe and notopleuron not joined by a yellow band **22**

22 Abdomen tergites III–V entirely black **23**

– Abdomen tergites III–V orange-brown with dark markings **25**

23 Wing membrane almost entirely fuscous; abdomen tergite II largely fulvous, contrasting with the black tergites III–V (Fig. 22J–L) (methyl eugenol) ....***B.* (*Bactrocera*) *pepisalae* (Froggatt)**

– Wing membrane colorless with distinct fuscous markings; abdomen entirely black, or with at most an orange-brown band along posterior margin of tergite II.....**24**

24 r-m crossvein strongly oblique; broad dark fuscous band across wing from costal band to hind margin, enclosing both crossveins; legs entirely fulvous (Fig. 23A–C) (methyl eugenol) .....***B.* (*Bactrocera*) *obliquivenosa* Drew & Romig**

– r-m crossvein not oblique; transverse fuscous band across wing broad and covering more than outer half of discal medial cell; legs fulvous with apical half of mid and hind femur black (Fig. 23D–F) (methyl eugenol)..... .....***B.* (*Bactrocera*) *biarcuata* (Walker)**

25 Z-shaped fuscous pattern across wing.....**26**

– Single fuscous band of variable shape across wing **27**

26 Lateral postsutural vitta short and tapering posteriorly; wing markings dark fuscous; lateral and medial longitudinal black stripes on abdominal tergites III–V sometimes joined across base of tergite III (Fig. 23G–I) (cue-lure)..... .....***B.* (*Bactrocera*) *nigrescentis* (Drew)**

– Lateral postsutural vitta broad, parallel sided and reaching to intra-alar seta; wing markings pale fuscous; lateral and medial longitudinal black stripes on abdominal tergites III–V not joined (Fig. 23J–L) (cue-lure) (bred from *Pycnarrhena ozantha* in Vanuatu)..... ***B.* (*Bactrocera*) *redunca* (Drew)**

27 Large species (body length 11 mm or more); transverse fuscous band across wing broad and covering more than outer half of discal medial cell (Fig. 24A–C) (methyl eugenol).....***B.* (*Bactrocera*) *confluens* (Drew)**

– Moderately sized species (body length 9 mm or less); transverse fuscous band across wing of medium width, covering outer third of discal medial cell **28**

28 Wing crossband dark fuscous and broad; costal band confluent with R_{4+5} and greatly expanded at apex of wing (Fig. 24D–F) (cue-lure) (bred from *Burckela* sp.).....***B.* (*Bactrocera*) *decumana* (Drew)**

– Wing crossband light fuscous; costal band not greatly expanded at apex of wing. **29**

29 Scutum dark fuscous to black with a broad orange-brown medial stripe, starting before notopleural suture and enlarged posteriorly to cover entire posterior margin region of scutum; scutellum largely orange-brown, and yellow ventrally and narrowly on dorsolateral surface; anepisternal stripe moderately broad, reaching to mid distance between anterior and posterior notopleural setae dorsally (Figs 14A–I, 15) (zingerone)..... ***B.* (*Bactrocera*) *tsatsiai* sp. nov.**

– Scutum predominantly to entirely black, at most narrowly orange-brown laterally and posteriorly; scutellum yellow; anepisternal stripe broad, almost reaching to anterior notopleural seta dorsally.....**30**

30 Scutum entirely black, except for yellow postpronotal lobe, notopleuron and lateral postsutural vitta; abdominal tergites III–V with moderately broad medial

longitudinal black stripe and lateral black markings on tergite IV not narrowed posteriorly; fuscous crossband on wing clearly defined (Fig. 4A–E) (cue-lure) .... ***B.* (*Bactrocera*) *pseudodistincta* (Drew)**

– Scutum predominantly black with orange-brown laterally and posteriorly; abdominal tergites III–V with narrower medial longitudinal black stripe and lateral black markings on tergite IV narrowed posteriorly; fuscous crossband on wing diffuse (Fig. 3A–F) (cue-lure) ..... ***B.* (*Bactrocera*) *allodistincta* sp. nov.**

31 Lateral postsutural vitta absent **32**

– Lateral postsutural vitta present **34**

32 Scutellum entirely yellow; abdominal tergites orange-brown with a narrow median longitudinal stripe on tergites III–V (Fig. 24G–I) (cue-lure) (bred from *Cerbera* spp and *Antiaris toxicaria* in Vanuatu) ..... ***B.* (*Bactrocera*) *minuta* (Drew)**

– Scutellum yellow and broadly black medially; abdominal tergites black **33**

33 Scutellum with two pairs of setae; anepisternal stripe narrow and reaching to mid distance between anterior and posterior notopleural setae dorsally (Fig. 10A–F) (zingerone) ..... ***B.* (*Parazeugodacus*) *kolombangarae* sp. nov.**

– Scutellum with one pair of setae; anepisternal stripe broader and reaching posterior notopleural seta dorsally (Fig. 11A–E) (cue-lure) .... ***B.* (*Bactrocera*) *morula* Drew**

34 Costal band confluent with or overlapping R_{4+5} **35**

– Costal band not reaching to R_{4+5} **43**

35 Scutum and abdominal tergites mostly red-brown **36**

– Scutum black or dark fuscous with a pair of longitudinal black bands; abdominal tergites mostly black or orange-brown or red-brown with dark markings **37**

36 Anepisternal stripe reaching to anterior notopleural seta; pecten present on male abdominal tergite III (Fig. 24J–L) (methyl eugenol) (bred from *Nauclea* sp.) .... ***B.* (*Bactrocera*) *naucleae* Drew & Romig**

– Anepisternal stripe ending midway between anterior margin of notopleuron and anterior notopleural seta; pecten absent from male abdominal tergite III (Fig. 25A–C) (bred from *Spondias dulcis*) ..... ***B.* (*Calodacus*) *hastigerina* (Hardy)**

37 Abdominal tergites III–V red-brown with a black 'T'-shaped pattern and narrow lateral dark margins; pecten absent from male abdominal tergite III (Fig. 25D–F) (bred from *Calophyllum* spp) ..... ***B.* (*Calodacus*) *calophylli* (Perkins & May)**

– Abdominal tergites III–V mostly black or orange-brown with broad medial and longitudinal black stripes; pecten present on male abdominal tergite III **38**

38 Abdominal tergites III–V orange-brown with broad medial and lateral longitudinal black stripes that are not joined (Fig. 25G–I) (methyl eugenol) .... ***B.* (*Bactrocera*) *froggatti* (Bezzi)**

– Abdominal tergites mostly black **39**

39 Costal band overlapping R_{4+5} for entire length; abdominal tergites mostly black, with some orange-brown centrally on tergites IV and V **40**

– Costal band confluent with R_{4+5}; abdominal tergites entirely black **41**

40 Wing (Fig. 9E–G) with a light fuscous tinge as a broad, somewhat triangular area covering much of the middle of the wing, including the areas bordering r-m and dm-cu (Figs 6A–E, 9E–G) (cue-lure)..... ***B.* (*Bactrocera*) *geminosimulata* sp. nov.**

– Wing (Fig. 9A–D) without a light fuscous tinge in the area described above (Figs 7A–D, 9A–D) (cue-lure) (bred from *Coccinia grandis*) ..... ***B.* (*Bactrocera*) *simulata* (Malloch)**

41 Microtrichia covering all of basal costal and costal cells in wing (Fig. 25J–L) (dihydroeugenol, isoeugenol) (bred from *Allophylus cobbe* (formerly *Pometia pinnata*)) ..... ***B.* (*Bactrocera*) *quadrisetosa* (Bezzi)**

– Microtrichia restricted to posterodistal corner of costal cell in wing **42**

42 Legs mostly black; scutellum with a broad black basal band; anepisternal stripe narrow, just wider than notopleuron (Fig. 26A–C) (cue-lure) ..... ***B.* (*Bactrocera*) *epicharis* (Hardy)**

– Legs mostly fulvous; scutellum with a narrow black basal band; anepisternal stripe reaching to anterior notopleural seta (Fig. 26D–F) (cue-lure)..... ***B.* (*Bactrocera*) *atrabifasciata* Drew & Romig**

43 Scutellum yellow with dark markings or orange-brown and narrowly yellow laterally **44**

– Scutellum entirely yellow or entirely orange-brown **49**

44 Scutellum with a dark apical spot (Fig. 26G–I) (methyl eugenol) (bred from Moraceae in Australia and *Pimelodendron amboicinum* in Papua New Guinea) ... . **some specimens of *B.* (*Bactrocera*) *bancroftii* (Tryon)**

– Scutellum with a black or brown longitudinal marking over dorsal surface **45**

45 Scutum and abdomen predominantly black (Fig. 26J–L) (methyl eugenol)..... ***B.* (*Bactrocera*) *picea* (Drew)**

– Scutum and abdomen predominantly red-brown **46**

46 Postpronotal lobe fuscous or orange-brown anteriorly and yellow posteriorly; abdominal tergites III–V with a broad medial longitudinal black stripe and with or without narrow sublateral longitudinal black bands over tergites III–V which are all joined across posterior margin of tergite V by a narrow transverse black band **47**

– Postpronotal lobe entirely yellow; abdominal tergites III–V with either a narrow medial longitudinal black band on all tergites or a broad medial band on tergite V only **48**

47 Abdomen with broad sublateral black stripes on tergites III–V, in addition to medial stripe (Fig. 13A–E) (cue-lure) (bred from *Medusanthera laxiflora* in Papua New Guinea) ..... ***B.* (*Bactrocera*) *enochra* (Drew)**

– Abdomen with sublateral black stripes absent on tergites III–V (Fig. 12A–F) (cue-lure) ..... ***B.* (*Bactrocera*) *quasienochra* sp. nov.**

48 Anepisternal stripe reaching anterior notopleural seta; bulla present in male wing (Fig. 27A–D) (bred from *Gnetum gnemon*) ..... ***B.* (*Bulladacus*) *pacificae* Drew & Romig**

– Anepisternal stripe reaching midway between anterior margin of notopleuron and anterior notopleural seta; no bulla in male wing (Fig. 27E–G) (cue-lure) ..... ***B.* (*Neozeugodacus*) *buinensis* Drew**

49 Scutum basically red-brown **50**
– Scutum predominantly black **52**
50 Lateral postsutural vitta very short and tapering to a point posteriorly; a circular black spot present on tergite V (Fig. 27H–J) ..... ***B.* (*Bulladacus*) *unipunctata* (Malloch)**
– Lateral postsutural vitta long and reaching to intra-alar seta; abdominal tergites uniformly pale colored or with patterns of dark markings **51**
51 Costal cells colorless; abdominal tergites III–V with broad lateral longitudinal fuscous stripes (Fig. 27K–M) ..... ***B.* (*Bactrocera*) *aithogaster* Drew**
– Costal cells with pale fuscous coloration; abdominal tergites III–V uniformly orange-brown or with a black 'T'-shaped pattern (Fig. 28A–C) (cue-lure, zingerone) (bred from *Inocarpus fagifer*) ..... ***B.* (*Bactrocera*) *moluccensis* (Perkins)**
52 Postpronotal lobe dark fuscous (Fig. 28D–F) (cue-lure) ..... ***B.* (*Bactrocera*) *furvescens* Drew**
– Postpronotal lobe yellow **53**
53 Abdominal tergites entirely black (Fig. 28G–I) (cue-lure) ..... ***B.* (*Bactrocera*) *aterrima* (Drew)**
– Abdominal tergites orange-brown with or without dark color patterns..... **54**
54 Abdominal tergites either entirely orange-brown or with very narrow black lines anterolaterally on tergite III and occasionally with a narrow medial black stripe over tergites III–V (Fig. 26G–I) (methyl eugenol) (bred from Moraceae in Australia and *Pimelodendron amboicinum* in Papua New Guinea) ..... **some specimens of *B.* (*Bactrocera*) *bancroftii* (Tryon)**
– Abdominal tergites orange-brown with distinct dark markings laterally and medially **55**
55 Medial postsutural vitta present (Fig. 18E–H) (bred from *Terminalia catappa* and *Gnetum gnemon*) ..... **females of *B.* (*Bulladacus*) *penefurva* Drew**
– Medial postsutural vitta absent (Fig. 28J–L) (methyl eugenol) ..... ***B.* (*Bactrocera*) *parafroggatti* Drew & Romig**

Discussion

The snap-shot survey yielded 16,843 Dacine flies, belonging to 30 known and six new species, described herein, increasing the number of species known from the Solomon Islands from 48 to 54 (Table 1). Twenty-eight species were represented by at least ten specimens and the five most collected species were *Bactrocera frauenfeldi* (Schiner) (43.0% of all specimens), *B. froggatti* (Bezzi) (13.4%), *B. umbrosa* (Fabricius) (9.6%), *B. morula* Drew (7.1%), and *B. pagdeni* (Malloch) (7.0%). Our sampling effort was very fruitful, yielding 29 of the 37 species previously collected by trapping over eight years, plus we found six new species, and 18 new island records (Table 1). We collected 31 of 48, 22 of 31, and 8 of 14 species found on Guadalcanal, Kolombangara, and

Gizo, respectively. The species accumulation curves (Fig. 2) demonstrate the highest species diversity to be in the forests of Guadalcanal, with twice as many species as in agricultural sites (Fig. 2C). Despite the deployment of 36 sets of traps in the rich protected forests of Kolombangara (688 km^2), the number of collected and projected species was still half as many as on Guadalcanal (5,302 km^2) (Fig. 2B, C), consistent with previously published accounts (Drew and Romig 2001; Hollingsworth et al. 2003). The difference is related to island size, with number of fruit fly species clearly correlated (r^2 = 60.9%) to island size in the Solomon Islands (Suppl. material 3: Fig. S2).

In addition to collecting three new species, the use of zingerone lure revealed that *Bactrocera pagdeni*, formerly known only by its female holotype (Drew 1974), one specimen at the Bishop Museum collections (BPBM), and a few males recently captured in zingerone traps (Hancock and Drew 2018b), is actually a common and widespread species, with 1,174 specimens collected during our survey (Table 1). Likewise, the recent discovery of the attraction of *Bactrocera quadrisetosa* (Bezzi) to dihydroeugenol and isoeugenol lures in Vanuatu (Leblanc, unpublished) will likely reveal that this species is also common and widespread in the Solomon Islands. Clearly, many new species are awaiting discovery with the increasing availability of new generation lures (Manrakhan et al. 2017; Royer et al. 2018, 2019). Several rare species that require further attention in future surveys include: *B. aithogaster* Drew (known by only two specimens), *B. bancroftii* (Tryon) (one specimen of this Australian species from Guadalcanal), *B. furvescens* Drew, a Papua New Guinea species of which a single specimen was collected in 1971 in Honiara, and *B. unipunctata* (Malloch) known from a single specimen collected on Florida Island (Malloch 1939). The species from Mount Austen (Guadalcanal), identified as *B. musae* (Tryon) (Drew and Romig 2001), is likely a non-pest species member of the *B. musae* complex (Drew et al. 2011). *Bactrocera musae* is a major pest of banana, and no fruit fly infestations have been observed on banana in the Solomon Islands, even in recent years (FT, pers. obs.).

The COI sequences we obtained for the new species typically have large minimum pairwise distances to their nearest congeners, up to 12%, whereas the average minimum distance between species for *Bactrocera* is 6.09% (Suppl. material 2: Table S1; Doorenweerd et al. 2020). This is likely due to a lack of species from Papua New Guinea represented in the reference dataset, where there is a large, mostly unstudied, diversity of *Bactrocera* (White and Evenhuis 1999; Drew pers. comm.). As a consequence, the currently available reference data suggests that COI reliably distinguishes all newly described species, but further sampling of species in New Guinea may reduce the pairwise distance resolution (Doorenweerd et al. 2020). There is one potentially new species (*B.* spnSol08; molecular voucher UHIM.ms08767), for which we have one specimen, that we leave undescribed. Although its COI sequence is highly divergent, closest to *B. hantanae* Tsuruta & White at 9.89%, there is only a single specimen and its morphology has no apparent differences with that of *B. dorsalis* (Hendel). Future sampling will hopefully bring in a larger series of this potentially new species to enable further examination of the morphological characters.

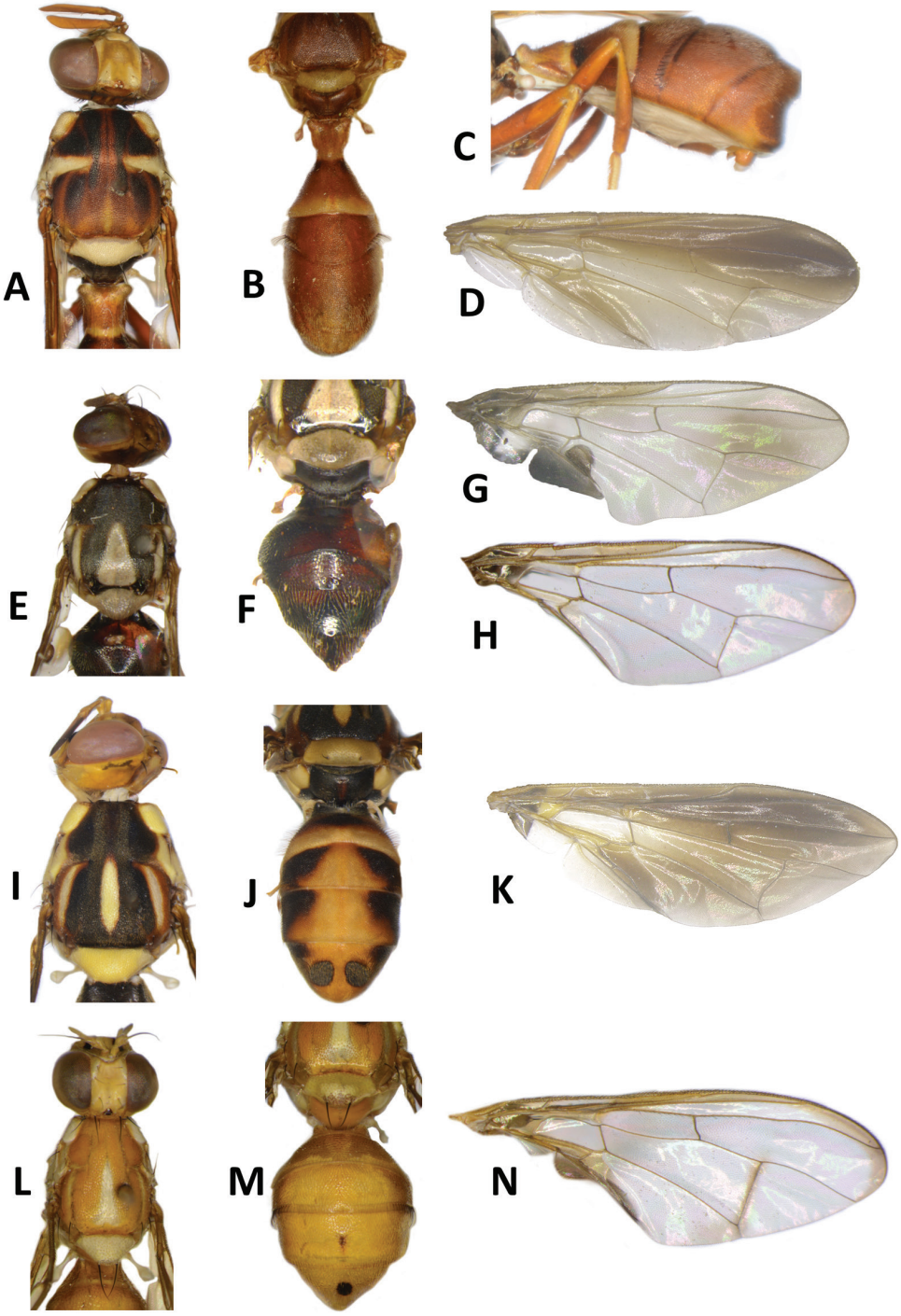

Figure 18. *Dacus solomonensis* Malloch **A** head and scutum **B, C** abdomen **D** wing. *Bactrocera penefurva* Drew **E** head and scutum **F** abdomen **G** male wing **H** female wing. *Bactrocera pagdeni* (Malloch) **I** head and scutum **J** abdomen **K** wing. *Zeugodacus univittatus* (Drew) **L** head and scutum **M** abdomen **N** wing.

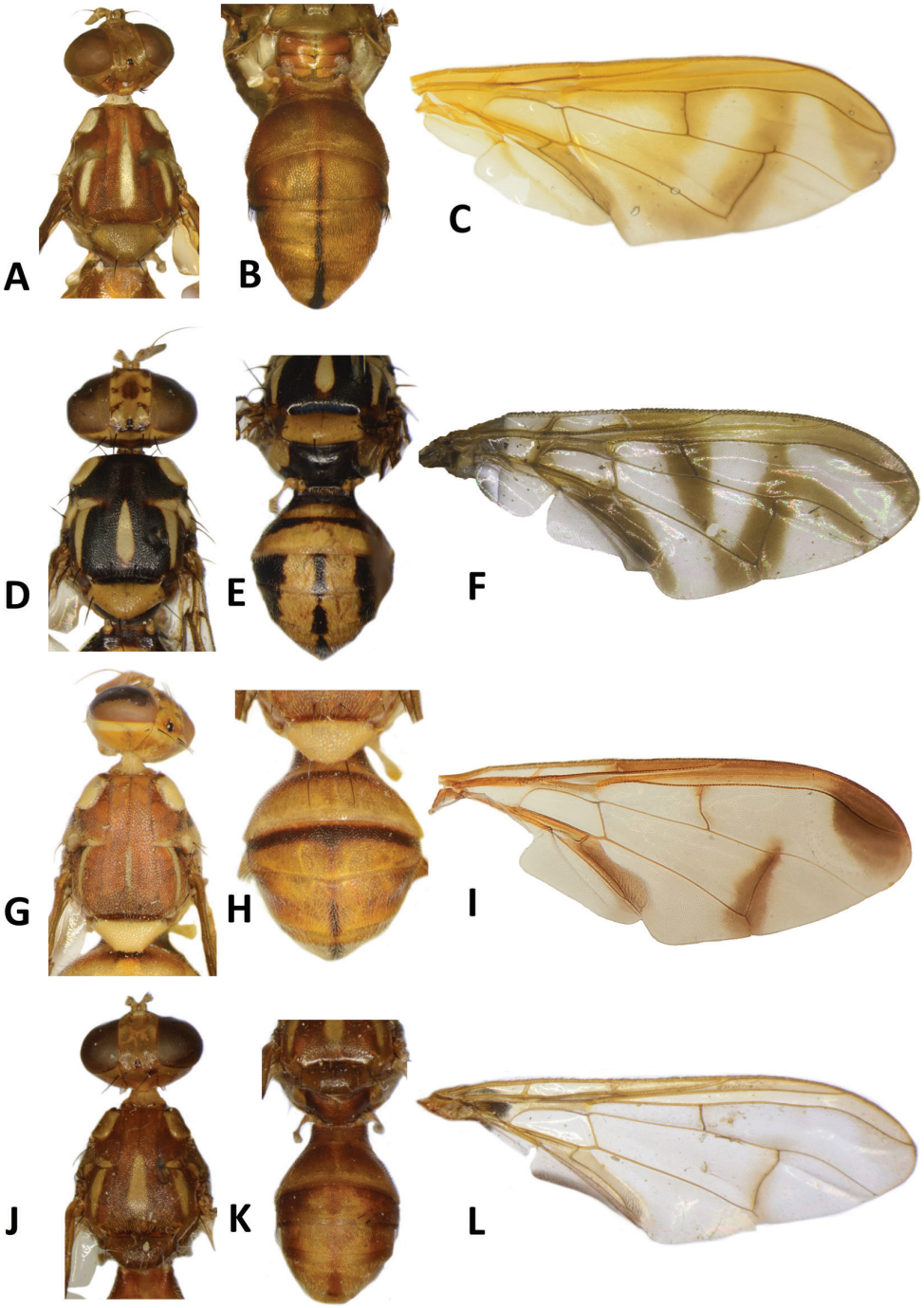

Figure 19. *Zeugodacus hamaceki* Drew & Romig **A** head and scutum **B** abdomen **C** wing. *Zeugodacus amoenus* (Drew) **D** head and scutum **E** abdomen **F** wing. *Zeugodacus cucurbitae* (Coquillett) **G** head and scutum **H** abdomen **I** wing. *Zeugodacus fuscipennulus* (Drew & Romig) **G** head and scutum **H** abdomen **I** wing.

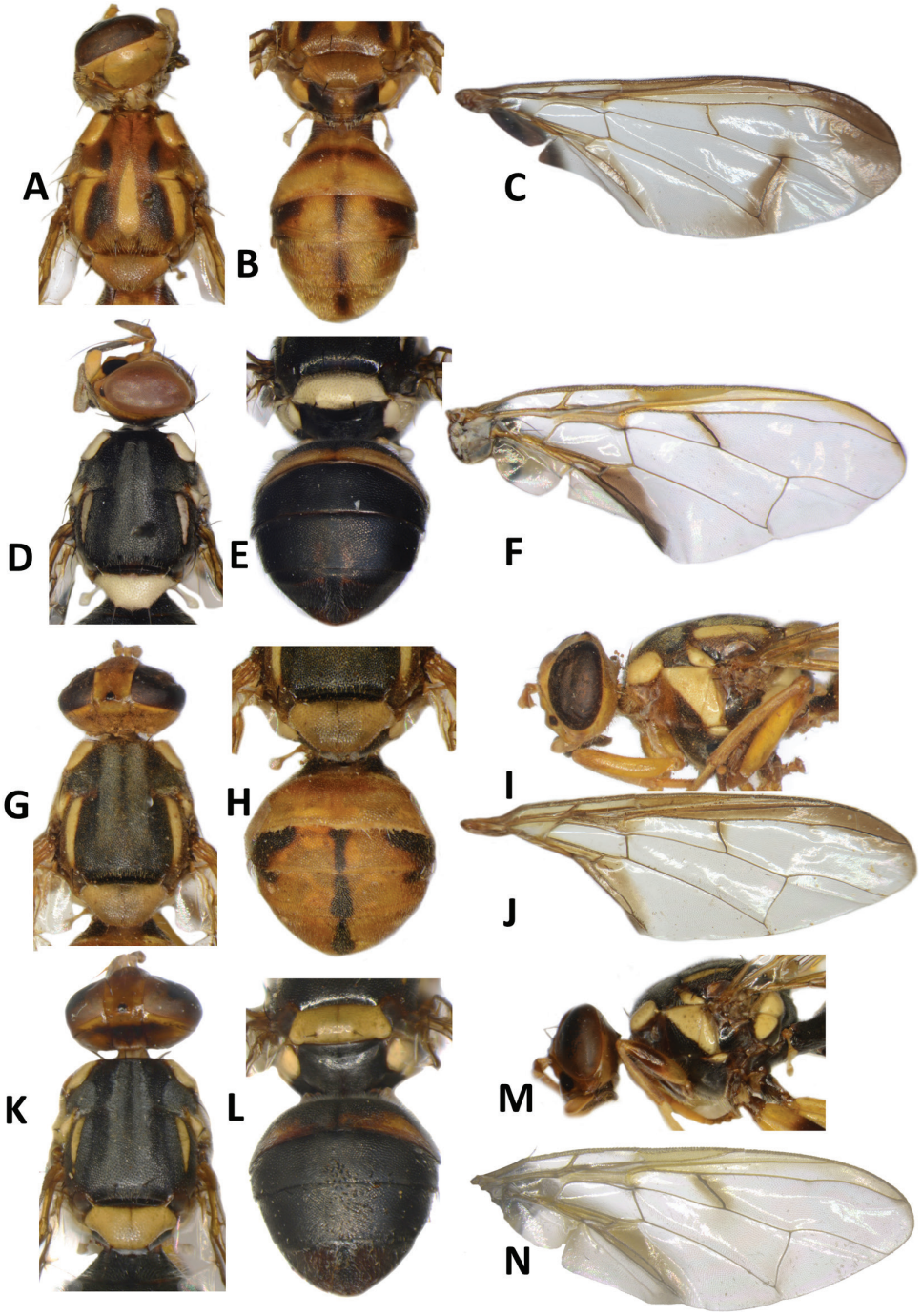

Figure 20. *Zeugodacus abdoangustus* (Drew) **A** head and scutum **B** abdomen **C** wing. *Bactrocera melanogaster* Drew **D** head and scutum **E** abdomen **F** wing. *Bactrocera phaea* (Drew) **G** head and scutum **H** abdomen **I** lateral view **J** wing. *Bactrocera neonigrita* Drew **K** head and scutum **L** abdomen **M** lateral view **N** wing.

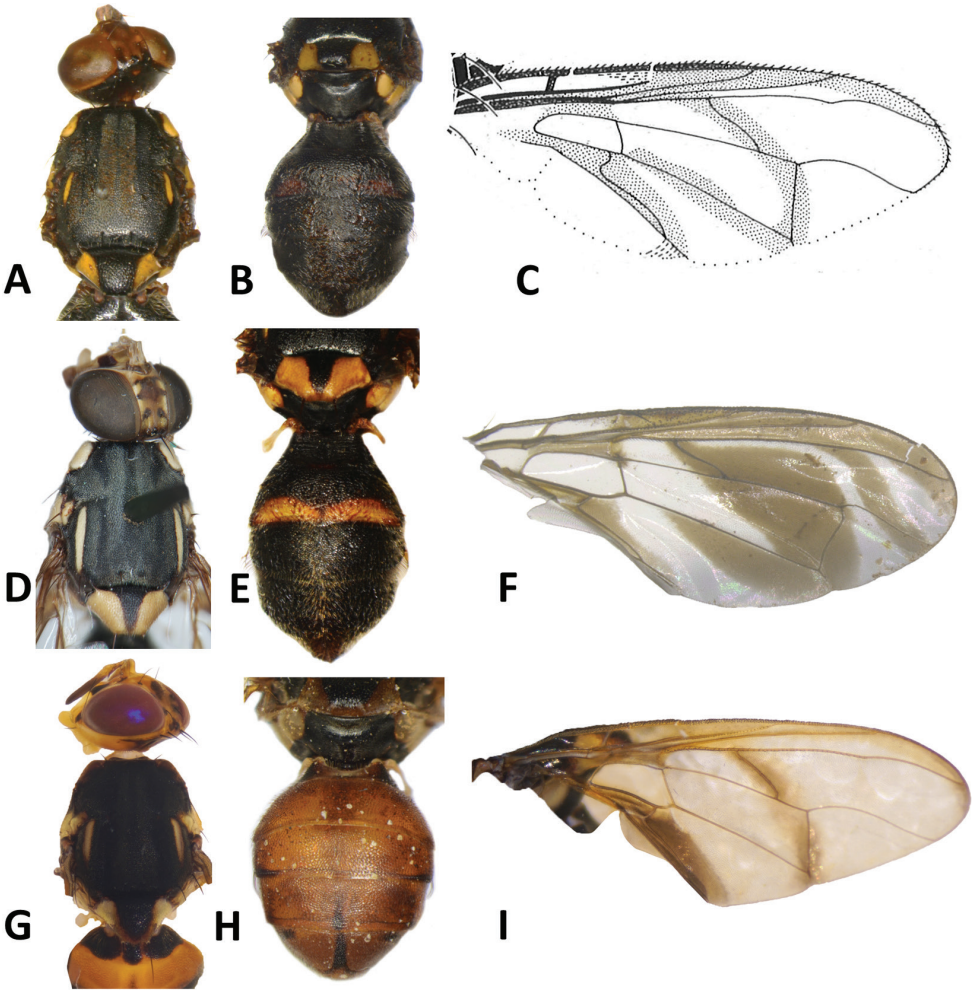

Figure 21. *Bactrocera reclinata* Drew **A** head and scutum **B** abdomen **C** wing (reproduced from Drew 1989). *Bactrocera longicornis* Macquart **D** head and scutum **E** abdomen **F** wing. *Bactrocera hollingsworthi* Drew & Romig **G** head and scutum **H** abdomen **I** wing.

In addition to the data from this survey, we summarized trapping data in the Solomon Islands generated during the Regional Fruit Fly Projects in the Pacific, as a further indication of the relative abundance and to update the distribution of each species (Table 1). Over 1.8 million flies were collected from 180 sites maintained throughout the archipelago between 1994 and 2001 (Vagalo et al. 1997; Drew and Romig 2001; Hollingsworth et al. 2003; Leblanc et al. 2012). A few specimens of then undescribed *B. geminosimulata* and *B. quasienochra* may have been included among these records.

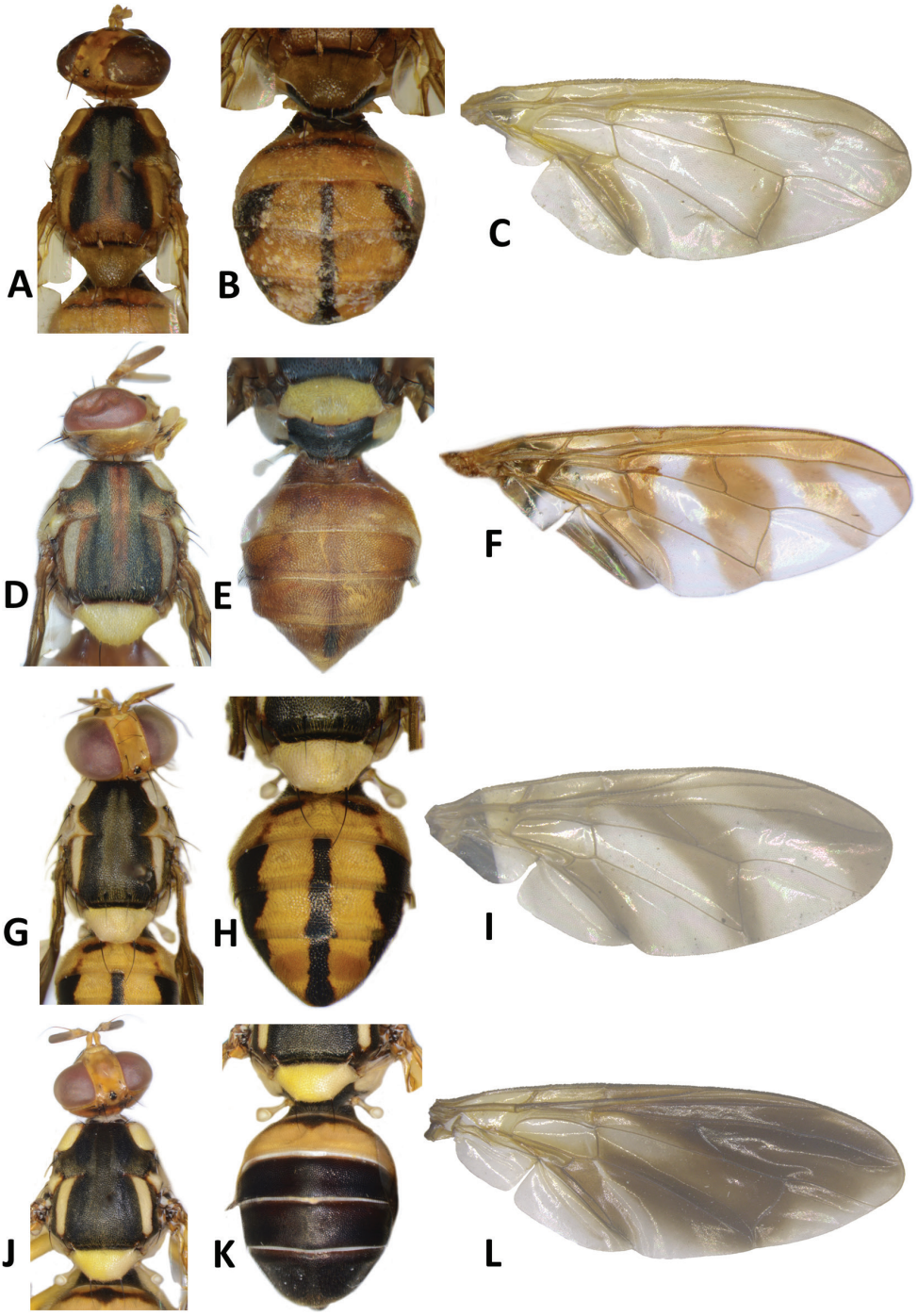

Figure 22. *Bactrocera unitaeniola* Drew & Romig **A** head and scutum **B** abdomen **C** wing. *Bactrocera umbrosa* (Fabricius) **D** head and scutum **E** abdomen **F** wing. *Bactrocera unifasciata* (Malloch) **G** head and scutum **H** abdomen **I** wing. *Bactrocera pepisalae* (Froggatt) **J** head and scutum **K** abdomen **L** wing.

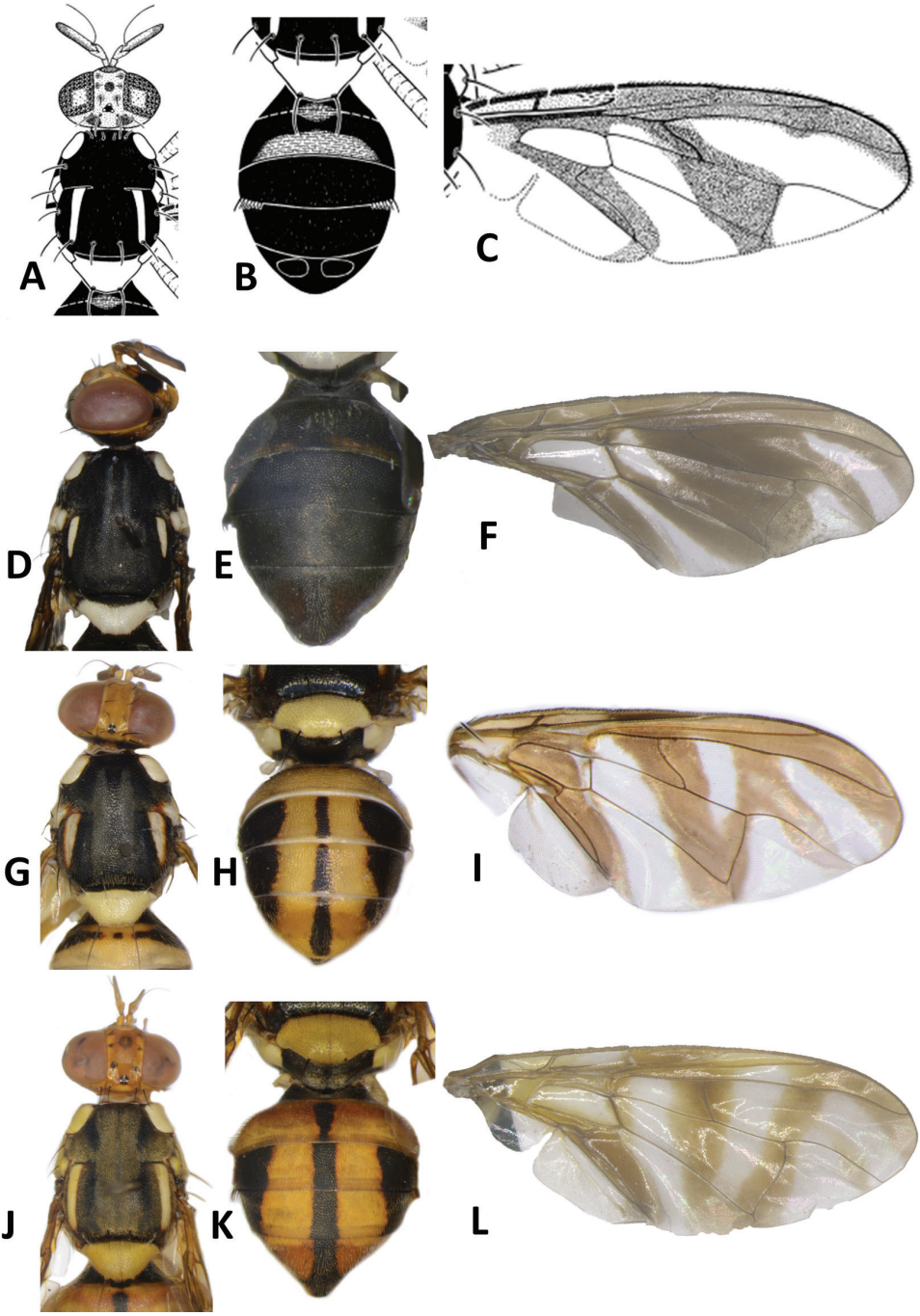

Figure 23. *Bactrocera obliquivenosa* Drew & Romig (reproduced from Drew and Romig 2001) **A** head and scutum **B** abdomen **C** wing. *Bactrocera biarcuata* (Walker) **D** head and scutum **E** abdomen **F** wing. *Bactrocera nigrescentis* (Drew) **G** head and scutum **H** abdomen **I** wing. *Bactrocera redunca* (Drew) **J** head and scutum **K** abdomen **L** wing.

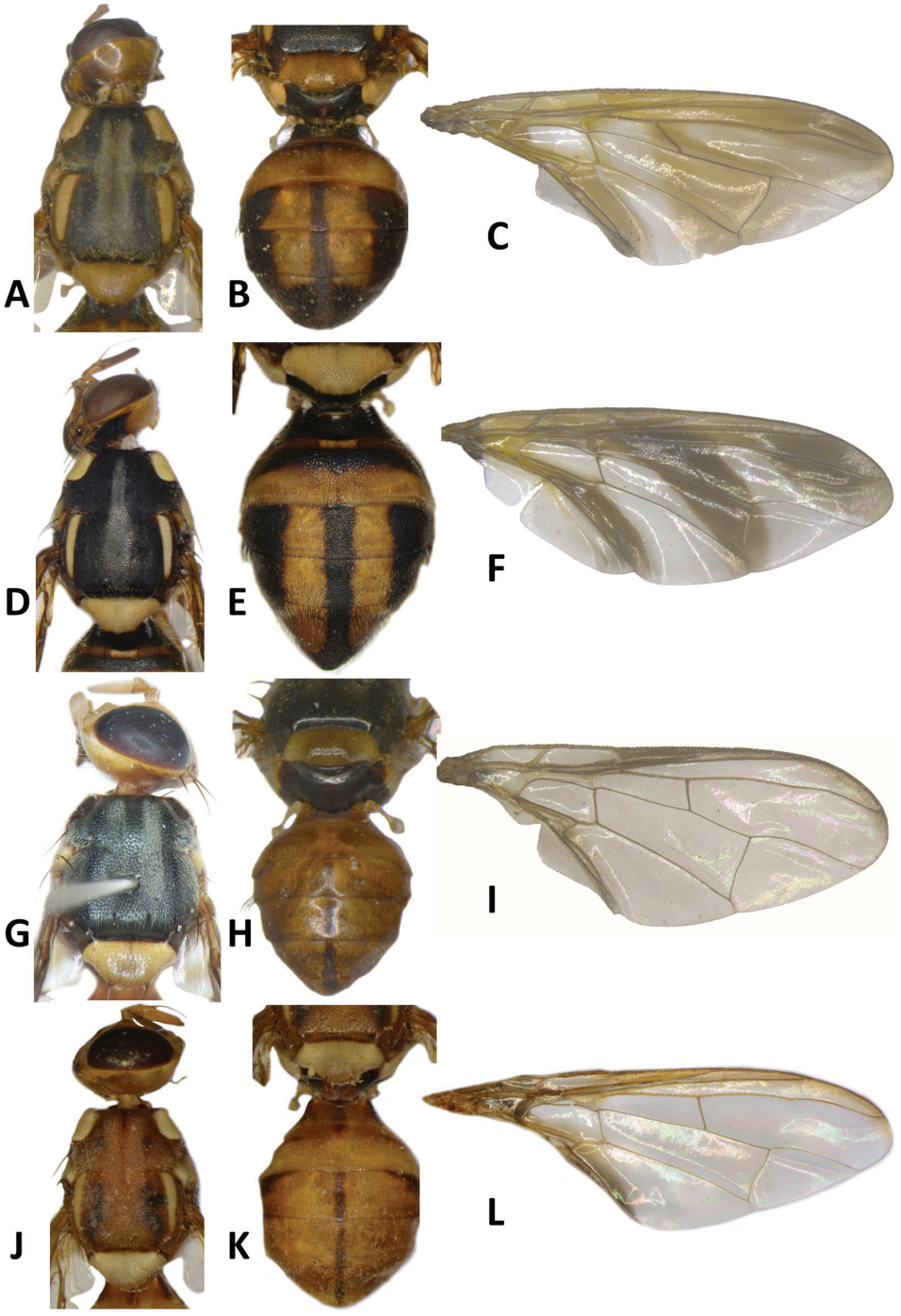

Figure 24. *Bactrocera confluens* (Drew) **A** head and scutum **B** abdomen **C** wing. *Bactrocera decumana* (Drew) **D** head and scutum **E** abdomen **F** wing. *Bactrocera minuta* (Drew) **G** head and scutum **H** abdomen **I** wing. *Bactrocera naucleae* (Drew & Romig) **J** head and scutum **K** abdomen **L** wing.

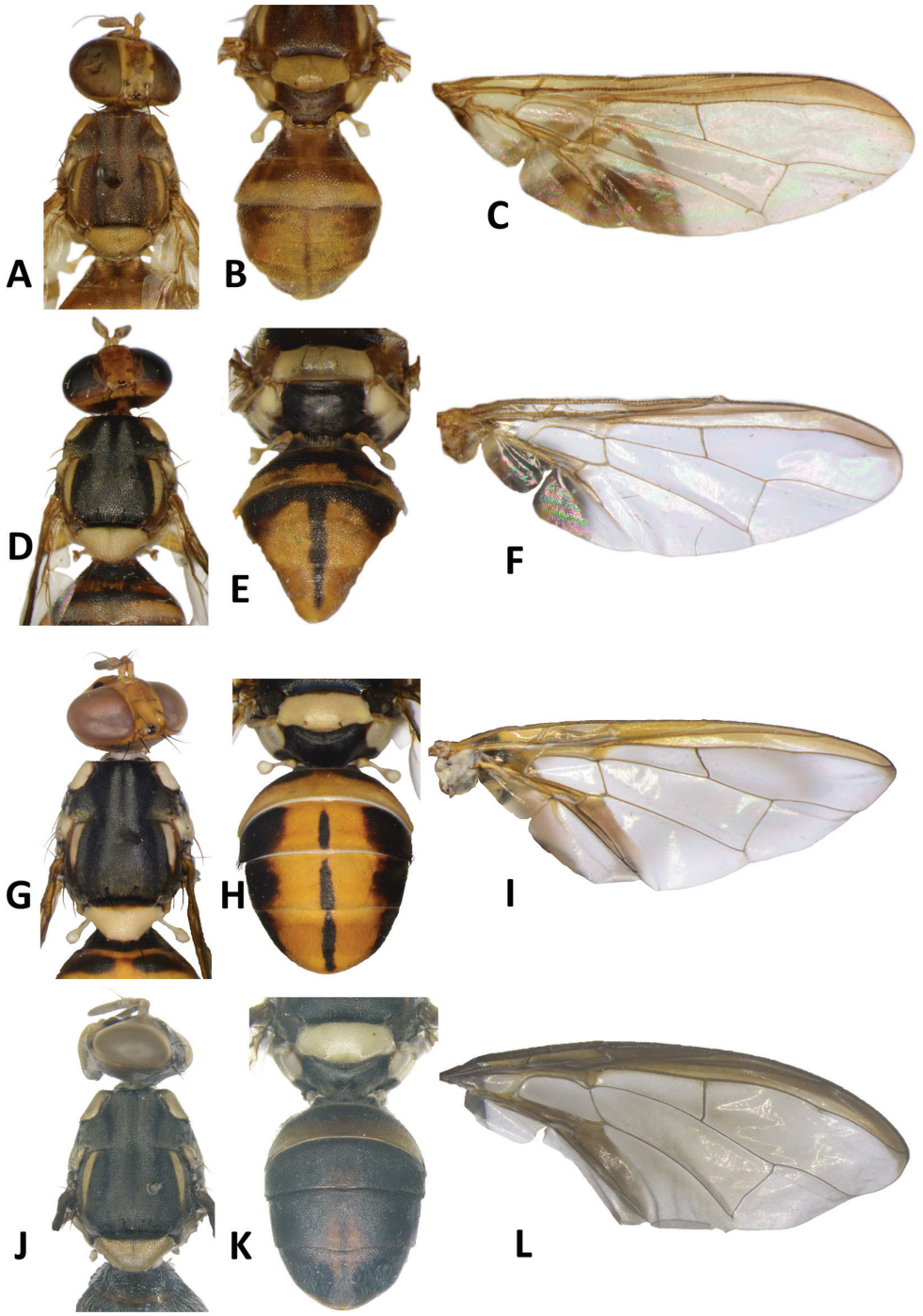

Figure 25. *Bactrocera hastigerina* (Hardy) **A** head and scutum **B** abdomen **C** wing. *Bactrocera calophylli* (Perkins & May) **D** head and scutum **E** abdomen **F** wing. *Bactrocera froggatti* (Bezzi) **G** head and scutum **H** abdomen **I** wing. *Bactrocera quadrisetosa* (Bezzi) **J** head and scutum **K** abdomen **L** wing.

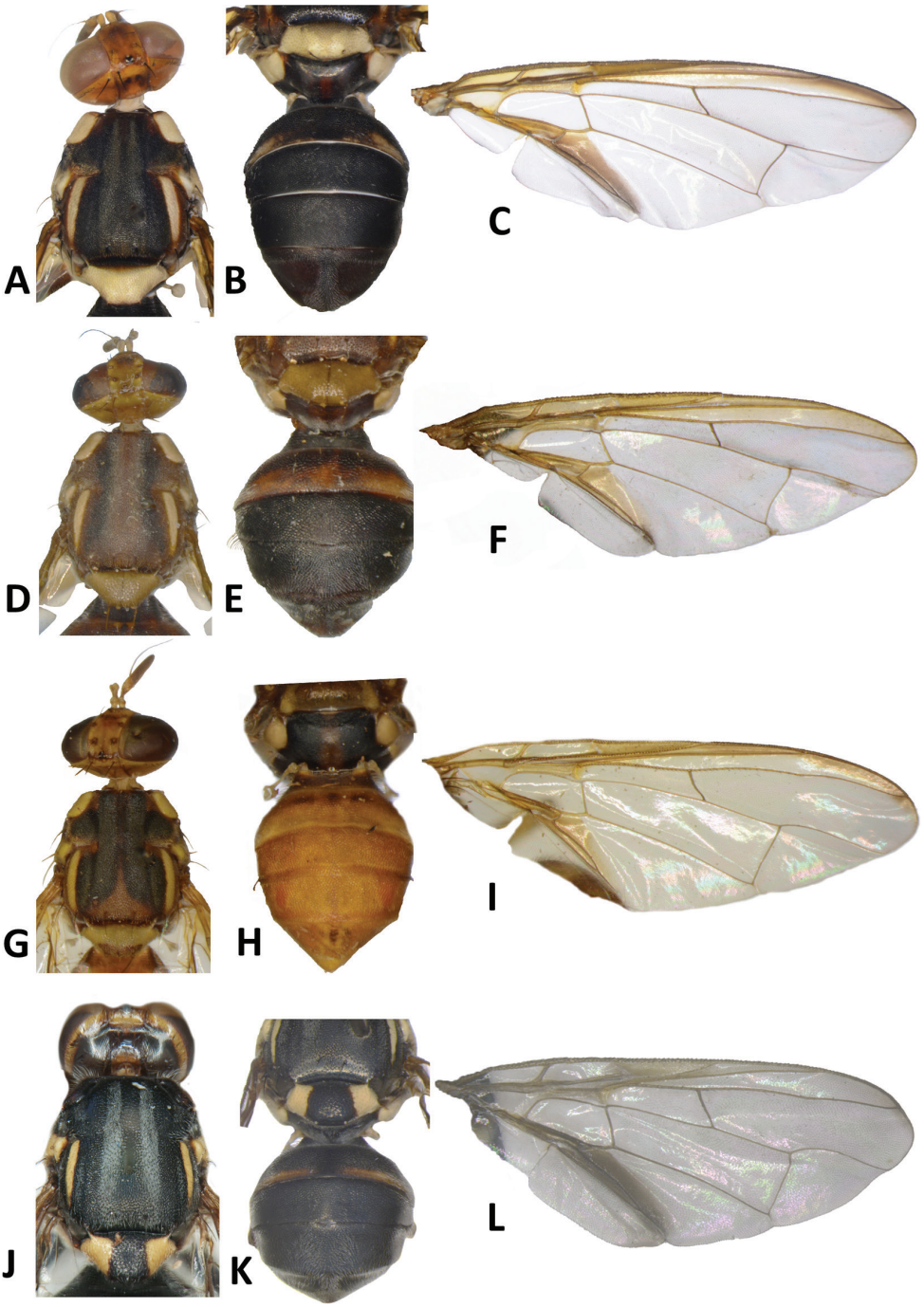

Figure 26. *Bactrocera epicharis* (Hardy) **A** head and scutum **B** abdomen **C** wing. *Bactrocera atrabifasciata* Drew & Romig **D** head and scutum **E** abdomen **F** wing. *Bactrocera bancroftii* (Tryon) (specimen from Australia) **G** head and scutum **H** abdomen **I** wing. *Bactrocera picea* (Drew) **J** head and scutum **K** abdomen **L** wing.

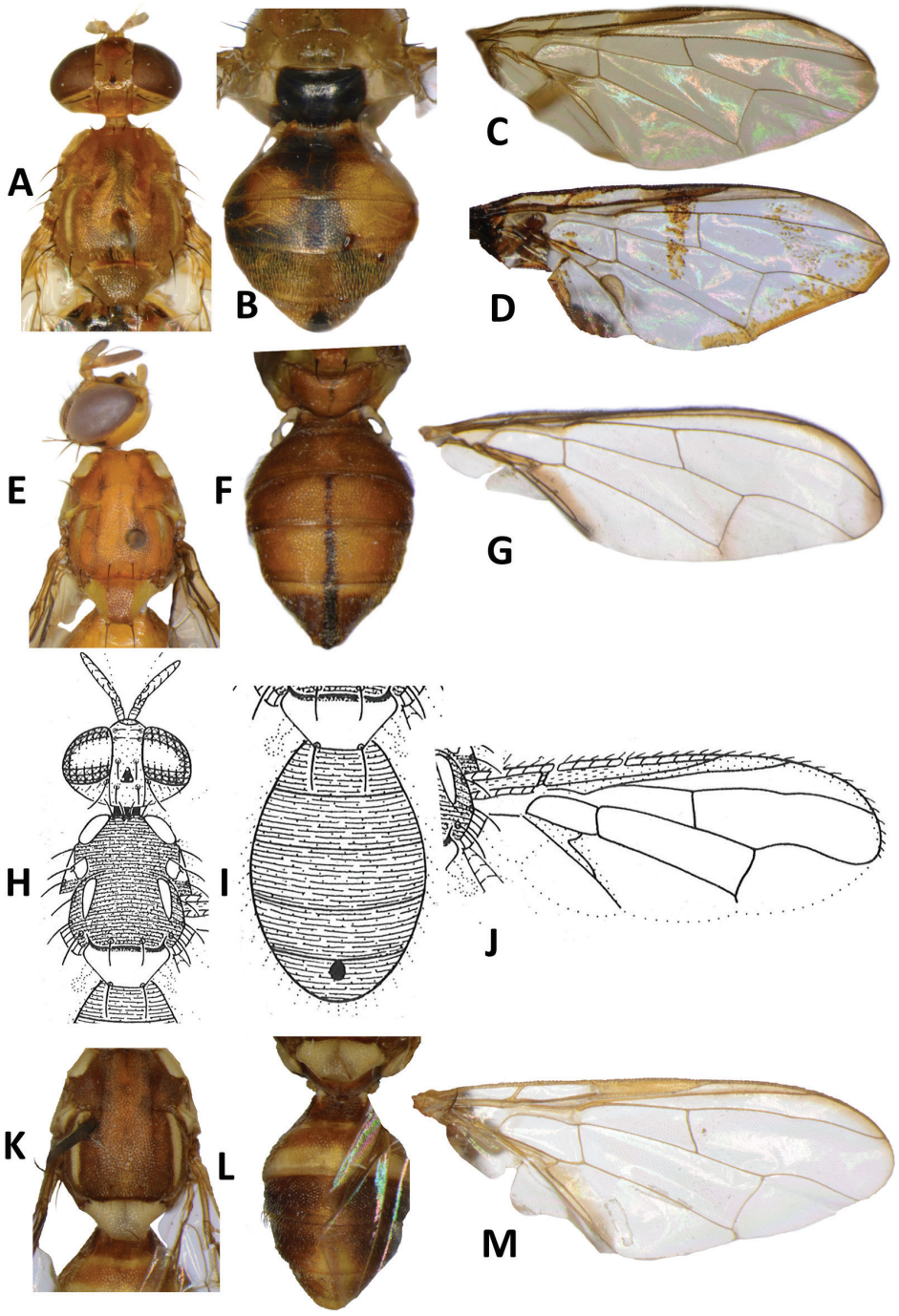

Figure 27. *Bactrocera pacificae* Drew & Romig **A** head and scutum **B** abdomen **C** female wing **D** male wing. *Bactrocera buinensis* Drew **E** head and scutum **F** abdomen **G** wing. *Bactrocera unipunctata* (Malloch) (reproduced from Drew 1989) **H** head and scutum **I** abdomen **J** wing. *Bactrocera aithogaster* Drew **K** scutum **L** abdomen **M** wing.

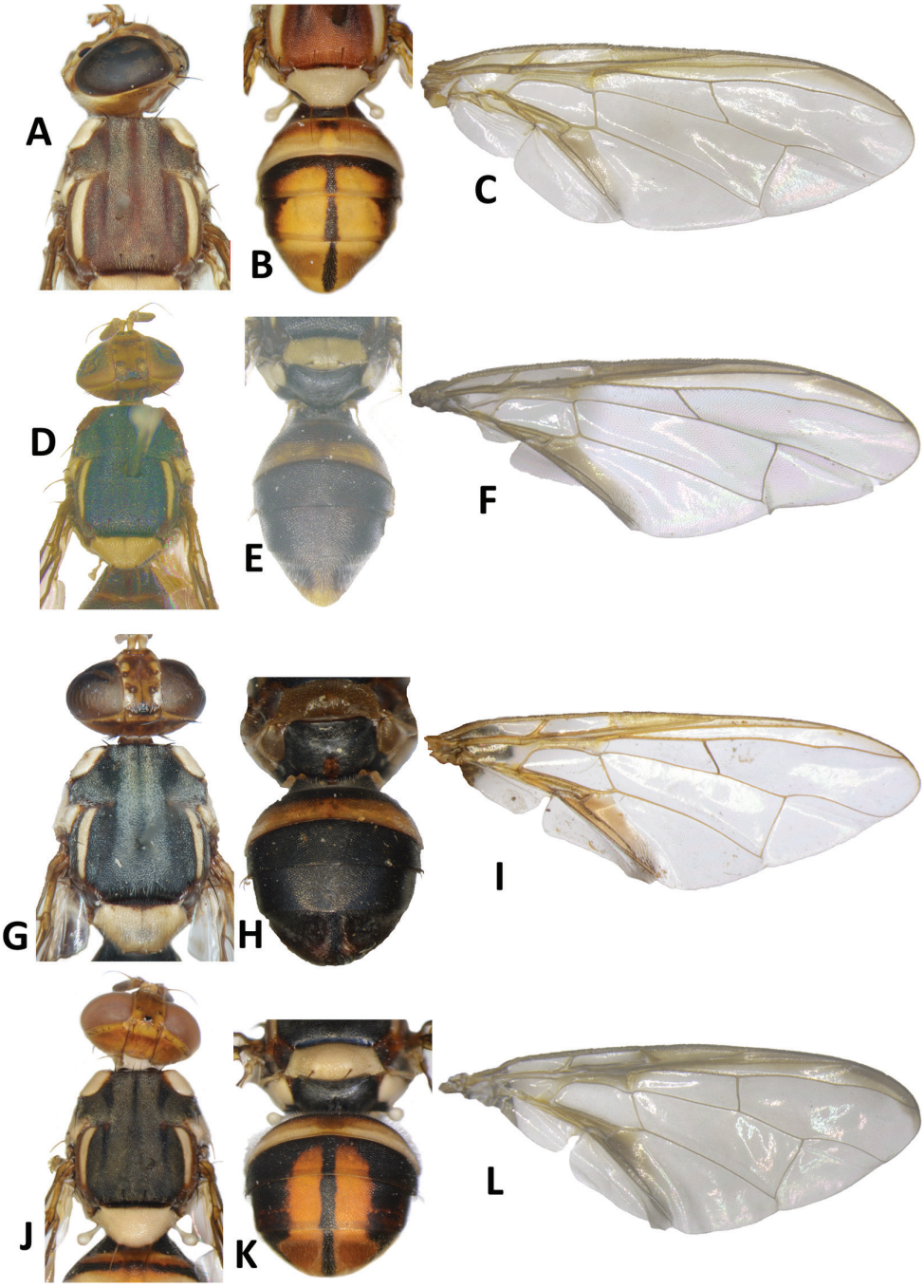

Figure 28. *Bactrocera moluccensis* (Perkins) **A** head and scutum **B** abdomen **C** wing. *Bactrocera furvescens* Drew **D** head and scutum **E** abdomen **F** wing. *Bactrocera aterrima* (Drew) **G** head and scutum **H** abdomen **I** wing. *Bactrocera parafroggatti* Drew & Romig **J** head and scutum **K** abdomen **L** wing.

Table 1. Checklist of Dacine fruit flies of Solomon Islands, including number of specimens collected during the Regional Fruit Fly Projects (1994–2001) and the 2018 survey. References to earliest record for each group on islands are: A: Macquart 1835, B: Froggatt 1910, C: Bezzi 1919, D: Malloch 1939, E: Hardy 1954, F: Drew 1972, G: Drew 1974, H: Eta 1985, I: Drew 1989, J: Waterhouse 1993; K: Hollingsworth et. al. 1997, L: Drew and Romig 2001, new: previously unpublished or new record, W: widespread species.

Species	Lure	# trapped Solomon Islands (1994–2001)	# trapped Gizo (2018)	# trapped Kolombangara (2018)	# trapped Guadalcanal (2018)	Shortland Group	Choiseul	Vella Lavella	Gizo	Kolombangara	New Georgia	Isabel	Russell	Florida (Ngella & Savo)	Guadalcanal	Malaita	San Cristobal	Rennell & Bellona	Santa Cruz	Reef Islands
BACTROCERA																				
B. aithogaster Drew, 1989	No known lure														I					
B. *allodistincta* Leblanc & Doorenweerd	Cue-lure				12										new					
B. aterrima (Drew, 1972)	Cue-lure	10			1	I	L			L		L			new					
B. atrabifasciata Drew & Romig, 2001	Cue-lure	14	1		1	L			L			L		L	new					
B. bancroftii (Tryon, 1927)	Methyl eugenol	118													L					
B. biarcuata (Walker, 1865)	Methyl eugenol	299		28	3	I	L		L	L	L	L	L	L	L		L			
B. buinensis Drew, 1989	Cue-lure	16		163			L			L					new		new			
B. calophylli (Perkins & May, 1949)	No known lure	bred from fruit													L					
B. confluens (Drew, 1971)	Methyl eugenol	412			1		new			new				L	I	new				
B. decumana (Drew, 1972)	Cue-lure	1,226		208		I	L	L	L	L		L	L	L	L	L	L			
B. enochra (Drew, 1972)	Cue-lure	33	1	19	1	F			new	L		L			L					
B. epicharis (Hardy, 1970)	Cue-lure	168		119	48	I	new			L		new		L	L	L				
B. frauenfeldi (Schiner, 1868)	Cue-lure, zingerone	1,271,832	1686	921	4636	W	W	W	W	W	W	W	D	W	W	W	W	W	W	W
B. froggatti (Bezzi, 1928)	Methyl eugenol	33,514	36	983	1236	I	L	L	G	L	L	L	C	D	D	L	L	L		
B. furvescens Drew, 1989	Cue-lure														I					
B. geminosimulata Leblanc & Doorenweerd	Cue-lure				14										new					
B. hastigerina (Hardy, 1954)	No known lure	bred from fruit													L					
B. hollingsworthi Drew & Romig, 2001	Cue-lure	5		1						new									L	
B. *kolombangarae* Leblanc & Doorenweerd	Zingerone			18	1					new					new					
B. longicornis Macquart, 1835	Cue-lure											A								

Species	Lure	# trapped Solomon Islands (1994–2001)	# trapped Gizo (2018)	# trapped Kolombangara (2018)	# trapped Guadalcanal (2018)	Shortland Group	Choiseul	Vella Lavella	Gizo	Kolombangara	New Georgia	Isabel	Russell	Florida (Ngella & Savo)	Guadalcanal	Malaita	San Cristobal	Rennell & Bellona	Santa Cruz	Reef Islands
B. melanogaster Drew, 1989	Methyl eugenol	820		2	10	new	I	new	new	I	I	I	I	I	I					
B. minuta (Drew, 1971)	Cue-lure	45																	L	
B. moluccensis (Perkins, 1939)	Cue-lure	71,499	9	5	435	L	L	L	L	L	L	L	L	L	L	L	L	L	L	
B. morula Drew, 1989	Cue-lure	861			1202				L						I		L			
B. naucleae Drew & Romig, 2001	Methyl eugenol	130					L					L			L					
B. neonigrita Drew, 1989	Methyl eugenol					I														
B. nigrescentis (Drew, 1971)	Cue-lure	279	1	32	331		L	L	new	new	new	L		L	L			L	L	
B. obliquivenosa Drew & Romig, 2001	Methyl eugenol	1								L										
B. pacificae Drew & Romig, 2001	No known lure	bred from fruit													L				L	
B. pagdeni (Malloch, 1939)	Zingerone			718	456					new				D	new					
B. parafroggatti Drew & Romig, 2001	Methyl eugenol	1,645			85		L			new	L	L		L	L		L	L		
B. penefurva Drew, 1989	No known lure	bred from fruit													I					
B. pepisalae (Froggatt, 1910)	Methyl eugenol	7,746			35	new	L	E		L	L	L	B	D	G	L	G			
B. phaea (Drew, 1971)	Cue-lure	97										L		L	L					
B. picea (Drew, 1972)	Methyl eugenol	726		227	19	I	L	L	L	L	L	L	I	L	L	new				
B. pseudodistincta (Drew, 1971)	Cue-lure	433		5			L			L		L		L	L	L	L	L	L	
B. quadrisetosa (Bezzi, 1928)	Dihydroeugenol, isoeugenol	bred from fruit									L			D	I				L	
B. *quasienochra* Leblanc & Doorenweerd	Cue-lure				1										new					
B. reclinata Drew, 1989	Methyl eugenol	1													L					
B. redunca (Drew, 1971)	Cue-lure	7,031			524	I	L			L		L	L	L	L	L	new		L	
B. simulata (Malloch, 1939)	Cue-lure	32,810		16	350	I	L	L	L	L	I	L	L	D	I	L	L	L	L	
B. *tsatsiae* Leblanc & Doorenweerd	Zingerone			20	9					new					new					
B. umbrosa (Fabricius, 1805)	Methyl eugenol	362,783	157	170	1296	new	W	W	W	W	W	W	W	D	W	W	W	W	D	W
B. unifasciata (Malloch, 1939)	Cue-lure	5		1	18					new		L			D					
B. unipunctata (Malloch, 1939)	No known lure													D						
B. unitaeniola Drew & Romig, 2001	Cue-lure	13					L					L			L					

Species	Lure	# trapped Solomon Islands (1994–2001)	# trapped Gizo (2018)	# trapped Kolombangara (2018)	# trapped Guadalcanal (2018)	Shortland Group	Choiseul	Vella Lavella	Gizo	Kolombangara	New Georgia	Isabel	Russell	Florida (Ngella & Savo)	Guadalcanal	Malaita	San Cristobal	Rennell & Bellona	Santa Cruz	Reef Islands
B. *vargasi* Leblanc & Doorenweerd	Zingerone			9	34					new					new					
DACUS																				
D. solomonensis Malloch, 1939	Cue-lure	23,085			60		L			new	L	L	L	L	D	L	L			
ZEUGODACUS																				
Z. abdoangustus (Drew, 1972)	Cue-lure	38			11							L			L	L				
Z. amoenus (Drew, 1972)	Cue-lure	3										L								
Z. cucurbitae (Coquillett, 1899)	Cue-lure, zingerone	43,294	7	305	44	H	J	J	J	J	J	J	K		K	K				
Z. fuscipennulus (Drew & Romig, 2001)	Cue-lure	101		1						L	new	new			L		new			
Z. hamaceki (Drew & Romig, 2001)	Cue-lure	115			5					L		L			L					
Z. univittatus (Drew, 1972)	Cue-lure	118			95					new		L			L		L			

Acknowledgements

Funding for this project was provided by the United States Department of Agriculture (USDA) Farm Bill Section 10007 Plant Pest and Disease Management and Disaster Prevention Program in support of suggestion "Genomic approaches to fruit fly exclusion and pathway analysis, FB3.0292.04-FY19". These funds were managed as cooperative agreements between USDA Animal and Plant Health Inspection Service and the University of Hawaii's College of Tropical Agriculture and Human Resources (AP20PPQS&T00C076) and the University of Idaho's College of Agriculture and Life Sciences (AP19PPQ&T00C084). We are very thankful to Roy Vaketo (Solomon Islands Ministry of Agriculture) for his invaluable assistance during the field collecting and to Kolombangara Forest Products Ltd for granting us access to their protected forest areas. Photographs were edited for publication by Ellie Hitchings (University of Idaho).

References

Allwood AJ, Drew RAI [Eds] (1997) Management of fruit flies in the Pacific. ACIAR Proceedings No 76.

Allwood AJ (2000) Regional approach to the management of fruit flies in the Pacific Island countries and territories. In: Tan KH (Ed.) Area-wide control of fruit flies and other insect pests. USM Press, Penang, 439–448.

Bezzi M (1919) Fruit flies of the genus *Dacus* sensu latiore (Diptera) from the Philippine Islands. Philippine Journal of Science 15: 411–443.

Colwell RK (2019) EstimateS: Statistical estimation of species richness and shared species from samples. Version 9.1.0 User's Guide and application. http://viceroy.eeb.uconn.edu/estimates/ [Accessed August 2020]

De Meyer M, Clarke A, Vera, T, Hendrichs J (2015) Resolution of cryptic species complexes of tephritid pests to enhance SIT application and facilitate international trade. ZooKeys 540: 1–557. https://doi.org/10.3897/zookeys.540.6506

Doorenweerd C, Leblanc L, Norrbom AL, San Jose M, Rubinoff R (2018) A global checklist of the 932 fruit fly species in the tribe Dacini (Diptera, Tephritidae). ZooKeys 730: 17–54. https://doi.org/10.3897/zookeys.730.21786

Doorenweerd C, Jose MS, Leblanc L, Barr N, Geib S, Chung AYC, Dupuis J, Ekayanti A, Fiegalan ER, Hemachandra KS, Chia-lung MAH (2020) DNA barcodes and reliable molecular identifications in a diverse group of invasive pests: lessons from *Bactrocera* fruit flies on variation across the COI gene, introgression, and standardization. bioRxiv. https://doi.org/10.1101/2020.11.23.394510

Drew RAI (1972) Additions to the species of Dacini (Diptera: Tephritidae) from the South Pacific area with keys to species. Journal of the Australian Entomological Society 11: 185–231. https://doi.org/10.1111/j.1440-6055.1972.tb01621.x

Drew RAI (1974) Revised descriptions of species of Dacini (Diptera: Tephritidae) from the South Pacific area. II. The *Strumeta* group of subgenera of genus *Dacus*. Queensland Department of Primary Industries, Division of Plant Industry. Bulletin 653: 1–101.

Drew RAI (1989) The tropical fruit flies (Diptera: Tephritidae: Dacinae) of the Australasian and Oceanian regions. Memoirs of the Queensland Museum 26: 1–521.

Drew RAI, Romig M (2001) The fruit fly fauna (Diptera: Tephritidae: Dacinae) of Bougainville, the Solomon Islands and Vanuatu. Australian Journal of Entomology 40: 113–150. https://doi.org/10.1046/j.1440-6055.2001.00222.x

Drew RAI, Ma J, Smith S, Hughes JM (2011) The taxonomy and phylogenetic relationships of species in the *Bactrocera musae* complex of fruit flies (Diptera: Tephritidae: Dacinae) in Papua New Guinea. Raffles Bulletin of Zoology 59: 145–162.

Drew RAI, Hancock DL (2016) A review of the subgenus *Bulladacus* Drew & Hancock of *Bactrocera* Macquart (Diptera: Tephritidae: Dacinae), with description of two new species from Papua New Guinea. Australian Entomologist 43: 189–210.

Dupuis JR, Bremer FT, Kauwe A, San Jose M, Leblanc L, Rubinoff D, Geib S (2017) HiMAP: Robust phylogenomics from highly multiplexed amplicon sequencing. bioRxiv. https://doi.org/10.1101/213454

Eta CR (1985) Eradication of the melon fly from Shortland Islands, Western province, Solomon Islands (special report). Solomon Islands Agricultural Quarantine Service, Annual Report, Ministry of Agriculture and lands, Honiara, 14–23.

Froggatt WW (1910) Notes on fruit-flies (Trypetidae) with descriptions of new species. Proceedings of the Linnaean Society of New South Wales 35: 862–872. https://doi.org/10.5962/bhl.part.25563

Hancock DL (2015) A new subgenus for six Indo-Australian species of *Bactrocera* Macquart (Diptera: Tephritidae: Dacinae) and subgeneric transfer of four other species. Australian Entomologist 42: 39–44.

Hancock DL, Drew RAI (2015) A review of the Indo-Australian subgenus *Parazeugodacus* Shiraki of *Bactrocera* Macquart (Diptera: Tephritidae: Dacinae). Australian Entomologist 42: 91–104.

Hancock DL, Drew RAI (2018a) A review of the subgenera *Apodacus* Perkins, *Hemizeugodacus* Hardy, *Neozeugodacus* May, stat. rev., *Semicallantra* Drew and *Tetradacus* Miyake of *Bactrocera* Macquart (Diptera: Tephritidae: Dacinae). Australian Entomologist 45: 105–132.

Hancock DL, Drew RAI (2018b) A review of the subgenus *Zeugodacus* Hendel of *Bactrocera* Macquart (Diptera: Tephritidae: Dacinae): an integrative approach. Australian Entomologist 45: 251–272.

Hardy DE (1954) The *Dacus* subgenera *Neodacus* and *Gymnodacus* of the world. Proceedings of the Entomological Society of Washington 56: 5–23.

Hollingsworth RG, Vagalo M, Tsatsia F (1997) Biology of melon fly, with special reference to Solomon Islands. In: Allwood AJ, Drew RAI (Eds) Management of fruit flies in the Pacific. ACIAR Proceedings No 76: 140–144. https://aciar.gov.au/publication/technical-publications/management-fruit-flies-pacific-0

Hollingsworth RG, Drew RAI, Allwood AJ, Romig M, Vagalo M, Tsatsia F (2003) Host plants and relative abundance of fruit fly (Diptera: Tephritidae) species in the Solomon Islands. Australian Journal of Entomology 42: 95–108. https://doi.org/10.1046/j.1440-6055.2003.00337.x

Krosch MN, Schutze MK, Armstrong KF, Graham G, Yeates DK, Clarke AR (2012) A molecular phylogeny for the Tribe Dacini (Diptera: Tephritidae): Systematic and biogeographic implications. Molecular Phylogenetics and Evolution 64: 513–523. https://doi.org/10.1016/j.ympev.2012.05.006

Leblanc L, Tora Vueti E, Drew RAI, Allwood AJ (2012) Host plant records for fruit flies (Diptera: Tephritidae: Dacini) in the Pacific Islands. Proceedings of the Hawaiian Entomological Society 44: 11–53. http://hdl.handle.net/10125/25459

Leblanc L, Fay H, Sengebau F, San Jose M, Rubinoff D, Pereira R (2015) A survey of fruit flies (Diptera: Tephritidae: Dacinae) and their Opiine parasitoids (Hymenoptera: Braconidae) in Palau. Proceedings of the Hawaiian Entomological Society 47: 55–66. http://hdl.handle.net/10125/38673

Lidner B, McLeod P (2008) A review and impact assessment of ACIAR's fruit-fly research partnerships, 1984–2007. Australian Centre for International Agricultural Research (ACIAR). Impact Assessment Series 56. https://aciar.gov.au/publication/technical-publications/review-and-impact-assessment-aciars-fruit-fly-research-partnerships-1984-2007

Macquart J (1835) Histoire naturelle des insectes. Diptères. Volume 2. In: Nouvelles suites à Buffon, formant avec les œuvres de cet auteur, un cours complet d'histoire naturelle. Roret, Paris, 703 pp. https://doi.org/10.5962/bhl.title.14274

Malloch JR (1939) Solomon Islands Trypetidae. The Annals and Magazine of Natural History; Zoology, Botany, and Geology. Series 11, 4: 228–277. https://doi.org/10.1080/00222933908526987

Manrakhan A, Daneel J-H, Beck R, Virgilio M, Meganck K (2017) Efficacy of trapping systems for monitoring of Afrotropical fruit flies. Journal of Applied Entomology 141: 825–840. https://doi.org/10.1111/jen.12373

Ratnasingham S, Hebert PDN (2007) BOLD: The Barcode of Life Data System (www.barcodinglife.org). Molecular Ecology Notes 7: 355–364. https://doi.org/10.1111/j.1471-8286.2007.01678.x

Royer JE, Agovaua S, Bokosou J, Kurika K, Mararuai A, Mayer DG, Niangu B (2018) Responses of fruit flies to new attractants in Papua New Guinea. Austral Entomology 57: 40–49. https://doi.org/10.1111/aen.12269

Royer JE, Mille C, Cazeres S, Brinon J, Mayer DG (2019) Isoeugenol, a more attractive male lure for the Cue-Lure-responsive pest fruit fly *Bactrocera curvipennis* (Diptera: Tephritidae: Dacinae), and new records of species responding to Zingerone in New Caledonia. Journal of Economic Entomology 112: 1502–1507 https://doi.org/10.1093/jee/toz034.

San Jose M, Doorenweerd C, Leblanc L, Barr N, Geib SM, Rubinoff D (2018) Incongruence between molecules and morphology: A seven-gene phylogeny of Dacini fruit flies paves the way for reclassification (Diptera: Tephritidae). Molecular Phylogenetics and Evolution 121: 139–149. https://doi.org/10.1016/j.ympev.2017.12.001

Stark JD, Leblanc L, Mau RFL, Manoukis NC (2018) In memory of Roger Irvin Vargas (1947–2018). Proceedings the Hawaiian Entomological Society 50: v–vii. http://hdl.handle.net/10125/59374

Vagalo M, Hollingsworth RG, Tsatsia F (1997) Fruit fly fauna in Solomon Islands. In: Allwood AJ, Drew RAI (Eds) Management of fruit flies in the Pacific. ACIAR Proceedings No 76: 81–86. https://aciar.gov.au/publication/technical-publications/management-fruit-flies-pacific-0

Vargas RI, Pinero JC, Leblanc L (2015) An overview of pest species of *Bactrocera* fruit flies (Diptera: Tephritidae) and the integration of biopesticides with other biological approaches for their management with a focus on the pacific region. Insects 6: 297–318. https://doi.org/10.3390/insects6020297

Virgilio M, Jordaens K, Verwimp C, White IM, De Meyer M (2015) Higher phylogeny of frugivorous flies (Diptera, Tephritidae, Dacini): localised partition conflicts and a novel generic classification. Molecular Phylogenetics and Evolution 85: 171–179. https://doi.org/10.1016/j.ympev.2015.01.007

Waterhouse DF (1993) Pest fruit flies in the Oceanic Pacific. In: Waterhouse DF (Ed.) Biological control. Pacific Prospects. Supplement 2. ACIAR Monograph No 20: 4–47.

WFO (2021): World Flora Online. Published on the Internet. http://www.worldfloraonline.org [Accessed on: 20 Apr 2021]

White IM, Elson-Harris MM (1992) Fruit Flies of Economic Significance. CABI Publishing, 601 pp.

White IM, Headrick DH, Norrbom AL, Carroll LE (1999) Glossary. In: Aluja M, Norrbom AL (Eds) Fruit flies (Tephritidae): Phylogeny and evolution of behavior. CRC Press, Boca Raton, 881–924. https://doi.org/10.1201/9781420074468.sec8

White IM, Evenhuis NL (1999) New species and records of Indo-Australasian Dacini (Diptera: Tephritidae). The Raffles Bulletin of Zoology 47: 487–540.

Supplementary material 1

Figure S1. COI Phylogeny
Authors: Camiel Doorenweerd
Data type: phylogenetic
Explanation note: Maximum likelihood tree based on COI sequence data, modified from Doorenweerd et al. (2020) to have species / species complexes 'collapsed' into triangles where the horizontal width indicates the maximum pairwise distance of that clade. Newly described species are indicated in green.

Link: https://doi.org/10.3897/zookeys.1057.68375.suppl1

Supplementary material 2

Table S1. Pairwise molecular distance
Authors: Camiel Doorenweerd
Data type: phylogenetic
Explanation note: COI Pairwise distance statistics for the *Bactrocera* included in Doorenweerd et al. (2020), including the species newly described here.

Link: https://doi.org/10.3897/zookeys.1057.68375.suppl2

Supplementary material 3

Figure S2. Number of dacine fruit fly species in relation to island size in the Solomon Islands
Authors: Luc Leblanc, Francis Tsatsia, Camiel Doorenweerd
Data type: pdf. file

Link: https://doi.org/10.3897/zookeys.1057.68375.suppl3

ZooKeys 1057: 105–116 (2021)
doi: 10.3897/zookeys.1057.68175
https://zookeys.pensoft.net

SHORT COMMUNICATION

A peer-reviewed open-access journal
ZooKeys
Launched to accelerate biodiversity research

Synorthocladius federicoi sp. nov., a new species occurring in the middle basin of the Adige River, northern Italy (Diptera, Chironomidae, Orthocladiinae)

Valeria Lencioni[1], Joel Moubayed[2]

1 *Department of Invertebrate Zoology and Hydrobiology, MUSE-Museo delle Scienze, Corso del Lavoro e della Scienza 3, 38122 Trento, Italy* **2** *Freshwater and Marine biology, 10 ruez des Fenouils, 34070 Montpellier, France*

Corresponding author: Valeria Lencioni (valeria.lencioni@muse.it)

Academic editor: Fabio Laurindo da Silva | Received 2 May 2021 | Accepted 22 July 2021 | Published 27 August 2021

http://zoobank.org/88B7FF92-1EFF-47D6-A61C-1402C1C6515D

Citation: Lencioni V, Moubayed J (2021) *Synorthocladius federicoi* sp. nov., a new species occurring in the middle basin of the Adige River, northern Italy (Diptera, Chironomidae, Orthocladiinae). ZooKeys 1057: 105–116. https://doi.org/10.3897/zookeys.1057.68175

Abstract

An adult male *Synorthocladius* was collected in the middle basin of the Adige River in the city of Verona, northern Italy. A combination of atypical characters for the genus signalled a new species. *Synorthocladius federicoi* **sp. nov.** is here diagnosed and described. The new species is known only from its type locality and is presumed to be a local biogeographical representative of the Italian Pre-Alps. An emended generic diagnosis, a key to known *Synorthocladius* from Europe and comments on the taxonomic position of the new species are given.

Keywords

Adige River, Alps, chironomids, orthoclads, adult male, morphology

Introduction

According to data on the taxonomy and geographical distribution of known *Synorthocladius* species from the Palaearctic and neighbouring biogeographical regions (Pankratova 1970; Sasa and Yamamoto 1977; Sasa 1981; Cranston et al. 1989; Reiss 1989; Evrard 1995; Liu and Wang 2005; Langton and Pinder 2007; Lencioni et al. 2011,

2012, 2018; Ashe and O'Connor 2012; Moubayed-Breil and Ashe 2012; Plociennik and Pesic 2012; Sæther and Spies 2013; Plociennik and Karaouzas 2014; Makarchenko and Makarchenko 2017; Kettani and Moubayed-Breil 2018; Murray et al. 2018; Yavorskaya et al. 2018; Rossaro et al. 2019; Moubayed-Breil 2020), there are eight valid species of the genus worldwide, of which only one, *S. semivirens* (Kieffer, 1909), was reported from Europe. The present description of *S. federicoi* sp. nov. increases the total number valid species of *Synorthocladius* from Europe to two.

The emended generic diagnosis of the genus given in Cranston et al. (1989) and Liu and Wang (2005) is reviewed and supplemented with some additional characters found in the adult male of the new species.

Material and methods

The studied adult male was collected using a light trap along the banks of the Adige River (altitude = 61 m a.s.l.; 45°26'58.68"N, 10°58'52.81"E), preserved in 80% ethanol and cleared of musculature in 90% lactic acid for about 70 minutes. When clearing was complete, the material was washed in two changes of 50–60% ethanol to ensure that all traces of lactic acid were removed. It was then mounted in polyvinyl lactophenol. Before the final slide mount (dorsal), the hypopygium including tergite IX, the anal point, the gonocoxite and the gonostylus were viewed ventrally and laterally and all morphological details were drawn from all sides. The rest of the abdomen was preserved in 85% ethanol for possible future DNA analysis. Terminology and measurements follow those of Sæther (1980) and Langton and Pinder (2007). Taxonomic remarks and comments on the ecology of the new species are provided.

Taxonomy

Genus *Synorthocladius* Thienemann, 1935: emended generic diagnosis

Remarks. The generic diagnosis of *Synorthocladius* in Thienemann (1935), emended in Cranston et al. (1989) and Liu and Wang (2005), is here supplemented as follows. ***Head*:** Frontal tubercles present, circular or triangular; coronal triangle reduced or weakly developed; coronal setae present or absent; sensilla coeloconica on palpomere 3 present or absent. Antenna. Last flagellomere simply clubbed, or with bilobed or truncate apex; antennal ratio between 0.5 and 1.0. ***Thorax*:** Acrostichals 0–3, or about 9; scutellum with 2 or 4–6 setae; sensilla chaetica present on tibiae and tarsomeres ta_1–ta_5 of PI–PII, absent on tarsomeres of PIII. ***Abdomen*:** Tergite IX with or without a dorsal hump; anal point slightly to strongly curved upwards. Gonocoxite generally with slender dorsal and ventral inner margin, distinctly broad at base. Virga absent or well developed. Superior volsella flat or broadly swollen. Apex of inferior volsella single or double, long nose-like, lobe-like or truncate, subtriangular or spherical. Gonostylus generally slender to well developed, or atypically globular or bean-shaped as in the new species.

***Synorthocladius federicoi* sp. nov.**
http://zoobank.org/886D9D10-C7F4-4B3D-AA73-CE96DCF7C5E9

Material examined. *Holotype*: adult male, leg. L. Latella; Adige River in the city of Verona, Veneto Region, Italy (altitude = 61 m a.s.l.; 45°26'58.68"N, 10°58'52.81"E); 13 April 2020.

The holotype (on one slide and abdomen in one tube) is deposited in the entomological collection of MUSE-Museo delle Scienze, Trento, Italy (Accession number: cINV0017_s61v73).

Etymology. The new species is named '*federicoi*' after Federico, the first author's son, who has an inherited passion for insects and contributed to the collection of chironomids with the light trap.

Diagnostic characters. *Head*: Frontal tubercles broadly semi-circular, coronal triangle and coronal suture reduced, coronal setae absent; temporals 6; last flagellomere of antenna bilobed apically, with numerous curved sensilla chaetica; AR 0.90. Palpomere 3 without sensilla coeloconica. Clypeus inverted safety helmet shaped, with 5 setae. ***Thorax*:** Lobes of antepronotum not gaping, thinner basally; acrostichals 2; dorsocentrals 7–8, uniserial; prealars 4; humeral pit absent; scutellars 6; squama with 4–5 setae. Legs. Sensilla chaetica on tibiae and tarsomeres ta_1–ta_5 of PI–PII, only on tarsomeres ta_1–ta_5 of PIII. ***Abdomen*:** Tergites II–VI with a unique distribution of setae in two longitudinal rows. Tergite IX broadly semicircular, bearing a hump, posteromedian and caudal areas with 15 setae mostly located close to base of anal point. Anal point triangular, short and sharply pointed, distinctly curving upwards distally. Sternapodeme orally projecting; phallapodeme unusual comma-like. Virga present, branched apically. Gonocoxite with dorsal distal half parallel-sided; ventral side broadly expanded, bearing several stout setae placed in 2 arched rows. Superior volsella swollen. Inferior volsella subtriangular, inwardly projecting into a spherical lobe, which is hyaline and bare. Gonostylus atypically shaped; globular when viewed dorsally, bean-like in ventral view; crista dorsalis absent; megaseta well developed, tongs-like, visible only in dorsal view.

Description. Adult male (n = 1; Figs 1A, C–D, F, H, J, L; 2A, C–I). Medium- to large-sized *Synorthocladius* species. Total length 2.35 mm. Wing length 1.85 mm. TL/WL = 1.27.

***Colouration*.** Blackish species with greenish to brownish legs. Head dark brown including eyes and pedicel; antenna brownish. Thorax with contrasting blackish to dark green mesonotal stripes, area between thoracic stripes greenish; scutellum distinctly contrasting, blackish to brownish. Wing pale brown. Anal segment brown to dark brown with contrasting dark brown to pale gonostylus.

***Head*.** (Fig. 1A). Eyes bare, hairs absent on inner lateral margin; frontal tubercle spherical and well developed; coronal suture reduced, coronal setae absent; temporals 6, uniserial, including 4 inner and 2 outer verticals. Antenna 13-segmented, 790 µm long; last flagellomere (Fig. 1C–D, apical part) 265 µm long, strongly clubbed and bilobed apically, bearing numerous characteristic curved sensilla chaetica; antennal groove begins on segment 3 and reaches the last flagellomere; AR 0.9. Palp 5-segment-

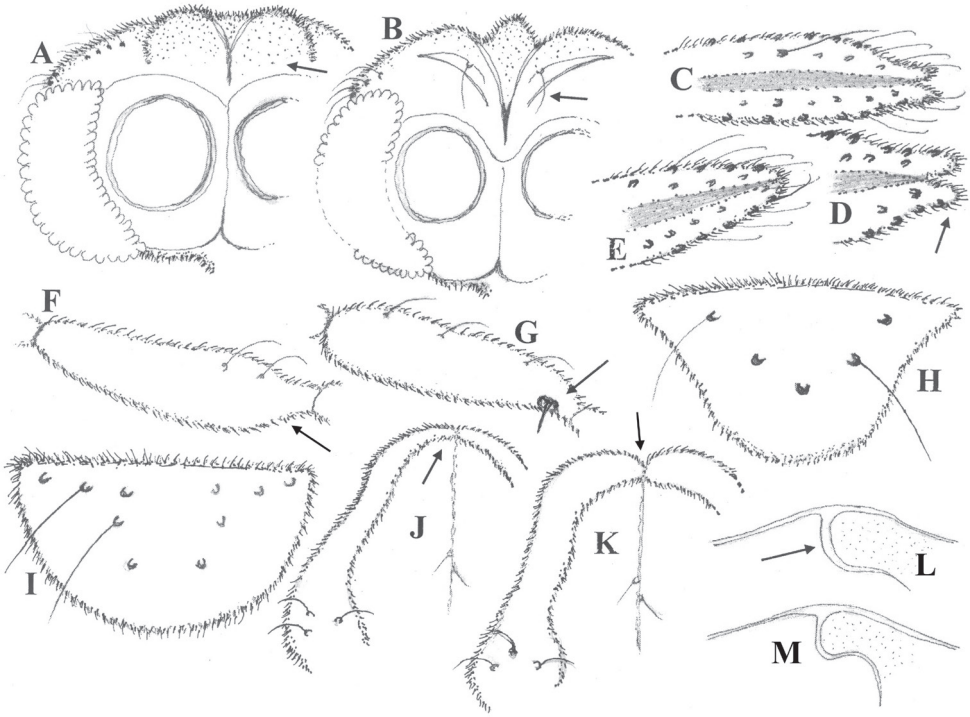

Figure 1. Male imago of *Synorthocladius* spp. Head (dorsal, left side) with vertex, coronal area and temporals of **A** *S. federicoi* sp. nov. **B** *S. semivirens*. Antenna, apex of last flagellomere of **C, D** *S. federicoi* sp. nov. **E** *S. semivirens*. Palpomere 3 of **F** *S. federicoi* sp. nov. **G** *S. semivirens*. Clypeus of **H** *S. federicoi* sp. nov. **I** *S. semivirens*. Lobes of antepronotum and acrostichals of **J** *S. federicoi* sp. nov. **K** *S. semivirens*. Humeral area of **L** *S. federicoi* sp. nov. **M** *S. semivirens*. The arrows indicate some distinguishing characters.

ed, segments 1–2 fused; length (in μm) of segments: 30, 45, 70, 65, 125; palpomere 3 (Fig. 1F) with 2 sensilla clavata, sensilla coeloconica absent. Clypeus (Fig. 1H) inverted safety helmet shaped, with 5 setae in 3 rows.

Thorax. Lobes of antepronotum (Fig. 1J) not gaping and thinner dorsally; acrostichals 2, starting about 150 μm from tip of antepronotum; dorsocentrals 7–8, uniserial; prealars 4; humeral pit absent, notopleural suture (Fig. 1L) with parapsidal fork bent forwards; scutellum with 6 uniserial setae, inserted medially (3 on each side of the midline); preepisternum bare.

Wing. Brachiolum with 1 seta. Number and distribution of setae on veins: R, 5; R_{1+2}, 0; R_{2+3}, 1; remaining veins bare; squama with 4–5 setae in 1 row.

Legs. Femora of PI and PII subequal, tarsomere ta_5 of PI–PIII of same size (100 μm long). Tibial spurs present on PI–PIII; length (in μm) of spurs: 50 (PI), 60 (PII), 25 (PIII); pseudospurs absent. Sensilla chaetica present on tibiae and tarsomeres ta_1–ta_5 of PI–PII, only present on tarsomeres ta_1–ta_5 of PIII. Length (μm) and proportions of legs as in Table 1.

Table 1. *Synorthocladius federicoi* sp. nov. Length (μm) and proportions of prothoracic (PI), mesothoracic (PII) and metathoracic (PIII) legs.

	fe	ti	ta_1	ta_2	ta_3	ta_4	ta_5	LR	BV	SV	BR
PI	625	710	425	355	245	150	100	0.60	2.07	3.14	2.40
PII	645	615	295	175	140	110	100	0.48	2.96	4.27	3.10
PIII	675	745	380	235	190	115	100	0.51	2.81	3.74	2.30

***Abdomen*.** Tergites II–VI (Fig. 2A) with a novel chaetotaxy: two longitudinal rows of setae, 3 to 6 setae on each side of the midline, fewer on tergites V and VI. Hypopygium as in Fig. 2C (dorsal) and G (ventral, with tergite IX, anal point and gonostylus ommited). Tergite IX about 50 μm long and 100 μm maximum width, broadly semi-circular, postero-median and caudal areas with 15 setae (5 located medially, 10 mostly located close to base of anal point); a distinct hump present medio-dorsally, clearly visible in lateral view (Fig. 2D). Anal point (Fig. 2C, D) 25 μm long, 30 μm wide at base, triangular, short and sharply pointed apically, distal part markedly curved upwards (when viewed laterally as in Fig. 2D), basal margin broadly semi-circular. Laterosternite IX with 8 setae (4 on each side). Sternapodeme and phallapodeme as in Fig. 2G, transverse sternapodeme bowed anteriorly; phallapodeme unusual, comma-like. Virga (Fig. 2C, I) well developed and branched apically. Gonocoxite 160 μm long, 80–90 μm wide at base; widest at base and rounded apically; dorsal distal half parallel-sided; ventrally broadly expanded (Fig. 2G), the lobe occupying about 75% of the total length of the gonocoxite, with several stout setae placed in 2 arched rows. Superior volsella swollen. Inferior volsella (Fig. 2C, H) broadly subtriangular at base, inwardly projecting and narrowing into a spherical transparent apex; anterior margin concave, with sclerotization; posterior margin convex, with 3–4 stout setae in 1 row. Gonostylus 55 μm long, 35 μm maximum width, atypically shaped for the genus as shown in Fig. 2C, E, F, globular or bean-like (depending on the angle of view); dorsally (Fig. 2C) with 3–4 stout setae located on distal and lateral parts, anteriorly with distinct sclerotization; ventrally (Fig. 2F) with conspicuous sclerotization anteriorly, with stout setae in a circular row; crista dorsalis absent; megaseta (Fig. 2C, E) 10–12 μm long, tongs-like and well-developed, inserted dorsally halfway from the apex, only visible in dorsal view. HV (total body length divided by length of gonostylus 10 times) = 4.27; HR (length of gonocoxite divided by length of gonostylus) = 2.91.

Female, pupa and larva: unknown.

Differential diagnosis. According to Ashe and O'Connor (2012), currently there are six valid *Synorthocladius* species reported from the Palaearctic Region: *S. asamasecundus* Sasa & Hirabayashi, 1991, *S. ginzanpequea* (Sasa & Suzuki, 2001), *S. mongolwexeus* (Sasa & Suzuki, 1997); *S. semivirens*; *S. tamaparvulus* Sasa, 1981 and *S. tusimoijekeus* (Sasa & Suzuki, 1999).

The new species is a *Synorthocladius* based on characters provided in the generic descriptions of Cranston et al (1989) and Liu and Wang (2005): small species (wing

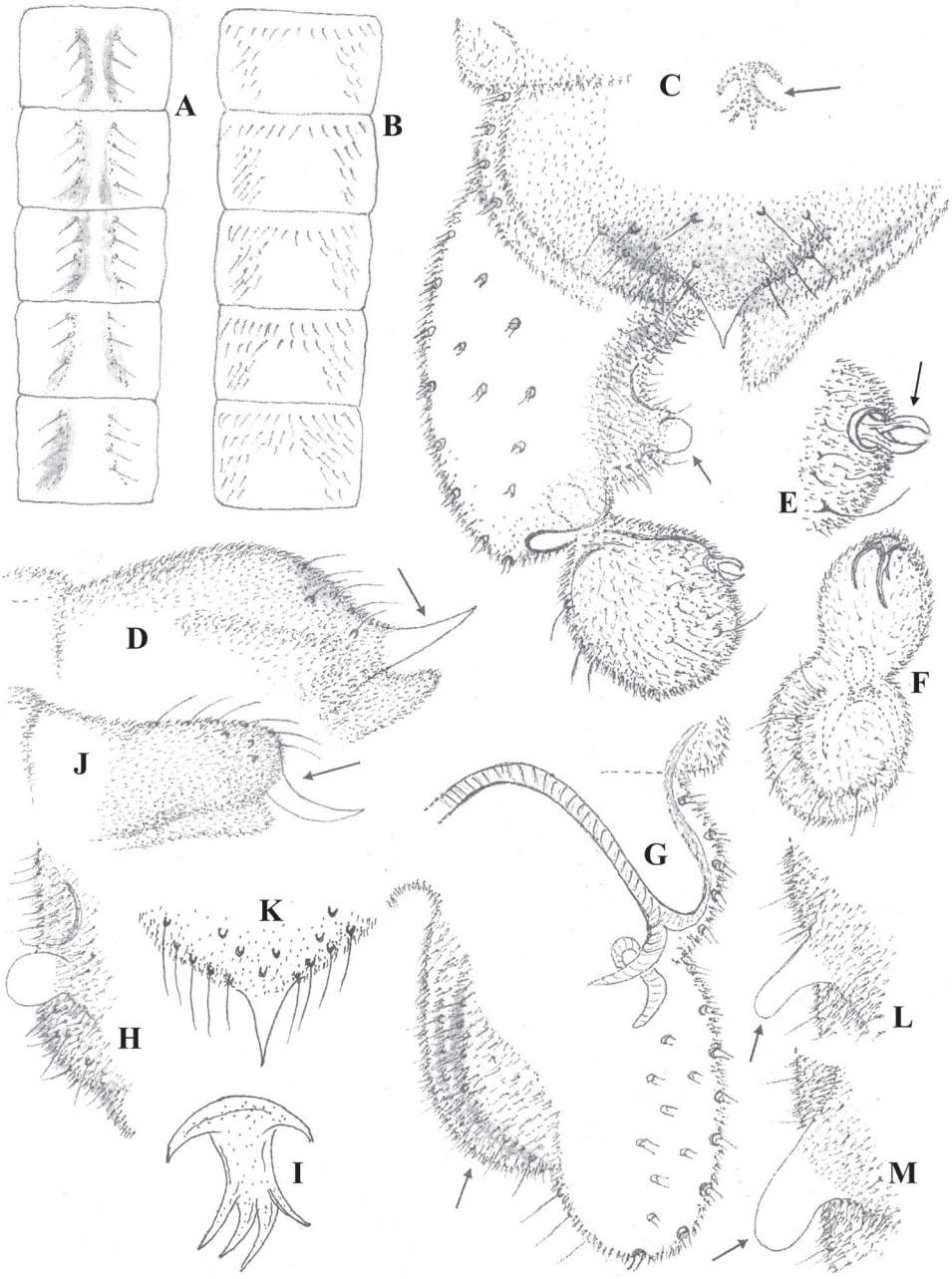

Figure 2. Male imago of *Synorthocladius* spp. Chaetotaxy of tergites II–VI of **A** *S. federicoi* sp. nov. **B** *S. semivirens*. *S. federicoi* sp. nov. **C** hypopygium in dorsal view **D** tergite IX and anal point in lateral view **E** megaseta, dorsal **F** gonostylus, other aspect in ventral view **G** hypopygium, ventral **H** inferior volsella **I** virga. *S. semivirens* **J** tergite IX and anal point in lateral view **K** anal point, dorsal **L, M** inferior volsella, two aspects. The arrows indicate some distinguishing characters.

length 1.85 mm); antenna with 13 flagellomeres, with groove beginning on flagellomere 3, apical flagellomere with characteristic curved sensilla chaetica, antennal ratio less than 1 (0.9); eyes bare, temporal setae few (6), uniserial; antepronotal lobes fused medially, acrostichals few (2), dorsocentrals and scutellars uniserial; wing membrane without setae, squama with sparse setal fringe (4/5); anal point short and without setae; inferior volsella bilobed. However, *S. federicoi* sp. nov. is very different from previously described species in the following respects:

- Frontal tubercles broadly globular (Fig. 1A); indistinct in *S. semivirens* (Fig. 11B), absent in *S. tamaparvulus* (Sasa 1981, fig. 11B);
- Inner temporals of 4 setae in 1 row (Fig. 1A); with a single seta in *S. semivirens* (Fig. 1B);
- Last flagellomere of antenna distinctly bilobed apically (Fig. 1C, D); rounded and simply clubbed in *S. semivirens* (Fig. 1E) and *S. tamaparvulus* (Sasa 1981, fig. 11C);
- Lobes of antepronotum not gaping (Fig. 1J); gaping in *S. semivirens* (Fig. 1K);
- Notopleural suture with parapsidal branch arched (Fig. 1L); sinuate in *S. semivirens* (Fig. 1M);
- Unusual pattern of setae on tergites II–VI (Fig. 2A); more generally distributed in *S. semivirens* (Fig. 2B) and *S. tamaparvulus* (Sasa 1981, fig. 11F);
- Tergite IX with a distinct hump (Fig. 2D); linearly elongate in *S. semivirens* (Fig. 2J);
- Basal part of anal point semi-circular and slightly bent downwards (Fig. 2C, dorsal; Fig. 2D, lateral); sub-circular and strongly projecting downwards in *S. semivirens* (Fig. 2K, dorsal; Fig. 2J, lateral);
- Virga branched (Fig. 2C, I); absent in *S. semivirens* and *S. tamaparvulus*;
- Inferior volsella broadly subtriangular basally, narrowing towards apex and ending in a unique (for the genus) spherical lobe; elongate finger-like to nose-like in both *S. semivirens* (Fig. 2L, M) and *S. tamaparvulus* (Sasa 1981, figs 12A, E);
- Gonostylus unusual in shape (globular or bean-like as in Fig. 2C, E, F); elongate and more or less parallel-sided in *S. semivirens* and *S. tamaparvulus*, as illustrated by Cranston et al. (1989, fig. 9.83E), Liu and Wang (2005, figs 4, 8), Langton and Pinder (2007, fig. 192D) and Sasa (1981, fig. 12A, E).

Key to adult males of known *Synorthocladius* species from Europe

1 Inferior volsella with spherical apex (Fig. 2C, H); last flagellomere of antenna bilobed apically (Fig. 1C, D); gonostylus globular dorsally (Fig. 2C, E)..... .....***S. federicoi* sp. nov.**

– Inferior volsella finger-like or nose-like (Fig. 2L, M); last flagellomere of antenna simply clubbed (Fig. 1E); gonostylus slender as in Sasa (1981, fig. 12E), Liu and Wang (2005, figs 4, 8), Langton and Pinder (2007, fig. 192D)..... .....***S. semivirens***

Discussion

The newly described species can be considered as a local biogeographic representative of the Venetian Pre-Alps. Consequently, the description here of *S. federicoi* sp. nov. increases the total number of valid species of *Synorthocladius* from Europe to two.

Larvae of *Synorthocladius* species are typically rheobiontic, occurring especially in rheocrene mountain springs and streams fed by groundwater (krenal) (Reiss 1968, 1989; Evrard 1995; Lindegaard 1995; Lencioni et al. 2011, 2012, 2018; Kettani and Moubayed-Breil 2018; Murray et al. 2018), but also in the rhithral and potamal reaches of rivers with high current velocity (Rossaro 1982). The holotype and only known specimen of the new species was collected in a moderately shaded lotic habitat with sandy to gravely substrate supplied by fresh groundwater, which maintains a low annual variation of temperature. The type locality (Fig. 3) is in the hyporhithral sector of the Adige River (Braioni and Ruffo 1986). It includes stones covered by submerged and emerged bryophytes and microalgae, which provide favourable microhabitats for chironomid larval stages. The environmental data of water recorded in the type locality are: conductivity = 262 µS/cm; pH = 8.4; temperature = 12.5 °C. Emergence of adult chironomids is usually observed in early spring (March–April).

Synorthocladius federicoi sp. nov. is known only from its type locality in the Venetian Pre-Alps (a mountain range of the Italian Alps). It would appear to be a biogeographic representative of lotic habitats delimited by the south-eastern part of the Italian Alps. It is likely to be more widespread in similar lotic habitats or Alpine streams of northern Italy.

Chironomid species encountered with *S. federicoi* sp. nov. include: *Conchapelopia pallidula* (Meigen, 1818), *C. melanops* (Meigen, 1818), *Paramerina cingulata* (Walker,

Figure 3. Type locality of *Synorthocladius federicoi* sp. nov., Adige River, Verona (northern Italy) (by V. Lencioni).

1856), *Cardiocladius fuscus* Kieffer, 1924, *Cricotopus annulator* Goetghebuer, 1927, *C. levantinus occidentalis* Moubayed-Breil & Ashe, 2011, *C. tremulus* (Linnaeus, 1758), *Eukiefferiella devonica* (Edwards, 1929), *E. ilkleyensis* (Edwards, 1929), *E. lobifera* Goetghebuer, 1934, *Paracricotopus niger* (Kieffer, 1913), *Parametriocnemus stylatus* (Spärck, 1923), *Rheocricotopus chalybeatus* (Edwards, 1929), *Synorthocladius semivirens* (Kieffer, 1909), *Tvetenia calvescens* (Edwards, 1929), *Micropsectra atrofasciata* (Kieffer, 1911) and *Rheotanytarsus curtistylus* (Goetghebuer, 1921).

Acknowledgements

The authors are grateful to Leonardo Latella (Natural History Museum of Verona, Italy) for collecting the holotype, to Patrick Ashe for his helpful reading before submission, and to the two reviewers Peter Langton and Eugenyi Makarchenko for their constructive corrections that greatly improved the manuscript.

References

Ashe P, O'Connor J (2012) A World Catalogue of Chironomidae (Diptera). Part 2. Orthocladiinae. Irish Biogeographical Society and National Museum of Ireland, Dublin, 968 pp.

Braioni G, Ruffo S (1986) Ricerche sulla qualità delle acque dell'Adige. Memorie del Museo Civico di Storia Naturale di Verona, Sez. Biologica 6: 1–341.

Cranston P, Oliver DR, Sæther OA (1989) The adult males of Orthocladiinae (Diptera, Chironomidae) of the Holarctic Region – Keys and diagnoses. In: Wiederholm T (Ed.) Chironomidae of the Holarctic region. Keys and diagnoses. Part 3-Adult males. Entomologica Scandinavica Supplement 34: 164–352.

Evrard M (1995) The chironomid fauna of the Ourthe basin, Belgium: additions the Belgian check-list of Chironomidae (Diptera). Annales de Limnologie 31(3): 215–221. https://doi.org/10.1051/limn/1995019

Kettani K, Moubayed-Breil J (2018) Communities of Chironomidae from four ecological zones delimited by the Mediterranean coastal ecosystem of Morocco (Moroccan Rif). Updated list and faunal data from the last two decades. Journal of Limnology 77(1): 141–144. https://doi.org/10.4081/jlimnol.2018.1727

Langton PH, Pinder LCV (2007) Keys to the adult males of Chironomidae of Britain and Ireland. Volume 1 (pp. 1–239) and volume 2 (pp. 1–68). Freshwater Biological Association, Scientific Publication, n° 64.

Lencioni V, Marziali L, Rossaro B (2011) Diversity and distribution of chironomids (Diptera, Chironomidae) in pristine Alpine and pre-Alpine springs. Journal of Limnology 71(1): 106–121. https://doi.org/10.4081/jlimnol.2011.s1.106

Lencioni V, Marziali L, Rossaro B (2012) Chironomids as bio-indicators of environmental quality in mountain springs. Freshwater Science 31(2): 525–541. https://doi.org/10.1899/11-038.1

Lencioni V, Mezzanotte E, Spagnol C, Latella L (2018) Effect of human impacts on diversity and distribution of chironomids (Diptera, Chironomidae) in pre-Alpine springs. Journal of Limnology 77(1): 203–212. https://doi.org/10.4081/jlimnol.2018.1804

Lindegaard C (1995) Chironomidae (Diptera) of European cold springs and factors influencing their distribution. Journal of the Kansas Entomological Society, Supplement 68(2): 108–131. https://www.jstor.org/stable/25085637

Liu Y, Wang X (2005) *Synorthocladius* Thienemann from China, with a review of the genus (Diptera: Chironomidae: Orthocladiinae). Zootaxa 1057: 51–60. https://doi.org/10.11646/zootaxa.1057.1.3

Makarchenko EA, Makarchenko MA (2017) Fauna and distribution of the Podonominae, Diamesinae, Prodiamesinae and Orthocladiinae (Diptera, Chironomidae) of the Russian Far East and bordering territory // Vladimir Ya. Levanidov's Biennial Memorial Meetings. Vol. 7. Vladivostok, FSCEATB FEB RAS, 127–142.

Moubayed-Breil J (2020) Chironomidae from the Mediterranean ecosystem of continental France. Faunal and biogeographic data over the last four decades [Diptera]. Ephemera 21(1): 31–69.

Moubayed-Breil J, Ashe P (2012) An updated checklist of the Chironomidae of Corsica with an outline of their altitudinal and geographical distribution (Diptera). Ephemera 13(1): 13–39.

Murray D, O'Connor J, Ashe P (2018) Chironomidae (Diptera) of Ireland. A review, checklist and their distribution in Europe. Irish Biogeographical Society 12: 1–390.

Pankratova VYa (1970) Lichinki i kukolki komarov podsemeistva Orthocladiinae fauny SSSR (Diptera, Chironomidae = Tendipedidae) (Larvae and pupae of midges of the subfamily Orthocladinae (Diptera, Chironomidae = Tendipedidae) of the USSR fauna). Opredeliteli po Faune SSSR, izdavaemye Zoologicheskim Institutom AN SSSR, 102: 1–344. Izdatel'stvo Nauka, Leningrad.

Paasivirta L (2014) Checklist of the family Chironomidae (Diptera) of Finland. Zookeys 441: 63–93. https://doi.org/10.3897/zookeys.441.7461

Plociennik M, Pesic V (2012) New records and list of non-biting midges (Chironomidae) from Montenegro. Biologia Serbica 34(1–2): 36–50. https://ojs.pmf.uns.ac.rs/index.php/dbe_serbica/article/view/1279

Plociennik M, Karaouzas I (2014) The Chironomidae (Diptera) fauna of Greece, ecological distributions and patterns, taxa list and new records. International Journal of Limnology 50: 19–34. https://doi.org/10.1051/limn/2013066

Reiss F (1968) Verbreitung lakustrischer Chironomiden (Diptera) des Alpengebietes. Annales Zoologici Fennici 5: 119–123.

Reiss F (1989) Die Chironomidae der Türkei. Teil 1, Podonominae, Diamesinae, Prodiamesinae, Orthocladiinae (Diptera, Nematocera, Chironomidae). Entomofauna, Zeitschrift Für Entomologie 10(8/1): 105–160.

Rossaro B (1982) Guide per il riconoscimento delle specie animali delle acque interne italiane. 16. Chironomidi, 2 (Diptera, Chironomidae, Orthocladiinae). CNR AQ/1/171: 1–80.

Rossaro B, Pirola N, Marziali L, Magoga G, Boggero A, Montagna M (2019) An updated list of chironomid species from Italy with biogeographic considerations (Diptera, Chironopmi-

dae). Biogeographia – The Journal of Integrative Biogeography 34: 59–85. https://doi.org/10.21426/B634043047

Sasa M (1981) A morphological study of adults and immature stages of 20 Japanese species of the family Chironomidae (Diptera). Research Report from the National Institute of Environmental studies 7: 1–158.

Sasa M, Yamamoto M (1977) A checklist of Chironomidae recorded from Japan. Japanese Journal of Sanitary Zoology 28(3): 301–318. https://doi.org/10.7601/mez.28.301

Sæther OA (1980) Glossary of chironomid morphology terminology (Diptera, Chironomidae). Entomologica Scandinavica, Supplement 14: 1–51.

Sæther OA, Spies M (2013) Fauna Europaea: Chironomidae. In: Beuk P, Pape T (Eds) Fauna Europaea: Diptera Nematocera. Fauna Europaea version 2.6. [Internet data base at] http://www.faunaeur.org

Yavorskaya N, Makarchenko MA, Orel OV, Makarchenko EA (2018) An updated checklist of Chironomidae (Diptera) from the Amur River basin (Russian Far East). Journal of Limnology 77(1): 155–159. https://doi.org/10.4081/jlimnol.2018.1785

ZooKeys 1057: 117–148 (2021)
doi: 10.3897/zookeys.1057.71451
https://zookeys.pensoft.net

RESEARCH ARTICLE

A peer-reviewed open-access journal
ZooKeys
Launched to accelerate biodiversity research

Revision of the genus *Furusawaia* Chûjô, 1962 (Coleoptera, Chrysomelidae, Galerucinae)

Chi-Feng Lee[1], Jan Bezděk[2]

1 *Applied Zoology Division, Taiwan Agricultural Research Institute, Taichung 413, Taiwan* **2** *Mendel University in Brno, Department of Zoology, Fisheries, Hydrobiology and Apiculture, Zemědělská 1, 613 00 Brno, Czech Republic*

Corresponding author: Chi-Feng Lee (chifeng@tari.gov.tw)

Academic editor: Michael Schmitt | Received 12 July 2021 | Accepted 16 August 2021 | Published 27 August 2021

http://zoobank.org/B6A748DE-942C-4932-8D86-6F522081AF98

Citation: Lee C-F, Bezděk J (2021) Revision of the genus *Furusawaia* Chûjô, 1962 (Coleoptera, Chrysomelidae, Galerucinae). ZooKeys 1057: 117–148. https://doi.org/10.3897/zookeys.1057.71451

Abstract

Yunnaniata Lopatin, 2009 is regarded as a junior synonym of *Furusawaia* Chûjô, 1962 **syn. nov**. *Yunnaniata konstantinovi* Lopatin, 2009 **comb. nov.** is transferred to the genus *Furusawaia* Chûjô and redescribed. *Furusawaia continentalis* Lopatin, 2008 and *F. yosonis* Chûjô are recognized as valid species and redescribed. Four new species are described from Taiwan: *F. jungchani* **sp. nov.**, *F. lui* **sp. nov.**, *F. tahsiangi* **sp. nov.**, and *F. tsoui* **sp. nov.** A key to Taiwanese and Chinese species of *Furusawaia* is provided.

Keywords

Caryophyllaceae, citizen scientists, Food plant, leaf beetles, new species, new synonym, *Stellaria*, taxonomy, winglessness, *Yunnaniata*

Introduction

Furusawaia Chûjô, 1962 is a little known galerucine genus, with *F. yosonis* Chûjô from Taiwan as the type and only species. No additional species were described until Lopatin (2008) described the second species, *F. continentalis* Lopatin from China (Yunnan, Sichuan). *Furusawaia* Chûjô was initially placed in the section Hylaspites within the tribe Sermylini (Wilcox 1971, 1975). It was transferred to section Capulites by Seeno and Wilcox (1982), containing four genera: *Capula* Jacobson, 1925; *Furusawaia* Chûjô, 1962; *Nepalogaleruca* Kimoto, 1970; and *Himaplosonyx* Chen, 1976. The section Capulites was

redefined by Bezděk and Beenen (2009) and *Yunnaniata* Lopatin, 2009 (in Lopatin and Konstantinov 2009) was included and considered closely related to *Furusawaia* Chûjô. The taxonomic status of both genera was re-evaluated in the present study.

The Taiwan Chrysomelid Research Team (TCRT) was founded in 2005 and is composed of ten members. All of them are amateurs interested in producing a complete inventory of chrysomelid species in Taiwan. Specimens of *Furusawaia* are difficult to collect, with only a few individuals collected on or under stones along forest trails at mid-altitudes (above 2,000 m). This habitat is similar to that of *Yunnaniata konstantinovi* (Bezděk and Beenen 2009). Due to this problem, more citizen scientists were recruited using internet social media. Pin-Hsun Ko (柯品薰) was the first person to observe that adults of *Furusawaia* species fed on leaves of *Stellaria media* (L.) Vill (Caryophyllaceae) on March 30, 2015. Members of the TCRT started to focus searches for adults where these food plants grew. However, specimens were still difficult to find during numerous field trips, with one exception. Ten individuals were collected from Huakang (華崗) by Jung-Chan Chen (陳榮章) on April 24, 2019 (see *F. jungchani* sp. nov.). Fortunately, many more were collected thanks to the efforts of citizen scientists resulting in 96 specimens that were available for this study.

Materials and methods

For taxonomic study, the abdomens of adults were separated from the forebodies and boiled in 10% KOH solution, followed by washing in distilled water to prepare genitalia for illustrations. The genitalia were then dissected from the abdomens, mounted on slides in glycerin, and studied and drawn using a Leica M165 stereomicroscope. A Nikon ECLIPSE 50i microscope was used for detailed examinations.

At least two pairs from each species were examined to delimit variability of diagnostic characters. For species collected from more than one locality, at least one pair from each locality was examined. Length was measured from the anterior margin of the eye to the elytral apex, and width at the greatest width of the elytra.

Specimens studied herein are deposited at the following institutes and collections:

BPBM Bernice P. Bishop Museum, Hawaii, USA [James Boone];
IZAS Institute of Zoology, Chinese Academy of Sciences, Beijing, China [Ruie Nie];
JBCB Jan Bezděk collection, Brno, Czech Republic;
KMNH Kitakyushu Museum of Natural History and Human History, Kitakyushu, Japan [Yûsuke Minoshima];
TARI Taiwan Agricultural Research Institute, Taichung, Taiwan;
USNM Smithsonian Institution, National Museum of Natural History, Washington, U.S.A. [Alexander S. Konstantinov];
TCRT Taiwan Chrysomelid Research Team;
ZIN Zoological Institute, Russian Academy of Sciences, St. Peterburg, Russia [Alexey Moseyko];

Exact label data are cited for all type specimens of previously described species; a double slash (//) divides the data on different labels and a single slash (/) divides the data in different rows. Other comments and remarks are in square brackets: [p] – preceding data are printed, [h] – preceding data are handwritten, [w] – white label, [r] – red label, [b] – blue label.

Identified specimens of the following species are included in the study:

Himaplosonyx apterus Chen, 1976 (Fig. 1A–C): holotype ♀ (IZAS, based on photographs): "Himaplosonyx / ♀ aptera Chen [h] / 鑑定者 [identifier] : 陳世驤 [Sicien Chen] 19 [p, w] // HOLOTYPE [p, r] // 1966.V.11 / T66-20 [p] / 采集者 [collector] 王書永 [Shu-Yung Wang] [p, w] // 西藏 [Tibet]: 聂拉木 [Nielamu] 樟木 [Camphor wood] / (郭沙寺[Guosha Temple]) 2750米 [2750 m] / 中國科學院 [Chinese Academy of Sciences] [p, w]".

Nepalogaleruca angustilineata Kimoto & Takizawa, 1972 (Fig. 1D): NEPAL. 1♂ (JBCB), Chomrong, 9.V.1994, leg. P. Hesoun.

Nepalogaleruca elegans Kimoto, 1970: Nepal. 1♂ (KMNH), Prov. Nr. 3 East Dudh Kosi Tal under Thangpoche, 3400 m, 29–31.V.1964, leg. W. Dierl; 1♀ (KMNH), Prov. Nr. 3 East Jubing, 1600 m, 2.V. 1964, leg. W. Dierl; 1♂ (KMNH), C. Baroni U., Thodung via Those, 3100 m, 29–31.V.1976, leg. W. Wittmer.

Capula apicalis Chen et al., 1986 (Fig. 1E): China. Sichuan: 1♂ (JBCB), Sa'de env., alpine meadows, 29°36.4'N, 101°22.9'E, 4500 m, V.2004, leg. Hackel & Sehnal.

Capula caudata Chen et al., 1986 (Fig. 1F): China. Sichuan: 1♀ (JBCB), Sabde, 4200 m, 29°04'168"N, 101°25'720"E, 25.V.2001, leg. M. Janata.

Taxonomic results

Furusawaia Chûjô, 1962

Furusawaia Chûjô, 1962: 107 (type species: *Furusawaia yosonis* Chûjô, 1962, by original designation); Wilcox 1971: 210 (catalogue); Kimoto and Chu 1996: 91 (catalogue); Kimoto and Takizawa 1997: 298 (key); Beenen 2010: 458 (catalogue); Yang et al. 2015: 187 (catalogue).

Yunnaniata Lopatin in Lopatin and Konstantinov 2009: 8 (type species: *Yunnaniata konstantinovi* Lopatin, 2009, by original designation); Yang et al., 2015: 184 (catalogue). syn. nov.

Included species. *Furusawaia continentalis* Lopatin, 2008, *F. konstantinovi* (Lopatin, 2009) comb. nov., *F. jungchani* sp. nov., *F. lui* sp. nov., *F. tahsiangi* sp. nov., *F. tsoui* sp. nov., and *F. yosonis* Chûjô, 1962.

Diagnosis. Adults of *Furusawaia* Chûjô are similar to those of *Capula* Jacobson in possessing a black general color pattern and midcoxae widely separated, the distance between them at least as wide as half of transverse diameter of coxa; but they differ from

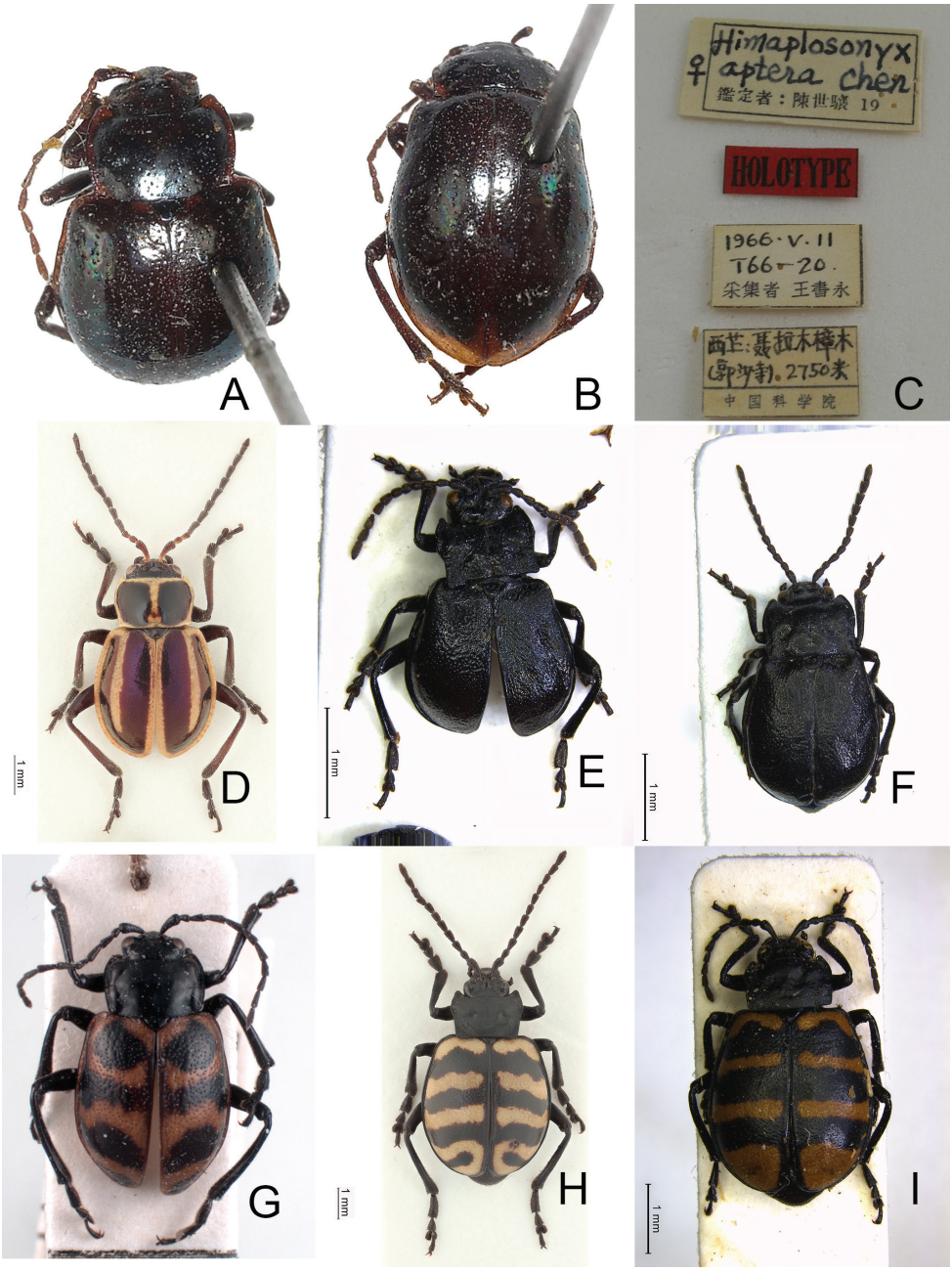

Figure 1. Habitus, dorsal view **A** *Himaplosonyx apterus* Chen, holotype, female, front view **B** ditto, back view **C** same, labels **D** *Neplogaleruca angustilineata* Kimoto & Takizawa, male **E** *Capula apicalis* Chen et al., male **F** *C. caudata* Chen et al., female **G** *Furusawaia continentalis* Lopatin, holotype, male **H** *F. konstantinovi* (Lopatin), male **I** same species, female.

those of *Capula* Jacobson by the red or orange transverse stripes on the elytra (elytra entirely metallic or black in *Capula* (Fig. 1E, F), humeral calli absent (humeral calli present in *Capula*), antenna elongate, length to width ratios of antennomeres IV-VII more than 1.9 × (antennae shorter, length to width rations of antennomeres IV–VII 1.5–1.7 ×, length to width ratios of antennomeres I–XI in male of *Capula apicalis* 2.4: 1.9: 1.8: 1.6: 1.5: 1.5: 1.6: 1.6: 1.7: 1.5: 2.7 (Fig. 2A); length to width ratios of antennomeres I–XI in female of *Capula caudata* 2.3: 1.7: 1.8: 1.5: 1.5: 1.5: 1.6: 1.5: 1.6: 1.6: 3.0 (Fig. 2B)). Genitalic characters are also diagnostic. In *Capula*, the aedeagus lacks endophallic sclerites (Fig. 2C, D) (at least primary endophallic sclerite present in *Furusawaia*), the gonocoxae (Fig. 2E) of *Capula* females are much wider than those of *Furusawaia* and the spermatheca (Fig. 2F) possesses a short and strongly swollen receptacle (elongate and slightly swollen receptacle of spermatheca in *Furusawaia*). Abdominal ventrites VIII (Fig. 2G) are similar in both genera. Members of *Himaplosonyx* (Fig. 1A, B) differ from those of *Furusawaia* in possessing explanate lateral margins of the pronotum, disc with two foveae in the middle, and the pronotal anterior margin bordered but posterior marginal border absent. Members of *Nepalogaleruca* (Fig. 1D) differ from those of *Furusawaia* in the yellow general color pattern, pronotum with two longitudinal black or metallic spots, elytra with two pairs of longitudinal black or metallic stripes, and the midcoxae closer to each other, distance between them less than half of transverse diameter of coxa.

Remarks. Bezděk and Beenen (2009) separated *Yunnaniata* from *Furusawaia* based on the flat pronotum, however, convexity of the pronotum varies among different species and populations of *Furusawaia* in Taiwan. Thus, both genera are regarded as synonyms here. Although *Yunnaniata* males possess more complicated sclerites in the aedeagus, no additional characters separate the two genera.

Biology. Adults were observed walking or resting on forest trails (e.g., Fig. 3A) at low altitudes (above 1,000 m) in northern Taiwan or middle and high altitudes (above 2,000 m) in China, central and southern Taiwan. They feed on leaves of *Stellaria* species (Caryophyllaceae) in Taiwan.

Distribution. West China (Yunnan, Sichuan), Taiwan.

Chinese species

***Furusawaia continentalis* Lopatin, 2008**
Figs 1G, 4A, D, E

Furusawaia continentalis Lopatin, 2008: 925; Beenen 2010: 458 (catalogue).

Types. ***Holotype*** ♂ (ZIN): "**CH**. Yunnan. N. Baoshan / 25 29 10 N / 99 04 38 E / H 3530 m, 10.05 2006 / Belousov & Kabak leg [p, w] // Holotypus [p, r] // Furosawaia [sic!] / continentalis sp. n. [h] / det. I. Loptatin, 200[p]8[h, w]".

Other material. China. Yunnan: 1♂ (JBCB), 30 km mer.-occ ad Daochang, 2800 m, 9.VI.2001, leg. local collector.

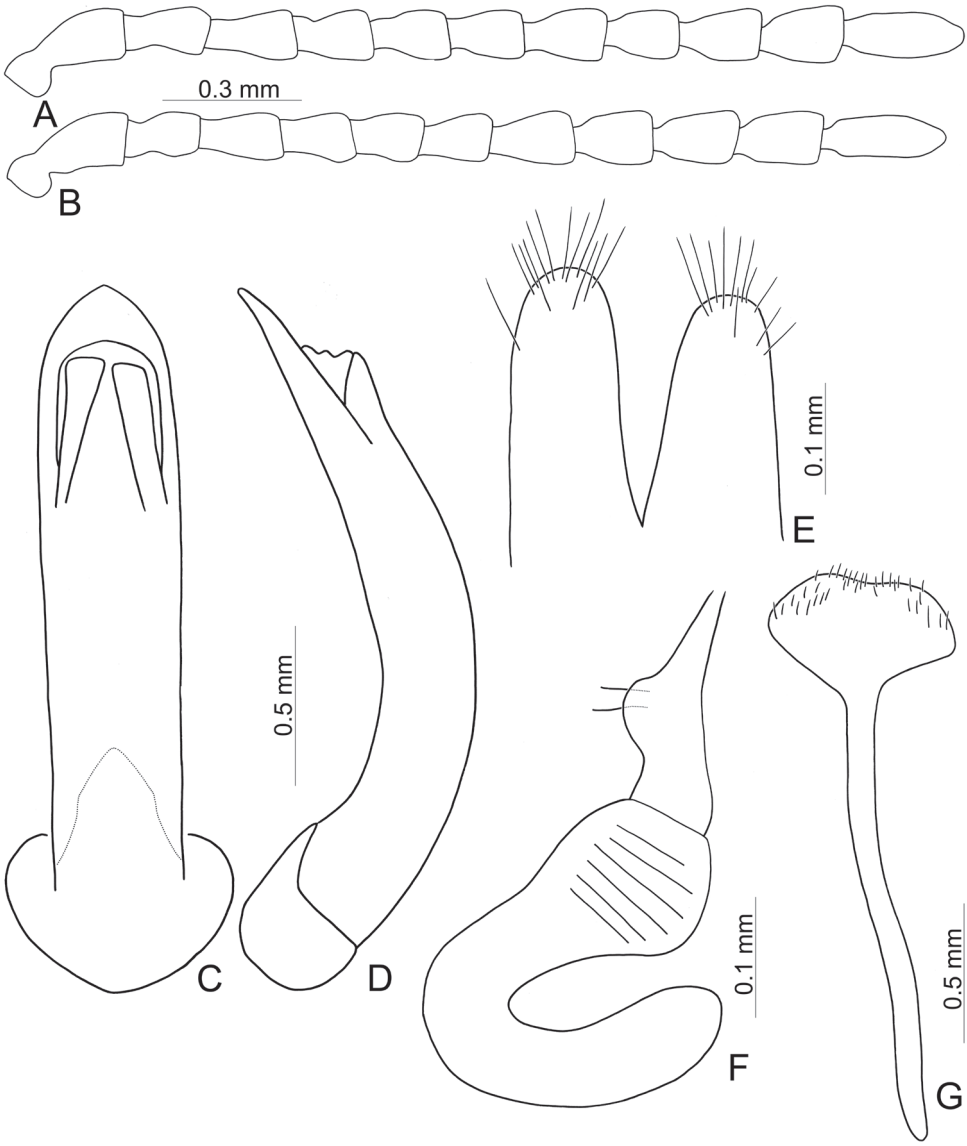

Figure 2. Diagnostic characters of *Capula apicalis* Chen et al. (**A, C, D**) and *C. caudata* Chen et al. (**B, E–G**) **A** antenna, male **B** antenna, female **C** aedeagus, dorsal view **D** ditto, lateral view **E** gonocoxae **F** Spermatheca **G** abdominal ventrite VIII, female.

Redescription. Male: Length 8.1 mm, width 4.5 mm. Body color (Fig. 1G) black, elytra with red circular stripes along basal and lateral margins, anterior transverse red stripe at basal 1/4, red stripe along basal margin extending downwards at suture and humeral calli connected with anterior red stripe, two oblique stripes at middle and apical 1/4. Antennae filiform in males (Fig. 4A), length ratios of antennomeres I–XI

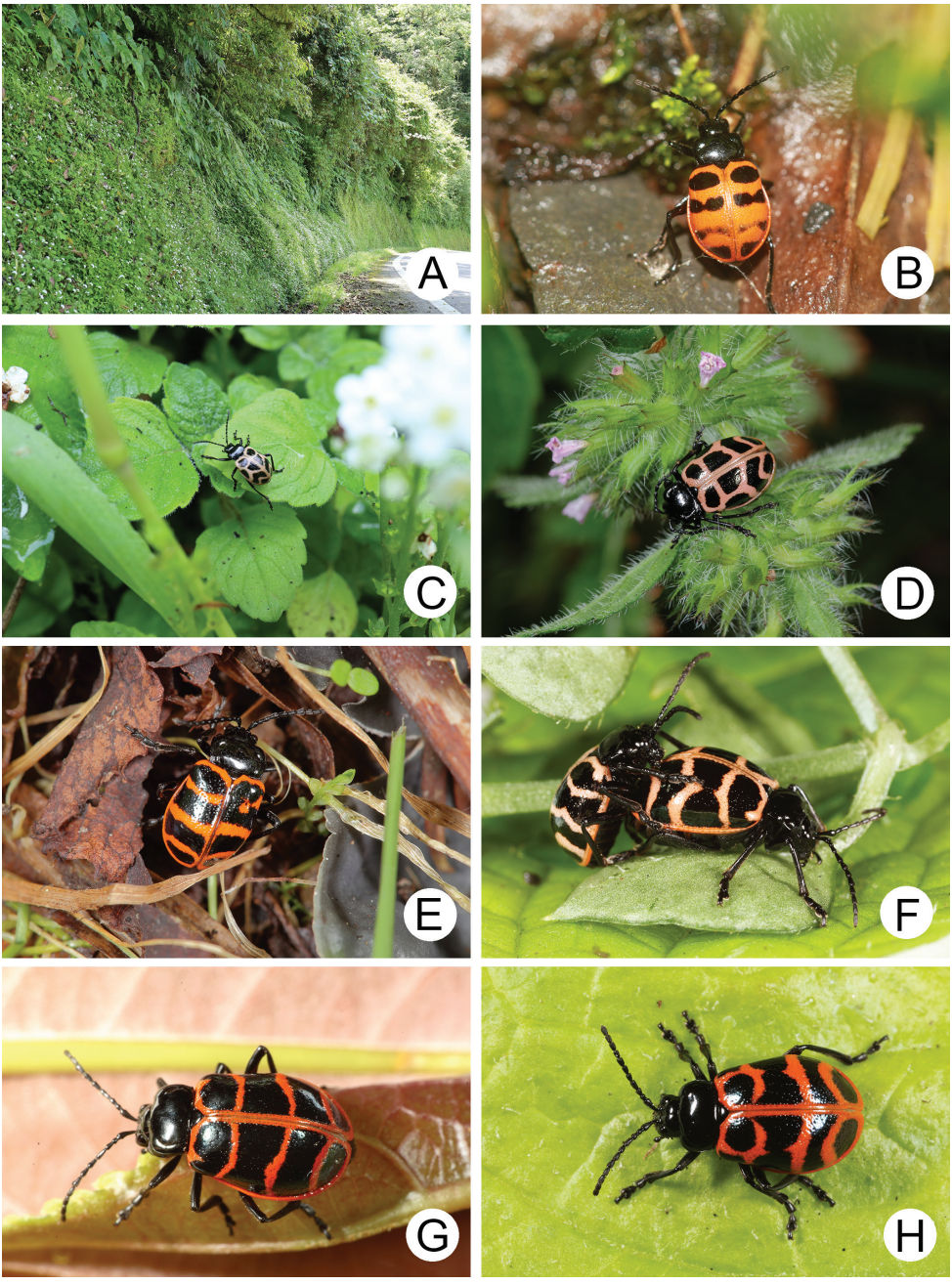

Figure 3. Field photographs of *Furusawaia* species **A** microhabitat for *F. lui* sp. nov. in Hsinpaiyang (新白楊) **B** adult of *F. jungchani* sp. nov. in the daytime, Huakang (華崗) **C** adult of *F. lui* sp. nov. in the daytime, Hsinpaiyang (新白楊) **D** adult of *F. lui* sp. nov. at night, Hsinpaiyang (新白楊) **E** adult of *F. tahsiangi* sp. nov. in the daytime, Hsuehshan (雪山) **F** adult of *F. tsoui* sp. nov. at night, Jianqing trail (見晴步道) **G** adult of *F. yosonis* at night, Alishan (阿里山) **H** adult of an undescribed species, Tianchi Lodge (天池山莊)

1.0: 0.3: 0.5: 0.7: 0.6: 0.6: 0.6: 0.6: 0.5: 0.5: 0.7, length to width ratios of antennomeres I–XI 2.8: 1.4: 1.9: 2.8: 2.7: 2.9: 3.0: 3.0: 2.7: 2.6: 4.4. Pronotum 1.8 × wider than long, disc generally flat; dull, with reticulate microsculpture; with sparse minute punctures confused with few fine, but slightly larger, punctures, with lateral groove extending posterior to base; basal margin straight; apical margin moderately concave; anterior angles obtuse; lateral margins distinct and rounded. Elytra with rounded lateral margins, widest behind middle, 1.2 × longer than wide; disc with dense, coarse punctures; shining, without reticulate microsculpture. Aedeagus (Fig. 4D, E) slender in dorsal view, 7.2 × longer than wide, parallel-sided, strongly narrowed apically, apex narrowly rounded; ostium large, covered by membrane; slightly curved in lateral view; endophallic sclerite extremely elongate, 0.7 × as long as aedeagus.

Diagnosis. Adults of *Furusawaia continentalis* can be recognized by the following combination of characters: elongate antennae, length to width ratios of antennomeres IV–X more than 2.5 × (less than 2.5 × in others); disc of pronotum generally flat (more or less convex in Taiwanese species), dull and with reticulate microsculpture (only shared with *F. konstantinovi*), apical margin moderate concave (straight apical margin in others); anterior angles obtuse (anterior angles strongly produced to distinct bulb in others); disc of elytra smooth, lacking reticulate microsculpture, with dense coarse punctures (disc dull, with reticulate microsculpture and dense coarse punctures in *F. konstantinovi*; disc smooth, lacking reticulate microsculpture but with sparse punctures in Taiwanese species); red stripe along suture abbreviated behind anterior stripe at basal 1/3 (Fig. 1E) (red stripe entirely absent in *F. konstantinovi* (Fig. 1E, F), but present in Taiwanese species). In males of *F. continentalis*, aedeagus (Fig. 4D, E) with elongate primary endophallic sclerite, 0.7 × as long as aedeagus (small primary endophallic sclerite, 0.4–0.5 × as long as aedeagus), without lateral expansions near apex (with lateral expansions near apex in others).

Food plants. Unknown.

Distribution. China: Sichuan, Yunnan.

***Furusawaia konstantinovi* (Lopatin, 2009), comb. nov.**
Figs 1H, I, 4B, C, F–J

Yunnaniata konstantinovi Lopatin in Lopatin and Konstantinov 2009: 10; Bezděk and Beenen 2009: 46 (redescription); Yang et al. 2015: 184 (catalogue).

Types. ***Holotype*** ♂ (USNM, by monotype): "China. Yunnan, Lijiang 29. V. / Yulongshan, Prim. forest 2002 / 2800 m N27°08'20", E100°14'6" / leg. A. Konstantinov & M. Volkovitsh [p, w] // Yunnaniata / konstantinovi sp. n. [h] / det. I. Lopatin, 200[p]5[h, w] // Holotypus [p, r] // BLNO / 002622 [p, b] // USNMENT / 00871439 [p, w]".

Other material. China. Yunnan: 4♂ 1♀ (JBCB, 1♂ TARI), 32 km N. Lijiang, 21.VI.2007, Maoniuping (Yak meadows), 27°9.9'N, 100°14.5E, 3540 m, leg. J. Hájek & J. Růžička [Individually collected on wet vegetation and under stones and logs, wet yak pasture]; 1♀ (TARI); Yulong Mts., 4000 m, 27.V.1993, leg. Bolm.

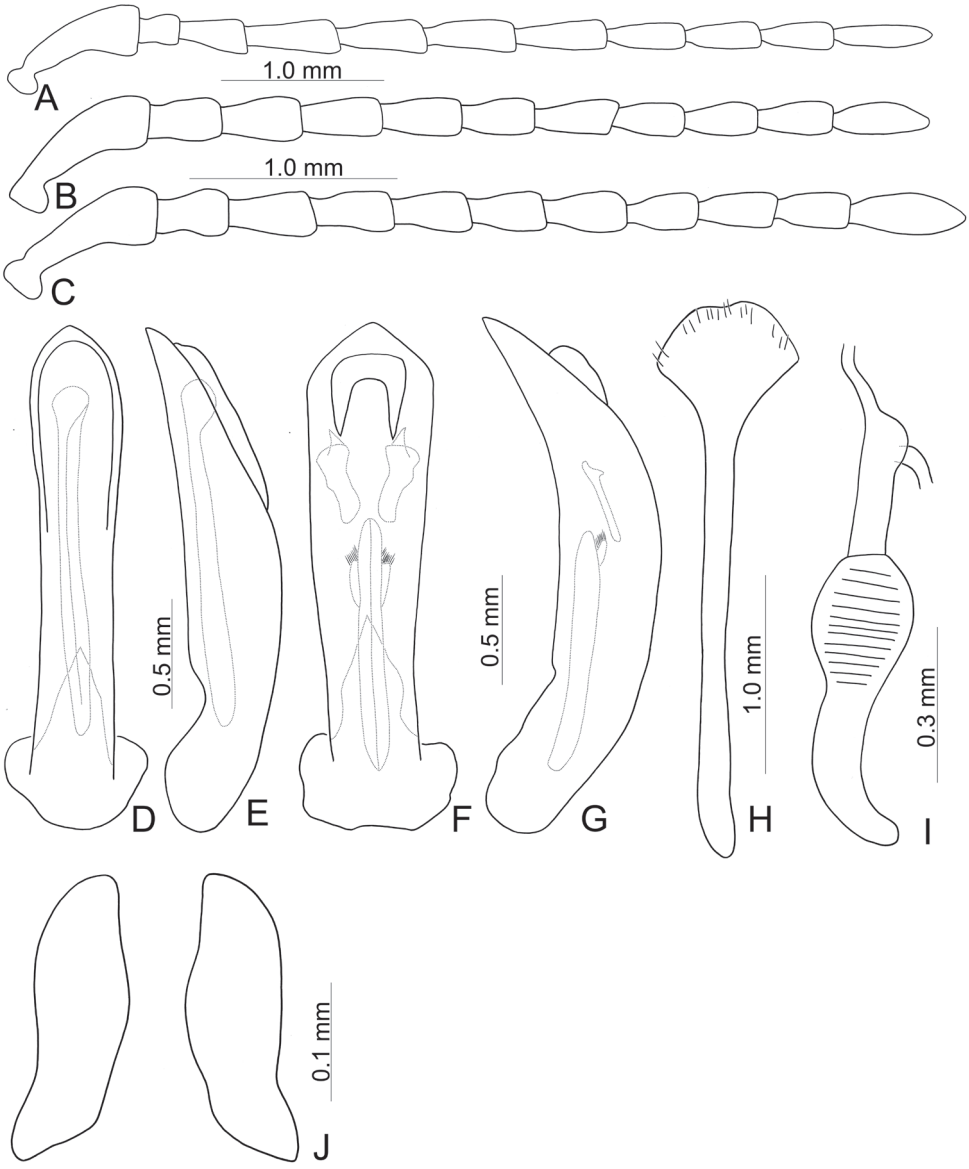

Figure 4. Diagnostic characters of *Furusawaia continentalis* Lopatin and (**A, D, E**) and *Furusawaia konstantinovi* (Lopatin) comb. nov. (**B, C, F–J**) **A, B** antenna, male **C** antenna, female **D, F** aedeagus, dorsal view **E, G** ditto, lateral view **H** abdominal ventrite VIII, female **I** spermatheca **J** gonocoxae.

Redescription. Length 8.0–9.3 mm, width 4.8–5.2 mm. Body color (Fig. 1H, I) black, elytra four transverse yellow stripes behind base, at basal 1/4, middle, and apical 1/4 respectively, three anterior stripes straight, posterior stripe curved posteriorly near suture and extending into apex; in some individuals the entire apical 1/4 is yellow except the margin. Antennae filiform in males (Fig. 4B), length ratios of antennomeres

I–XI 1.0: 0.4: 0.5: 0.5: 0.5: 0.4: 0.5: 0.4: 0.4: 0.5: 0.6, length to width ratios of antennomeres I–XI 3.1: 1.7: 1.7: 2.1: 2.1: 2.0: 2.2: 2.1: 2.1: 2.2: 3.0; similar in females (Fig. 4C), length ratios of antennomeres I–XI 1.0: 0.4: 0.5: 0.5: 0.5: 0.5: 0.5: 0.4: 0.5: 0.5: 0.7, length to width ratios of antennomeres I–XI 2.8: 1.6: 1.9: 2.0: 1.9: 1.9: 2.1: 2.0: 2.1: 2.1: 2.9. Pronotum 1.6–1.7 × wider than long, disc generally flat; dull, with reticulate microsculpture; with sparse fine confused punctures mixed with a few coarse punctures, with lateral shallow depressions; lateral margins distinct, more so in males, less so in females; apical and basal margins straight; anterior angles strongly produced to distinctly acute angles. Elytra with rounded lateral margin, widest behind middle, 1.1–1.2 × longer than wide; disc dull, with reticulate microsculpture, and dense, fine punctures. Aedeagus (Fig. 4F, G) slender in dorsal view, sides gradually narrowed to base, strongly, abruptly narrowed subapically, apex narrowly rounded; ostium with one median longitudinal sclerite; strongly curved in lateral view; primary endophallic sclerite elongate, 0.4 × as long as aedeagus, one pair of short lateral expansions near apex, covered with fine setae, and with one additional pair of short longitudinal sclerites above apex of primary endophallic sclerite, with irregular margins and apical horns. Gonocoxae (Fig. 4J) reduced into one pair of small flattened sclerites. Ventrite VIII (Fig. 4H) with apex well sclerotized and extremely small, several short setae along apical margin, spiculum extremely long. Receptacle of spermatheca (Fig. 4I) slightly swollen, separated from pump; pump short and slightly curved; sclerotized proximal spermathecal duct separated from receptacle, moderately long, with wide base.

Diagnosis. Adults of *Furusawaia konstantinovi* can be recognized by the following combination of characters: disc of pronotum generally flat (more or less convex in Taiwanese species), dull and with reticulate microsculpture (only shared with *F. continentalis*), lateral margin narrowed at posterior half (lateral margins rounded in others); disc of elytra dull, with reticulate microsculpture, with dense coarse punctures (disc smooth, lacking reticulate microsculpture and dense coarse punctures in *F. continentalis*; disc smooth but with sparse punctures in Taiwanese species); suture and lateral margins of elytra black (Fig. 1E, F) (lateral margins and at least part of suture of elytra with stripes in others). In males of *F. continentalis*, aedeagus (Fig. 4F, G) with one additional pair of small elongate endophallic sclerites above primary endophallic sclerite (no additional sclerites in others).

Food plants. Unknown.

Distribution. China: Yunnan.

Taiwanese species

***Furusawaia jungchani* sp. nov.**
http://zoobank.org/FCD26A55-C260-4977-A894-B25BA485A9E7
Figs 3B, 5, 6, 7

Types (n = 19). ***Holotype*** ♂ (TARI), Taiwan. Nantou: Huakang (華崗), 10.IV.2019, leg. J.-C. Chen (陳榮章). ***Paratypes***. 3♂, 2♀ (TARI), same data as holotype; 8♂, 2♀ (TARI), same but with "24.IV.2019"; 1♂, 1♀ (TARI), same but with "23.V.2017"; 1♂ (TARI), Hohuansi trail (合歡溪步道 = Huakan, 華崗), 15.V.2017, leg. J.-C. Chen.

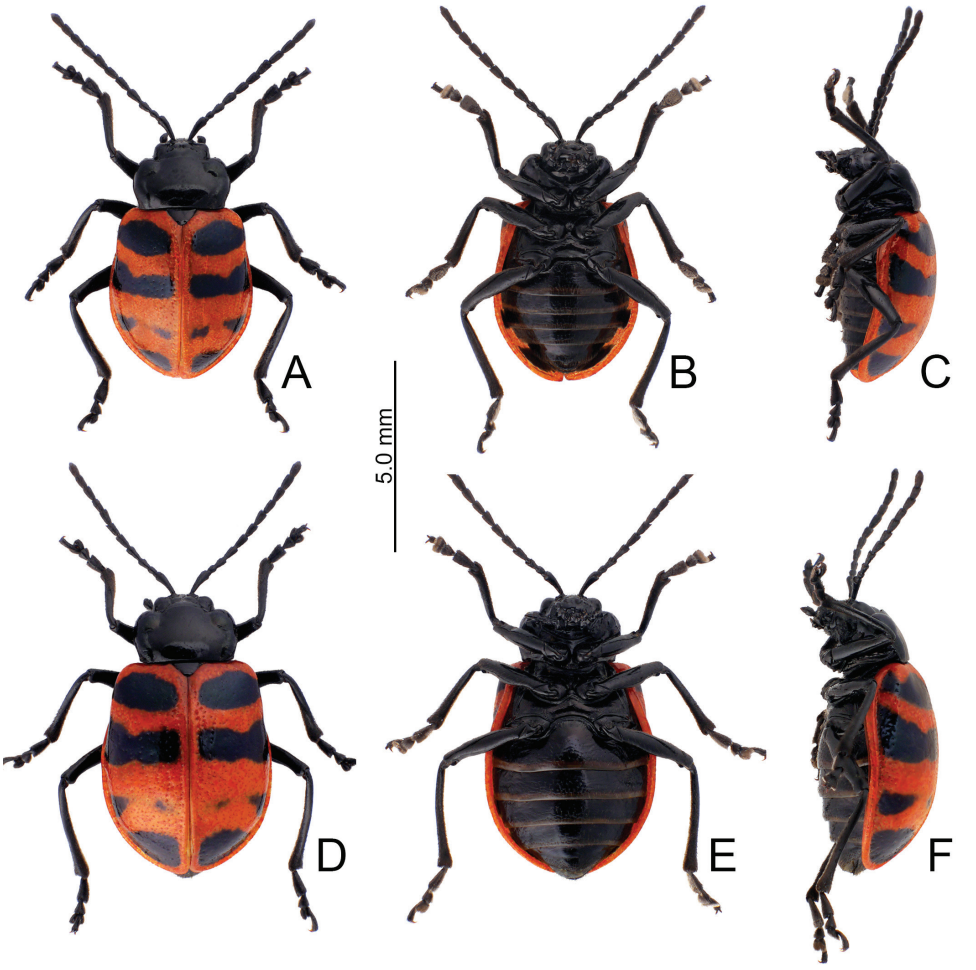

Figure 5. Habitus, *Furusawaia jungchani* sp. nov. **A** male**,** dorsal view **B** ditto, ventral view **C** ditto, lateral view **D** female, dorsal view **E** ditto, ventral view **F** ditto, lateral view.

Description. Length 6.8–8.3 mm, width 4.1–5.1 mm. Body color (Fig. 5) black, elytra with red or orange stripes along basal and lateral margins, and suture, three transverse red or orange stripes at basal 1/4, middle, and apical 1/4 respectively, anterior and median stripes straight, posterior stripe curved anteriorly at middle, median and posterior stripes wider, sometimes connected with each other, in some individuals anterior stripe also wider. Antennae filiform in males (Fig. 6A), length ratios of antennomeres I–XI 1.0: 0.3: 0.4: 0.6: 0.6: 0.5: 0.6: 0.6: 0.5: 0.5: 0.6, length to width ratios of antennomeres I–XI 3.2: 1.4: 1.7: 2.2: 2.3: 2.1: 2.3: 2.3: 2.1: 2.2: 2.4; similar in females (Fig. 6B), length ratios of antennomeres I–XI 1.0: 0.4: 0.4: 0.5: 0.5: 0.5: 0.5: 0.5: 0.5: 0.5: 0.6, length to width ratios of antennomeres I–XI 3.0: 1.5: 1.6: 2.2: 2.1: 2.1: 1.9: 2.4: 2.1: 2.0: 2.4. Pronotum 1.7–1.8 × wider than long, disc strongly convex; smooth, without reticulate microsculpture; with punctures obsolete, with lateral

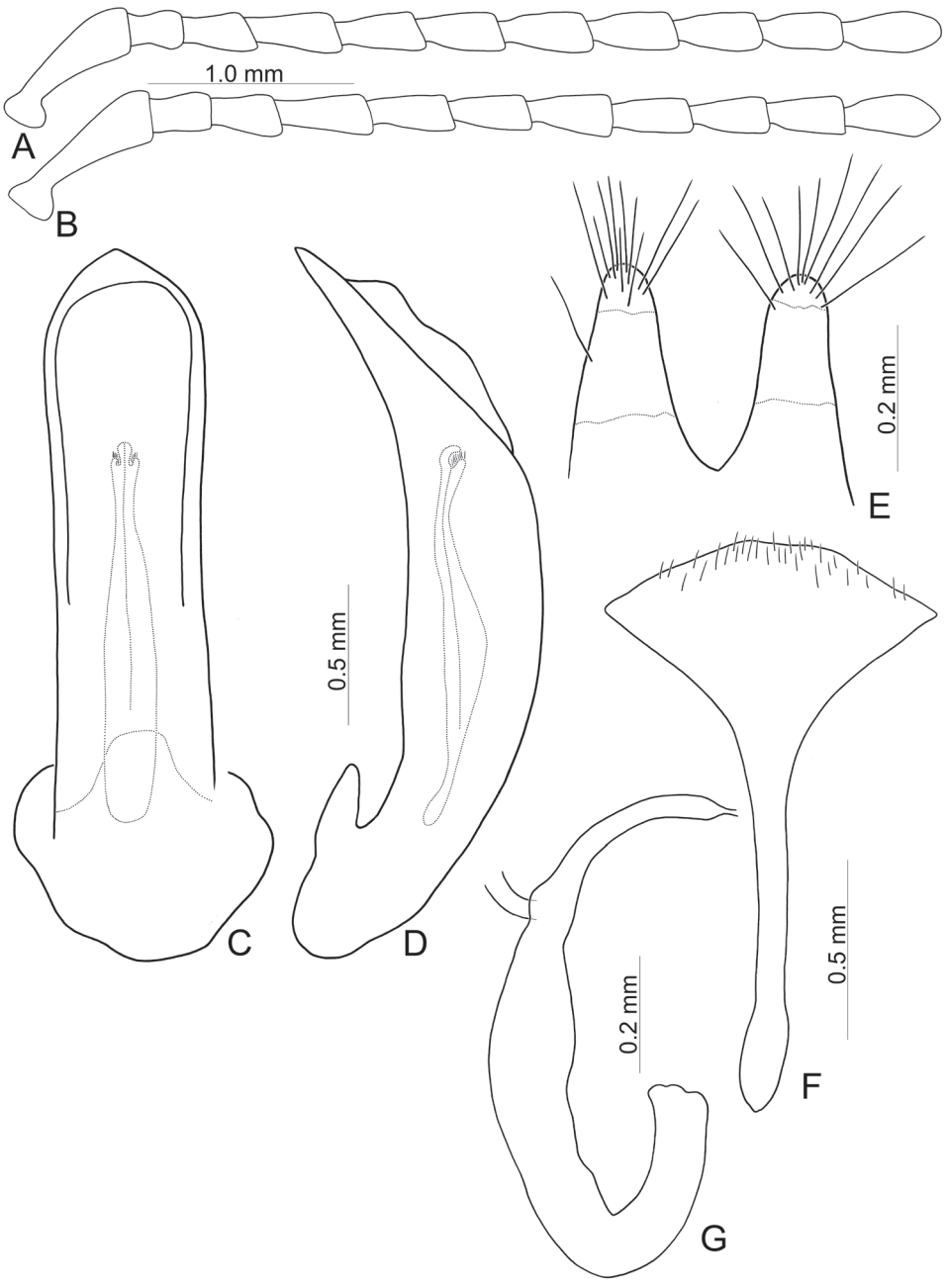

Figure 6. Diagnostic characters of *Furusawaia jungchani* sp. nov. **A** antenna, male **B** antenna, female **C** aedeagus, dorsal view **D** ditto, lateral view **E** gonocoxae **F** abdominal ventrite VIII, female **G** spermatheca.

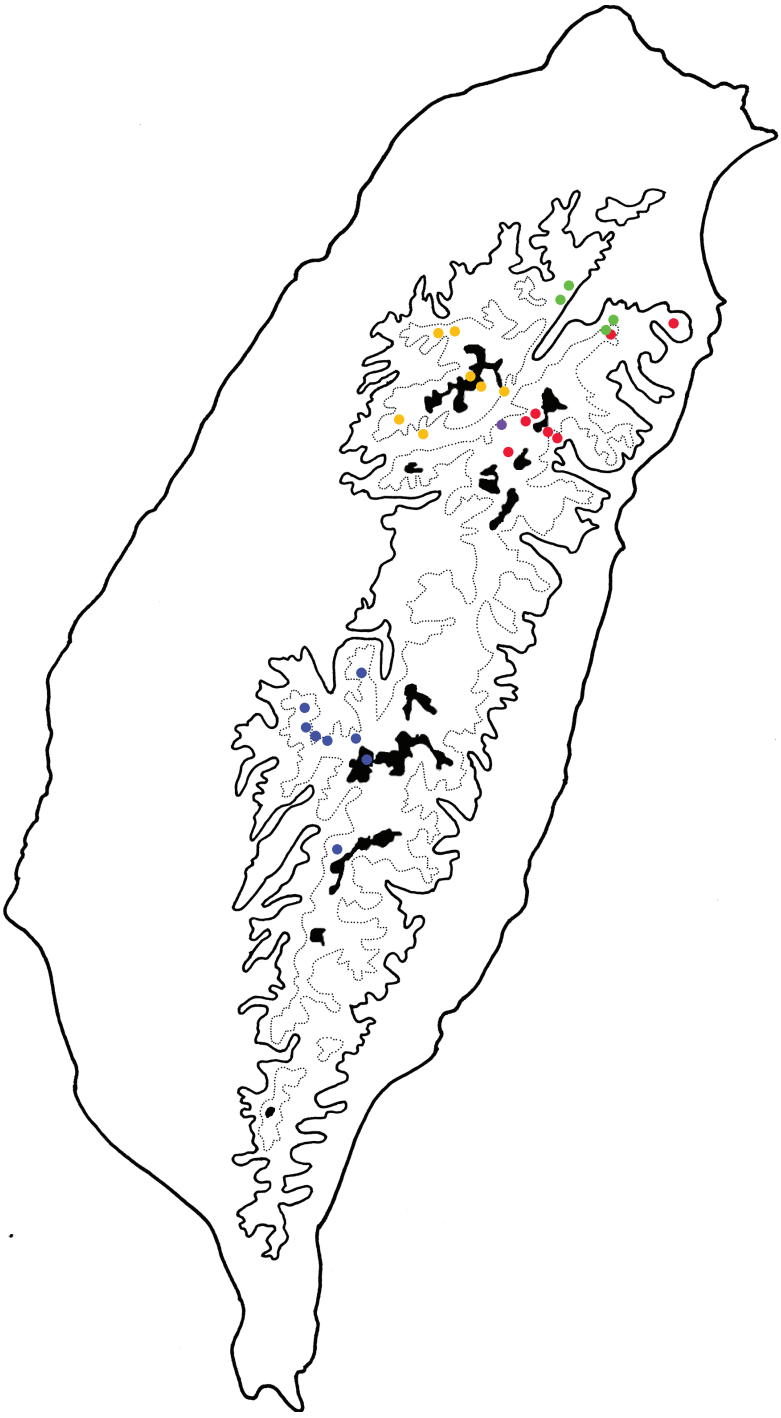

Figure 7. Distribution map of *Furusawaia* species inTaiwan, solid line: 1000 m, broken line: 2000 m, black areas: 3000 m. Key: Red Dots *F. lui* sp. nov. Blue Dots *F. yosonis* Chûjô Green Dots *F. tsoui* sp. nov. Yellow Dots *F. tahsiangi* sp. nov. Purple Dot *F. jungchani* sp. nov.

impressions; lateral margins distinct, rounded, and widest at apical 1/3, reduced at anterior angles; apical and basal margins straight; anterior angles strongly produced to a bulbous point. Elytra with rounded lateral margins, widest behind middle, 1.2–1.3 × longer than wide; disc smooth, without reticulate microsculpture; and with sparse, coarse punctures. Aedeagus (Fig. 6C, D) slender in dorsal view, 5.7 × longer than wide, parallel-sided, narrowed near apex, apex narrowly rounded; ostium large, covered by membrane; strongly curved in lateral view; endophallic sclerite elongate, 0.5 × as long as aedeagus, one pair of short lateral expansions near apex, covered with fine setae; basal 2/3 widened and parallel-sided. Only median areas of apices of gonocoxae (Fig. 6E) sclerotized, elongate, apex narrowly rounded, with several long setae near apex. Ventrite VIII (Fig. 6F) with apex well sclerotized and small, several short setae along apical margin, spiculum long. Receptacle of spermatheca (Fig. 6G) slightly swollen, undivided from pump; pump long and strongly curved; sclerotized proximal spermathecal duct undivided from receptacle, moderately long.

Diagnosis. Adults of *Furusawaia jungchani* sp. nov. are similar to those of *F. tahsiangi* sp. nov. in sharing straight median and posterior stripes on the elytra but differ by the wider median and posterior stripes (Fig. 5) (median and posterior stripes not so modified in *F. tahsiangi* sp. nov. (Fig. 10)); and strongly convex pronotum with reduced lateral margin at anterior angles (less convex pronotum with lateral margin at anterior angles in *F. tahsiangi* sp. nov.). In males of *F. jungchani* sp. nov., the aedeagus is strongly curved in lateral view (Fig. 6D) (moderately curved in *F. yosonis* (Fig. 15D), slightly curved in others (Figs 9F, 11D, 13D)); endophallic sclerite (Fig. 6C) similar to that of *F. yosonis* (Fig. 15C) with basal 2/3 wider and parallel-sided (only wider at middle in *F. lui* sp. nov. (Fig. 9C); basal 2/3 widened but basally narrowed, and strongly widened at middle in *F. tahsiangi* sp. nov. (Fig. 11C); basal 2/3 widened but basally and in basal 3/7 narrowed in *F. tsoui* sp. nov. Fig. 13C)). In females of *F. jungchani* sp. nov., the spermathecae (Fig. 6G) are similar to those of *F. yosonis* (Fig. 15G) with slightly swollen receptacle (moderately swollen receptacle in *F. lui* sp. nov. (Fig. 9I) and *F. tahsiangi* sp. nov. (Fig. 11F); strongly swollen receptacle in *F. tsoui* sp. nov. (Fig. 13G)) and apex undivided from sclerotized proximal duct (Fig. 6G) (apex truncate and divided from sclerotized proximal duct in *F. lui* sp. nov. (Fig. 9G, I) and *F. tahsiangi* sp. nov. (Fig. 11F)); abdominal ventrite VIII (Fig. 6F) similar to that of *F. lui* sp. nov. (Fig. 9H) with large, well sclerotized apex (membranous apex in *F. tsoui* sp. nov. (Fig. 13F) and *F. yosonis* (Fig. 15F); sclerotized and small apex in *F. tahsiangi* sp. nov. (Fig. 11G)); gonocoxae (Fig. 6E) similar to those of *F. tahsiangi* sp. nov. (Fig. 11E) and *F. tsoui* sp. nov. (Fig. 13E) with rounded apices (acute apices in *F. yosonis* (Fig. 15E)) and dense setae present only at apical area (dense setae present at apical and lateral area in *F. lui* sp. nov. (Fig. 9J)).

Food plants. *Stellaria reticulivena* Hayata (Caryophyllaceae).

Biological notes. All adults were found on forest trails during daytime (Fig. 3B).

Distribution. Only known from the type locality (Fig. 7).

Etymology. The species name is dedicated to Mr Jung-Chan Chen (陳榮章) who collected all specimens of this new species.

***Furusawaia lui* sp. nov.**
http://zoobank.org/A03781BE-A4ED-49A4-A7E9-B2D2643C6657
Figs 1A, C, D, 8, 9

Furusawaia yosonis Chûjô, 1962: 108 (part).

Types (n = 21). ***Holotype*** ♂ (TARI), Taiwan. Hualien: Pilu (碧綠), 27.IV.2018, leg. H.-F. Lu (陸錫峯). ***Paratypes***. 1♀ (TARI), same data as holotype; 1♀ (TARI), same but with "25.V.2018"; 1♀ (TARI), same but with "17.VI.2018"; 1♀ (TARI), same but with "23.VI.2018"; Hualien: 1♂, 1♀ (TARI), Hsiaofengkou (小風口), 11.V.2017, leg. C.-T. Yao (姚正得); 1♂ (TARI), same but with "22.VI.2017"; 1♂ (TARI), same locality, 2.VIII.2017, leg. 何彬宏 (B.-H. Ho); 1♂ (TARI), Hsinpaiyang (新白楊), 18.V.2018, leg. H.-F. Lu; 1♂, 2♀♀ (TARI), Karenko (= Hualien, 花蓮), 20.VII.-4.VIII.1919, leg. T. Okuni; Ilan: 1♀ (TARI), Lankanshan (蘭坎山), 1.VII.2017, leg. P.-Y. Chen (陳柏彥); 1♂ (JBCB), Taipingshan (太平山), 19.VI.2008, leg. S.-F. Yu (余素芳); Nantou: 2♀♀ (TARI), 820 Forest road (820 綠林道), 6.VII.2015, leg. T.-H. Lee (李大翔); Taichung: 1♂, 2♀ (TARI), Pilu (畢祿), 7.VII.2015, leg. C.-F. Lee (李奇峯); 1♀ (TARI), same locality, 2.VI.2016, leg. Y.-T. Chung (鍾奕霆).

Description. Length 8.4–9.3 mm, width 4.8–5.5 mm. Body color (Fig. 8) black, elytra with pink (yellow in dead specimens) stripes along basal and lateral margins, and suture, three transverse pink stripes at basal 1/4, middle, and apical 1/4 respectively, anterior stripe curved posteriorly and connected with basal stripe, median angular at middle and connected anteriorly with anterior stripe, posterior stripe angular at middle, basal stripe extending posteriorly from humeral calli and connected with anterior stripe. Antennae filiform in males (Fig. 9A), length ratios of antennomeres I–XI 1.0: 0.3: 0.4: 0.6: 0.5: 0.5: 0.5: 0.5: 0.4: 0.4: 0.5, length to width ratios of antennomeres I–XI 3.3: 1.4: 1.4: 2.1: 1.9: 1.8: 2.0: 1.9: 1.7: 1.7: 2.1; similar in females (Fig. 9B), length ratios of antennomeres I–XI 1.0: 0.3: 0.4: 0.5: 0.4: 0.4: 0.5: 0.4: 0.5: 0.4: 0.5, length to width ratios of antennomeres I–XI 3.2: 1.4: 1.8: 2.3: 2.2: 2.0: 2.1: 2.1: 2.2: 2.2: 2.6. Pronotum 1.8–1.9 × wider than long, disc strongly convex; smooth, without reticulate microsculpture; with punctures obsolete; with lateral impressions; lateral margins distinct including anterior angles, rounded and widest at apical 1/3; apical and basal margin straight; anterior angles strongly produced to a bulbous point. Elytra with rounded lateral margin, widest behind middle, 1.2–1.3 × longer than wide; disc smooth, with sparse, coarse punctures. Aedeagus (Fig. 9E, F) slender in dorsal view, 5.8 × longer than wide, parallel-sided, narrowed near apex, apex narrowly rounded; ostium large, membranous; slightly curved in lateral view; endophallic sclerite elongate, 0.4× as long as aedeagus, widened only at middle, one pair of short lateral expansions near apex, covered with fine setae. Only apices of gonocoxae (Fig. 9J) sclerotized, elongate, apex narrowly rounded, with extremely dense, short setae near apex. Ventrite VIII (Fig. 9G) with apex well sclerotized, several short setae along apical margin, spiculum short. Receptacle of spermatheca (Fig. 12G, I) moderately or slightly swollen, with

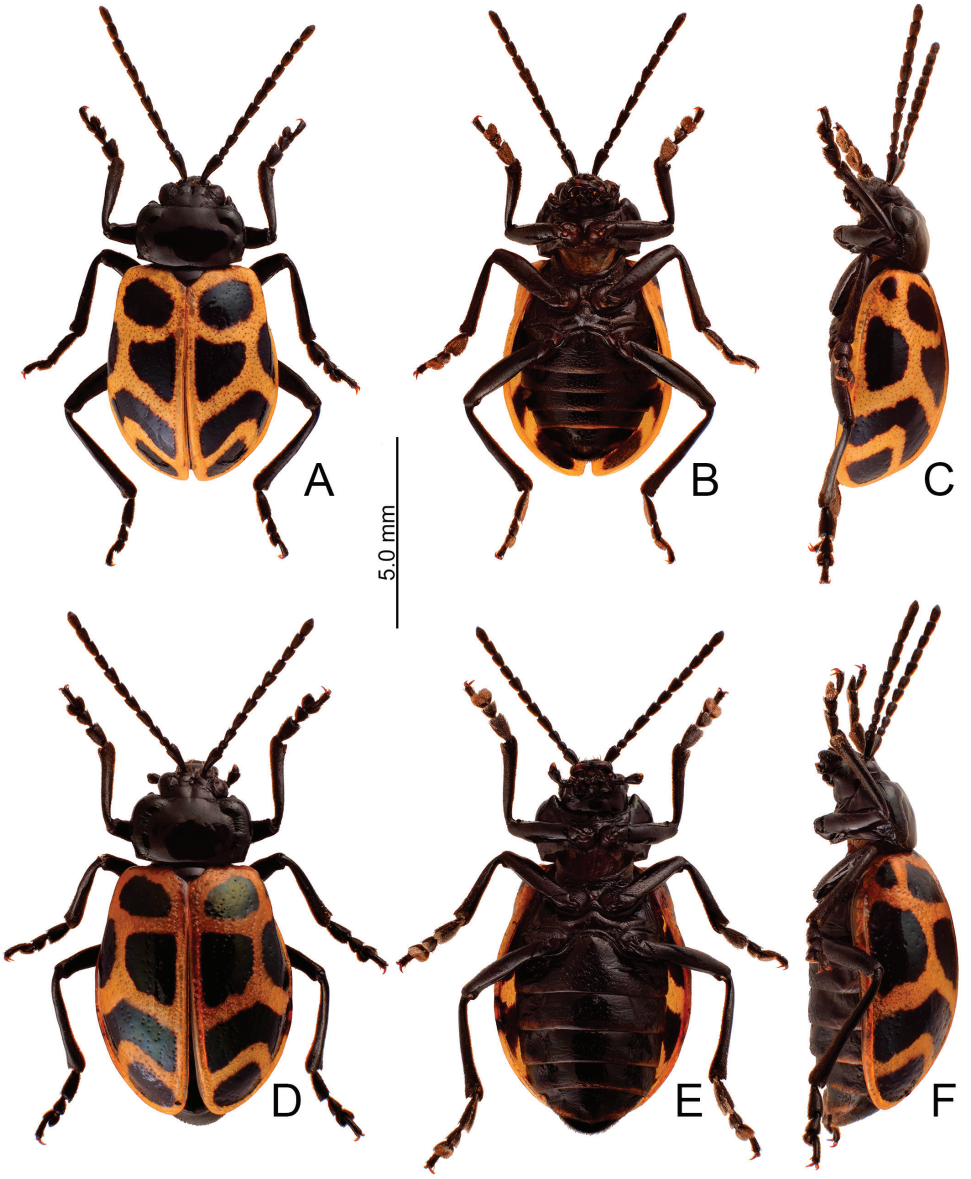

Figure 8. Habitus, *Furusawaia lui* sp. nov. **A** male**,** dorsal view **B** ditto, ventral view **C** ditto, lateral view **D** female, dorsal view **E** ditto, ventral view **F** ditto, lateral view.

apex truncate, undivided from pump; pump long and strongly curved; sclerotized proximal spermathecal duct separated from receptacle, short to moderately long.

Variations. Populations in lower altitudes such as Pilu (碧綠, 2200 m) and Hsinpaiyang (新白楊, 1600 m) have more slender antennae, length ratios of antennomeres I–XI in males 1.0: 0.4: 0.5: 0.7: 0.5: 0.5: 0.6: 0.6: 0.6: 0.6: 0.5 (Fig. 9C), length to width ratios of antennomeres I–XI 2.9: 1.5: 1.6: 2.4: 2.1: 2.1: 2.1: 2.3: 2.2: 2.4: 2.9;

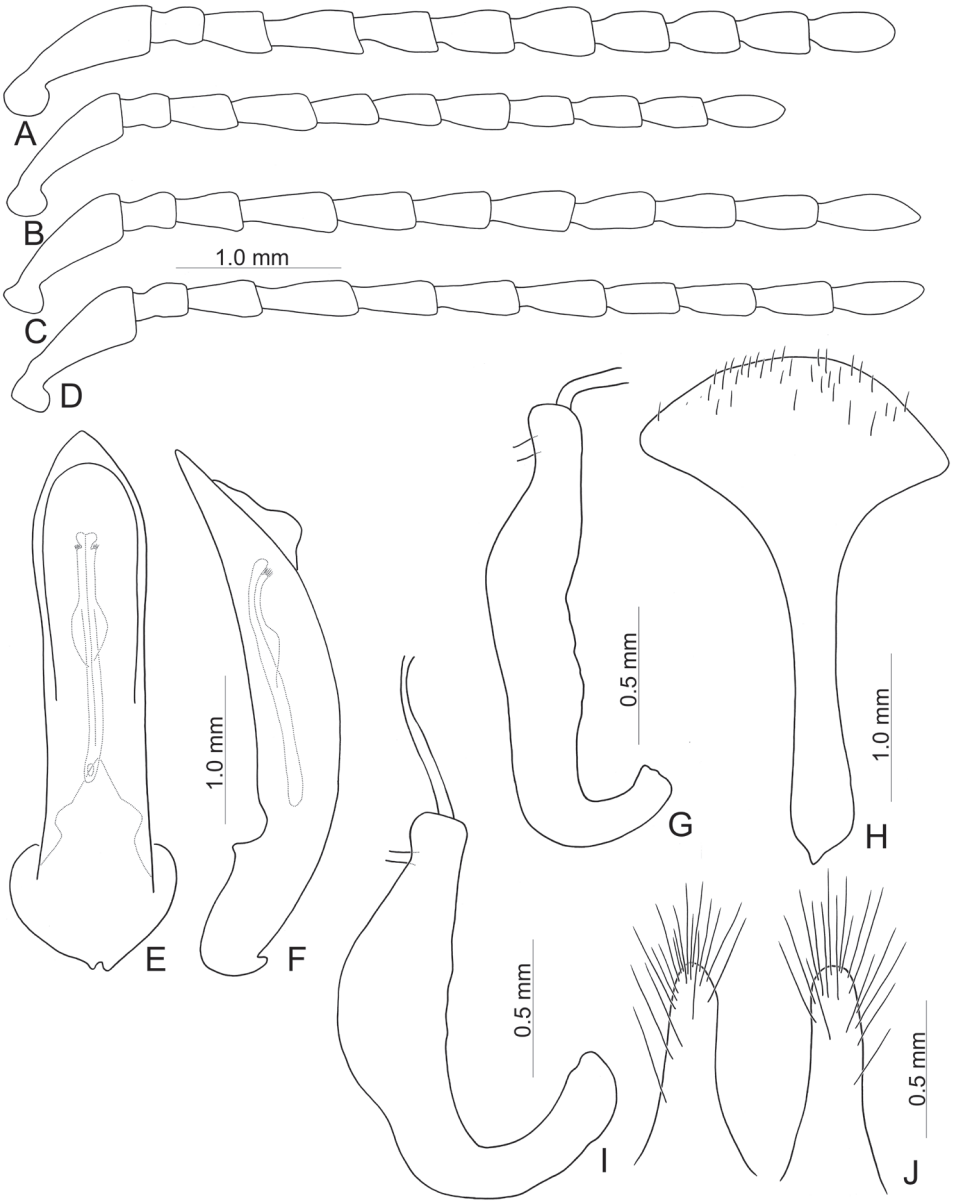

Figure 9. Diagnostic characters of *Furusawaia lui* sp. nov. **A** antenna, male, Hsiaofengkou (小風口) **B** antenna, female, Pilu (畢祿) **C** antenna, male, Hsinpaiyang (新白楊) **D** antenna, female, Pilu (碧綠) **E** aedeagus, dorsal view **F** ditto, lateral view **G** spermatheca **H** abdominal ventrite VIII, female **I** spermatheca, variation **J** gonocoxae.

similar in females (Fig. 9D), length ratios of antennomeres I–XI 1.0: 0.4: 0.5: 0.6: 0.6: 0.5: 0.5: 0.5: 0.5: 0.5: 0.6, length to width ratios of antennomeres I–XI 2.7: 1.6: 1.9: 2.6: 2.5: 2.4: 2.3: 2.4: 2.4: 2.5: 2.9. Northern populations, including specimens collected from Taipingshan and Lankanshan, have less convex pronota.

Diagnosis. Adults of *Furusawaia lui* sp. nov. are characterized by the longitudinal stripes connected between basal and anterior stripes, and anterior and median stripes (Fig. 8). In males of *F. lui* sp. nov., the aedeagus (Fig. 9F) is similar to that of *F. tahsiangi* sp. nov. (Fig. 11D) and *F. tsoui* sp. nov. (Fig. 13D), slightly curved in lateral view (strongly curved in *F. jungchani* sp. nov. (Fig. 6D), moderately curved in *F. yosonis* (Fig. 15D)); endophallic sclerite only widened at middle (Fig. 9E) (basal 2/3 widened and parallel-sided in *F. jungchani* sp. nov. (Fig. 6C) and *F. yosonis* (Fig. 15C), basal 2/3 widened but basally narrowed, and strongly widened at middle in *F. tahsiangi* sp. nov. (Fig. 11C); basal 2/3 widened but basally and at basal 3/7 narrowed in *F. tsoui* sp. nov. (Fig. 13C)). In females of *Furusawaia lui* sp. nov., the spermatheca (Fig. 9G, I) is similar to those of *F. tahsiangi* sp. nov. (Fig. 11F), *F. jungchani* sp. nov. (Fig. 6G), and *F. yosonis* (Fig. 15G) with moderately or slightly swollen receptacle (strongly swollen receptacle in *F. tsoui* sp. nov. (Fig. 13G)) and apex truncate and divided from sclerotized proximal duct (apex undivided from sclerotized proximal duct in *F. jungchani* sp. nov. (Fig. 6G), *F. tsoui* sp. nov. (Fig. 13G), and *F. yosonis* (Fig. 15G)); abdominal ventrite VIII (Fig. 9H) is similar to that of *F. jungchani* sp. nov. (Fig. 6F) with well sclerotized and large apex (membranous apex in *F. tsoui* sp. nov. (Fig. 13F) and *F. yosonis* (Fig. 15F); sclerotized and smaller apex in *F. tahsiangi* sp. nov. (Fig. 11G)); the gonocoxae (Fig. 9J) are similar in most Taiwanese species with rounded apices (pointed apices in *F. yosonis* (Fig. 15E)) but dense setae at apical and lateral areas (dense setae only at apical area in *F. jungchani* sp. nov. (Fig. 6E), *F. tahsiangi* sp. nov. (Fig. 11E), and *F. tsoui* sp. nov. (Fig. 13E)).

Remarks. Three paratypes of *Furusawaia yosonis* labeled as "Formosa / Karenko (= Hualien, 花蓮), -19 / VII 20-VIII 4. / T. Okuni [p, w] // Para / Type [p, green letters, circle label with border // Furusawaia / yosonis / CHÛJÔ [h] / DET. M. CHUJO [p, w] // 1912 (♂), 1914 (♀), 2168 (♀) [p, w]" belong to this new species and are designated as paratypes.

Food plants. *Stellaria media* (L.) Vill (Caryophyllaceae).

Biological notes. Adults were active on forest trails during daytime at Hsinpaiyang (新白楊) (Fig. 3A, C), Pilu (碧綠), and Hsiaofengkou (小風口). They were nocturnal at Pilu (畢祿) (Fig. 3D).

Distribution. This new species is widespread between middle and high altitudes (above 1,500) in north and east Taiwan (Fig. 7). It is sympatric with *F. tsoui* sp. nov. in Taipingshan.

Etymology. The species name is dedicated to Mr Hsi-Feng Lu (陸錫峯), the member of TCRT who collected most specimens of this new species.

***Furusawaia tahsiangi* sp. nov.**

http://zoobank.org/17C8C5CC-7C9C-4EC7-B3AA-7266AD638AFB

Figs 3E, 10, 11

Furusawaia yosonis Chûjô, 1962: 108 (part).

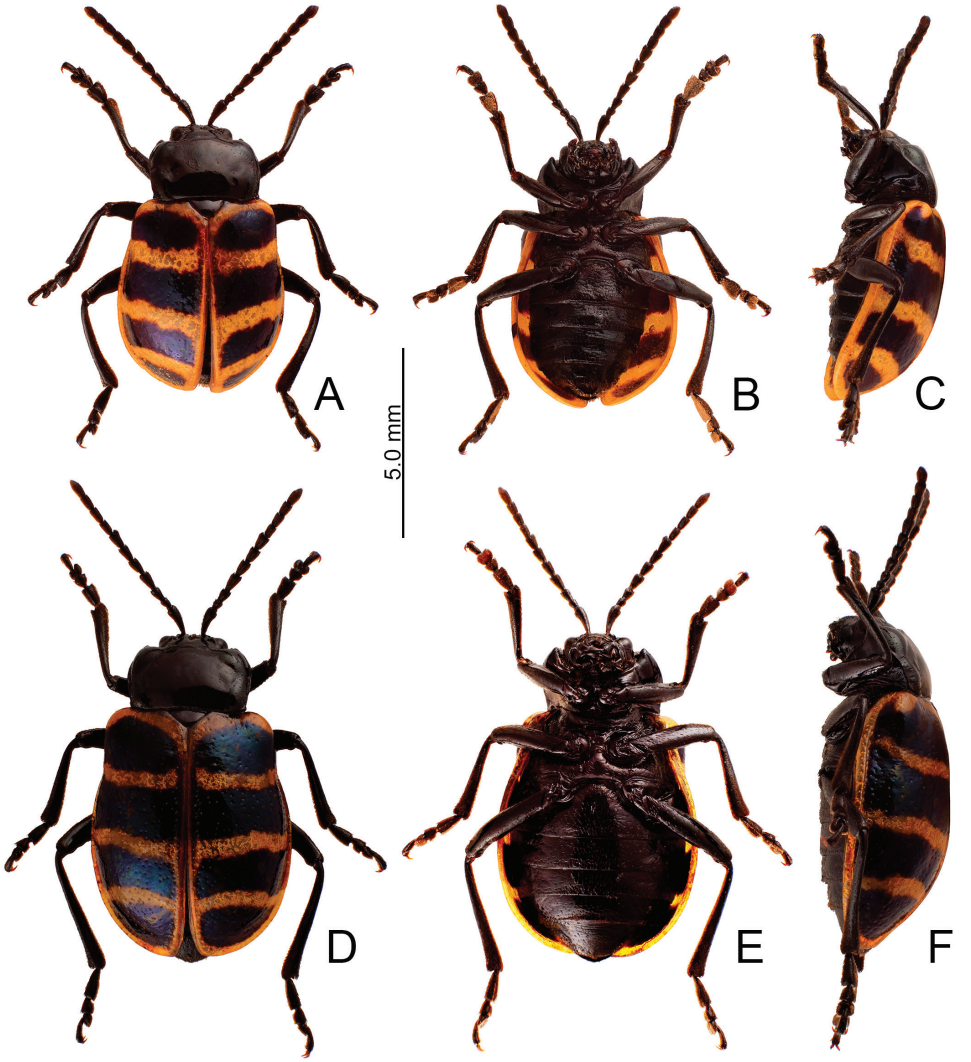

Figure 10. Habitus, *Furusawaia tahsiangi* sp. nov. **A** male**,** dorsal view **B** ditto, ventral view **C** ditto, lateral view **D** female, dorsal view **E** ditto, ventral view **F** ditto, lateral view.

Types (n = 17). ***Holotype*** ♂ (TARI), Taiwan. Taichung: Tahsuehshan (大雪山), 7.VI.2010, leg. T.-H. Lee (李大翔). ***Paratypes.*** 1♀, same data as holotype; Hsinchu: 1♀ (TARI), Kuanwu (觀霧), 4.IV.2017, leg. C.-Y. Chuang (莊靜宜); Ilan: 1♂, 1♀ (TARI), Siyuanyakou (思源啞口), 30.III.2015, leg. P.-H. Ko (柯品薰); Miaoli: 1♂ (TARI), Kueishan (檜山), 27.VII.2020, leg. S.-F. Yu (余素芳); Taichung: 1♂, 1♀ (TARI), Hsuehshan (雪山), 1.IV.2010, leg. W.-B. Yeh (葉文斌); 1♀ (TARI), same locality, 10.VI.2010, leg. P.-L. Tian (田佩玲); 1♂ (TARI), same locality, 1.V.2012, leg. J.-C. Chen (陳榮章); 1♀ (TARI), same locality, 1.V.2012, leg. T.-H. Lee (李大翔);

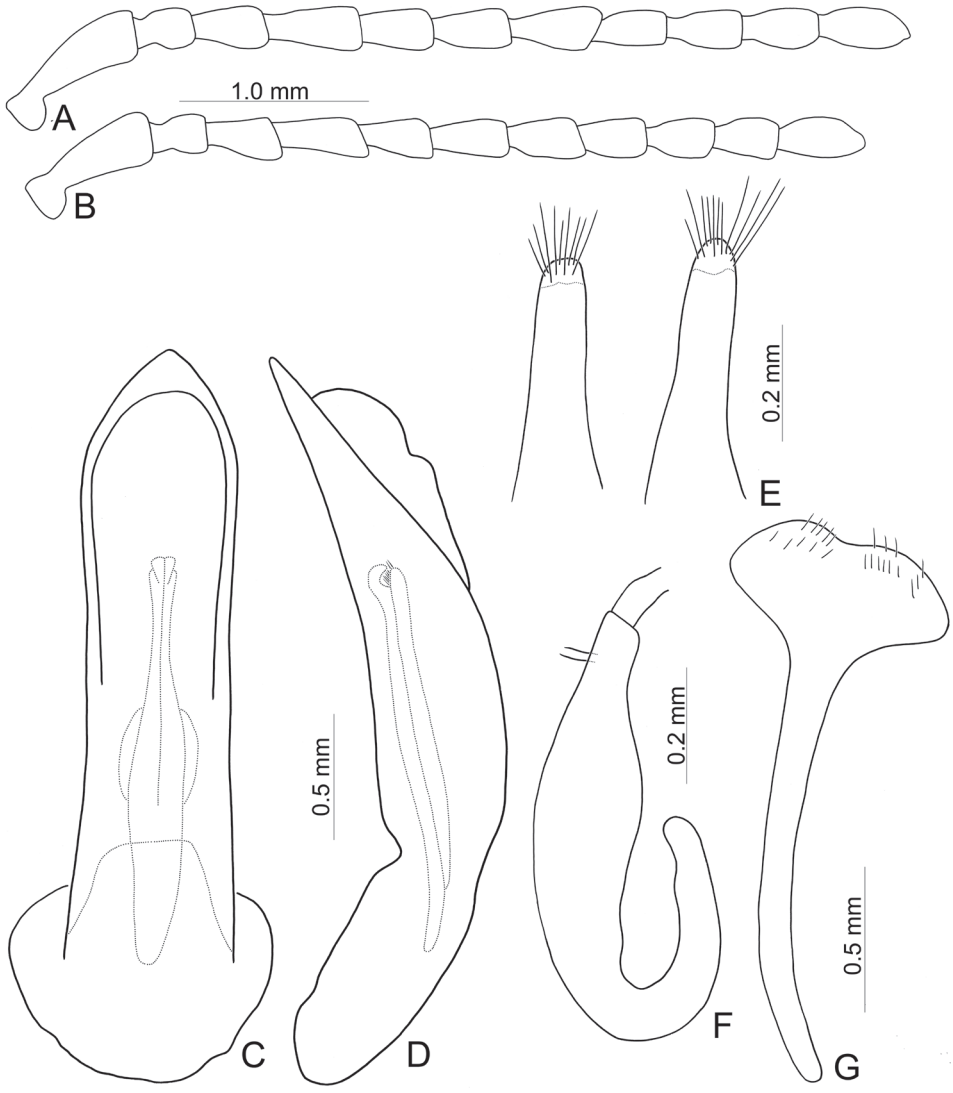

Figure 11. Diagnostic characters of *Furusawaia tahsiangi* sp. nov. **A** antenna, male **B** antenna, female **C** aedeagus, dorsal view **D** ditto, lateral view **E** gonocoxae **F** spermatheca **G** abdominal ventrite VIII, female.

1♂ (TARI), same locality, 8.V.2015, leg. C.-Y. Hsu (許志遠); 1♂, 1♀ (TARI), same but with "24.IV.2019; 1♀ (TARI), same locality, 20.IV2021, leg. W.-J. Chien (簡畹融); 1♂ (TARI), Hassenzan (= Pahsienshan, 八仙山), 6.VI.1942, leg. A. Mutuura; 1♂ (TARI), Tsuichih (翠池), 1.V.2012, leg. F.-S. Huang (黃福盛).

Description. Length 7.9–8.9 mm, width 4.5–5.5 mm. Body color (Fig. 10) black, elytra with orange stripes along basal and lateral margins, and suture, three transverse orange stripes at basal 1/4, middle, and apical 1/4 respectively, anterior and middle transverse stripes straight, posterior transverse stripe curved slightly anteriorly. Antennae filiform in males (Fig. 11A), length ratios of antennomeres I–XI 1.0: 0.4: 0.5: 0.6: 0.5:

0.5: 0.6: 0.5: 0.5: 0.5: 0.6, length to width ratios of antennomeres I–XI 2.9: 1.5: 1.7: 2.1: 1.8: 1.9: 2.3: 2.1: 2.0: 2.0: 2.3; similar in females (Fig. 11B), length ratios of antennomeres I–XI 1.0: 0.4: 0.5: 0.6: 0.5: 0.5: 0.5: 0.5: 0.5: 0.5: 0.6, length to width ratios of antennomeres I–XI 2.6: 1.5: 1.6: 2.3: 1.8: 2.0: 1.9: 1.7: 1.7: 1.7: 2.2. Pronotum 1.6–1.7 × wider than long, disc slightly convex; smooth, without reticulate microsculpture; with punctures obsolete, with lateral impressions reduced; lateral margins distinct, including anterior angles, rounded and widest at apical 1/3; apical and basal margin straight; anterior angles strongly produced to a bulbous point. Elytra with rounded lateral margin, widest behind middle, 1.2–1.3 × longer than wide; disc smooth, without reticulate microsculpture; and with sparse, coarse punctures. Aedeagus (Fig. 11C, D) slender in dorsal view, 5.5 × longer than wide, parallel-sided, narrowed near apex, apex narrowly rounded; ostium large, membranous; slightly curved in lateral view; endophallic sclerite elongate, 0.5 × as long as aedeagus, basal 2/3 widened but basally narrowed, strongly widened at middle, one pair of short lateral expansions near apex, covered with fine setae. Only apices of gonocoxae (Fig. 11E) sclerotized, elongate, apex narrowly rounded, with dense long setae near apices. Ventrite VIII (Fig. 11G) with apex well sclerotized and small, several short setae along apical margin, spiculum long. Receptacle of spermatheca (Fig. 11F) moderately swollen, undivided from pump, apex truncate; pump long and strongly curved; sclerotized proximal spermathecal duct separated from receptacle, short.

Diagnosis. Adults of *Furusawaia tahsiangi* sp. nov. are similar to those of *F. jungchani* sp. nov. based on the straight anterior and median stripes on the elytra but they differ in the having narrower median and posterior stripes (Fig. 10) (wider median and posterior stripes in *F. jungchani* sp. nov.(Fig. 5)); and less convex pronotum with lateral margin at anterior angles (strongly convex pronotum with reduced lateral margin at anterior angles in *F. jungchani* sp. nov.). In males of *F. tahsiangi* sp. nov., the aedeagus (Fig. 11D) is similar to those of *F. lui* sp. nov. (Fig. 9F) and *F. tsoui* sp. nov. (Fig. 13D), slightly curved in lateral view (strongly curved in *F. jungchani* sp. nov. (Fig. 6D), moderately curved in *F. yosonis* (Fig. 15D)); endophallic sclerite with basal 2/3 wider but basally narrowed, strongly wider at middle (Fig. 11C) (basal 2/3 widened and parallel-sided in *F. jungchani* sp. nov. (Fig. 6C) and *F. yosonis* (Fig. 15C); widened only at middle in *F. lui* sp. nov. (Fig. 9E); basal 2/3 wider, but basally and at basal 3/7 narrowed in *F. tsoui* sp. nov. (Fig. 13C)). In females of *F. tahsiangi* sp. nov., the spermatheca (Fig. 11F) is similar that of *F. lui* sp. nov. (Fig. 9I), with moderately swollen receptacle (slightly swollen receptacle in *F. jungchani* sp. nov. (Fig. 6G) and *F. yosonis* (Fig. 15G); strongly swollen receptacle in *F. tsoui* sp. nov. (Fig. 13G)) and apex truncate and divided from sclerotized proximal duct (apex undivided from sclerotized proximal duct in others); abdominal ventrite VIII (Fig. 11G) well sclerotized, with small apex (membranous apex in *F. tsoui* sp. nov. (Fig. 13F) and *F. yosonis* (Fig. 15F); sclerotized and large apex in *F. jungchani* sp. nov. (Fig. 6F) and *F. lui* sp. nov. (Fig. 9H)); gonocoxae (Fig. 11E) similar to those of *F. jungchani* sp. nov. (Fig. 6E) and *F. tsoui* sp. nov. (Fig. 13E) with rounded apices (pointed apices in *F. yosonis* (Fig. 15E)) and dense setae present only at near apices (dense setae present at apical and lateral areas in *F. lui* sp. nov. (Fig. 9J)).

Remarks. One paratype of *Furusawaia yosonis* labeled: "Taiwan / Hassenzan [p] (= Pahsienshan, 八仙山) / 6.VI.1942 [h] / A. MUTUURA [p, w] // 新八仙山 [h, on the

back of the same label] // Para / Type [p, green letters, circle label with border // Furusawaia / yosonis / CHÛJÔ [h] / DET. M. CHUJO [p, w] // 2318 [p, w]". Chûjô (1962) typed the locality of this specimens as Mt. Shinhassenza which is translated from 新八仙山.

Food plants. *Stellaria media* (L.) Vill (Caryophyllaceae).

Biological notes. Adults were active on forest trails during daytime from Hsuehshan (雪山) (Fig. 3E) and Siyuanyakou (思源啞口); while they were nocturnal at Tahsuehshan (大雪山).

Distribution. This new species is widespread at high altitudes (above 2,000 m) in central Taiwan (Fig. 7).

Etymology. The species name is dedicated to Mr. Ta-Hsiang Lee (李大翔). He and the first author were the first ones of TCRT to find this new species.

***Furusawaia tsoui* sp. nov.**
http://zoobank.org/85943675-C6B4-4E08-A7DF-BFC5B78E7DC4
Figs 3F, 12, 13

Furusawaia yosonis: Kimoto, 1969: 66 (part).

Types (n = 12). ***Holotype*** ♂ (TARI), Taiwan. Ilan: Jianqing trail (見晴步道), 19.V.2015, leg. S.-F. Yu (余素芳). ***Paratypes.*** 1♂, 2♀ (TARI), same data as holotype; Ilan: 1♂ (TARI), Mingchi (明池), 29.VII.2007, leg. M.-H. Tsou (曹美華); 1♀ (BPBM), Taiheizan (= Taipingshan, 太平山); 1♂ (BPBM), same locality, 5.V.1932, leg. J. L. Gressitt; 1♂ (BPBM), same but with "6.VII.1934"; 1♀ (BPBM), same but with "29.VI.193?"; 2♀ (BPBM), same locality, V-VII.1934, leg. L. & M. Gressitt; Hsinchu: 1♀ (TARI), Yuanyanghu (鴛鴦湖), 30.VI.2021, leg. T.-Y. Chien (簡廷仰) & S,-P. Wu (吳書平).

Description. Length 8.1–10.0 mm, width 4.7–5.9 mm. Body color (Fig. 12) black, elytra with pink stripes along basal and lateral margins, and suture, three transverse pink stripes at basal 1/4, middle, and apical 1/4 respectively, anterior stripe subtruncate, median angular at middle, posterior stripe curved upwards, basal stripe extending posterior a little from humeral calli. Antennae filiform in males (Fig. 13A), length ratios of antennomeres I–XI 1.0: 0.4: 0.5: 0.6: 0.6: 0.5: 0.6: 0.6: 0.6: 0.6: 0.7, length to width ratios of antennomeres I–XI 2.9: 1.5: 1.9: 2.4: 2.4: 1.9: 2.2: 2.2: 2.3: 2.3: 2.7; similar in females (Fig. 13B), length ratios of antennomeres I–XI 1.0: 0.4: 0.5: 0.6: 0.6: 0.5: 0.5: 0.4: 0.5: 0.5: 0.6, length to width ratios of antennomeres I–XI 3.2: 1.8: 2.0: 2.7: 2.6: 2.3: 2.2: 2.1: 2.1: 2.3: 2.8. Pronotum 1.7 × wider than long, disc slightly convex; smooth, without reticulate microsculpture; with punctures obsolete, with lateral impressions; lateral margins distinct, rounded, and widest at apical 1/3; apical and basal margin straight; anterior angles strongly produced to bulbous point. Elytra with rounded lateral margin, widest behind middle, 1.2–1.3 × longer than wide; disc smooth, without reticulate microsculpture; and with sparse, coarse punctures. Aedeagus (Fig. 13C, D) slender in dorsal view, 5.8 × longer than wide, parallel-sided,

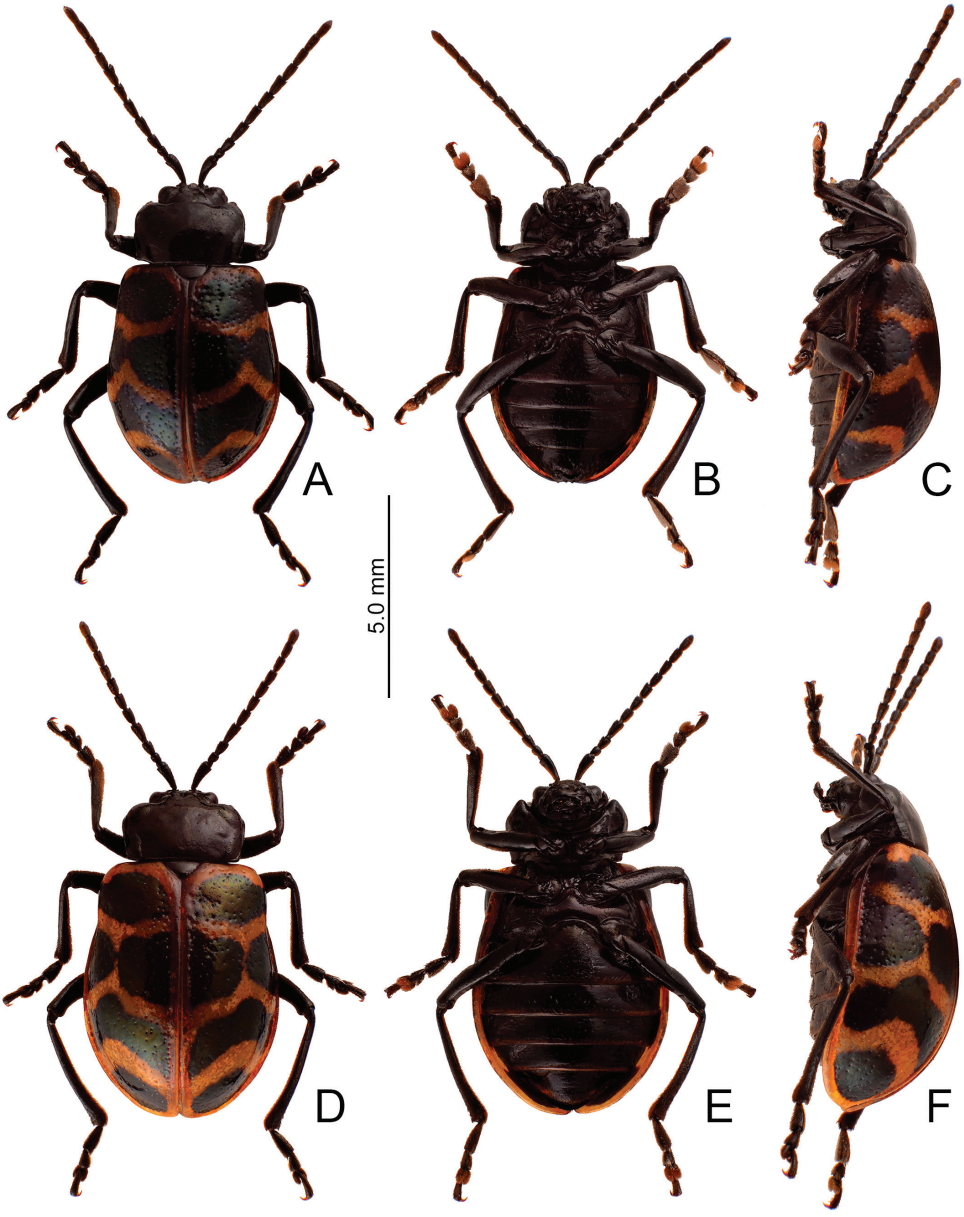

Figure 12. Habitus, *Furusawaia tsoui* sp. nov. **A** male**,** dorsal view **B** ditto, ventral view **C** ditto, lateral view **D** female, dorsal view **E** ditto, ventral view **F** ditto, lateral view.

narrowed near apex, apex narrowly rounded; ostium large, covered membranous; slightly curved at apical 1/3 in lateral view; endophallic sclerite elongate, 0.5 × as long as aedeagus, basal 2/3 widened, but basally and at basal 3/7 narrower, one pair of short lateral expansions near apex, covered with fine setae. Only apices of gonocoxae

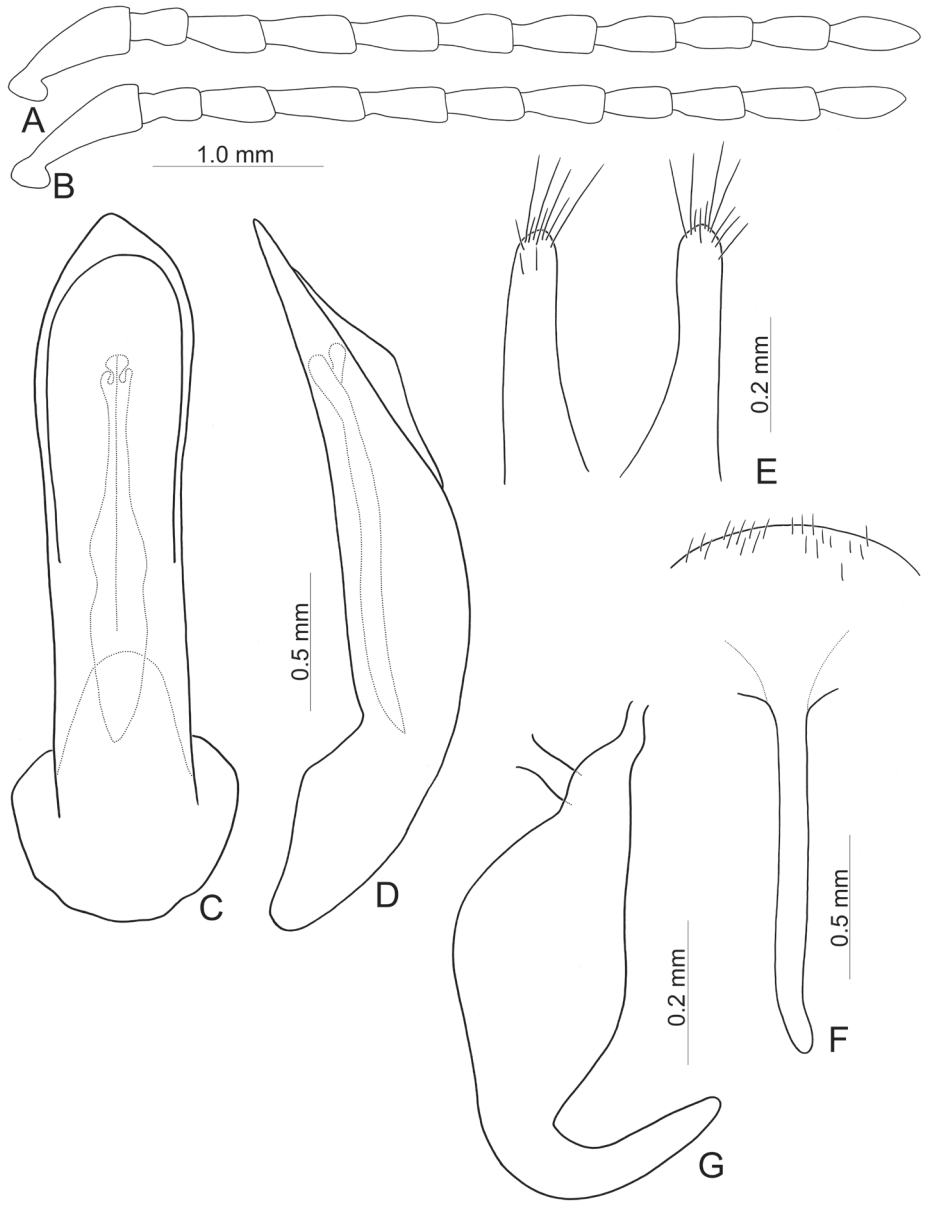

Figure 13. Diagnostic characters of *Furusawaia tsoui* sp. nov. **A** antenna, male **B** antenna, female **C** aedeagus, dorsal view **D** ditto, lateral view **E** gonocoxae **F** abdominal ventrite VIII, female **G** spermatheca.

(Fig. 13E) sclerotized, elongate, apex narrowly rounded, with dense, short setae near apices. Ventrite VIII (Fig. 13F) membranous apically, several short setae along apical margin, spiculum long. Receptacle of spermatheca (Fig. 13G) strongly swollen, undivided from pump; pump long and strongly curved; sclerotized proximal spermathecal duct undivided from receptacle, short.

Diagnosis. Adults of *Furusawaia tsoui* sp. nov. (Fig. 12) are similar to *F. yosonis* Chûjô (Fig. 14) based on the curved median and posterior stripes on the elytra (straight median and posterior stripes on the elytra in *F. jungchani* sp. nov. (Fig. 5) and *F. tahsiangi* sp. nov. (Fig. 10)) and without longitudinal stripes connecting basal and anterior stripes, anterior and median stripes (with longitudinal stripes connecting basal and anterior stripes, anterior and median stripes in *F. lui* sp. nov. (Fig. 8)) but differing by the less convex pronotum with lateral margin present at anterior angles (strongly convex pronotum with lateral margin reduced at anterior angles in *F. yosonis*). In males of *F. tsoui* sp. nov., aedeagus (Fig. 13D) similar to those of *F. lui* sp. nov. (Fig. 9F) and *F. tahsiangi* sp. nov. (Fig. 11D), slightly curved in lateral view (strongly curved in *F. jungchani* sp. nov. (Fig. 6D), moderately curved in *F. yosonis* (Fig. 15D)); endophallic sclerite with basal 2/3 widened, but basally and at basal 3/7 narrowed in *F. tsoui* sp. nov. (Fig. 13C) (basal 2/3 widened and parallel-sided in *F. jungchani* sp. nov. (Fig. 6C) and *F. yosonis* (Fig. 15C), widened only at middle in *F. lui* sp. nov. (Fig. 9E), basal 2/3 widened but basally narrowed, strongly widened at middle in *F. tahsiangi* sp. nov. (Fig. 11C)). In females of *F. tsoui* sp. nov., spermatheca (Fig. 13G) with strongly swollen receptacle (slightly or moderately swollen receptacle in others) and apex undivided from sclerotized proximal duct (apex truncate and separate from sclerotized proximal duct in *F. lui* sp. nov. (Fig. 9G, I) and *F. tahsiangi* sp. nov. (Fig. 11F)); abdominal ventrite VIII (Fig. 13F) similar to those of *F. yosonis* (Fig. 15F) membranous apex (well sclerotized small apex in *F. tahsiangi* sp. nov. (Fig. 11G), sclerotized large apex in *F. jungchani* sp. nov. (Fig. 6F) and *F. lui* sp. nov. (Fig. 9H)); gonocoxae (Fig. 13E) similar to *F. jungchani* sp. nov. (Fig. 6E) and *F. tahsiangi* sp. nov. (Fig. 11E) with rounded apices (pointed apices in *F. yosonis* (Fig. 15E)) and dense setae present only near apex (dense setae present at apical and lateral area in *F. lui* sp. nov. (Fig. 9J)).

Remarks. The specimens identified by Kimoto (1969) as *Furusawaia yosonis* collected from Taipingshan (太平山) belong to this new species and are designated as paratypes.

Food plants. *Stellaria media* (L.) Vill and *Cucubalus baccifer* L. (Caryophyllaceae).

Biological notes. Adults were active on forest trails during daytime at Mingchi (明池). They were nocturnal on Jianqing trail (見晴步道) (Fig. 3F).

Distribution. This species is widespread at low and mid-altitudes (above 1,000 m) in northern Taiwan (Fig. 7). It is sympatric with *F. lui* sp. nov. in Taipingshan (太平山).

Etymology. The species name is dedicated to Mr Mei-Hua Tsou (曹美華). He was the first to collect adults of this new species in Mingchi (明池).

Furusawaia yosonis Chûjô, 1962

Figs 3G, 14, 15

Furusawaia yosonis Chûjô, 1962: 109 (Alishan, 阿里山); Kimoto 1969: 66 (part); Wilcox 1971: 210 (catalogue); Kimoto and Chu 1996: 91 (catalogue); Kimoto and Takizawa 1997: 310; Beenen 2010: 458 (catalogue); Yang et al. 2015: 187 (catalogue).

Types. ***Holotype*** ♂ (TARI, by original designation): "Holo / Type [p, circle label with letters faded out] // Arisan (= Alishan, 阿里山) / FORMOSA / 24–25.V.1933 / Col. M. CHUJO [p, w] // Furusawaia / yosonis / CHÛJÔ [h] / DET. M. CHUJO [p, w] // 2320 [p, w]". ***Paratypes*****:** 1♀ (TARI): "Allo / Type [p, gray letters, circle label with border] // Arisan (= Alishan, 阿里山) / FORMOSA / 24–25.V.1933 / Col. M. CHUJO [p, w] // Furusawaia / yosonis / CHÛJÔ [h] / DET. M. CHUJO [p, w] // 2319 [p, w]"; 1♂ (TARI): "Hunkiko (= Fenchihu, 奮起湖) / VII.6.1928 [p, letters faded out] // R. Takahashi / ???? [p, letters faded, illegible] // Para / Type [p, green letters, circle label with border // Furusawaia / yosonis / CHÛJÔ [h] / DET. M. CHUJO [p, w] // 2319 [p, w]".

Other material (n = 28). Taiwan. Chiayi: 2♀ (TARI), Arisan (= Alishan, 阿里山), V.1935, leg. Y. Miwa; 1♂ (TARI), same locality, 31.III.1939, leg. A. Aoki; 1♂, 1♀ (TARI), same locality, 20–23.VI.1956, leg. S. C. Chiu; 1♂ (KMNH), same locality, 8.IV.1965, leg. S. Miyamoto; 1♀ (KMNH), 6.VII.1965, leg. T. Yamasaki; 1♂ (TARI), same locality, 17–20.VIII.1982, leg. K. C. Chou & C. C. Pan; 1♂ (JBCB), same locality, 17–26.VI.1995, leg. P. Moravec; 1♀ (TARI), same locality, 26.III.2009, leg. G. Shang (向高世); 1♀ (TARI), same locality, 17.V.2010, leg. T.-H. Lee (李大翔); 1♂, 3♀ (TARI), same locality, 10.V.2021, leg. T.-Y. Chien (簡廷仰); 1♂ (KMNH), Chaoping (沼平), Alishan, 6.VII.1961, leg. S. Ueno; 1♂ (TARI), same locality, 10.V.2021, leg. B.-X. Guo; 1♀ (KMNH), Niitakaguchi (新高山 = Yushankou, 玉山口), – Alishan, 6.IV.1967, leg. T. Shirozu; 1♂ (TARI), Shishan race (石山引水道), 8.III.2020, leg. B.-H. Ho (何彬宏); 1♂ (TARI), Tatachia (塔塔加), 17–24.VII.2008, leg. G.-S. Tung (董景生); 1♂ (TARI), same locality, 7.VI.2009, leg. C.-F. Lee (李奇峯); 1♀ (KMNH), Tzuchung (自忠), 3.VII.1961, leg. S. Ueno; 1♂, 1♀ (TARI), same locality, 8.V.2015, leg. J.-C. Chen (陳榮章); 1♂ (KMNH), Yushan (玉山), 20.V.1981, leg. F. Kimura; Kaohsiung: 1♂ (TARI), Tianchi (天池), 15.IV.2021, leg. F.-S. Huang (黃福盛); Nnatou: 2♀ (KMNH), Tonpoge (= Tungpu, 東埔), 28.III.1967, leg. T. Shirozu.

Redescription. Length 7.8–9.1 mm, width 4.7–6.0 mm. Body color (Fig. 14) black, elytra with red stripes along basal and lateral margins, and suture, three transverse red stripes at basal ¼, middle, and apical ¼ respectively, anterior stripe curved downwards, two posterior stripes curved upwards, basal stripe extending posterior from humeral calli, more or less connected with anterior stripe. Antennae filiform in males (Fig. 15A), length ratios of antennomeres I–XI 1.0: 0.4: 0.4: 0.7: 0.6: 0.5: 0.6: 0.5: 0.5: 0.5: 0.7, length to width ratios of antennomeres I–XI 2.9: 1.8: 1.8: 2.7: 2.8: 2.4: 2.6: 2.3: 2.3: 2.3: 2.9; similar in females (Fig. 15B), length ratios of antennomeres I–XI 1.0: 0.4: 0.5: 0.6: 0.6: 0.5: 0.5: 0.5: 0.5: 0.5: 0.7, length to width ratios of antennomeres I–XI 3.3: 1.7: 2.1: 3.0: 2.7: 2.5: 2.5: 2.6: 2.4: 2.4: 2.9. Pronotum 1.7–1.8 × wider than long, disc strongly convex; smooth, without reticulate microsculpture; with punctures obsolete, with lateral impressions; lateral margins reduced, visible only near basolateral angles, or visible in some individuals, rounded and widest at apical 1/3; apical and basal margin straight; anterior angles strongly produced to bulbous point. Elytra with rounded lateral margins, widest behind middle, 1.2–1.3 × longer than wide; disc smooth, without reticulate microsculpture;

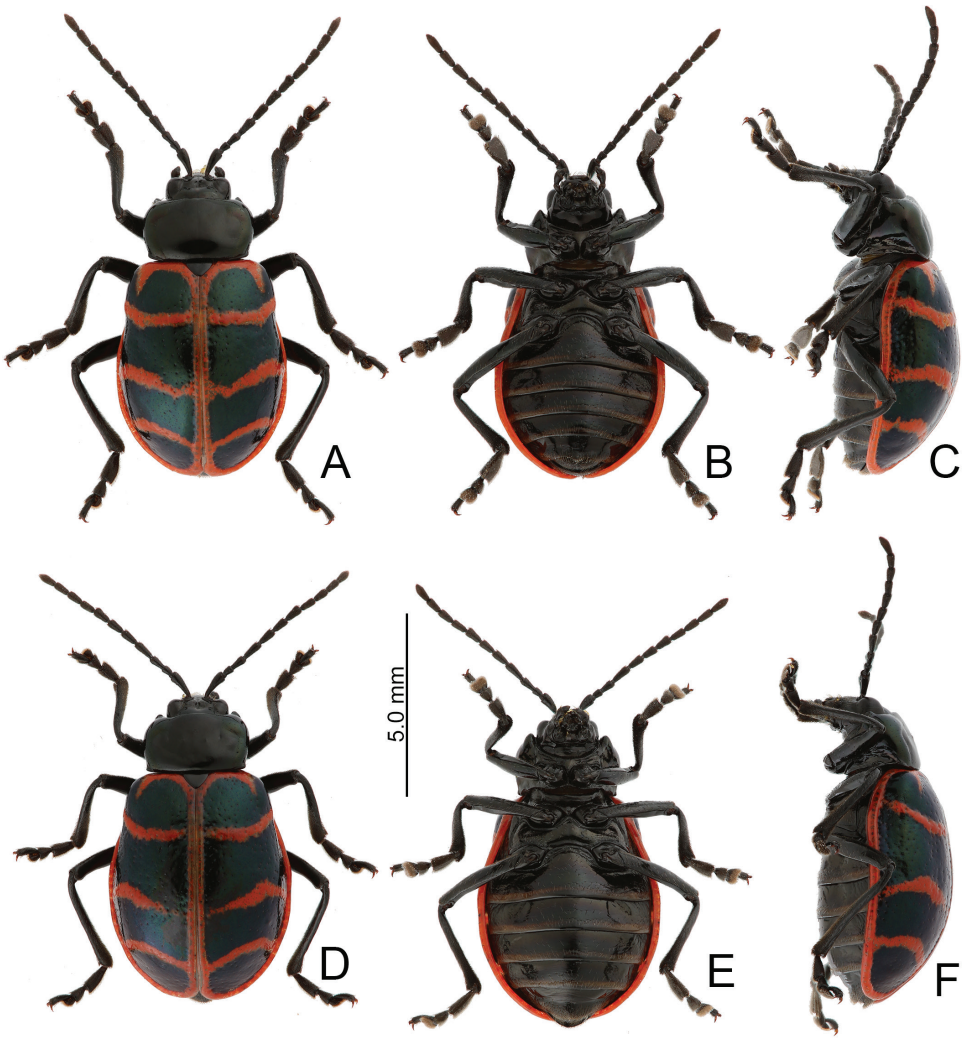

Figure 14. Habitus, *Furusawaia yosonis* Chûjô **A** male**,** dorsal view **B** ditto, ventral view **C** ditto, lateral view **D** female, dorsal view **E** ditto, ventral view **F** ditto, lateral view.

and with sparse, coarse punctures. Aedeagus (Fig. 15C, D) slender in dorsal view, 5.9 × longer than wide, parallel-sided, narrowed near apex, apex narrowly rounded; ostium large, membranous; moderately curved in lateral view; endophallic sclerite elongate, 0.4 × as long as aedeagus, basal 2/3 widened and parallel-sided, one pair of short lateral expansions near apex, covered with fine setae. Only apices of gonocoxae (Fig. 15E) sclerotized, elongate, apices pointed, with dense, short setae at near apex, and several short setae along lateral margin. Ventrite VIII (Fig. 15F) membranous apically, several short setae along apical margin, spiculum long. Receptacle of spermatheca (Fig. 15G) as slender as pump, undivided from pump; pump long and strongly curved; sclerotized proximal spermathecal duct undivided from receptacle, extremely long.

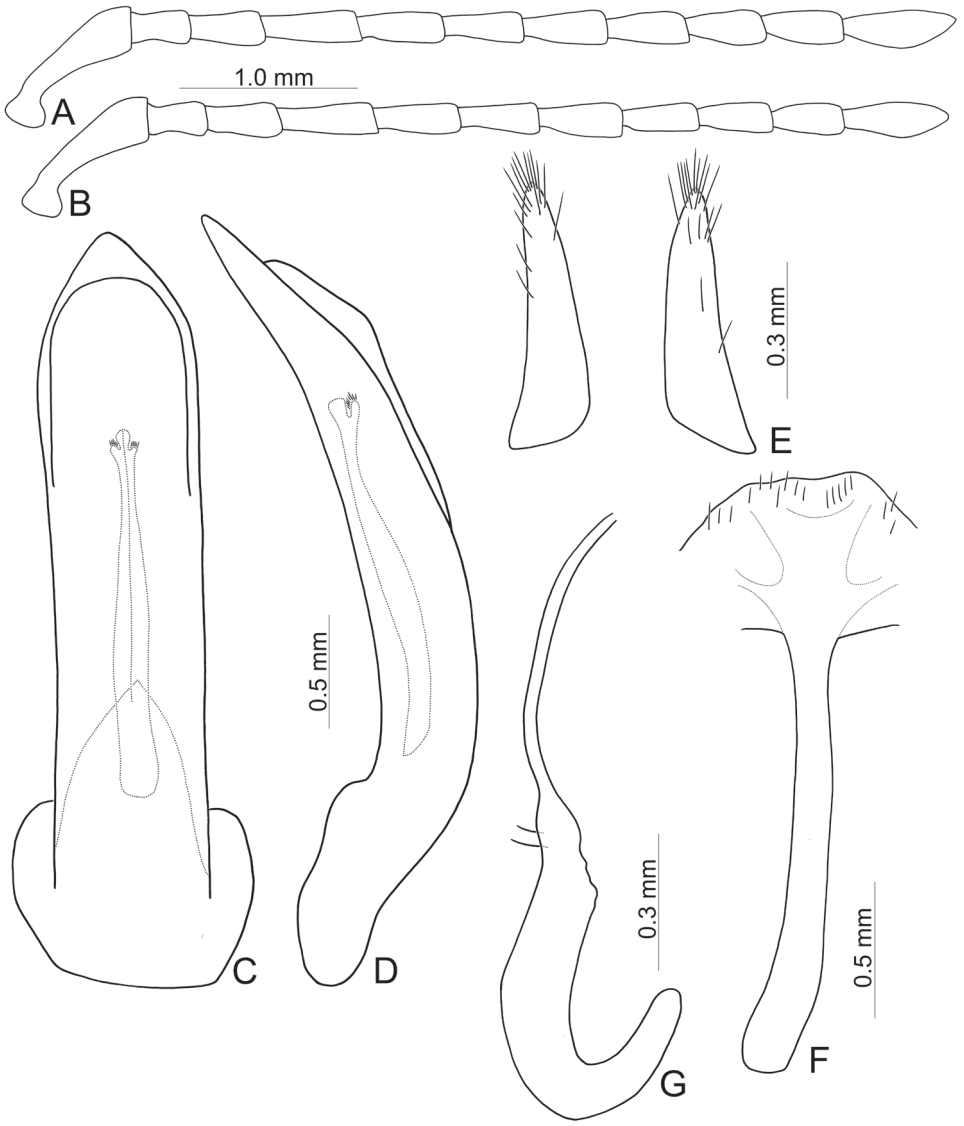

Figure 15. Habitus, *Furusawaia yosonis* Chûjô **A** male**,** dorsal view **B** ditto, ventral view **C** ditto, lateral view **D** female, dorsal view **E** ditto, ventral view **F** ditto, lateral view.

Diagnosis. Adults of *Furusawaia yosonis* Chûjô (Fig. 14) are similar to those of *F. tsoui* sp. nov. (Fig. 12) based on the curved median and posterior stripes on the elytra (straight median and posterior stripes on the elytra in *F. jungchani* sp. nov. (Fig. 5) and *F. tahsiangi* sp. nov. (Fig. 10)) and without longitudinal stripes connecting basal and anterior stripes, and anterior and median stripes (with longitudinal stripes connecting basal and anterior stripes, anterior and median stripes in *F. lui* sp. nov. (Fig. 8)). It differs by the more convex pronotum with lateral margins reduced at anterior angles (less convex pronotum with lateral margins present at anterior angles in *F. tsoui* sp. nov.). In

males of *F. yosonis*, the aedeagus (Fig. 15D) is moderately curved in lateral view (strongly curved in *F. jungchani* sp. nov. (Fig. 6D), slightly curved in others (Figs 9F, 11D, 13D); the endophallic sclerite (Fig. 15C) similar to that of *F. jungchani* sp. nov. (Fig. 6C) with basal 2/3 wider and parallel-sided (only widened at middle in *F. lui* sp. nov. (Fig. 9E); basal 2/3 widened but basally narrowed, and strongly widened at middle in *F. tahsiangi* sp. nov. (Fig. 11C); basal 2/3 widened, but basally and at basal 3/7 narrower in *F. tsoui* sp. nov. (Fig. 13C)). In females of *F. yosonis* Chûjô, the spermathecae (Fig. 15G) are similar to those of *F. jungchani* sp. nov. (Fig. 6G) with slightly swollen receptacle (moderately swollen receptacle in *F. lui* sp. nov. (Fig. 9I) and *F. tahsiangi* sp. nov. (Fig. 11F); strongly swollen receptacle in *F. tsoui* sp. nov. (Fig. 13G)) and apex undivided from sclerotized proximal duct (apex truncate and separated from sclerotized proximal duct in *F. lui* sp. nov. (Fig. 9G, I) and *F. tahsiangi* sp. nov. (Fig. 11F)); abdominal ventrites VIII (Fig. 15F) are similar to those of *F. tsoui* sp. nov. (Fig. 13F), with membranous apex (well sclerotized and small apex in *F. tahsiangi* sp. nov. (Fig. 11G), sclerotized and larger apex in *F. jungchani* sp. nov. (Fig. 6F) and *F. lui* sp. nov. (Fig. 9H)); gonocoxae (Fig. 15E) with pointed apices (rounded apices in others) and dense setae present only at apical area (dense setae present at apical and lateral area in *F. lui* sp. nov. (Fig. 9J)).

Food plants. *Stellaria media* (L.) Vill (Caryophyllaceae).

Biological notes. All adults were found on forest trails at night (Fig. 3G).

Distribution. This species is widespread at high altitudes (above 2,000 m) in southern Taiwan (Fig. 7).

Key to species of *Furusawaia*

1 Pronotum dull, with reticulate microsculpture, generally flat; elytra with dense, coarse punctures, stripe along suture entirely absent (Fig. 1E, F) or present only from base to basal 1/3 (Fig. 1D)..... **2 (Chinese species)**

– Pronotum shining, without reticulate microsculpture, more or less convex; elytra with sparse coarse punctures, stripes along suture entirely present .... **3 (Taiwanese species)**

2 Pronotum with lateral margins rounded, anterior angles obtuse; elytra shining, without reticulate microsculpture, stripe along lateral margin entirely present, stripe along suture only appear from base to basal 1/3 (Fig. 1D) .... ***F. continentalis* Lopatin**

– Pronotum with lateral margin narrowed at posterior half, anterior angle strongly produced to bulbous point; elytra dull, with reticulate microsculpture, stripes along lateral margins and suture absent (Fig. 1E, F). .... ***F. konstantinovi* (Lopatin)**

3 Median and posterior stripes on elytra straight (Figs 5, 10). **4**

– Median and posterior stripes on elytra curved (Figs 8, 12, 14). **5**

4 Pronotum strongly convex, lateral margins reduced behind anterior angles; median and posterior stripes on elytra widened (Fig. 5) ..... ***F. jungchani* sp. nov.**

– Pronotum less convex, lateral margin visible behind anterior angles; median and posterior stripes on elytra normal (Fig. 10)..... ***F. tahsiangi* sp. nov.**

5 Basal, anterior, and median stripes on elytra connected by longitudinal stripes (Fig. 8)..... ***F. lui* sp. nov.**
– Basal, anterior, and median stripes on elytra separated (Figs. 12, 14)..... **6**
6 Pronotum strongly convex, lateral margins reduced behind anterior angles... ..... ***F. yosonis* Chûjô**
– Pronotum less convex, lateral margin visible behind anterior angles..... ..... ***F. tsoui* sp. nov.**

Discussion

Adults of *Furusawaia* Chûjô represent one of the wingless galerucine genera with reduced humeral calli in Taiwan. Most of the wingless galerucines in Taiwan have been studied, including *Taiwanoshaira* Lee & Beenen (2020), *Lochmaea* Weise (Lee 2018), *Shairella* Chûjô (Lee and Beenen 2017), and *Sikkimia* Duvivier (Lee and Bezděk 2016). Members of these genera are exclusively nocturnal. However, adults of *Furusawaia* exhibit bizarre behavior in being diurnal or nocturnal in different populations of the same species. Such behaviors may be associated with bicolored elytra, which are unique among wingless galerucines. The function of the bicolored elytra requires further study to determine if they are aposematic or part of a mimicry complex.
In addition, the difficulty in collecting adults of *Furusawaia* may result from such bizarre behavior. Adults of wingless galerucines are generally easy to collect by searching food plants at night, except this genus. Usually single or a pair of adults of *Furusawaia* were collected during each field trip based on this collecting method. Citizen scientists play an important role in obtaining sufficient material for study by collecting adults. Twenty citizen scientists were involved and collected about 80% of specimens available for study.

Adults of most *Furusawaia* species are capable for dispersal judging from the distribution maps (Fig. 7), except those of *F. jungchani* sp. nov. Even adults of *F. lui* sp. nov. and *F. tsoui* are sympatric in Taipingshan (太平山). Most adults of the species studied were collected at lower altitudes (belong 2,500 m) where they are easily accessible to collectors. One undescribed female was collected at Tianchi Lodge (天池山莊) (Fig. 3H), 2,860 m, at Nantou county. Some additional undescribed species were found at Mt. Mabolasi (馬博拉斯山, 3,785 m) and Mt. Malichianan (馬利加南山, 3,546 m). They are not described here due to insufficient material. More undescribed species are expected in high mountains that are extremely difficult access. Male aedeagi in the section Capulites are uniform (Bezděk and Beenen 2009), and those of Taiwanese *Furusawaisa* species played a minor role in diagnosis. Besides color patterns on the elytra and convexity of pronota, female genitalic characters are more or less diagnostic, including gonocoxae, spermathecae, and abdominal ventrites VIII. Future molecular studies may test the morphological taxonomy and clarify relationships among species.

Acknowledgements

We thank the following citizen scientists for collecting material: Jung-Chan Chen (陳榮章), Po-Yen Chen (陳柏彥), Ting-Yang Chien (簡廷仰), Wan-Jung Chien (簡畹融), Ching-Yi Chuang (莊靜宜), Yi-Ting Chung (鍾奕霆), Bin-Hong Ho (何彬宏), Bo-Xin Guo (郭泊鑫), Chih-Yuan Hsu (許志遠), Fu-Shen Huang (黃福盛), Pin-Hsun Ko (柯品薰), Ta-Hsiang Lee (李大翔), Hsi-Feng Lu (陸錫峯), Gaus Shang (向高世), Pei-Ling Tian (田佩玲), Mei-Hua Tsou (曹美華), Gene-Sheng Tung (董景生), Shu-Ping Wu (吳書平), Cheng-Te Yao (姚正得), Wen-Bin Yeh (葉文斌), and Su-Fang Yu (余素芳). We especially thank Yi-Chia Chiu (邱奕家), Chi-Lung Lee (李其龍), and Hsing-Tzung Cheng (鄭興宗) for photographs of specimens, Hsueh Lee (李雪), Ta-Hsiang Lee (李大翔), Hsi-Feng Lu (陸錫峯), Mei-Hua Tsou (曹美華), and Jung-Chan Chen (陳榮章) for their field photography, and Chih-Kai Yang (楊智凱) for identification of host plants. This study was supported by the Ministry of Science and Technology MOST 109-2313-B-055-003 and Shei-Pa National Park SP110113. We especially thank Chang Chin Chen for assisting our study in various ways and Chris Carlton for reading the draft and editing for American English style.

References

Beenen R (2010) Galerucinae. In: Löbl I, Smetana A (Eds) Catalogue of Palaearctic Coleoptera, Volume 6. Chrysomeloidea. Apollo Books, Stenstrup, 443–491.

Bezděk J, Beenen R (2009) Addition to the description of *Yunnaniata konstantinovi* Lopatin, 2009, and its classification in the section Capulites (Coleoptera: Chrysomelidae: Galerucinae: Hylaspini). Zootaxa 2303: 45–52. https://www.mapress.com/zt/article/view/zootaxa.2303.1.2

Chen S (1976) [new taxon]. In: Chen S, Yu P-Y, Wang S-Y, Jiang S-Q: New leaf beetles from West China. Acta Entomologica Sinica 19: 205–224.

Chen S, Wang S-Y, Jiang S-Q (1986) The galerucine genus *Capula* from West China (Coleoptera: Chrysomelidae). Acta Zootaxonomica Sinica 11: 398–400.

Chûjô M (1962) A taxonomis study on the Chrysomelidae (Insecta: Coleoptera) from Formosa. Part XI. Subfamily Galerucinae. The Philippine Journal of Science 91: 1–239.

Jacobson GG (1925) De Chrysomelidis palaearcticis. Descriptionum et annotationum series III. Russkoe Entomologischeskoe Obozrenie 19: 143–148.

Kimoto S (1970) A list of the Nepalese chrysomelid specimens preserved in Zoologische Sammlung des Bayerischen Staates, München. Khumbu Himal 3: 412–421.

Kimoto S, Takizawa H (1972) Chrysomelid-beetles of Nepal, collected by the Hokkaido University scientific expedition to Nepal Himalaya, 1968. Part I. Kontyû 40: 215–223.

Kimoto S, Chu Y-I (1996) Systematic catalog of Chrysomelidae of Taiwan (Insecta: Coleoptera). Bulletin of the Institute of Comparative Studies of International Cultures and Societies 16: 1–152.

Kimoto S, Takizawa H (1997) Leaf beetles (Chrysomelidae) of Taiwan. Tokai University Press, Tokyo, 581 pp.

Lee C-F (2018) The genus *Lochmaea* Weise, 1883 in Taiwan: results of taxonomic expeditions by citizen scientists (Coleoptera, Chrysomelidae, Galerucinae). ZooKeys 856: 75–100. https://doi.org/10.3897/zookeys.856.30838

Lee C-F, Beenen R (2017) Revision of the genus *Shairella* Chûjô, 1962 (Coleoptera: Chrysomelidae: Galerucinae) from Taiwan, with description of five new species. Zootaxa 4268: 489–507. https://doi.org/10.11646/zootaxa.4268.4.2

Lee C-F, Beenen R (2020) *Taiwanoshaira* Lee & Beenen, a new genus and first record of moss-inhabiting Galerucinae *sensu strico* (Coleoptera, Chrysomelidae) from Taiwan. ZooKeys 944: 129–146. https://doi.org/10.3897/zookeys.944.53099

Lee C-F, Bezděk J (2016) Revision of the wingless *Sikkimia* Duvivier (Coleoptera, Chrysomelidae, Galerucinae) from Taiwan, including a new generic synonymy and four new species descriptions. ZooKeys 553: 79–106. https://doi.org/10.3897/zookeys.553.6576

Lopatin IK (2008) New leaf-beetle species (Coleoptera, Chrysomelidae) from China: IX. Entomological Review 88: 918–927. https://doi.org/10.1134/S001387380808006X

Lopatin IK, Konstantinov AS (2009) New genera and species of leaf beetles (Coleoptera: Chrysomelidae) from China and South Korea. Zootaxa 2083: 1–18. https://doi.org/10.11646/zootaxa.2083.1.1

Seeno TN, Wilcox JA (1982) Leaf beetle genera (Coleoptera: Chrysomeldiae). Entomography 1: 1–221.

Wilcox JA (1971) Chrysomelidae: Galerucinae (Oidini, Galerucini, Metacyclini, Sermylini). In: Wilcox JA (Ed.) Coleopterorum Catalogus Supplementa. Pars 78(1), 2nd edn. W. Juunk, ‘s-Gravenhage, 1–220.

Wilcox JA (1975) Chrysomelidae: Galerucinae. Addenda et index. In: Wilcox JA (Ed.) Coleopterorum Catalogus Supplementa. Pars 78(4), 2nd edn. W. Juunk, ‘s-Gravenhage, 667–770.

Yang X, Ge S, Nie R, Ruan Y, Li W (2015) Chinese leaf beetles. Science Press, Beijing, 507 pp.

ZooKeys 1057: 149–184 (2021)
doi: 10.3897/zookeys.1057.66675
https://zookeys.pensoft.net

RESEARCH ARTICLE

A peer-reviewed open-access journal
ZooKeys
Launched to accelerate biodiversity research

A review of the *Eviota zebrina* complex, with descriptions of four new species (Teleostei, Gobiidae)

Luke Tornabene[1], David W. Greenfield[2,3], Mark V. Erdmann[4,5]

1 *School of Aquatic and Fishery Sciences, and the Burke Museum of Natural History and Culture, University of Washington, 1122 NE Boat Street, Seattle, Washington, 98105, USA* **2** *Research Associate, Department of Ichthyology, California Academy of Sciences, 55 Music Concourse Dr., Golden Gate Park, San Francisco, California 94118-4503, USA* **3** *Professor Emeritus, University of Hawaii. Mailing address: 944 Egan Ave., Pacific Grove, CA 93950, USA* **4** *Conservation International Aotearoa, University of Auckland, 23 Symonds Street, Auckland 1010, New Zealand* **5** *Research Associate, Department of Ichthyology, California Academy of Sciences, 55 Music Concourse Dr., Golden Gate Park, San Francisco, CA 94118-4599, USA*

Corresponding author: Luke Tornabene (Luke.Tornabene@gmail.com)

Academic editor: Nina Bogutskaya | Received 30 March 2021 | Accepted 20 July 2021 | Published 27 August 2021

http://zoobank.org/30DE300C-11FF-4858-8A7F-F40361CDBEE6

Citation: Tornabene L, Greenfield DW, Erdmann MV (2021) A review of the *Eviota zebrina* complex, with descriptions of four new species (Teleostei, Gobiidae). ZooKeys 1057: 149–184. https://doi.org/10.3897/zookeys.1057.66675

Abstract

The *Eviota zebrina* complex includes eight species of closely-related dwarfgobies, four of which are herein described as new. The complex is named for *Eviota zebrina* Lachner & Karnella, 1978, an Indian Ocean species with the holotype from the Seychelles Islands and also known from the Maldives, which was once thought to range into the Gulf of Aqaba and the Red Sea eastward to the Great Barrier Reef of Australia. Our analysis supports the recognition of four genetically distinct, geographically non-overlapping, species within what was previously called *E. zebrina*, with *E. zebrina* being restricted to the Indian Ocean, *E. marerubrum* **sp. nov.** described from the Red Sea, *E. longirostris* **sp. nov.** described from western New Guinea, and *E. pseudozebrina* **sp. nov.** described from Fiji. The caudal fin of all four of these species is crossed by oblique black bars in preservative, but these black bars are absent from the four other species included in the complex. Two of the other species within the complex, *E. tetha* and *E. gunawanae* are morphologically similar to each other in having the AITO cephalic-sensory pore positioned far forward and opening anteriorly. *Eviota tetha* is known from lagoonal environments in Cenderawasih Bay and Raja Ampat, West Papua, and *E. gunawanae* is known only from deeper reefs (35–60 m) from Fakfak Regency, West Papua. The final two species are *E. cometa* which is known from Fiji and Tonga and possesses red bars crossing the caudal fin (but lost in preservative) and a 9/8 dorsal/anal-fin formula, and *E. oculineata* **sp. nov.**, which is described as new from New Guinea and the Solomon Islands, and possesses an 8/7 dorsal/anal-fin formula and lacks red caudal bars. *Eviota oculineata* has been confused with *E. cometa* in the past.

Keywords
coral-reef fishes, dwarfgoby, *Eviota cometa*, gobies, ichthyology, taxonomy, systematics

Introduction

The genus *Eviota*, commonly known as dwarfgobies, contains 124 species (Greenfield 2021; Greenfield and Erdmann 2021), making it one of the most speciose genera of marine fishes. Several putatively widespread species of *Eviota* displaying morphological variation have recently been shown to be complexes of distinct species that are often distinguishable by a combination of genetic differences, subtle morphological characters, and/or differences in live coloration (Greenfield and Tornabene 2014; Tornabene et al. 2015, 2016). Another example of this phenomenon is demonstrated by the *Eviota zebrina* complex, a group containing eight genetic lineages based on mtDNA, including the nominal species *Eviota zebrina* Lachner & Karnella, 1978, *E. cometa* Jewett & Lachner, 1983, *E. gunawanae* Greenfield et al., 2019, *E. tetha* Greenfield & Erdmann, 2014, and several undescribed species (Greenfield et al. 2019). All species in this complex possess: (i) unbranched pectoral-fin rays; (ii) reduced fifth pelvic-fin rays (absent or rudimentary to ~ 15% length of fourth ray); (iii) pore patterns lacking only the IT pores, or both the IT and nasal pores Figure 1); (iv) fourth pelvic-fin ray with only 3–7 branches; (v) a red or dark brown lateral stripe on the body (stripe faint in *E. pseudozebrina* sp. nov.) that terminates in distinct black spot on the base of the caudal fin that is sometimes bordered with yellow in life (spot faint in *E. tetha*). The combination of the lateral stripe and black caudal spot are present only in two other species, *E. sebreei* Jordan & Seale, 1906 and *E. punyit* Tornabene et al., 2016, both of which differ from the *E. zebrina* complex in having a pore pattern lacking the PITO pore, and in having a fourth pelvic-fin ray with many more branches (11–15 vs. 3–7).

Eviota zebrina was described based on type material from the Seychelles Islands, with non-type specimens from the Red Sea and other Indian Ocean localities east to the Great Barrier Reef, Australia. Lachner and Karnella (1978) noted geographic variation in meristic characters and pigmentation patterns among populations but refrained from splitting the groups into named species. During their survey of the marine fishes of Fiji (1999–2003), Greenfield and Randall identified one of the dwarfgobies collected as *Eviota zebrina*, the first record of that species from Oceania at that time (Randall 2005). When Herler and Hilgers (2005) published color photographs of *E. zebrina* from the Red Sea that differed from the color of specimens from Fiji, it raised suspicions that the specimens from Fiji might be undescribed. In 2017 MVE collected specimens and DNA tissue of *E. zebrina* from the southern Lau Islands, Fiji, and in 2018 specimens and tissue of *E. zebrina* from the Maldives, an Indian Ocean location. Greenfield et al. (2019) included DNA sequences of *E. zebrina* from the Red Sea, the Maldives, Seychelles Islands, western New Guinea, and Fiji in a molecular phylogeny of this complex (Figure 2), spanning most of the known range of *E. zebrina*. These

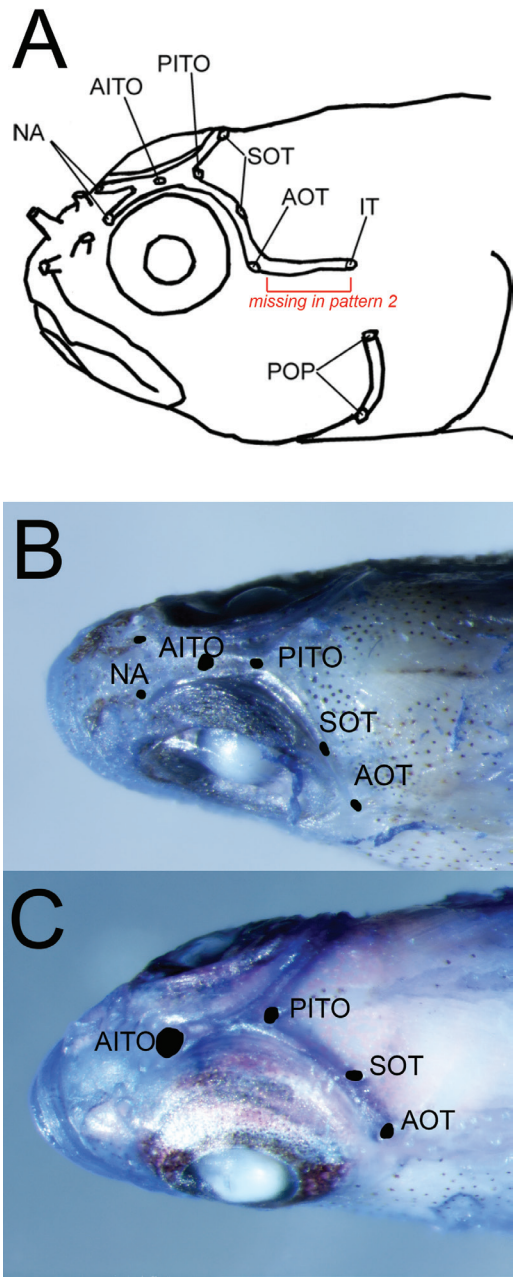

Figure 1. Head pore patterns relevant to the *Eviota zebrina* complex **A** complete pore pattern (pattern 1 of Lachner and Karnella 1980). Note that the IT pore and associated section of the lateralis canal are absent in pore pattern 2 and in all species of the *E. zebrina* complex. Figure modified from Tornabene et al. (2013) **B** pattern 2, found in all species of the *E. zebrina* complex except *E. tetha* and *E. gunawanae*. Photograph of CAS 246248, *E. longirostris* **C** pattern found in *E. tetha* and *E. gunawanae*. Photograph of CAS 246247, *E. tetha*. Note the absence of NA pores and the anterior-facing AITO pore. Pore abbreviations follow Lachner and Karnell (1980).

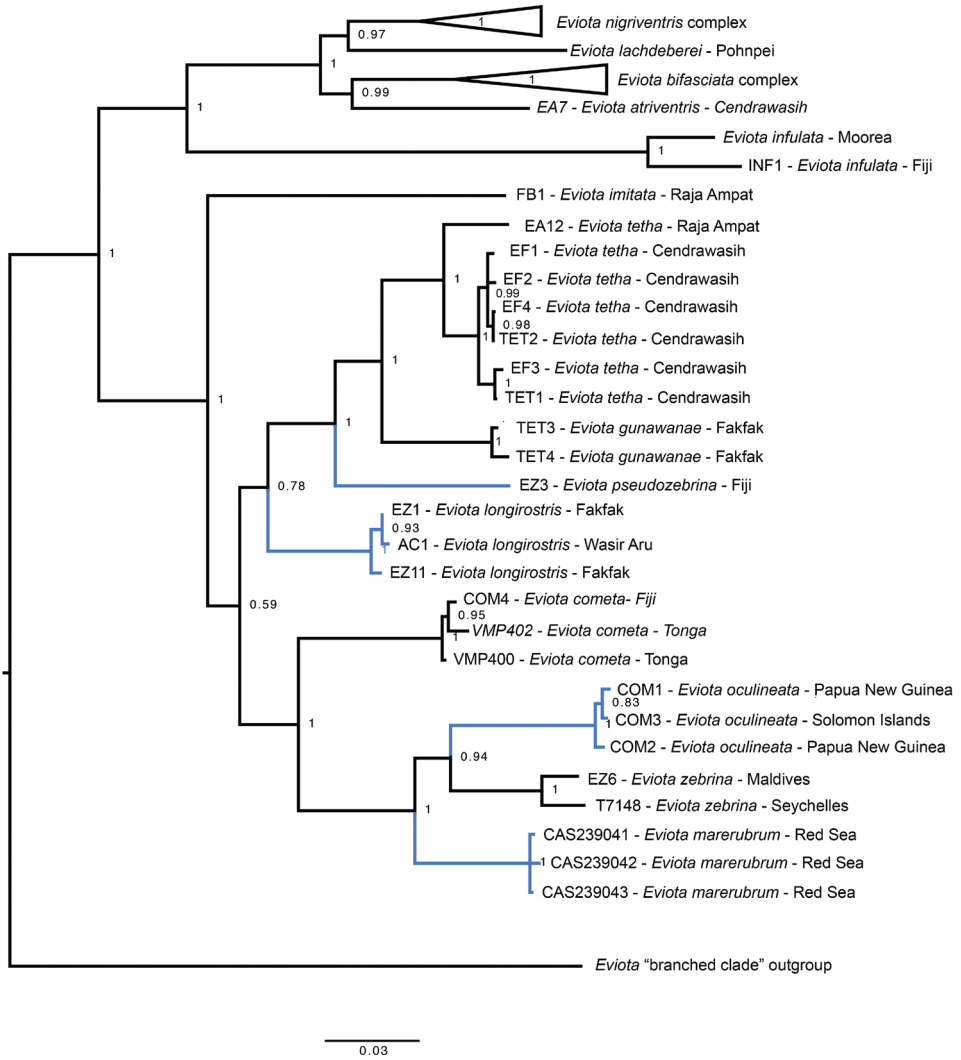

Figure 2. Molecular phylogeny based on COI and Ptr sequences. Branch lengths are substitutions/site, node labels are Bayesian posterior probabilities. Blue branches indicate new species described here. Labels before species name refer to tissue numbers.

data showed that *E. zebrina* indeed represented a species complex, with specimens of *Eviota "zebrina"* from the Red Sea, western New Guinea, and Fiji all representing lineages that are distinct from those in the Indian Ocean. We herein describe the specimens from Fiji as *Eviota pseudozebrina* sp. nov., those from western New Guinea as *E. longirostris* sp. nov., and the Red Sea specimens as *E. marerubrum* sp. nov.

Eviota cometa is also a member of the *E. zebrina* complex, and based on the phylogenetic tree of Greenfield et al. (2019), there are two lineages putatively identified as *E. cometa*. *Eviota cometa* was described by Jewett and Lachner (1983) from specimens

in Fiji (type locality) and many non-type specimens across the western and central Pacific Ocean. As was the case with *E. zebrina*, the authors noted that *E. cometa* displayed some morphological variation across its geographic range but refrained from recognizing morphotypes as distinct species. Specifically, Jewett and Lachner (1983) noted that there were two distinct counts in the dorsal- and anal-fin rays, 9/8 (as in the holotype) vs 8/7, but in some locations, including the type locality in Fiji, both counts were present, leading to the conclusion that this was intraspecific variation. No differences in live coloration were noted at the time of description. Recent live photographs of specimens of *E. cometa* have revealed the presence of two distinct color morphs, both of which occur near the type locality of Fiji, and correspond to the genetic lineages shown by Greenfield et al. (2019). We show here that these genetically distinct color morphs correspond to the groups of possessing two different fin-ray counts noted by Jewett and Lachner (1983). We describe the new species here as *E. oculineata* sp. nov. Lastly, we provide a detailed comparison of the eight known species in this complex and a taxonomic key to aid in their identification.

The addition of these four new species raises the total number of species in the genus to 127.

Materials and methods

Counts and measurements, descriptions of fin morphology and the cephalic sensory-canal pore patterns follow Lachner and Karnella (1980) and Jewett and Lachner (1983). Dorsal/anal fin-ray formula counts (e.g., 9/8) only include segmented rays. For counts of rays in dorsal, anal, and pectoral fins in the Description sections below, we list the holotype first followed by the range of counts for the entire type series, with the frequency of that count in square brackets.

Measurements were made to the nearest 0.1 mm using an ocular micrometer or dial calipers, and are presented as percentage of Standard Length (**SL**). Measurements of the holotype are listed first, followed by the range and average for all measured specimens of the type series in parenthesis. Lengths are given as standard length (SL), measured from the median anterior point of the upper lip to the base of the caudal fin (posterior end of the hypural plate); origin of the first dorsal fin is measured from the median anterior point of the upper lip to the anterior base of the first dorsal-fin spine; origin of the second dorsal fin is measured from the median anterior point of the upper lip to the anterior base of its spine; origin of the anal fin is measured from the median anterior point of the upper lip to the anterior base of its spine; body depth is measured at the center of the first dorsal fin; head length is taken from the upper lip to the posterior end of the opercular membrane; orbit diameter is the greatest fleshy diameter; snout length is measured from the median anterior point of the upper lip to the nearest fleshy edge of the orbit; upper jaw length is the distance from the anterior tip of the premaxilla to the end of the upper margin of the dentary where the maxilla joins; caudal-peduncle depth is the least depth, and caudal-peduncle length the

horizontal distance between verticals at the rear base of the anal fin and the caudal-fin base; pelvic-fin length is measured from the base of the pelvic-fin spine to the tip of the longest pelvic-fin soft ray. Cyanine Blue 5R (acid blue 113) stain and an air jet were used to make the cephalic sensory-canal pores more obvious (Akihito et al. 1993, 2002; Saruwatari et al. 1997). A digital radiograph was taken of the holotype of *Eviota cometa* to confirm counts of dorsal- and anal-fin rays.

Sequences for the new species and additional specimens from the *E. zebrina* complex were sequenced in Greenfield et al. (2019) and our prior studies on *Eviota* (Tornabene et al. 2013, 2015, 2016; Greenfield et al. 2019). For those studies, we sequenced a segment of the mitochondrial gene *cytochrome c oxidase subunit I* (COI) using the primers GobyL6468 and GobyH7696 (Thacker 2003) or FishF-1 and FishR-1 (Ward et al. 2005), and the nuclear gene *Protease III* (Ptr) using the primers PtrF2 and PtrR2 (Yamada et al. 2009). The PCR conditions follow that of Tornabene et al. (2016). Additional sequences that were putatively identified as *E. zebrina* were added from BOLD or GenBank. Sequences were aligned in Geneious v.6.0.6 (Biomatters; www.geneious.com). The final alignment consisted of 1173 bp of COI, and 614 bp of Ptr. A phylogenetic analysis of the concatenated alignment was done using Bayesian Inference in the software MrBayes v.3.2 (Ronquist et al. 2012), partitioning by gene. Substitution models were chosen using PartitionFinder2 (Lanfear et al. 2016). The analysis was run for 10^6 generations, discarding the first 10% of trees as burn-in.

Taxonomic account

Eviota pseudozebrina **Tornabene, Greenfield & Erdmann, 2021**
Fijian zebra Dwarfgoby
Figures 3–5

Eviota cf. *zebrina*: Greenfield et al. 2019: 64, fig. 9 (Fiji).

Material. ***Holotype*****.** CAS 228614, 16.6 mm SL male, Fiji, N. Lau Group, Vanua Balavu Id., Bay of Islands, cove in Bay, 17°10.679'S, 179°01.558'W, 0–2.4 m, rock with green algae, rotenone, field number G03-40, 13 January 2003, D.W. Greenfield, R. Langston, & K. Longenecker. ***Paratypes*****.** CAS 246310, 10 males, 14.0–18.3 mm SL, 11 females, 11.6–14.8 mm SL, taken with holotype. CAS 244078, male, 10.4 mm SL, Fiji, S. Lau Group, Matuku Lagoon, 19°09.115'S, 179°44.732'E, 3–5 m, clove oil & hand net, field number MVE-17-016, 14 May 2017, M.V. Erdmann. CAS 246250, 10.5 mm SL, Fiji, S. Lau Group, Matuku Lagoon, 19°09.115'S, 179°44.732'E, 3–5 m, tissue number EZ3, clove oil & hand net, field number MVE-17-016, 14 May 2017, M.V. Erdmann.

Non-type material. All from Fiji - CAS 219786 (3), Viti Levu Id., off Suva; 228677 (8), Vanua Balavu Id., Bay of Islands; 228731 (1), Vanau Balavu Id., Bay of Islands; 228732 (2), Vanua Balavu Id., Balavu Harbor; 228743 (1), Viti Levu Id., Vatunisogasoga Reef; 228744 (1), Mago Id., Lau Group; 229544 (1), Viti Levu Id., E.

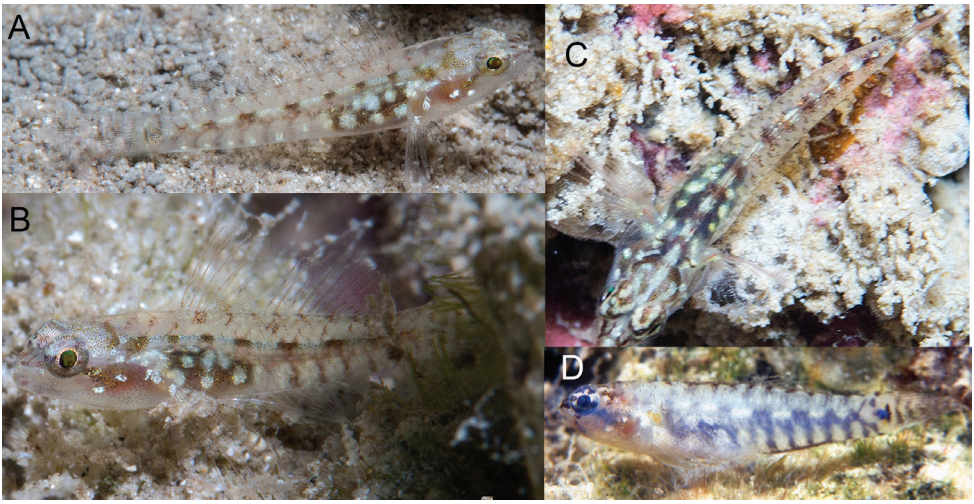

Figure 3. *Eviota pseudozebrina*, live. **A–C** CAS 244078, 10.4 mm SL male, Fiji **D** Underwater photograph of fresh specimen from Fiji, reproduced with permission from Randall (2005).

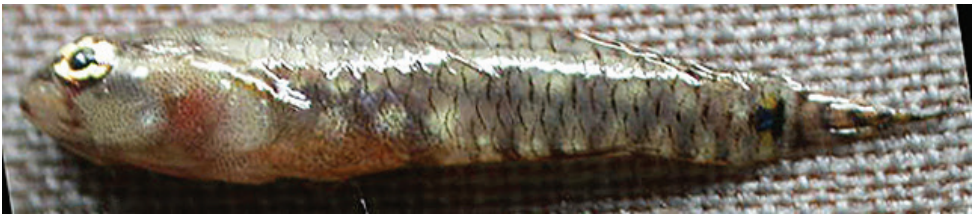

Figure 4. *Eviota pseudozebrina*, fresh specimen, type series, CAS 246310.

of Nananu Passage; 229568 (2), Yadua Id., Talai Harbor; 229580 (14), Yadua Id., Tali Harbor; 229608 (15), Viti Levu Id., Nananui-i-cake Id.

Diagnosis. A species of *Eviota* with a cephalic sensory-canal pore pattern lacking only the IT pore, pectoral-fin rays not branched, dorsal/anal-fin ray formula 9/8, 5th pelvic-fin ray 6–16% of 4th ray; dark rectangular to round spot on area of preural centrum followed by a dark vertical line over end of hypural plate; caudal fin crossed by six or seven dark vertical bars in preservation, naris long and black, body deep, 22–26% SL; usually 15 pectoral-fin rays. Color of body a translucent gray background and markings of white, brown, or black, with no red coloration.

Description. Dorsal-fin elements VI+I,9, first dorsal triangular in shape, first three spines filamentous, 2nd or 3rd longest, reaching to 6th soft ray of second dorsal fin in holotype when adpressed, all second dorsal-fin soft rays branched, last ray branched to base; anal-fin elements I,8 (7[1],8[9])), all soft rays branched, last ray branched to base; pectoral-fin rays 16 (14[1], 15 [11], 16 [5]), all unbranched, pointed, reaching to below second dorsal fin; 5th pelvic-fin ray ~ 16% (6–16) of length of 4th pelvic-fin ray; 4th ray with 7 (3–7) branches, four segments between consecutive branches of 4th pelvic-fin ray, pelvic-fin membrane reduced, no basal membrane; caudal fin with 11

Figure 5. *Eviota pseudozebrina*, preserved holotype, CAS 228614, 16.6 mm SL male, Fiji.

branched and 17 segmented rays; lateral-line scales 24 (24[8], 25[2]); transverse scale rows 7; urogenital papilla of male smooth, long and narrow, expanded into a lateral horn at tip, extending past anal-fin spine; female papilla smooth, bulbous, with short finger-like projections on end; front of head rounded with an angle of ~ 60° from horizontal axis; mouth slanted obliquely upwards, forming an angle of ~ 60° to horizontal axis of body, lower jaw not projecting; maxilla extending posteriorly to rear of pupil; anterior tubular nares long, black, extending to center of upper lip; gill opening extending forward to below posteroventral edge of preoperculum; cephalic sensory-pore system missing only IT pore, cutaneous sensory papilla system similar to papilla pattern B-1 (of Lachner and Karnella 1980).

Measurements. In percent SL, value of holotype followed by range and mean of holotype and nine other paratypes in parentheses. Head length 28 (27–32, 29); origin of first dorsal fin 36 (33–37, 35); origin of second dorsal fin 57 (54–60, 57); origin of anal fin 59.9 (56–62, 59); caudal-peduncle length 24 (23–30, 25); caudal-peduncle depth 12 (10–13, 12); body depth 23 (23–26, 23); eye diameter 9 (8–10, 9); snout length 5 (4–5, 4); upper-jaw length 11 (females 9–11, 10, males 10–12, 11); pectoral-fin length 39 (31–39, 33); greatest pelvic-fin length 33 (27–36, 32).

Color in life. (Figure 3) Background color of head and body translucent gray. Body with eight yellow-white spots along vertebral column, separated by black areas. A faint, dusky brown lateral stripe positioned below vertebral column, starting over abdomen and continuing onto caudal peduncle. Abdomen dark brown to black with seven large, irregularly shaped bright white spots spaced over dark area. Ventral portion of flank with six short, faint, vertical brown bars connected to dusky lateral stripe, each bar separated from one another by a small, bright yellow-white iridescent spot. Dorsal midline with approximately 11–13 brown spots, starting on predorsal area and ending over caudal-fin base, spots formed from coalescing dark anterior scale margins. Caudal-fin base with group of large melanophores in advance of posterior end of hypural plate, followed by a dark brown vertical line over end of plate. Top of head with long white line in center extending from between eyes back to nape, a curved white line on each side of line, curved out and back to nape. A line of faint melanophores extending from 7 o'clock position of eye down across cheek. Reddish color of gill filaments shows through cheek, with two white spots at end of dark stripe from eye. Dark stripe extending onto snout from 3 o'clock position of eye, with another line medial to

it, the two lines joining anteriorly to meet black tubular nares, diverging posteriorly to form a Y shape. Pupil of eye black with iridescent greenish-yellow hue, upper half of eye surface cream colored with scattered melanophores, lower half darker. Pectoral-fin base with single white spot and another on base of fin rays. The dark bars crossing the caudal fin in freshly dead specimens not as visible in life.

Color in freshly dead specimen. (Figure 4). Generally pigmented as described for live specimens, but with the lateral stripe and ventral vertical bars on flank considerably darker than in life. Dark bars on caudal fin much darker in preservation than in life. A distinct vertical bar of melanophores extending ventrally from eye (positioned at ~ 7 o'clock) extending over cheek and jaws. Vertical bar on cheek present in life, but much lighter. Anterior scale margins over entire body with dark pigment, versus only some dorsal scales pigmented in live specimens.

Color in preservative. (Figure 5). Background color of head and body light cream. Scale anterior margins lined with melanophores, making scale pattern obvious. Side of head and jaws, pectoral-fin base and nape peppered with large melanophores. Tubular nares entirely black. Dark cluster of melanophores on lower jaw at rictus. Dark blotch at center of preoperculum at level of bottom of eye, another above it at level of pupil and dark blotch behind upper half of eye. Pupil of eye gray, iris black. Lower surface of abdomen dark brown. Series of dark brown spots extending from front of first dorsal fin back along fin bases to caudal-fin base. Similar series of dark spots along anal-fin base and onto caudal peduncle. Caudal-fin base with distinct rectangular-shaped dark brown spot in advance of posterior end of hypural plate, followed by a dark brown vertical line over end of plate. Caudal fin peppered with melanophores and crossed by seven dark brown bars. Filamentous spines of first dorsal fin dark brown, remainder of fin heavily peppered with melanophores. Second dorsal fin peppered with melanophores and crossed by 4 dark brown bars. Anal fin peppered with melanophores. Pectoral and pelvic fins lightly peppered with melanophores.

Etymology. The specific epithet is an adjective combining the Greek *pseudos* (lie) and *zebrina* (New Latin meaning zebra-marked), referring to its similarity to *Eviota zebrina*.

Distribution and habitat. Definitively known only from Fiji, but specimens identified as *E. zebrina* are known from Wallis & Futuna and Tonga in Oceania; genetic analysis of specimens from these areas is required to verify if they in fact represent *E. pseudozebrina*. In our CAS collections, the largest samples were from habitats with rock and green algae (Greenfield and Randall 2016). Individuals collected by MVE were similarly from a lagoonal habitat with mixed sand, coral rubble, macroalgae and scattered live coral; in all cases specimens were collected from the intertidal to a maximum depth of 5 m.

Eviota longirostris **Tornabene, Greenfield & Erdmann, 2021**

Long-snout Dwarfgoby
Figures 6, 7

Eviota cf. *zebrina*. Greenfield et al. 2019: 64, fig. 9 (West Papua).

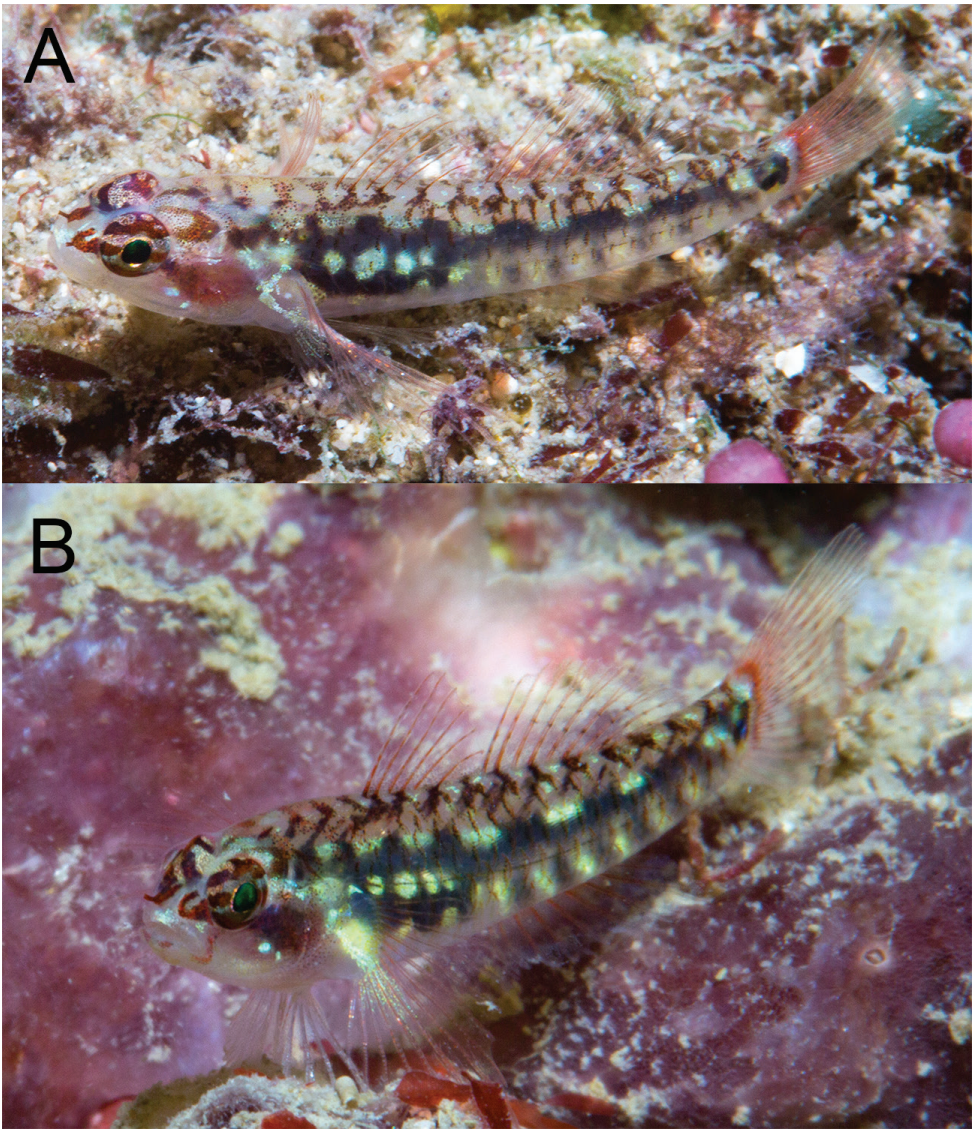

Figure 6. Underwater photograph of *Eviota longirostris* **A** paratype, CAS 246538, near type locality, West Papua, MVE-18-018 **B** specimen from type locality, West Papua, MVE-18-014.

Material. ***Holotype.*** MZB 26096, 17.6 mm SL female, Sariga, Kokas, Fakfak, West Papua, 02°36.367'S, 132°24.746'E, 5 m, clove oil & hand net, field number MVE-18-014, 8 March 2018, M.V. Erdmann. ***Paratypes.*** CAS 2246249, 5, taken with holotype. CAS 246249, 13.2 mm SL male, taken with holotype, tissue numbers EZ11-EZ15, preserved in 95% ethanol. CAS 246538, 15.0 mm SL male, 15.2 mm SL female, 02°38.527'S, 132°31.363'E, Fuum, Kokas, Fakfak, West Papua, 3 m, clove oil & hand net, field number MVE-18-018, 10 March 2018, M.V. Erdmann. CAS 246779

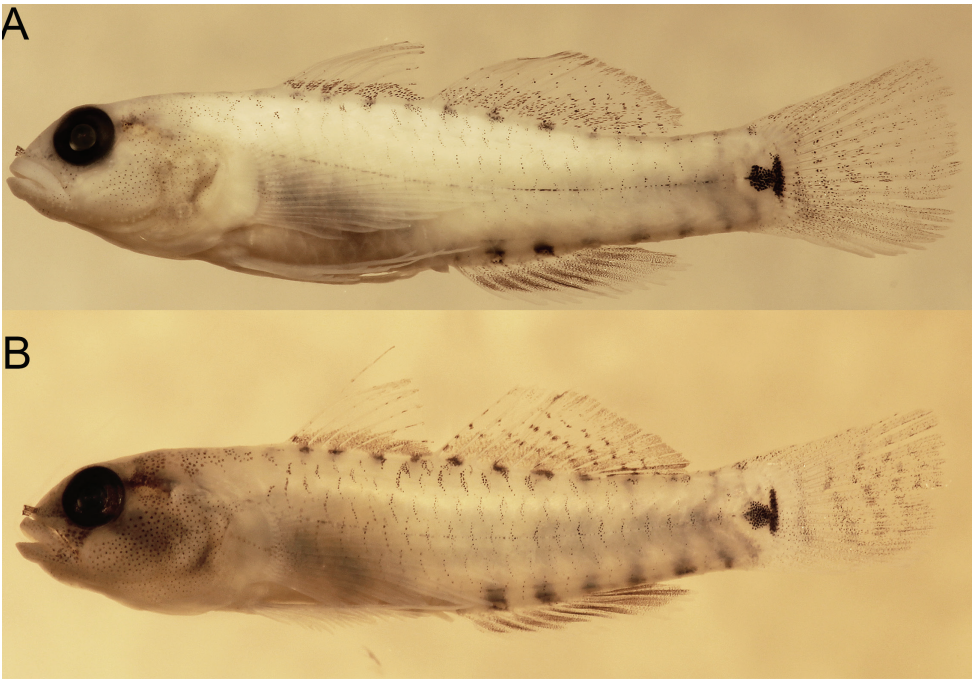

Figure 7. A *Eviota longirostris*, preserved holotype, MZB 26096 **B** paratype, CAS 246538, 15.0 mm SL male.

17.8 mm SL male, 03°54.784'S, 134°07.333'E, Bo's Rainbow, Kaimana, West Papua, 2 m, clove oil & had net, field number MVE 19-026, 21 April 2019, M.V. Erdmann. CAS 246248, 2, tissue numbers EZ1 and EZ2, preserved in 95% ethanol, 5°34.288'S, 134°48.416'E, Wasir, northeast Aru, 1–5 m, clove oil & hand net, field number MVE-16-077, 6 Dec 2016, M.V. Erdmann.

Diagnosis. A species of *Eviota* with a cephalic sensory-canal pore pattern lacking only the IT pore, pectoral-fin rays not branched, dorsal/anal-fin formula 9/8, 5th pelvic-fin ray 0–16% of 4th ray; dark triangular spot on area of preural centrum followed by a narrow dark vertical line over end of hypural plate; caudal fin crossed by six dark vertical bars, naris long and black, body slender 17–20% SL; snout long, 4–6% SL, and usually 16 pectoral-fin rays.

Description. Dorsal-fin elements VI+I,9, first dorsal triangular in shape, second spine slightly elongated in males, all second dorsal-fin soft rays branched, last ray branched to base; anal-fin elements I, 8, all soft rays branched, last ray branched to base; pectoral-fin rays 16 (15[1], 16[5], 17[1]), all unbranched, pointed, reaching to below second dorsal fin; 5th pelvic-fin ray variable ~ 8% (0–16) of length of 4th pelvic-fin ray; 4th ray with 6 branches, 4 segments between consecutive branches of 4th pelvic-fin ray, pelvic-fin membrane well developed, no basal membrane; caudal fin with 11 branched and 17 segmented rays; lateral-line scales 24; transverse scale rows 7; urogenital papilla of male smooth, long and narrow, expanded into a lateral horn at tip; female papilla smooth, bulbous, with short finger-like projections on end; front of

head rounded at an angle of ~ 60° from horizontal axis; mouth slanted obliquely upwards, forming an angle of ~ 60° to horizontal axis of body, lower jaw not projecting; maxilla extending posteriorly to front of pupil; anterior tubular nares black, extending past rear margin of upper lip; gill opening extending forward to below posteroventral edge of preoperculum; cephalic sensory-pore system missing only IT pore, cutaneous sensory papilla system similar to papilla pattern B-1 (of Lachner and Karnella 1980).

Measurements. In percent SL, value of holotype followed by range and mean of holotype and six other paratypes in parentheses. Head length 28 (28–32, 30); origin of first dorsal fin 36 (32–36, 34); origin of second dorsal fin 55 (52–58, 55); origin of anal fin 62 (54–62, 59); caudal-peduncle length 26 (23–31, 28); caudal-peduncle depth 13 (13–15, 14); body depth 20 (17–20, 19); eye diameter 9 (8–10, 9); snout length 6 (4–6, 5); upper-jaw length 9 (females 7–9, 8; males 9v12, 10.0); pectoral-fin length 37 (29–41, 34); greatest pelvic-fin length 36 (30–38, 33).

Color in life. (Figure 6). Background color of head and body translucent gray. Body with black subcutaneous lateral stripe, stripe beginning over abdomen as a large irregular blotch, narrowing posteriorly and terminating over caudal-fin base, stripe interrupted along dorsal edge by a series of 6 or 7 short and narrow white dashes. Black blotch over abdomen with several distinct iridescent yellow-white spots over dark area. Ventral portion of flank with six evenly-spaced dark spots, starting above origin of anal and continuing onto caudal peduncle, each spot loosely connected by faint dark pigment to aforementioned black lateral stripe, and each separated from one another by small yellow-white iridescent spots. On dorsal portion of flank, anterior margins of scales strongly marked with melanophores, dark scale margins coalescing along dorsal midline to loosely form a series of 14 black spots extending from predorsal area to caudal peduncle. A bold black spot at caudal-fin base consisting of two parts, a posterior narrow line centered over posterior end of hypural plate, the anterior half a roundish spot that looks triangular in shape with one point against the line when preserved. Yellow spots dorsal and ventral dark marking on the caudal peduncle, positioned above and below the posterior end of the triangular blotch and the vertical line. Reddish color of gill filaments shows through cheek from eye to pectoral-fin base. Pectoral-fin base crossed posterioventrally by a white line extending onto rays, connecting to white spot above base. A narrow red line below eye at 6 o'clock position extending down across end of jaws; this color feature is usually prominent but can also be muted quickly. Snout bright white, top of head white, peppered with melanophores, a reddish horseshoe-shaped mark behind each eye with the opening towards the eye. Jaws, underside of head and belly translucent gray. Two red stripes at front of eye, one at 9 o'clock position the other at 10 o'clock, running forward to meet at anterior tubular naris to form a V. Eye with black pupil surrounded by a narrow gold ring, iris pinkish and crossed by reddish horizontal stripe at center of pupil, a similar stripe on iris below pupil. Upper half of iris reddish with irregular pink marks. All fin rays and spines with a reddish tinge, a distinct reddish area at caudal-fin base.

Color in preservative. (Figure 7). Background color of head and body light yellow. Scale anterior margins outlined with melanophores, a narrow line of melanophores later-

ally over length of vertebral column. A bold black spot at caudal-fin base consisting of two parts, a posterior narrow line centered over posterior end of hypural plate, the anterior half triangular in shape with one point against the line. A series of 11 black spots extending along dorsal-fin bases onto caudal peduncle. Six postanal spots, two above anal fin. Side of head with a band of melanophores under eye at 6–8 o'clock positions extending down across jaws. Another dark band behind eye at 2 o'clock position above preoperculum. Side of head peppered with melanophores. Pectoral-fin base crossed by a narrow posteroventral line of melanophores. Top of head and nape crossed by four bands of melanophores, the first behind the eyes, the last at the first dorsal-fin base, each band with a central horizontal black line. First dorsal fin with narrow band of melanophores along its lower quarter, distal end of spines with melanophores. Second dorsal fin similar to first but basal dark band ~ 1/3–1/2 of fin and distal margin with dark band. Anal fin mostly black except at its base and distal margin. Pectoral and pelvic fins immaculate. Caudal fin crossed by six or seven vertical bands of melanophores with peppering at dorsal and ventral portions of fin.

Etymology. The specific epithet is an adjective derived from the Latin *longus* (long) and *rostrum* (snout), alluding to the relatively long snout of this species compared to others in the complex.

Distribution and habitat. Currently known only from the southern coastal region of West Papua, from southern Raja Ampat (based on photos only) to Fakfak, Kaimana, and the Aru Archipelago, although possibly more widespread including perhaps to Australia. Observed in shallow depths of 2–8 m on coastal reefs exposed to significant terrigenous influences (freshwater influx and sedimentation) and moderate to strong currents. Observed individually on coralline algae and dead coral substrates.

Eviota marerubrum **Tornabene, Greenfield & Erdmann, 2021**

Red Sea Dwarfgoby
Figures 8, 9

Eviota cf. *zebrina*. Greenfield et al. (2019: 64, fig. 9 (Red Sea).
Eviota zebrina (non Lachner & Karnella). Atta et al. (2019: 8); Troyer et al. (2018: 8); Meadows et al. (2014: 3, figs 2, 3); Golani and Bogorodsky (2010: 47); Herler (2007: 85); Herler and Hilgers (2005: 114, fig. 8).

Material. ***Holotype.*** USNM 218035, 14.1 mm SL male, Bay at El Himeira, Egypt, Gulf of Aqaba, Red Sea, 21–27 m, 9 September 1969, V. Springer et al. ***Paratypes.*** USNM 447872 (collected with holotype), 105, Bay at El Himeira, Egypt, Gulf of Aqaba, Red Sea, 21–27 m, 9 September 1969, Victor Springer et al.; USNM 218034, 163, Bay at El Himeira, Egypt, Gulf of Aqaba, Red Sea, 9–12 m, 8 September 1969, V. Springer, G. Raz & L. Hughes-Gannes; UW 159939 (previously in USNM 218034), 2, Bay at El Himeira, Egypt, Gulf of Aqaba, Red Sea, 9–12 m, 8 September 1969, V. Springer, G. Raz & L. Hughes-Gannes; CAS 247198 (previously in USNM 218034), 2f, Bay at El Himeira, Egypt, Gulf of Aqaba, Red Sea, 9–12 m, 8 September 1969, V. Springer,

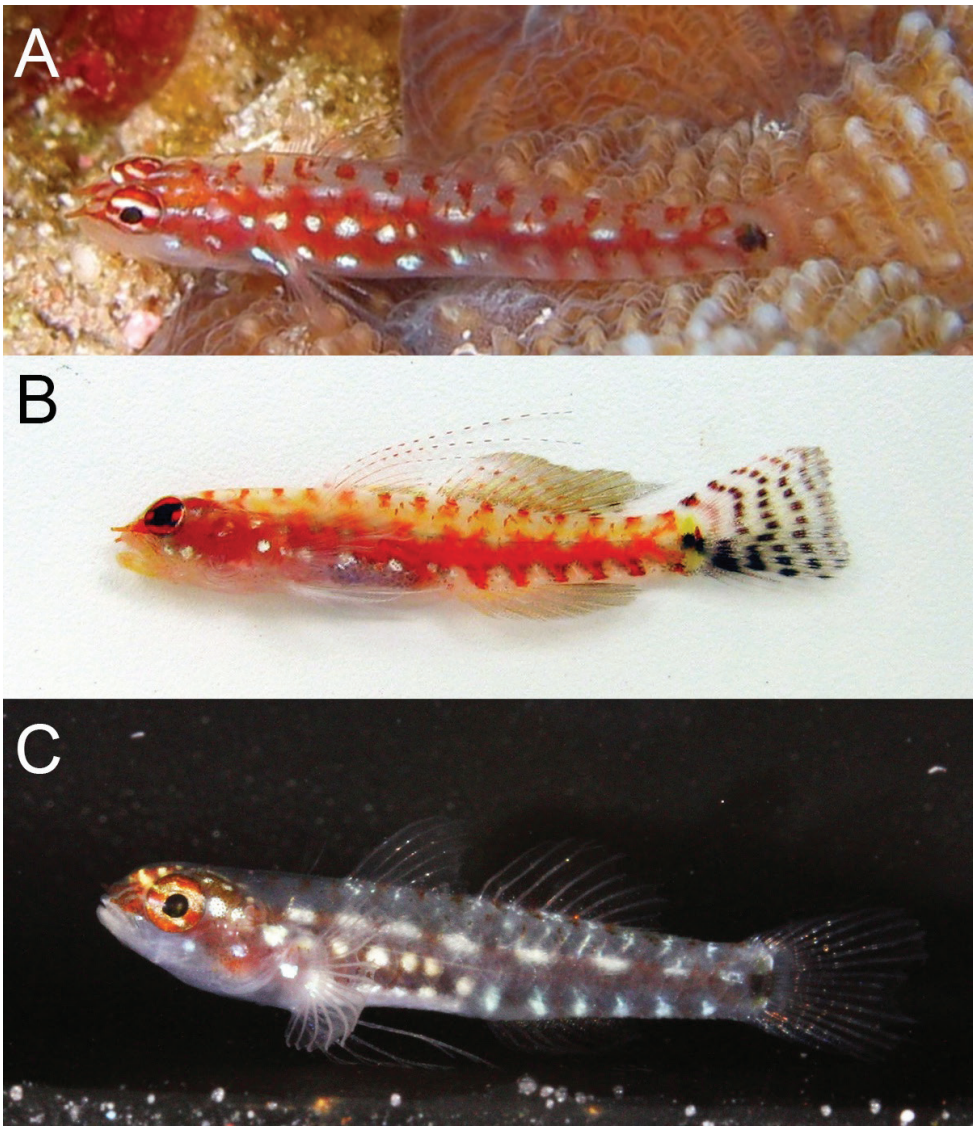

Figure 8. *Eviota marerubrum*, live. **A, B** Egypt (photograph J. Herler, with permission) **C** Israel (photograph R. Holzman, with permission).

G. Raz & L. Hughes-Gannes; USNM 218031, 23, Bay at El Himeira, Egypt, Gulf of Aqaba, Red Sea, 0–18 m, 16 July 1969, V. Springer, A. Amir, G. Raz & H. Harpaz.

Non-type material. CAS 239041, 1, preserved in 95% ethanol, Al Lith, Shi'b Habil reef, Station 24, exposed inner shelf, 8.1 m depth, 30 Jan 2015, D.J. Coker, J.D. DiBattista, T.H. Sinclair-Taylor, and M.L. Berumen; CAS 239042, 1, preserved in 95% ethanol, Al Lith, Marmar reef, Station 29, sheltered outer shelf, cave next to station, 10.3 m depth, 31 Jan 2015, D.J. Coker, J.D. DiBattista, T.H. Sinclair-Taylor,

Figure 9. *Eviota marerubrum*, preserved **A** holotype, USNM 218035 **B** freshly preserved specimen from Egypt, 16.5 mm SL (photograph J. Herler, with permission).

and M.L. Berumen; CAS 239043, 1, preserved in 95% ethanol, Thuwal, Abu Madafi reef, Station 31, exposed outer shelf, 14 m depth, 5 Feb 2015, D.J. Coker, J.D. DiBattista, T.H. Sinclair-Taylor, and M.L. Berumen. Examined by Lachner and Karnella (1978), all from the Red Sea: USNM 218030, 3 (13.0–16.5); USNM 218031, 23 (8.4–15.3); USNM 218032, 6 (8.1–11.4); USNM 218033, 6 (8.8–11.2); FMNH 83851, 2; FMNH 83850, 1; BPBM 13428, 1.

Diagnosis. A species of *Eviota* with a cephalic sensory-canal pore pattern lacking only the IT pore, AITO small and opening dorsally; pectoral-fin rays not branched; dorsal/anal-fin formula 8/7; 5th pelvic-fin ray 8–15% of 4th ray; small dark circular spot on area of preural centrum connected to a short, narrow dark vertical line over end of hypural plate; caudal fin of freshly dead specimens crossed by five or six dark vertical bars, naris long and reddish brown; eye with two distinct white horizontal stripes, one crossing through upper margin of eye, another crossing through lower margin of eye; body depth approximately 20–25% SL; usually 15 pectoral-fin rays.

Description. Fin-ray counts for dorsal, anal, and pectoral fins in the following description are based on specimens examined by Lachner and Karnella (1978) from the Red Sea. We reexamined ten specimens each from three of the lots from that study from Egypt, Northern Gulf of Aqaba, Red Sea, which were used to obtain morphometrics and to confirm meristic characters. The holotype was selected from one of those three lots (USNM 218035) and all other specimens in this lot are designated as paratypes and given a new catalog number, USNM 447872. Four specimens were removed from USNM 218034, two of which are now paratypes CAS 247198 and two

are paratypes UW 159939. The remaining specimens in USNM 218034, and USNM 218031, are also designated as paratypes.

Dorsal-fin elements VI+I,8 (7[1], 8[29], 9[2]), first dorsal triangular in shape, first or second spine elongated in some specimens of both sexes, ranging from slightly elongate (extending to first ray of second dorsal fin when depressed) in some smaller males and females of all sizes, to extremely elongate (extending to beyond last ray of second dorsal-fin when depressed) in largest males, all second dorsal-fin soft rays branched, last ray branched to base; anal-fin elements I, 7 (in all specimens examined), all soft rays branched, last ray branched to base; pectoral-fin rays 15 (14[3], 15[15], 16[7]), all unbranched, pointed, reaching to below second dorsal fin; 5th pelvic-fin ray variable ~ 10% (8–15%) of length of 4th pelvic-fin ray; 4th ray with 4–6 branches, 1–3 segments between consecutive branches of 4th pelvic-fin ray, pelvic-fin membrane not well developed, no basal membrane; caudal fin with 11 branched and 17 segmented rays (caudal fin broken in holotype and some paratypes, unable to count segmented rays); lateral-line scales 23 (22[2], 23[4], 24[2], 25[1], 26[1]); transverse scale rows 8 (7[6], 8[3]); urogenital papilla of male smooth, long and narrow, expanded into two lateral horns at tip; female papilla smooth, bulbous, with short finger-like projections on end; front of head sloping at an angle of ~ 50° up from horizontal axis; mouth slanted obliquely upwards, forming an angle of ~ 30° upwards from horizontal axis of body, lower jaw not projecting; maxilla extending posteriorly to posterior margin of pupil; anterior tubular nares reddish brown in life, extending past rear margin of upper lip; gill opening extending forward to below posteroventral edge of preoperculum; cephalic sensory-pore system missing only IT pore, AITO pore small and opening dorsally, cutaneous sensory papilla system similar to papilla pattern B-1 (of Lachner and Karnella 1980).

Measurements. In percent SL, value of holotype followed by range and mean of holotype and ten other paratypes in parentheses. Head length 28 (27–31, 29); origin of first dorsal fin 35 (33–38, 35); origin of second dorsal fin 53 (52–59, 55); origin of anal fin 58 (56–64, 60); caudal-peduncle length 26 (22–29, 26); caudal-peduncle depth 12 (10–13, 11); body depth 25 (20–25, 22); eye diameter 9 (9–11, 10); snout length 5 (4–5, 4); upper-jaw length 11 (females 9 or 10, 10; males 10–12, 10); pectoral-fin length 23 (21–29, 24); greatest pelvic-fin length 39 (27–39, 31).

Color in life. (Figure 8). Background color of head and body translucent gray. Body with broad red stripe extending from tip of snout to caudal peduncle, stripe interrupted by eight or nine iridescent white dashes evenly spaced along dorsal margin of stripe on body, dashes beginning above the operculum and terminating on caudal peduncle.

Six short red bars extending ventrally from red lateral stripe, first bar just posterior to origin of anal fin, last bar at the posterior margin of caudal peduncle, each bar separated by a white (sometimes iridescent) space. Dorsal midline with 13 or 14 small evenly spaced red spots beginning on nape at a vertical above operculum and extending posteriorly to posterodorsal margin of caudal peduncle. Abdomen and side of body behind pectoral fin with six to eight iridescent white spots over red lateral stripe. Pectoral-fin base red with iridescent white spot in center. Pair of small dark spots at base of caudal fin, anterior spot centered just anterior to origin

of caudal rays and circular in shape, posterior spot more vertically elongate, located on base of caudal rays.

Head pale gray ventrally, with red snout, nares, and nape. Eyes red with two horizontal white stripes on iris, above and below pupil. Short white stripe on head extending from behind eye, in line with upper stripe on iris, to operculum; white stripe sometimes broken into two small spots rather than continuous stripe. One or two iridescent white spots, slightly smaller than diameter of pupil, on side of head posterior to jaws. First three spines of the dorsal fin with evenly spaced red spots along entirety of spine. Second dorsal-fin rays each with two red spots evenly spaced along rays. Pectoral fins and pelvic fins white. Caudal fin pale with four faint red vertical bands.

Color in preservative. (Figure 9). Background color of head and body yellowish pale. Side of body without prominent markings except for a very narrow stripe line of single melanophores along lateral midline (present only in well-preserved specimens). Dorsal margin of body with 13 small evenly spaced dark spots beginning on nape at a vertical above operculum and extending posteriorly to posterodorsal margin of caudal peduncle. Dorsal and anal fins unpigmented in type series, however recently preserved specimens may have a dark band of melanophores at the base of first dorsal fin, and second dorsal and anal fins uniformly covered with small melanophores. Pelvic fins without pigment. Caudal fin with four faint brown vertical bands, band more pronounced in freshly preserved specimens.

Etymology. The specific epithet is an adjective combining the Latin *maris* (sea) and *ruber* (red) referring to the type locality, the Red Sea.

Distribution and habitat. Currently known only from specimens examined from the Red Sea, ranging from the Gulf of Aqaba in the northern Red Sea to the central Red Sea off the coast of Saudi Arabia.

Eviota oculineata Tornabene, Greenfield & Erdmann, 2021

False-comet Dwarfgoby
Figures 10, 11

Eviota cf. *cometa* Greenfield et al. 2019: 64, fig. 9 (New Guinea and Solomon Islands).
Eviota cometa (non Lachner & Karnella). Greenfield et al. (2019: fig. 8); Greenfield and Randall (2016: fig. 35); Allen and Erdmann (2012: 913); Randall (2005: 530); Suzuki et al. (2004: 131); Nakabo (2002: 1181).

Material. ***Holotype.*** CAS 247279, 10.9 mm SL male, tissue number COM5, preserved in 95% ethanol, 01°37.300'S, 138°43.395'E, Pulau Liki West, northern New Guinea, 30 m, clove oil & hand net, field number MVE-19-006, 12 Feb 2019, M.V. Erdmann. ***Paratypes.*** CAS 246244, 2, tissue numbers COM1 and COM2, preserved in 95% ethanol, 10°53.773'S, 150°44.637'E, Dumoulins, Milne Bay, Papua New Guinea, 20 m, clove oil & hand net, field number MVE-16-020, 23 May 2016, M.V. Erdmann. CAS 246245, 9.9 mm SL male, tissue number COM3, preserved in 95%

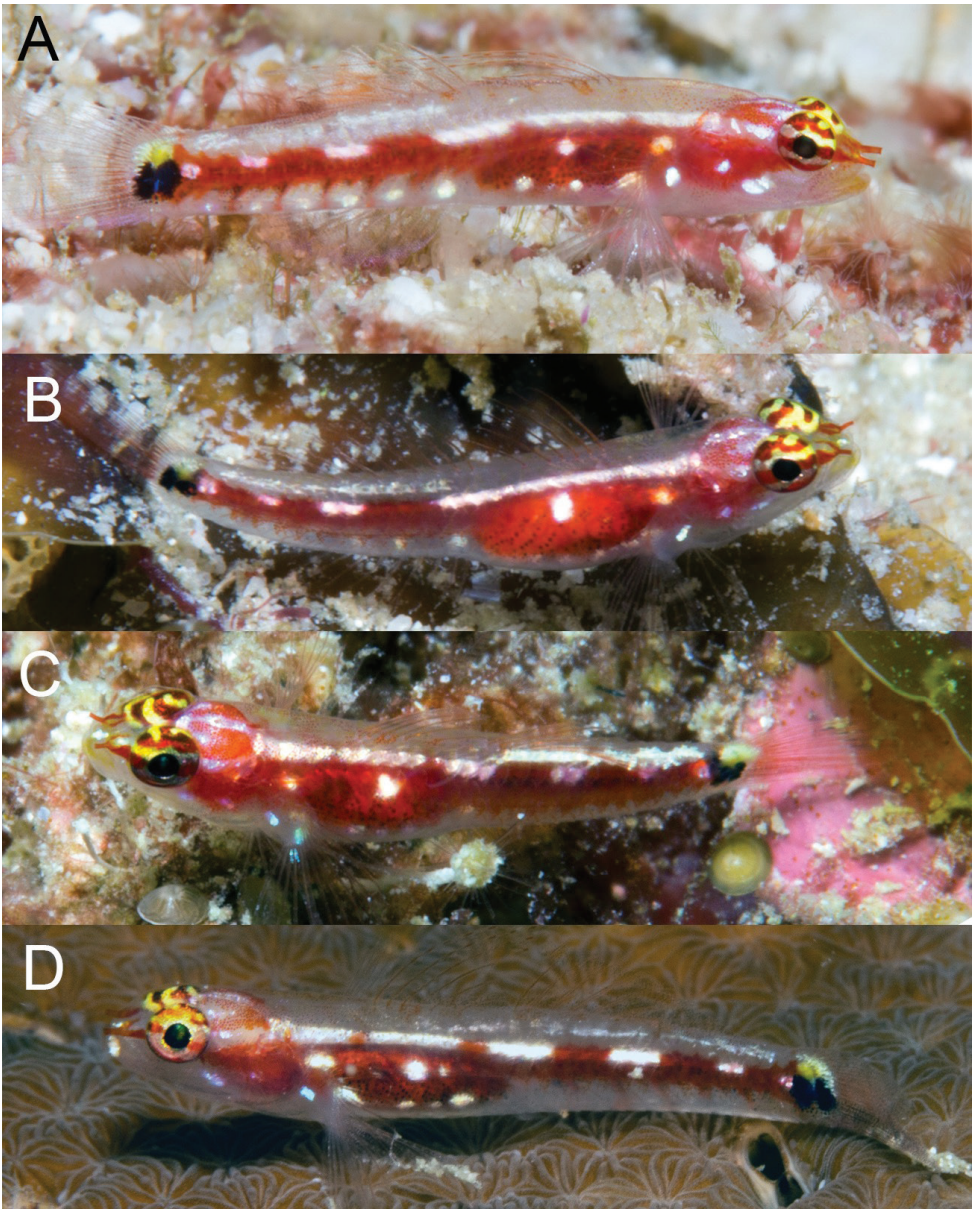

Figure 10. *Eviota oculineata*, live, New Guinea.

ethanol, 09°19.954'S, 160°17.946'E, Shoal near Nugu Island, Florida Island Group, Solomon Islands, 35 m, 11 October 2016, M.V. Erdmann.

Non-type material. Fiji - CAS 228684, 2, field number G02-146, Naigani Island, patch reef, clear water, coral wall overhang with black coral, 17°34.611'S, 178°40.217'E, 5.4–9. 1 m, rotenone, 4 November 2002, Greenfield, et al.; CAS 238063, 2, field

Figure 11. *Eviota oculineata*, preserved holotype, CAS 247279.

number JVE-10-11-2015, Mt. Mutiny Dive site, N.E. of Viti Levu, off Nanukuloa, rubbly reef, 17°20.76'S, 178°31.35'E, 12 m, clove oil, 11 October 2015, J.V. Eyre.

Diagnosis. A species of *Eviota* with a cephalic sensory-canal pore pattern lacking only the IT pore, AITO small and opening dorsally; pectoral-fin rays not branched; dorsal/anal-fin formula 8/7; 5th pelvic-fin ray 8–15% of 4th ray; large dark oval spot on area of preural centrum connected to a short, vertically elongate spot over end of hypural plate; caudal fin of freshly dead specimens without prominent vertical bars; naris long and reddish brown; side of body with prominent red lateral streak bordered dorsally by three to five elongate white dashes; eye with two distinct horizontal stripes, one white crossing through lower margin of pupil, one yellow crossing upper margin of pupil; body depth approximately 27–31% SL; usually 14 pectoral-fin rays.

Description. Dorsal-fin elements VI+I,8, first dorsal triangular in shape, first or second spine elongated in some specimens of both sexes, ranging from slightly elongate (extending to first ray of second dorsal fin when depressed) in the smallest male, to extremely elongate (extending to beyond origin of last ray of second dorsal fin when depressed, as in holotype), all second dorsal-fin soft rays branched, last ray branched to base; anal-fin elements I, 7 (all soft rays branched, last ray branched to base; pectoral-fin rays 14 (14[3], 15[1]), all unbranched, pointed, reaching to below second dorsal fin; 5th pelvic-fin ray variable, ~ 10% (8–15%) of length of 4th pelvic-fin ray; 4th ray with four or five branches, one or two segments between consecutive branches of 4th pelvic-fin ray, pelvic-fin membrane not well developed, no basal membrane; caudal fin with 11 branched and 16 segmented rays; lateral-line scales 24 (22[1], 23[1], 24[1]), scales not countable on one specimen due to damage); transverse scale rows 7; urogenital papilla of male smooth, long and narrow, expanded into two lateral horns at tip; female papilla smooth, bulbous, with short finger-like projections on end; front of head sloping at an angle of ~ 60° up from horizontal axis; mouth slanted obliquely upwards, forming an angle of ~ 35° upwards from horizontal axis of body, lower jaw not projecting; maxilla extending posteriorly to center of pupil; anterior tubular nares extending past rear margin of upper lip; gill opening extending forward to below posteroventral edge of preoperculum; cephalic sensory-pore system missing only IT pore, AITO pore small and opening dorsally; cutaneous sensory papilla system similar to papilla pattern B-1 (of Lachner and Karnella 1980).

Measurements. In percent SL, value of holotype followed by range and mean of holotype and ten other paratypes in parentheses. Head length 27 (27–31, 28); origin of first dorsal fin 37 (35–37, 36); origin of second dorsal fin 57 (54–58, 56); origin of anal fin 59 (59–62, 60); caudal-peduncle length 25 (20–29, 25); caudal-peduncle depth 11 (11–13, 12); body depth 18 (18 or 19, 18); eye diameter 9 (8–10, 9); snout length 3 (3–6, 4); upper-jaw length 8 (females 9 or 10, 9; males 8 or 9, 9); pectoral-fin length 25 (22–29, 25); greatest pelvic-fin length 30 (28–33, 31).

Color in life. (Figure 10). Background color of head and body translucent gray. Body with broad red stripe extending from tip of snout to caudal peduncle, stripe interrupted by five iridescent white dashes evenly spaced along dorsal margin of stripe on body, dashes beginning above the operculum and terminating on caudal peduncle, with anterior three dashes sometimes merged as a continuous white stripe over abdomen.

Occasionally five short red bars extending ventrally from red lateral stripe, first bar just posterior to origin of anal fin, last bar at the posterior margin of caudal peduncle, each bar separated by a white (sometimes iridescent) space. Abdomen and side of body behind pectoral fin with two (sometimes three) iridescent white spots over red lateral stripe, first spot immediately above and posterior to axis of pectoral fin. Pectoral-fin base red with iridescent white spot in center. Pair of vertically elongate, broadly joined dark spots at base of caudal fin, anterior spot centered just anterior to origin of caudal rays, posterior spot located on base of caudal rays. Small yellow spot on base of caudal fin just dorsal to pair of dark spots.

Head pale gray ventrally, with red snout, nares, and nape. Eyes red with two horizontal stripes on iris, one yellow and passing through upper margin of pupil, one white and passing through lower margin pupil, dorsal margin of eye above stripe with yellow spots or mottling. Short white stripe on head behind eye, in line with upper stripe on iris, extending posteriorly to operculum; white stripe sometimes broken into two small spots rather than continuous stripe. One or two iridescent white spots, slightly smaller than diameter of pupil, on side of head posterior to jaws. First three spines of the dorsal fin with evenly spaced red spots along entirety of spine. Second dorsal-fin rays faintly tinged with red. Pectoral fins and pelvic fins white. Caudal fin lacking prominent vertical bands, lower half of caudal fin with faint red hue.

Color in preservative. (Figure 11). Based on holotype, preserved in 95% ethanol. Background color of head and body yellowish pale. Head without pigment except for a faint scattering of melanophores on nape. Abdomen uniformly covered with dark melanophores, remaining side of body lacking any pigmentation except for a row of scattered melanophores along the ventral midline of body, beginning at anal fin origin on continuing to middle of caudal peduncle. Pair of vertically elongate, broadly joined dark spots at base of caudal fin, anterior spot centered just anterior to origin of caudal rays, posterior spot located on base of caudal rays. Dorsal and anal fins with light scattering of chromatophores on inter-radial membranes and on rays of posterior half of fins. Caudal fin lacking pigmentation except for a faint horizontal streak of melanophores on five rays, the first of which is just below the lateral midline of the caudal fin, followed by the four subsequent ventral rays. Pectoral fin, pectoral-fin base, and pelvic fins without pigment.

Etymology. The specific epithet is an adjective combining the Latin *oculi* (eye) and *linea* (line, stripe) referring to the stripes through the eye, which distinguish this species from *E. cometa*.

Distribution. Currently known only from New Guinea and the Solomon Islands, but likely occurs in Fiji and the Banda Sea, Indonesia, and the Great Barrier Reef, Australia, based on live photographs as well as specimens previously identified as *E. cometa* that possess 8/7 counts in the dorsal/anal fins (Figure 12). The species seems to prefer outer reef slopes exposed to clear oceanic water in depths of 20–35 m and is frequently observed resting individually on coralline algae outcrops or live plate corals.

Remarks. When *E. cometa* was described, it was based on preserved material with no information on live coloration, with the holotype from Fiji. Specimens in the type series possessed both 8/7 and 9/8 dorsal/anal-fin formulas (Lachner and Karnella 1983). When Greenfield and Randall (2016) reviewed the dwarfgobies of Fiji they based their identification of preserved specimens as *E. cometa* on the description of the species by Lachner and Karnella (1983) and the underwater photographs identified as *E. cometa* in Suzuki et al. (2004), Randall (2005), and Allen and Erdmann (2012). In their review they provided two photographs (fig. 34 and fig. 35 of Greenfield and Randall 2016), one an underwater photograph by R. Whitworth taken in Fiji (Figure 12A) and a fresh specimen from CAS 222731 (Figure 13A). The underwater photograph (Figure 12A) was similar to the earlier underwater photos, showing only a clear caudal fin that was not crossed by oblique red bars, and eyes with white/yellow stripes, whereas the fin of the other fresh specimen (Figure 13A) had distinct red bars on the caudal (however, when preserved the red bars were not visible as dark bars as they are in *E. pseudozebrina*) and a solid red eye. This supported the idea that there were two species in Fiji, the type locality for *E. cometa*.

In 2017 MVE collected and photographed specimens (Figure 13D) from a silty lagoon in the Lau Archipelago, Fiji, that resembled the freshly dead specimen from Greenfield and Randall (2016, fig. 34) in that the eye was all red, different from the striped eyes in previous underwater photographs (e.g., Figures 10, 12; now *E. oculineata*). Similarly, photographs of specimens from Tonga of fish with red bars across the caudal fin and solid red eyes also appeared to be this same species (Figures 13B, C), and this was confirmed with DNA (Figure 2). Additionally, in 2020 Janet Eyre took an underwater photograph of a fish in Fiji with the same solid red eye color and red bars across the caudal fin (Figure 13E). These specimens with the red caudal-fin bars and solid red eyes have a dorsal/anal-fin formula of 9/8, the same as the holotype of *E. cometa*, whereas those individuals lacking the red bars and having striped eyes have a dorsal/anal-fin formula of 8/7 and are described here as *E. oculineata*.

The large collection of 30 *E. cometa* from Fiji, CAS 222731, came from a habitat of dead coral and silty sand, and the photographs taken by MVE (Figure 13D) and Janet Eyre (Figure 13E) were also both from protected, silty, patch reef habitat contrasting strongly with the clearer water, outer reef habitat where *E. oculineata* is found. Given

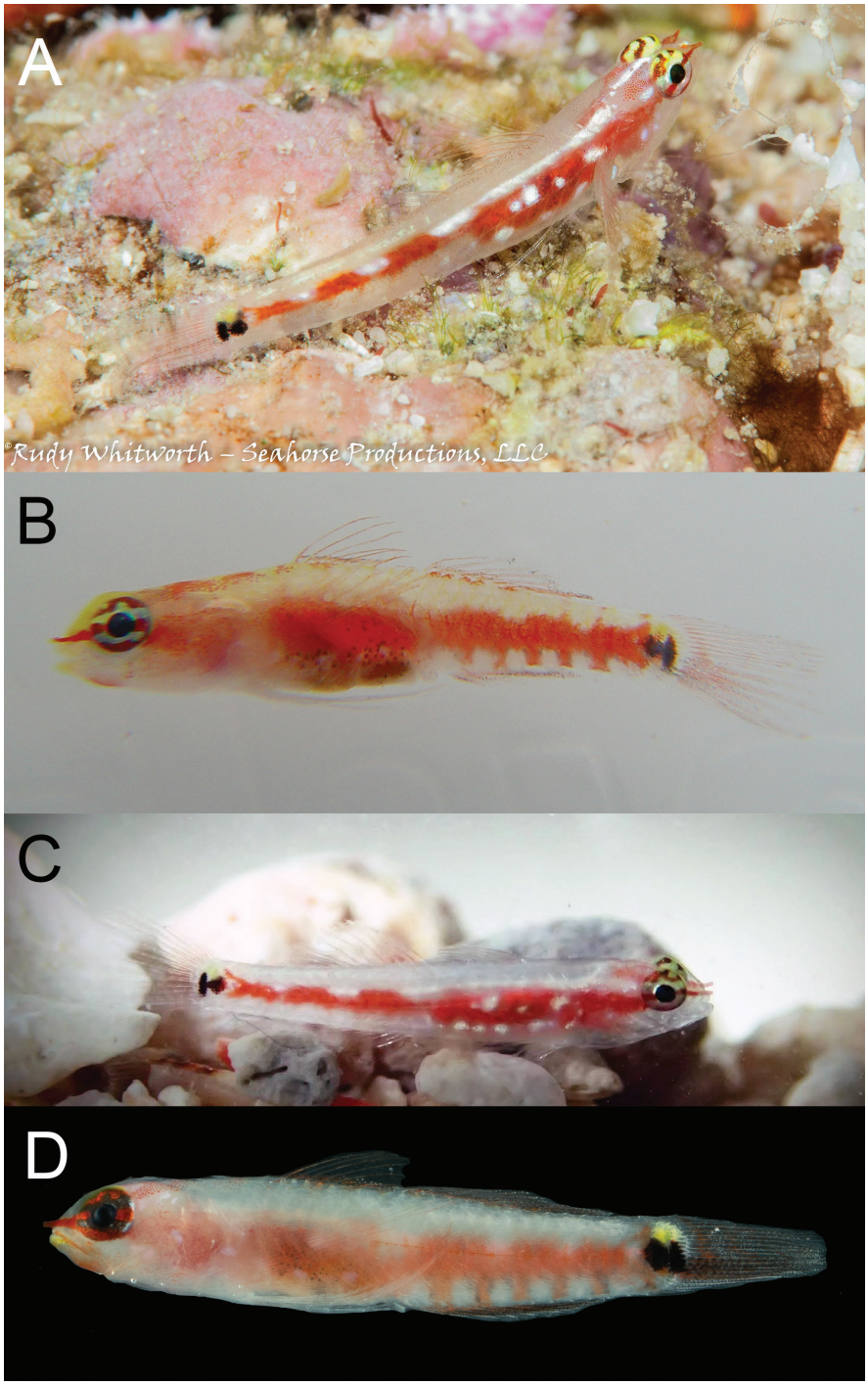

Figure 12. *Eviota oculineata* photographs from non-type specimens **A** Fiji (photograph R. Whitworth, with permission) **B** Fiji **C** Fiji (photograph J. Eyre, with permission) **D** Australia (photograph C. Goatley, with permission).

Table 1. Diagnostic characters for distinguishing species in the *Eviota zebrina* species complex. Counts for *E. marerubrum* and *E. zebrina* include data for specimens from the Red Sea and Seychelles, respectively, listed in Table 2 of Lachner and Karnella (1978), and morphometrics for *E. zebrina* are from 15 paratypes from CAS 40599. Data for *E. cometa* are from the holotype, tissue vouchers from the phylogeny, and Fiji specimens with 9/8 D2/A rays. Measurements are given in % SL.

	E. longirostris	***E. zebrina***	***E. pseudozebrina***	***E. cometa***	***E. oculineata***	***E. marerubrum***	***E. tetha***	***E. gunawanae***
Type locality	Indonesia	Seychelles	Fiji	Fiji	Papua New Guinea	Egypt	Indonesia	Indonesia
Pectoral rays - mode (range)	16 (15–17)	16 (15–17)	15 (14–16)	16 (16–17)	14 (14–15)	15 (14–16)	14 (14–15)	16 (16)
D2/A rays - mode	9/8	9/8	9/8	9/8	8/7	8/7	8/7	8/7
Length 5th pelvic-fin ray	absent to 15.8% of 4th	6–14% of 4th	6–16% of 4th	~ 10% of 4th	8–15% of 4th	8–15% of 4th	absent or rudimentary	~ 10% of 4th
AITO pore	small, opens dorsally	small, opens dorsally	small, opens dorsally	small, opens dorsally	small, opens dorsally	small, opens dorsally	large, opens anteriorly	large, opens anteriorly
IT pore	absent	absent	absent	absent	absent	absent	absent	absent
NA pores	present	present	present	present	present	present	absent	absent
Body depth - average (range)	18.7 (17.4–19.9)	19.2 (17.1–21.2)	23.2 (21.6–25.7)	21.1 (17.6–23.6)	28.4 (27.2–30.6)	22.3 (20.3–24.8)	19.6 (17.7–21.4)	19.6 (18.2–21.4)
Snout length - average (range)	5.3 (4.3–5.7)	3.4 (2.8–4.1)	4.3 (3.7–5.4)	3.7 (2.5–5.1)	4.3 (3.3–6.2)	4.3 (3.4–5.2)	4.5 (3.9–6.2)	4.4 (3.7–5.0)

the general preference of underwater photographers for clear water and healthy reefs, it is perhaps not surprising that the majority of underwater photographs in the literature appear to be *E. oculineata* and not the true *E. cometa*, given the latter species' apparent proclivity for silty inshore reefs. Additional photographs of fishes originally identified as *E. cometa* from Lizard Island, Australia (Figure 12D) also appear to be *E. oculineata*, based on dorsal/anal fin-ray counts and coloration.

Comparisons within the *Eviota zebrina* species complex

With the addition of the four species described here, the *E. zebrina* complex contains eight species: *E. cometa*, *E. gunawanae*, *E. longirostris*, *E. marerubrum*, *E. oculineata*, *E. pseudozebrina*, *E. tetha*, and *E. zebrina*. A combination of meristic features (e.g., counts of rays in the pectoral, dorsal, and anal fins), morphometric features (snout length, body depth), head pore patterns, and live and preserved coloration differentiate the species (Table 1). These characters are discussed in detail and are also presented in a taxonomic key below. We

Body coloration comparisons. All species in this group with the exception of *E. tetha* (Figure 14A) have large, prominent dark spots at the base of the caudal fin, which are often margined dorsally (and sometimes ventrally) by smaller yellow spots in life. The side of the body of most species in this group is characterized by a prominent red streak that ends at the base of the caudal fin; however *E. longirostris* (Figure 6) and *E. pseudozebrina* (Figure 3) lack red pigment and, instead, pigment on the side of the body is predominantly black or brown. *Eviota pseudozebrina* is the least colorful of all the species in the complex, with a translucent gray background and markings that are

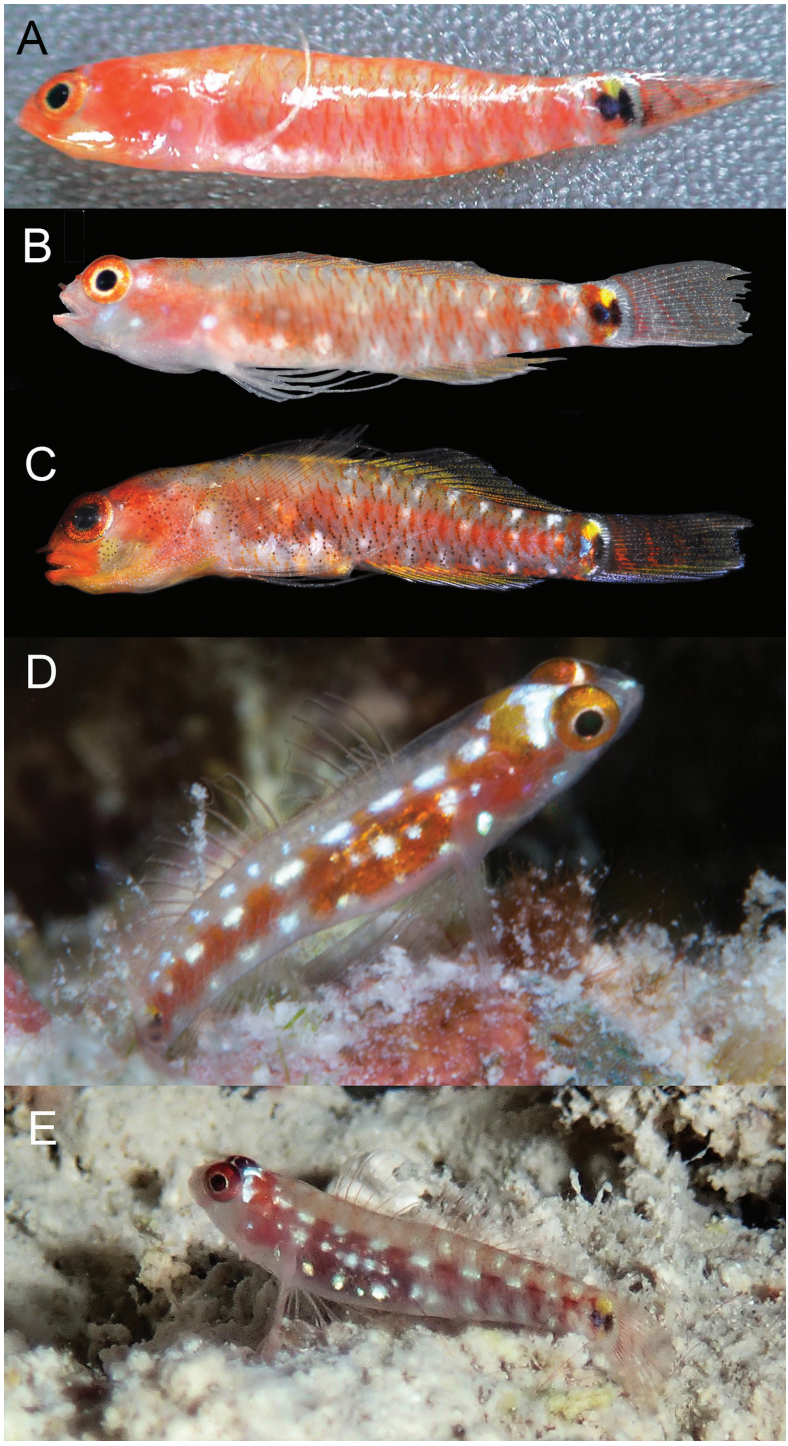

Figure 13. *Eviota cometa* **A** freshly dead specimen from Fiji **B, C** f reshly dead specimens from Vava'u, Kingdom of Tonga (photographs M. Gómez-Buckley, with permission) **D, E** live, Fiji (photograph **E** J. Eyre, with permission).

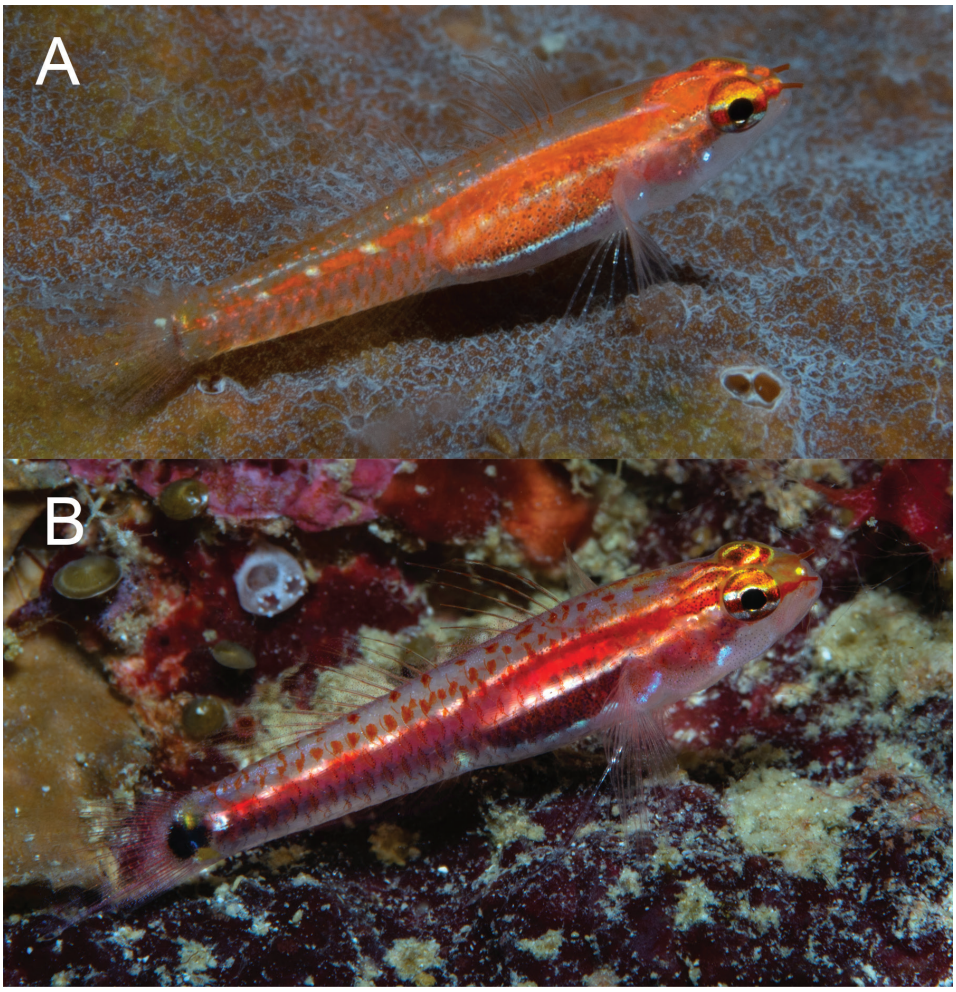

Figure 14. A *E. tetha*, Cendrawasih, West Papua **B** *Eviota gunawanae*, Fakfak, West Papua.

white, brown, or black. The upper half of the eye surface is cream colored with scattered melanophores, lower half darker. The overall coloration of *E. longirostris* is bolder with red markings on the head and eye and the spines and rays with a reddish tinge.

Five species have both a red body-stripe and the dark spot at the caudal-fin base: *E. cometa*, *E. gunawanae*, *E. marerubrum*, *E. oculineata*, and *E. zebrina*. *Eviota gunawanae* differs from the other four in having a solid white stripe on the mid-abdomen immediately posterior to the pectoral fin (Figure 14B), versus having a series of distinct white spots in this area (Figures 8, 10, 12, 13, 15). Above this region on the abdomen is a series of white stripes or dashes that extend from above the pectoral fin to the caudal fin base in all species in this complex. This series is made up of 3–6 elongate horizontal white dashes in *E. oculineata* (Figures 10, 12) versus being made up by eight or more short white dashes or spots in *E. marerubrum* (Figure 7), *E. cometa* (Figure 13), and *E. zebrina* (Figure 15). *Eviota cometa* differs from *E. marerubrum*, *E. oculine-*

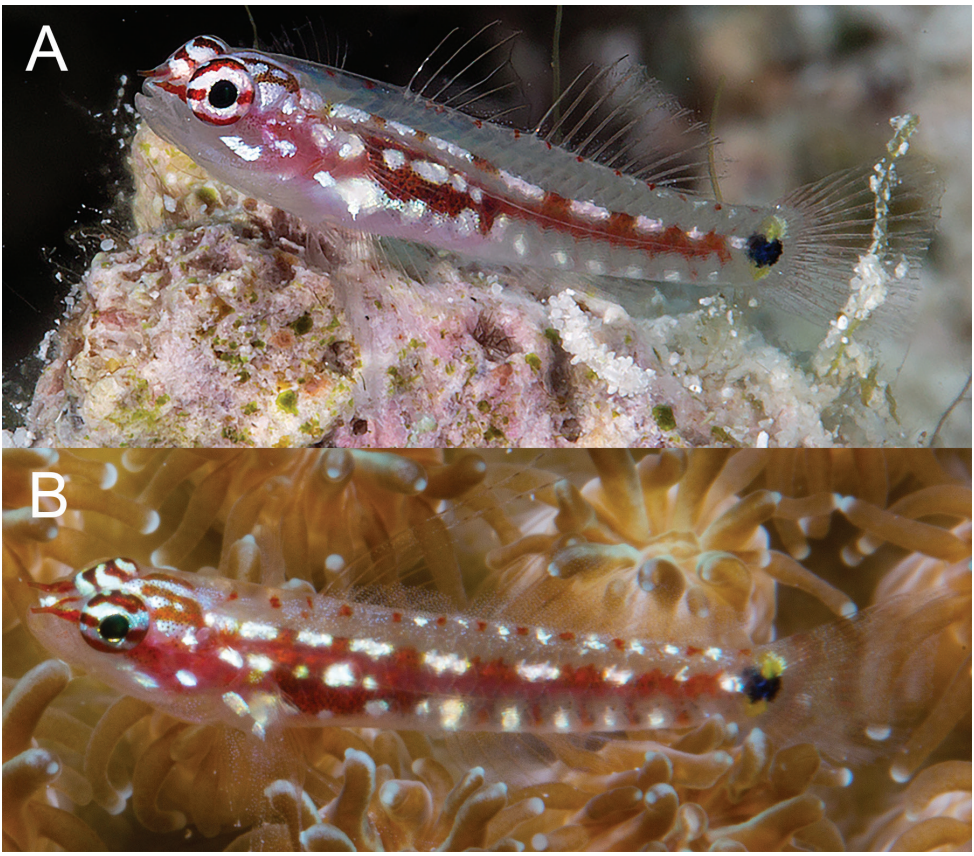

Figure 15. *Eviota zebrina* **A** Seychelles (photograph J. Greenfield, with permission) **B** Maldives.

ata, and *E. zebrina* in having a large, prominent V-shaped white patch on the nape immediately posterior to the eyes (Figure 13D, E), whereas the other four species possess short horizontal white stripes in this region (Figures 8, 10, 12, 15).

Eye coloration comparisons (Figure 16). As discussed by Greenfield (2017), eye coloration patterns in species of *Eviota* exhibit great variation and have been used in recognizing different species. Often dwelling in rock or coral crevices, dwarfgoby eyes are the body part that are most easily seen by other fishes, so it follows that eye coloration is a character that would be useful in species recognition and hence under selective pressure. Two of the species within the *E. zebrina* species complex differ from the others in lacking a reddish stripe crossing the center of the eye at the pupil. *Eviota pseudozebrina* is the most different by lacking any red in the eye, with the upper half of the eye gray and heavily peppered with melanophores, and the lower half dark (Figure 16F). From a lateral view, the entire iris of *E. cometa* is dark reddish, with the pupil surrounded by a white ring (Figure 16C). The dorsal side of the eye next to the interorbital area has a short white bar not visible laterally.

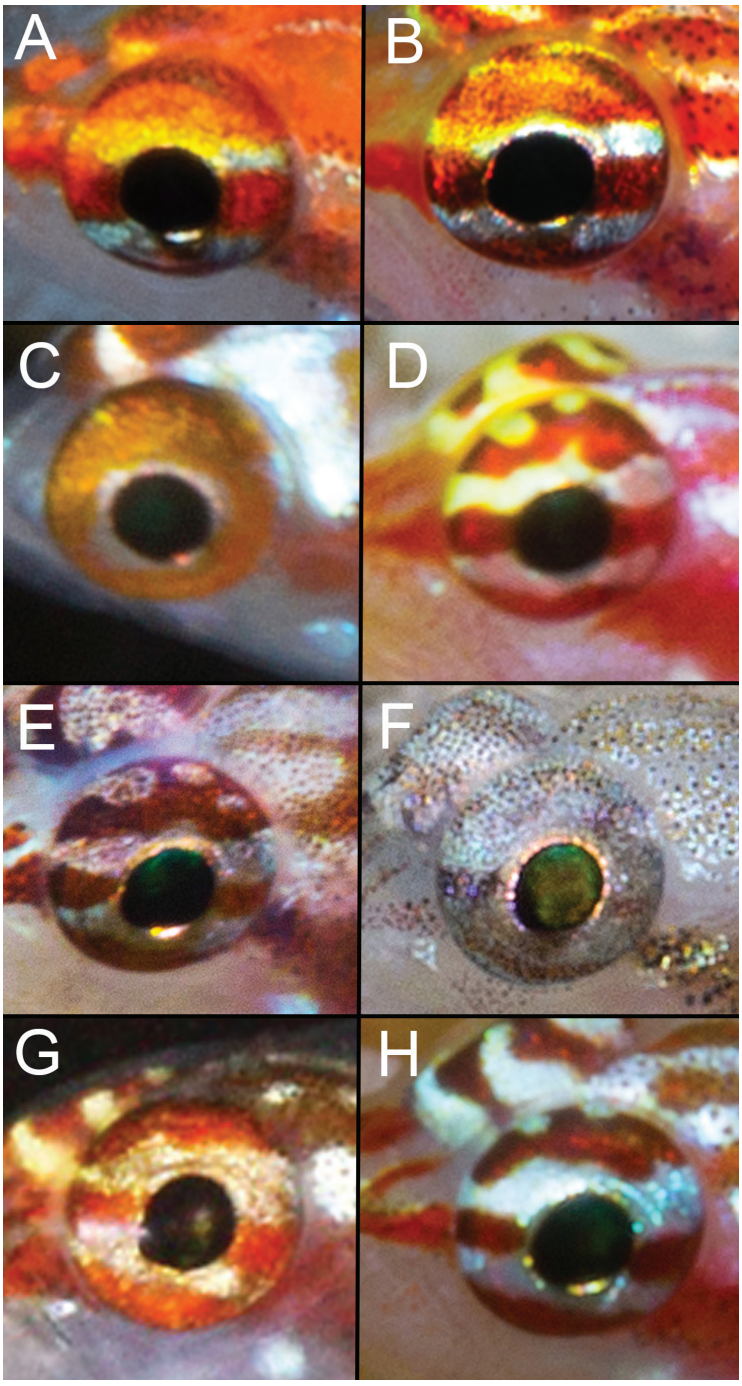

Figure 16. Eye coloration of the *Eviota zebrina* complex species **A** *E. tetha*, Kwatisore, West Papua; **B** *gunawanae*, Karas, West Papua **C** *E. cometa*, Lau Archipelago, Fiji **D** *E. oculineata*, Milne Bay, Papua New Guinea **E** *E. longirostris*, Fakfak, West Papua **F** *E. pseudozebrina*, Lau Archipelago, Fiji **G** *E. mareru-brum*, Israel, Red Sea **H** *E. zebrina*, Laamu Atoll, Maldives (photograph **G** R. Holzman, with permission).

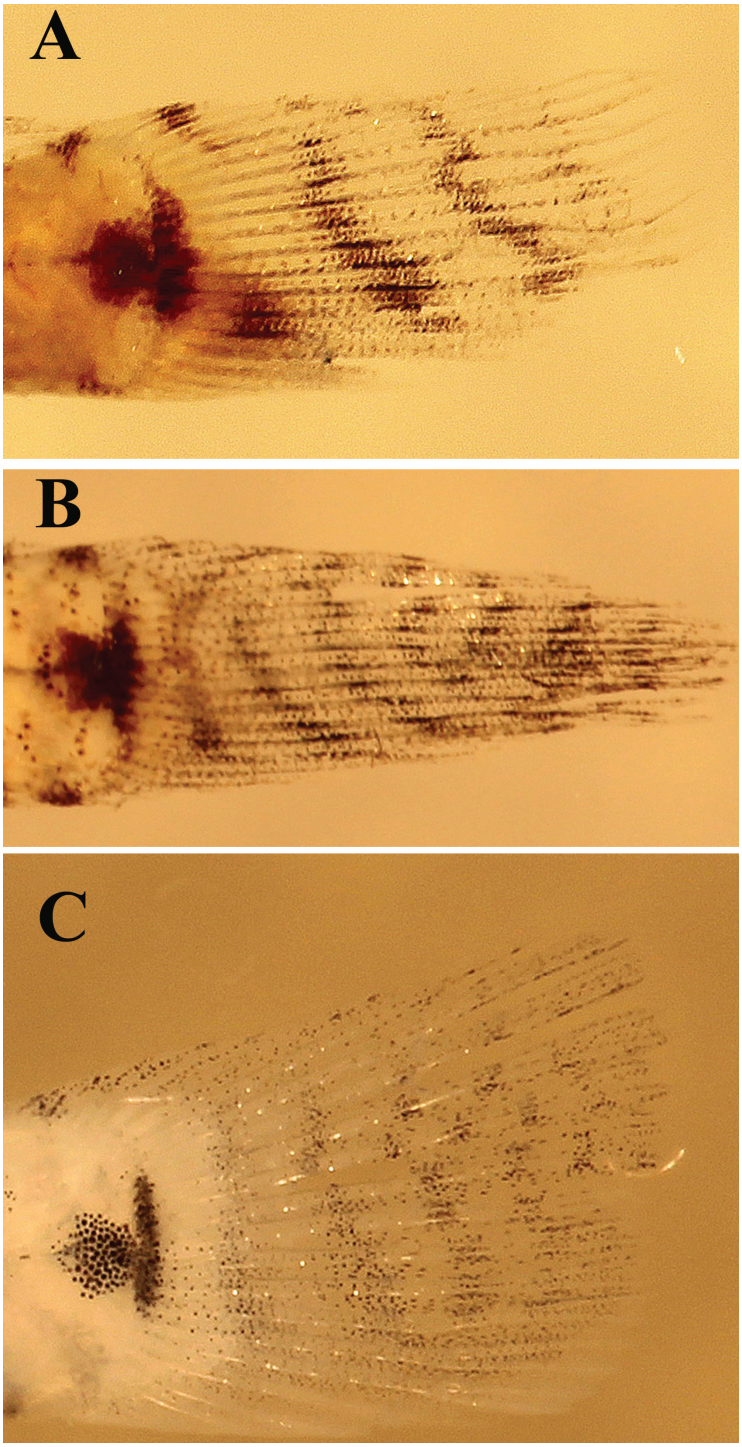

Figure 17. Comparison of caudal fin pigmentation in preserved specimens **A** *Eviota zebrina* paratype, CAS 040599 **B** *E. pseudozebrina* holotype, CAS 228614 **C** *E. longirostris*, paratype, CAS 246538.

Eviota tetha (Figure 16A) and *E. gunawanae* (Figure 16B) both have a yellow bar crossing the eye above the pupil, a solid unbroken bar above that, a narrow white bar crossing below the pupil and a solid bar below that. *Eviota tetha* differs from *E. gunawanae* by having the bars red-orange, whereas they are darker, almost brown in *E. gunawanae*.

The remaining four species have a light bar crossing above and below the pupil, but from a lateral view only *E. marerubrum* (Figure 16G) has a solid red bar across the top of the eye, whereas the others have the upper bar broken by irregular light areas. The light bar above the pupil in *Eviota oculineata* (Figure 16D) is yellow, unlike the other two species where the bar is white. *Eviota longirostris* (Figure 16E) and *E. zebrina* (Figure 16) are similar but the bars in *E. zebrina* are bright red whereas they are a dark reddish color in *E. longirostris*.

Caudal fin markings (Figure 17). Several species have oblique dark bars crossing the caudal fin that are obvious in freshly dead or preserved specimens, but are faint or absent in underwater photographs of live fishes. *Eviota zebrina* from the Seychelles Islands has three or four distinctive oblique black bars crossing the caudal fin. There also is a dark mark extending out from the caudal spot over the hypural plate onto the lower portion of the fin. *Eviota pseudozebrina* has 7 black bars crossing the caudal fin and no dark spot at the lower part of the fin. *Eviota longirostris* has six or seven black bars crossing the caudal fin and no dark spot at the lower part of fin. *Eviota marerubrum* has four black bars crossing the fin with the lower portion of the bars enlarged forming spots. *Eviota cometa* has four or five red bars crossing the fin when fresh, but these are lost in preservative. *Eviota oculineata*, *E. tetha*, and *E. gunawanae* lack black bars on the caudal fin.

Morphological characters. *Eviota tetha* and *E. gunawanae* are similar in morphology and both can be distinguished from the rest of the complex in lacking NA pores and in having the AITO pore enlarged and opening anteriorly, versus having a small AITO pore that opens dorsally. The remaining species in the complex have all pores present except the IT pore. The six species within the complex that lack only IT pores can be distinguished primarily on the basis of dorsal/anal-fin formula and coloration. Both *E. oculineata* and *E. marerubrum* have 8/7 dorsal-anal-fin formulas (as do *E. tetha* and *E. gunawanae*) and usually have fewer pectoral-fin rays (modally 14 or 15) whereas *E. cometa*, *E. longirostris*, *E. pseudozebrina*, and *E. zebrina* have 9/8 dorsal/anal-fin formulas and modally 15 (*E. pseudozebrina*) or 16 pectoral-fin rays (*E. cometa*, *E. zebrina*, *E. longirostris*). The species in the complex with 9/8 dorsal/anal-fin formulas vary interspecifically in some morphometric features. Specifically, snout length and body depth may be useful for distinguishing between *E. cometa*, *E. longirostris*, *E. pseudozebrina*, and *E. zebrina* (Figure 18).

Key to the species of the *Eviota zebrina* complex

Locations in parentheses only include type localities and other locations where we are confident in their occurrence based on a combination of live photographs, genetics, and specimens examined morphologically.

1 NA pores absent; AITO pore large, opening anteriorly; dorsal/anal-fin formula 8/7 ..... **2**

– NA pores present; AITO pore small, opening dorsally; dorsal/anal-fin formula 8/7 or 9/8 ..... **3**

2 Pectoral-fin rays 16; 5th pelvic-fin ray ~10% of 4th; dark spot at the base of the caudal fin is larger and extends anteriorly as a partially overlapping paired spots ..... ***Eviota gunawanae*** **(West Papua)**

– Pectoral-fin rays 14 or 15; 5th pelvic-fin ray rudimentary or absent; dark spot at the base of the caudal fin is restricted to the posterior end of the hypural plate..... ***Eviota tetha*** **(West Papua)**

3 Dorsal/anal-fin formula 8/7 ..... **4**

– Dorsal/anal-fin formula 9/8 ..... **5**

4 Eye with two horizontal white stripes; body depth 20–25% SL .... ***Eviota marerubrum*** **sp. nov. (Red Sea)**

– Eye with two horizontal stripes, the upper yellow, the lower white, with yellow mottling along dorsal surface of eye; body depth 27–31% SL ....***Eviota oculineata*** **sp. nov. (New Guinea, Solomon Islands, Fiji, Australia)**

5 Body markings predominantly red or reddish brown **6**

– Body markings predominantly dark brown to black..... **7**

6 Eye without prominent horizontal stripes, only a narrow gold rim around pupil over red iris; caudal fin crossed by several red vertical bars when fresh that are lost in preservation ..... ***E. cometa*** **(Fiji, Tonga)**

– Eye with pair of horizontal stripes; caudal fin crossed by several black vertical bars that are usually retained in preservation .... ***Eviota zebrina*** **(Maldives, Seychelles)**

7 Body deep 22–26, 23% SL; anterior part of dark spot at caudal-fin base a distinct rectangular shape in advance of dark line over hypural plate; upper half of eye gray, heavily peppered with melanophores..... ..... ***Eviota pseudozebrina*** **sp. nov. (Fiji)**

– Body more slender, depth 17–20, 19% SL; anterior part of dark spot at caudal-fin base triangular with one point against posterior dark line; upper half of eye with irregular reddish areas with white areas peppered with melanophores..... ***Eviota longirostris*** **sp. nov. (New Guinea)**

Discussion

The combination of molecular data, live coloration, and re-examination of preserved specimens including type series have shown that the *Eviota zebrina* complex contains at least eight species. The integrative approach taken here was first used in this complex to recognize *E. gunawanae* as being distinct from *E. tetha* (Greenfield et al. 2019), and here we expanded our taxonomic scope within the complex to recognize *E. longirostris*, *E. marerubrum*, *E. oculineata*, and *E. pseudozebrina* as being distinct from *E. zebrina*

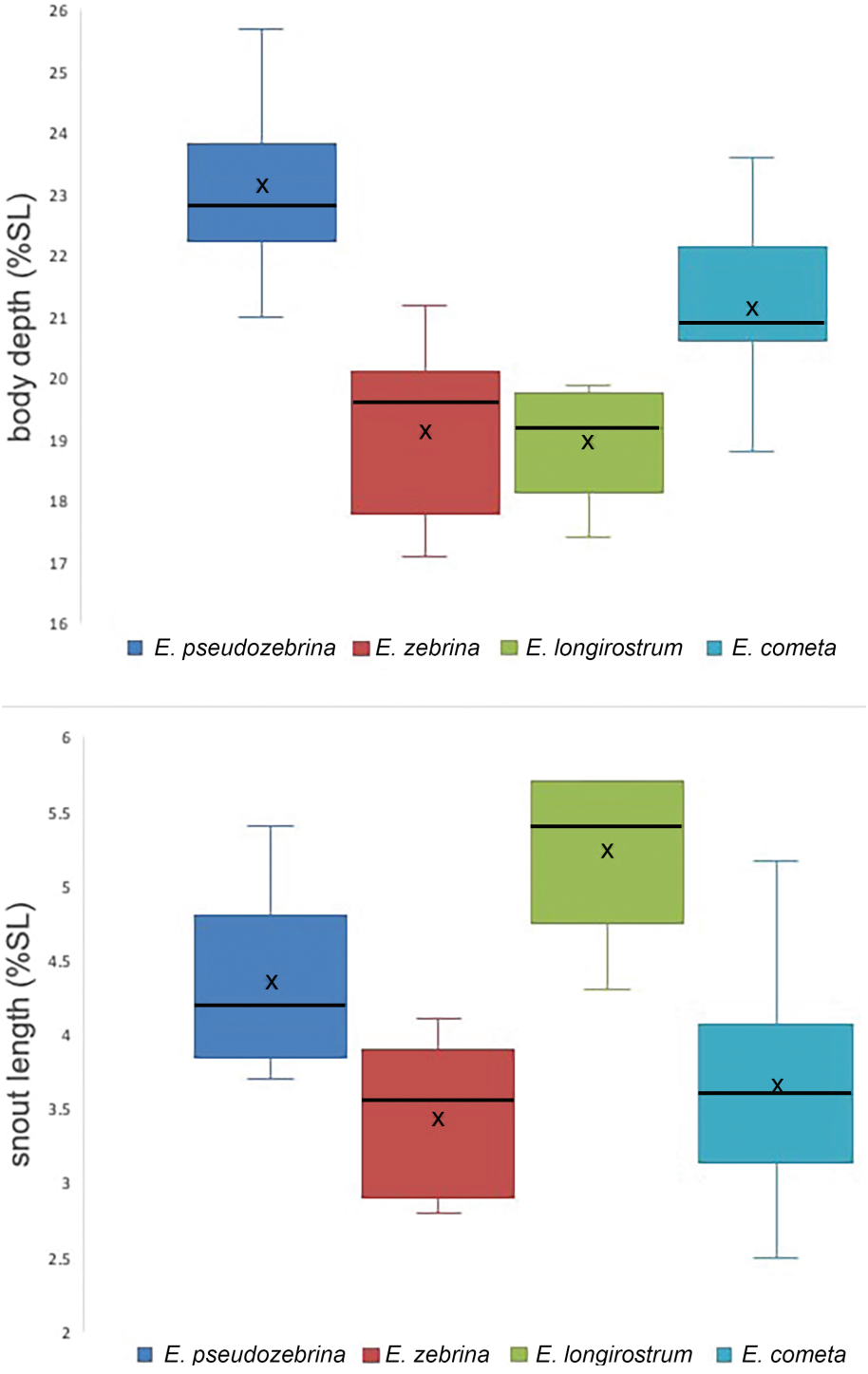

Figure 18. Morphometric ranges for body depth (top) and snout length (bottom) for the species of the *Eviota zebrina* complex with 9/8 dorsal-anal-fin formulas. X's are means, bars through boxes are medians.

Figure 19. Distribution map of *E. marerubrum*, *E. oculineata*, *E. zebrina*, and *E. cometa*. Points represent localities of specimens examined in this study or verified photographs.

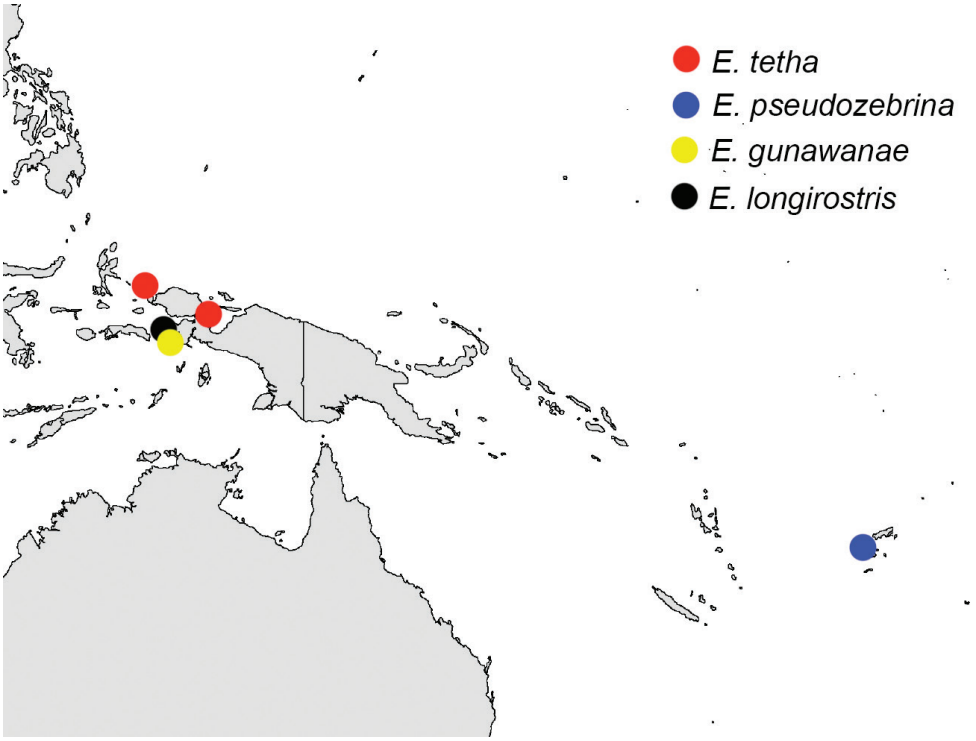

Figure 20. Distribution map of *E. tetha*, *E. pseudozebrina*, *E. gunawanae*, and *E. longirostris*. Points represent localities of specimens examined in this study or verified photographs.

and *E. cometa*, two species that they were previously confused when molecular data and color images of live specimens were unavailable.

We were unable to examine preserved specimens from throughout the range of the *E. zebrina* complex, nor would this be particularly informative given the importance

of live coloration as a taxonomic character. We have also not photographed specimens or taken genetic samples throughout the *E. zebrina* complex range, so exact boundaries of species ranges given here are considered preliminary. Nevertheless, some preliminary biogeographic patterns can be observed, ranging from species pairs/groups that are predominantly allopatric to those that have ranges that overlap significantly. *Eviota zebrina* and *E. marerubrum* appear to be restricted to the Indian Ocean and Red Sea respectively, and form a clade with *E. oculineata*, which occurs from Australia and New Guinea east to Fiji, and *E. cometa* which is currently known from Fiji and Tonga (Figures 2, 19). Another large clade within this complex contains species entirely from the Central and Western Pacific (Figures 2, 20), including *E. tetha*, *E. gunawanae*, and *E. longirostris*, all from West Papua, and *E. pseudozebrina*, which is currently known only from Fiji. Interestingly, Fiji and West Papua are each home to at least three species in this complex, and are also the regions where the authors have the most live photos coupled with tissue samples. A search of museum records from 71 collections using Fishnet2 (accessed through the Fishnet2 Portal, www.fishnet2.org, 2020-11-12) showed that specimens identified as *E. cometa* or *E. zebrina* exist from many other localities including the Philippines, Australia, Thailand, China, Vietnam, Vanuatu, New Caledonia, Pohnpei, Japan, Kiribati, Palau, the Marshall Islands, Sri Lanka, and Mauritius. It is likely that increased sampling efforts in these areas will uncover additional undescribed species within this complex (and other complexes within *Eviota*) or expand the known ranges of existing species, and reveal a more complete picture of the patterns of diversification and evolution within dwarfgobies.

Acknowledgements

Authors would like to thank R.C. Langston, K.R. Longenecker, K. Tang, and Captain B. Vasconcellos and the crew of the *Moku Mokua Hine* for assistance in the field. We are grateful to the late J. Seeto, G.R. South, and R.W. Tuxton of the University of the South Pacific, Fiji for facilitating our collecting in Fiji, and a special thanks to R.R. Thaman, also of U.S.P., for his unending assistance; without his help this project literally would not have been possible. MVE would like to thank the Fiji Department of Fisheries and Conservation International Fiji for hosting the 2017 Lau biodiversity survey that enabled us to obtain tissue samples and live color photographs of *E. cometa*, *E. oculineata* and *E. pseudozebrina*, and is particularly thankful to Roko Sau Joesefa Cinavilakeba, Susana Waqainabete-Tuisese and Semisi Meo, as well as the Captain and crew of the MV *Sea Rakino* for their excellent support during the 2017 survey, and to the Fijian Government and Lau Province village chiefs for permission to collect fishes. MVE also thanks G. Allen for his companionship during the numerous field surveys during which many of the new species were collected, and the owners, captains, and crews of the following vessels that supported collections: the MV *Putiraja*, the MV *Silolona*, the MY *Rascal*, S.Y. *Wyuna*, and the MV *Chertan*. We thank D. Catania, J. Fong, M. Hoang and L. Rocha of CAS, D. Pitassy and J. Williams of USNM, and K.

Maslenikov of UW for assistance with specimens. J. DiBattista and colleagues kindly provided samples from Saudi Arabia. E. McFarland assisted with molecular work. We thank M. Gómez-Buckley, R. Buckley, K. Stone, T. Halafihi, the Vava'u Environmental Protection Association, and the Kingdom of Tonga Ministry of Fisheries for their support of fieldwork in Tonga. Finally, we thank M. Gómez-Buckley, E. Troyer, J. Eyre, R. Whitworth, R. Holzman, J. Herler, J. Greenfield, R. Winterbottom, and S. Raredon for photographs or radiographs. This research was supported by National Science Foundation grants INT97-29666 and DEB0-1027545, and Sea Grant Project R/FM-6PD, as well as grants to Conservation International by W.M. Brooks, the Paine Family Trust, the Henry Foundation, and D. Arnall.

References

Akihito, Sakamoto K, Iwata A, Ikeda Y (1993) Cephalic sensory organs of the gobioid fishes. In: Nakabo T (Ed.) Fishes of Japan with pictorial keys to the species. Tokai University Press, Tokyo, 1088–1116. [1474 pp.] [In Japanese]

Akihito, Sakamoto K, Ikeda Y, Sugiyama K (2002) Gobioidei. In: Nakabo T (Ed.) Fishes of Japan with pictorial keys to the species. English edition. Vol. II, Tokai University Press, Tokyo, 1139–1310: 1596–1619.

Allen GE, Erdmann MV (2012) Fishes of the East Indies. Vols I–III, Tropical Reef Research, Perth, 1292 pp.

Atta CJ, Coker DJ, Sinclair-Taylor TH, DiBattista JD, Kattan A, Monroe AA, Berumen ML (2019) Conspicuous and cryptic reef fishes from a unique and economically important region in the northern Red Sea. PLoS ONE 14(10): e0223365. https://doi.org/10.1371/journal.pone.0223365

Fishnet2 (2020) Fishnet2. www.fishnet2.org [accessed 2020-11-12]

Golani D, Bogorodsky SV (2010) The Fishes of the Red Sea – reappraisal and updated checklist. https://doi.org/10.11646/zootaxa.2463.1.1

Greenfield DW (2021) Addendum to the 2016 key to the dwarfgobies (Teleostei: Gobiidae: *Eviota*). Journal of the Ocean Science Foundation 38: 1–12. https://doi.org/10.5281/zenodo.4458248

Greenfield DW (2017) An overview of the dwarfgobies, the second most speciose coral-reef fish genus (Teleostei: Gobiidae: *Eviota*). Journal of the Ocean Science Foundation 29: 32–54. https://doi.org/10.5281/zenodo.1115683

Greenfield DW, Erdmann MV (2021) *Eviota flaviarma*, a new dwarfgoby from Papua New Guinea (Teleostei: Gobiidae). Journal of the Ocean Science Foundation 38: 27–34. https://doi.org/10.5281/zenodo.5090376

Greenfield DW, Tornabene L (2014) *Eviota brahmi* sp. nov. from Papua New Guinea, with a redescription of *Eviota nigriventris* (Teleostei: Gobiidae). Zootaxa 3793: 13–146. https://doi.org/10.11646/zootaxa.3793.1.6

Greenfield DW, Randall JE (2016) A review of the dwarfgobies of Fiji, including descriptions of five new species (Teleostei: Gobiidae: *Eviota*). Journal of the Ocean Science Foundation 20: 25–75. https://doi.org/10.5281/zenodo.48268

Greenfield DW, Tornabene L, Erdmann MV, Pada DN (2019) *Eviota gunawanae*, a new dwarfgoby from Fakfak, West Papua (Teleostei: Gobiidae). Journal of the Ocean Science Foundation 32: 57–67. https://doi.org/10.5281/zenodo.2616753

Herler J (2007) Microhabitats and ecomorphology of coral- and coral rock-associated gobiid fish (Teleostei: Gobiidae) in the northern Red Sea. Marine Ecology 28: 82–94. https://doi.org/10.1111/j.1439-0485.2007.00165.x

Herler J, Hilgers H (2005) A synopsis of coral and coral-rock associated gobies (Pisces: Gobiidae) from the Gulf of Aqaba, northern Red Sea. Aqua, Journal of ichthyology and aquatic biology 10: 103–132. https://aqua-aquapress.com/?p=13644

Jewett SL, Lachner EA (1983) Seven new species of the Indo-Pacific genus *Eviota* (Pisces: Gobiidae). Proceedings of the Biological Society of Washington 96(4): 780–806.

Lachner EA, Karnella JS (1978) Fishes of the genus *Eviota* of the Red Sea with descriptions of three new species (Teleostei: Gobiidae). Smithsonian Contributions to Zoology 286: 1–23.

Lachner EA, Karnella JS (1980) Fishes of the Indo-Pacific genus *Eviota* with descriptions of eight new species (Teleostei: Gobiidae). Smithsonian Contributions to Zoology 315: 1–127.

Lanfear R, Frandsen PB, Wright AM, Senfeld T, Calcott B (2016) PartitionFinder 2: new methods for selecting partitioned models of evolution for molecular and morphological phylogenetic analyses. Molecular Biology and Evolution 34(3): 772–773. https://doi.org/10.1093/molbev/msw260

Meadows MG, Anthes N, Dangelmayer S, Alwany MA, Gerlach, T, Schulte G, Sprenger D, Theobald J, Michiels NK (2014) Red fluorescence increases with depth in reef fishes, supporting a visual function, not UV protection. Proceedings of the Royal Society B 281: e20141211. https://doi.org/10.1098/rspb.2014.1211

Nakabo T [Ed.] (2002) Fishes of Japan with pictorial key to the species, English edition II. Tokai University Press, Japan, 1749 pp.

Randall JE (2005) Reef and shore fishes of the South Pacific, New Caledonia to Tahiti and the Pitcairn Islands. University of Hawai'i Press, Honolulu, 707 pp.

Ronquist F, Teslenko M, van der Mark P, Ayres DL, Darling A, Hohna S, Larget B, Liu L, Suchard MA, Huelsenbeck JP (2012) MrBayes 3.2: Efficient Bayesian Phylogenetic Inference and Model Choice Across a Large Model Space. Systematic Biology 61(3): 539–542. https://doi.org/10.1093/sysbio/sys029

Saruwatari T, JA Lopez, Pietsch TW (1997) Cyanine blue: a versatile and harmless stain for specimen observations. Copeia 1997(4): 840–841. https://doi.org/10.2307/1447302

Suzuki T, Shibukawa K, Yano K, Senou H (2004). A photographic guide to the gobioid fishes of Japan. Heibosha Co., Japan, 536 pp.

Thacker CE (2003) Molecular phylogeny of the gobioid fishes (Teleostei: Perciformes: Gobioidei). Molecular Phylogenetics and Evolution 26: 354–368. https://doi.org/10.1016/S1055-7903(02)00361-5

Tornabene L, Ahmadia GN, Berumen ML, Smith DJ, Jompa J, Pezold F (2013) Evolution of microhabitat association and morphology in a diverse group of cryptobenthic coral reef

fishes (Teleostei: Gobiidae: *Eviota*). Molecular Phylogenetics and Evolution 66: 391–400. https://doi.org/10.1016/j.ympev.2012.10.014

Tornabene, L, Valdez S, Erdmann MV, Pezold F (2015) Support for a 'Center of Origin' in the Coral Triangle: cryptic diversity, recent speciation, and local endemism in a diverse lineage of reef fishes (Gobiidae: *Eviota*). Molecular Phylogenetics and Evolution 82: 200–210. https://doi.org/10.1016/j.ympev.2014.09.012

Tornabene L, Valdez S, Erdmann MV, Pezold F (2016) Multi-locus sequence data reveal a new species of coral reef goby (Teleostei: Gobiidae: *Eviota*), and evidence of Pliocene vicariance across the Coral Triangle. Journal of Fish Biology 88: 1811–1834. https://doi.org/10.1111/jfb.12947

Troyer EM, Coker DJ, Berumen ML (2018) Comparison of cryptobenthic reef fish communities among microhabitats in the Red Sea. PeerJ 6: e5014. https://doi.org/10.7717/peerj.5014

Ward RD, Zemlak TS, Innes BH, Last PR, Hebert PDN (2005) DNA barcoding Australia's fish species. Philosophical Transactions of the Royal Society, series B 360: 1847–1857. https://doi.org/10.1098/rstb.2005.1716

Yamada T, Sugiyama T, Tamaki N, Kawakita A, Kato M (2009) Adaptive radiation of gobies in the interstitial habitats of gravel beaches accompanied by body elongation and excessive vertebral segmentation. BMC Evolutionary Biology 9: e145. https://doi.org/10.1186/1471-2148-9-145

ZooKeys 1057: 185–208 (2021)
doi: 10.3897/zookeys.1057.67621
https://zookeys.pensoft.net

RESEARCH ARTICLE

A peer-reviewed open-access journal
ZooKeys
Launched to accelerate biodiversity research

A new species of *Leucostethus* (Anura, Dendrobatidae) from Gorgona Island, Colombia

Taran Grant[1], Wilmar Bolívar-García[2]

1 *Department of Zoology, Institute of Biosciences, University of São Paulo, 05508-090, São Paulo, SP, Brazil*
2 *Grupo de Investigación en Ecología Animal, Departamento de Biología, Universidad del Valle, Calle 13 No. 100-00. Cali, Colombia. A.A. 25360, Cali, Colombia*

Corresponding author: Taran Grant (taran.grant@ib.usp.br)

Academic editor: Uri García-Vázquez | Received 23 April 2021 | Accepted 20 July 2021 | Published 27 August 2021

http://zoobank.org/5370E65C-5D76-4C37-B07F-7ED3ED1A2425

Citation: Grant T, Bolívar-García W (2021) A new species of *Leucostethus* (Anura, Dendrobatidae) from Gorgona Island, Colombia. ZooKeys 1057: 185–208. https://doi.org/10.3897/zookeys.1057.67621

Abstract

We describe a new species of *Leucostethus* from Gorgona Island, a small (13 km^2) island located 35 km from the Pacific coast of southern Colombia. The new species most resembles *L. argyrogaster* and *L. fugax* from western Amazonia at 340–870 m elev. in Peru and Ecuador, with which it shares pale ventral coloration and orange suffusion of the axilla, groin and concealed surfaces of the hind limb, but it is most closely related to *L. bilsa* from ca. 340 km SW in the southern Chocó at 420–515 m elev., northwestern Ecuador. We report miniscule white spots on the posteroventral surface of the thighs of the new species and, on the basis of our preliminary assessment of their taxonomic distribution, hypothesize that their presence is a synapomorphy of Dendrobatoidea with subsequent losses in a few groups. Given the apparent restriction of the new species to Gorgona Island, it is Vulnerable according to IUCN Red List criteria. In addition to naming the new species, we also propose the following new combinations: *L. alacris* (Rivero and Granados-Díaz, 1990) **comb. nov.**, *L. dysprosium* (Rivero and Serna, 2000) **comb. nov.**, and *L. yaguara* (Rivero and Serna, 1991) **comb. nov.**

Keywords

Amphibia, Chocó, Colostethinae, *Colostethus*, Dendrobatoidea, *Silverstoneia*, taxonomy

Introduction

Gorgona Island, located approximately 35 km from the Pacific coast of southern Colombia (Giraldo 2012), is a fragment of the Caribbean Large Igneous Province that formed in the Late Cretaceous and accreted to South America in the Eocene (Serrano et al. 2011). Although Gorgona is currently an island, the depths between it and the mainland are only ca. 60–120 m, so contiguous terrestrial habitat undoubtedly connected Gorgona and the mainland during the last glacial maximum (20–18 ka) and for a considerable time afterward (Fleming et al. 1998; Montealegre-Z et al. 2010). Indeed, Gorgona's coral reef is estimated to date to only 2–3 ka (Glynn et al. 1982), placing a lower bound on Gorgona's complete isolation from the mainland. Given its size (ca. 13 km^2; Giraldo 2012), proximity to the mainland, and recent isolation, it is unsurprising that Gorgona's biota is predominated by species that are widespread in the Chocó (Giraldo and Valencia 2012). Nevertheless, several putative endemics have been discovered on Gorgona, including species of Chelicerata (Lourenço and Flores 1989), Formicidae (Fernández and Guerrero 2008), Orthoptera (Montealegre-Z and Postiles 2010; Montealegre-Z et al. 2011; Baena-Bejarano and Heads 2015), and Psocodea (García Aldrete et al. 2011; Sarria-S et al. 2014; Manchola et al. 2014), although it is not uncommon for subsequent research to uncover species named from Gorgona on the mainland (e.g. Mendivil Nieto et al. 2017). Among vertebrates, the putative endemics include the catfish *Trichomycterus gorgona* Fernández & Schaefer, 2005, the anoles *Anolis gorgonae* Barbour, 1909 and *A. medemi* Ayala & Williams, 1988 (Phillips et al. 2019), the snake *Atractus medusa* Passos et al., 2009, and an undescribed species of dendrobatid frog reported as "*Colostethus* sp. Gorgona" by Grant et al. (2017). The objective of the present paper is to formally name and describe this new species.

Materials and methods

We conducted fieldwork on Gorgona Island (02°58'N, 78°10'W) from 23 to 28 May 2016. See Giraldo (2012) for a general description of the island and Vásquez-Vélez (2014) for a description of the vegetation. We euthanized specimens using 20% benzocaine (Orajel; Church & Dwight Co., Inc., Ewing, New Jersey, USA) applied to the skin or by pithing (McDiarmid 1994). Following preservation of one hind limb in 96–100% ethanol for DNA analysis and/or preservation of the skin in 100% methanol, specimens were fixed in formalin and subsequently transferred to 70% ethanol and deposited in the amphibian collection of the Colección de Prácticas Zoológicas, Universidad del Valle, Cali, Colombia (CPZ-UV). We also include in the type series one specimen from the National Museum of Natural History, Smithsonian Institution, Washington DC, USA (**USNM**).

We captured advertisement calls using a Tascam DR-40 linear pulse-code modulation (PCM) recorder and internal microphone at a sampling rate of 44.1 kHz with 16 bit encoding at 26.2°C ambient temperature. We also captured audio and video of the holotype vocalizing using a Canon EOS Rebel T3 and internal microphone and analyzed the audio (linear PCM recorder, 48 kHz sampling rate, 16 bit encoding). The calling males were observed directly and recorded at ca. 1 m distance. Acoustic analyses employed standard definitions and terminology for spectral and temporal variables (Köhler et al. 2017). We used Raven Pro 1.6 sound analysis software (Cornell Laboratory of Ornithology, NY) to score call duration (s), notes per call, note duration (ms), internote interval (ms), note repetition rate (notes/minute), number of pulses, fundamental and dominant frequencies (kHz), frequency modulation both within and among notes (kHz), and number and frequency of harmonics (kHz). We scored spectral parameters from spectrograms and power spectra (Hann window, 90% overlap, 512 point Fast Fourier Transformation resolution) and temporal parameters from expanded waveforms. The first 10–15 notes of each call were variable and differed from subsequent notes, all of which were emitted at higher amplitudes and varied little temporally and spectrally (i.e. they did not taper off toward the end of the call), so we report values for both entire calls and the first 10 and last 20 notes; as the latter values are most representative of the advertisement call, we used them for interspecific comparisons. We report statistical summaries as $\bar{x} \pm$ SE.

Given that individual units of sound were consistently (i.e. both in the recorded calls and the many calls that were heard, but not recorded) emitted in bouts of < 30 s duration, we classified the individual units of sound as notes grouped into calls. This treatment is consistent with the interpretation by Vigle et al. (2020) of *Leucostethus bilsa* Vigle et al. 2020, which emitted units of sound in bouts of < 60 s. In contrast, other species of trans-Andean *Leucostethus* emit sounds at regular intervals in bouts varying from less than one minute to several minutes in duration, forming continuous series of variable length (a few to more than 300; Grant and Castro 1998); as such, in those species, Grant and Castro (1998) and Marin et al. (2018) considered calls to comprise a single note. For comparison, we treat the values reported by Grant and Castro (1998) and Marin et al. (2018) for "calls" as equivalent to the values reported by Vigle et al. (2020) and us as "notes."

Information on phylogenetic relationships was taken from Grant et al. (2017), Marin et al. (2018), and Vigle et al. (2020). Although Grant et al. (2017) included the undescribed species from Gorgona Island in their *Colostethus fraterdanieli* group, Marin et al. (2018) subsequently transferred that group to *Leucostethus*, and we follow their taxonomy here. Character definitions follow Grant et al. (2006, 2017). For hand morphology, we follow Fabrezi and Alberch (1996) in considering finger I of other tetrapods to be absent in Anura and number fingers accordingly. As such, we follow Grant et al. (2017) in referring to the swollen third finger of earlier literature (e.g. Grant et al. 2006) as swollen finger IV. The webbing formulation is that of Savage and Heyer (1967), whereby webbing is quantified by the number and proportion of free phalanges (see also Myers and Duellman 1982; Savage and Heyer 1997). Jaw muscle

terminology follows Haas (2001). We took the following measurements with digital calipers to 0.1 mm:

SVL snout–vent length
FAL forearm length from proximal edge of palmar tubercle to outer edge of flexed elbow
HL hand length from proximal edge of palmar tubercle to tip of finger IV
TL tibia length from outer edges of flexed knee to heel
FL foot length from proximal edge of outer metatarsal tubercle to tip of toe IV
HW head width between angle of jaws
HL head length diagonally from corner of mouth to tip of snout
EL eye length from posterior to anterior corner
END eye-naris distance from anterior corner of eye to center of naris
IND internarial distance between centers of nares
SL snout length from anterior corner of eye to tip of snout
IOD interorbital distance
TD tympanum diameter

Unless otherwise noted, measurements and proportions are given only for adults and are summarized as $\bar{x} \pm$ SE. Males with vocal slits on both sides of the mouth were scored as adults, those with only one vocal slit as sub-adults, and those lacking slits on both sides as juveniles. Females with expanded, convoluted oviducts and enlarged oocytes were considered to be adults, those with only weakly expanded, non- or weakly convoluted oviducts and poorly differentiated oocytes to be sub-adults, and those with small, undifferentiated oocytes and unexpanded, straight oviducts to be juveniles. Color in life is based on field notes and digital photographs.

We compare the new species to other species of *Leucostethus* sensu Marin et al. (2018) [viz. *L. argyrogaster* (Morales & Schulte, 1993); *L. bilsa*, *L. brachistriatus* (Rivero & Serna, 1986), *L. fraterdanieli* (Silverstone, 1971), *L. fugax* (Morales & Schulte, 1993), *L. jota* Marin et al., 2018, and *L. ramirezi* (Rivero & Serna, "1995" 2000)], to which we add *L. alacris* (Rivero & Granados-Díaz, 1990) comb. nov., *L. dysprosium* (Rivero & Serna, "1995" 2000) comb. nov., and *L. yaguara* (Rivero & Serna, 1991) comb. nov. Although the precise phylogenetic relationships of these three species have not yet been tested in quantitative phylogenetic analyses, Grant and Castro (1998) noted the resemblance of *L. alacris* and *L. yaguara* to *L. fraterdanieli* and Grant et al. (2017) considered the possibility that their Cordillera Occidental clade of *L. fraterdanieli* might correspond to one or both of those names. Similarly, *L. dysprosium* shares a complete, continuous, pale oblique lateral stripe with other species of *Leucostethus* (see Discussion) and appears to differ from other trans-Andean species of *Leucostethus* except *L. alacris* only in possessing more extensive toe webbing (see Rivero and Serna "1995" 2000: 49, fig. 2C). We also compare the new species to similar colostethines from the Chocó.

Results

***Leucostethus siapida* Grant & Bolívar-García, sp. nov.**
http://zoobank.org/757C0F3D-D62C-40E2-8F77-195C9234842D
Figs 1–9, Tables 1–3

Colostethus sp. Gorgona: Grant et al. (2017)
Leucostethus sp. Gorgona: Marin et al. (2018), Vigle et al. (2020)

Type material. ***Holotype*.** CPZ-UV 7293 (field number WB 3045), an adult male collected by Taran Grant immediately west of the housing complex at El Poblado, Gorgona Island, Parque Nacional Natural Gorgona, Guapi, Cauca Department, Colombia, 02°58'00.6"N, 78°10'27.4"W, ca. 30 m elevation, 26 May 2016.

***Paratypes*.** CPZ-UV 5013–5014, CPZ-UV 7294–7297, collected at the type locality by Wilmar Bolívar-García, Taran Grant, David Andrés Velásquez-Trujillo, and Andrés Felipe Gómez Fernández, 26–27 May 2016. USNM 313893, collected by Humberto Granados Diaz, Gorgona Island, 1987.

Diagnosis. A moderate-sized *Leucostethus* (maximum SVL: males 23.0 mm, females 25.8 mm) with complete pale oblique and ventrolateral stripes, dorsolateral stripe absent, finger IV of adult males very weakly swollen (barely discernible), throat of adult males bearing, at most, faintly stippled spotting or reticulation on throat, pale paracloacal spots present, axilla, groin, and concealed surfaces of hind limb suffused with orange, and toes II–IV with basal webbing.

Comparisons. *Leucostethus siapida* sp. nov. differs from all congeners except the cis-Andean species *L. argyrogaster* and *L. fugax* in possessing orange axilla, groin, and concealed surfaces of hind limb (yellow in other species) and lacking conspicuous dark coloration on the throat of adult males (present in other species); it differs from both species in being larger (maximum SVL: *L. siapida* males 23.0 mm, females SVL 25.8 mm; *L. argyrogaster* males 19.8 mm, females 21.1 mm; *L. fugax* males 19.5 mm, females 20.1) and further differs from *L. fugax* in lacking conspicuous swelling of finger IV in adult males (strongly swollen in *L. fugax*).

Among the trans-Andean species of *Leucostethus*, *L. siapida* sp. nov. differs from all except *L. bilsa* (apparently unswollen) and *L. alacris* (unknown) in lacking conspicuous swelling of finger IV in adult (conspicuously swollen in *L. brachistriatus*, *L. dysprosium*, *L. fraterdanieli*, *L. fugax*, *L. jota*, *L. rodriguezi*, and *L. yaguara*). It differs from *L. bilsa* in the coloration of the axilla, groin, and concealed surfaces of the hind limb (orange in *L. siapida* sp. nov., "mustard-yellow" in *L. bilsa*; Vigle et al. 2020), definition and shape of the bright coloration of the axilla (suffused in *L. siapida*, discrete, forming well-defined crescent around dorsal, posterior, and ventral circumference of arm in *L. bilsa*), male throat coloration (at most faintly stippled spotting or reticulation on throat in *L. siapida* sp. nov.; more darkly spotted in *L. bilsa*), and female SVL (23.5–25.8 mm in *L. siapida*, 27.4–28.2 mm in *L. bilsa*; Vigle et al. 2020), as well as 6.25% of sites in

Table 1. Measurements in mm (minimum-maximum, $\bar{x} \pm$ SE) of the type series of *Leucostethus siapida* sp. nov. See text for measurement definitions.

	Males (n = 5)	Females (n = 3)
Snout-vent length	19.9–23.0, 22.1 ± 0.56	23.5–25.8, 24.6 ± 0.67
Forearm length	4.4–5.2, 5.0 ± 0.15	4.8–5.6, 5.2 ± 0.23
Hand length	4.7–5.5, 5.3 ± 0.15	5.5–5.8, 5.6 ± 0.09
Shank length	9.0–10.2, 9.9 ± 0.24	9.1–10.8, 10.1 ± 0.51
Foot length	8.1–9.5, 8.9 ± 0.24	8.4–9.8, 9.2 ± 0.41
Head width	7.1–7.8, 7.6 ± 0.13	7.5–8.7, 8.1 ± 0.35
Head length	6.5–7.5, 7.0 ± 0.19	7.0–8.4, 7.8 ± 0.41
Eye length	2.6–3.2, 2.9 ± 0.10	2.7–3.2, 3.0 ± 0.15
Eye-naris distance	2.0–2.5, 2.3 ± 0.09	1.9–2.7, 2.3 ± 0.23
Internarial distance	2.8–3.3, 3.1 ± 0.09	3.0–3.6, 3.4 ± 0.20
Snout length	3.4–4.0, 3.8 ± 0.12	3.2–4.5, 4.0 ± 0.39
Interorbital distance	2.3–2.6, 2.5 ± 0.05	2.4–2.7, 2.6 ± 0.09
Tympanum diameter	1.2–1.5, 1.3 ± 0.05	1.4–1.7, 1.6 ± 0.09

Table 2. Testis pigmentation in *Leucostethus siapida* sp. nov. See Remarks for comments on CPZ-UV 7295.

	Left	Right
CPZ-UV 5013	Pigmented	Unpigmented
CPZ-UV 5014	Unpigmented	Pigmented
CPZ-UV 7293 (holotype)	Pigmented	Pigmented
CPZ-UV 7295	Pigmented	–
CPZ-UV 7297	Unpigmented	Pigmented

Table 3. Characteristics of the advertisement call of *Leucostethus siapida* sp. nov. for the three recorded calls, including values for complete calls and the first 10 and last 20 notes, reported as minimum–maximum ($\bar{x} \pm$ SE). Peak values are reported for the fundamental and dominant frequencies. For notes per call and note repetition rate $n = 3$; for variables related to individual notes, sample size is equal to the corresponding number of notes analyzed; internote internal sample size is three less than the corresponding number of notes. The fundamental frequency is reported only for the last 20 notes because some early notes were too weak for the fundamental frequency to be clearly identified.

Notes	Notes per call	Note repetition rate (notes/minute)	Note Duration (ms)	Internote interval (ms)	Fundamental frequency (Hz)	Dominant frequency (Hz)
All (n = 237)	73–88 (79.0 ± 4.6)	223.7–237.5 (232.7 ± 4.5)	10.9–98.9 (67.1 ± 1.4)	104.3–1308.3 (192.4 ± 9.2)	–	3220–4737 (4381 ± 20)
First 10	–	98.5–159.1 (133.9 ± 18.2)	10.9–67.9 (32.1 ± 2.1)	232.1–1308 (472 ± 45.3)	–	3563–4307 (4328 ± 59)
Last 20	–	285.1–292.8 (287.9 ± 2.5)	72.9–98.9 (87.0 ± 0.7)	106.6–140.3 (127.8 ± 0.9)	1969–2411 (2309 ± 15)	4219–4737 (4544 ± 24)

the mitochondrial H-strand transcription unit 1 (146 of 2335 sites; Vigle et al. 2020). *Leucostethus siapida* sp. nov. differs from *L. alacris* in having only basal webbing between toes II and IV (moderate webbing between all toes, I 1–3 II 2–2.5 III 2.75–4 IV 4.5–3 V; Rivero and Granados-Diaz 1989).

Among species of *Leucostethus*, advertisement calls have been described for an apparently undescribed species from the Cordillera Occidental reported as *Colostethus fraterdanieli* (Grant and Castro 1998), *L. fraterdanieli* sensu stricto and

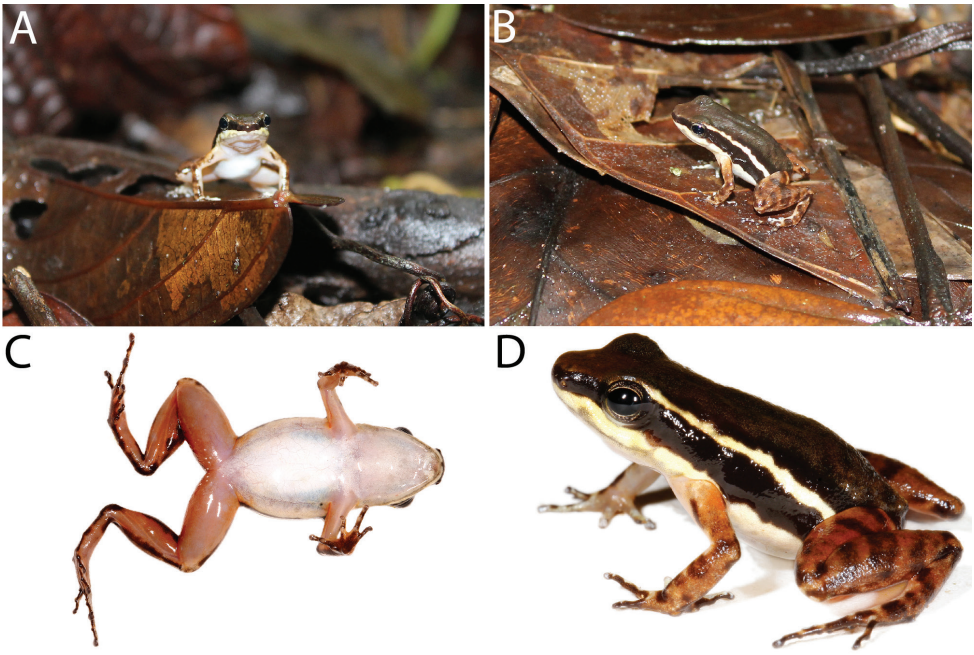

Figure 1. Holotype of *Leucostethus siapida* sp. nov. in life (adult male CPZ-UV 7293, 22.7 mm SVL) **A** frontal and **B** lateral views of holotype in situ while responding phonotaxically to playback of own vocalization **C** ventral view (note the suffusion of orange in axilla, groin, posteroventral thigh, and concealed surface of shank) **D** lateral view.

L. jota (Marin et al. 2018), and *L. bilsa* (Vigle et al. 2020). The note repetition rate ($\bar{x}$ = 287.9 notes/minute) of *L. siapida* sp. nov. is more than twice that of the other species (*L. bilsa*: 81.2 notes/minute; *L. fraterdanieli* sensu stricto: $\bar{x}$ = 98.2 notes/minute; *L. jota*: $\bar{x}$ = 21.8 notes/minute; Cordillera Occidental species: 120.4–132.8 notes/minute). The advertisement call of *L. siapida* sp. nov. also has a higher pitched dominant frequency than all species except *L. jota* (peak frequency 4219–4737 Hz in *L. siapida* sp. nov., $\bar{x}$ = 4400 Hz in *L. jota*, < 3800 Hz in other species).

Among other anurans in the Chocó, *Leucostethus siapida* sp. nov. most resembles *Silverstoneia dalyi* and *S. nubicola* from the adjacent mainland, with which it shares dorsal and lateral coloration, orange suffusion of flash marks and limbs, a well-defined oblique lateral stripe, and a pale ventrolateral stripe (Grant and Myers 2013). It differs from these species in being larger (maximum SVL: *L. siapida* sp. nov., male 23.0 mm, female 25.8 mm; *S. dalyi*, male 17.9 mm, female 19.0 mm; *S. nubicola*, male 20.6 mm, female 21.9 mm) and lacking a conspicuously swollen finger IV (conspicuously swollen in both species). It further differs from *S. dalyi* in lacking a discrete, dark brown postrictal spot and from *S. nubicola* in bearing, at most, faintly stippled spotting or reticulation on the throat (male throat solid black, often extending posteriad into anterior belly in *S. nubicola*).

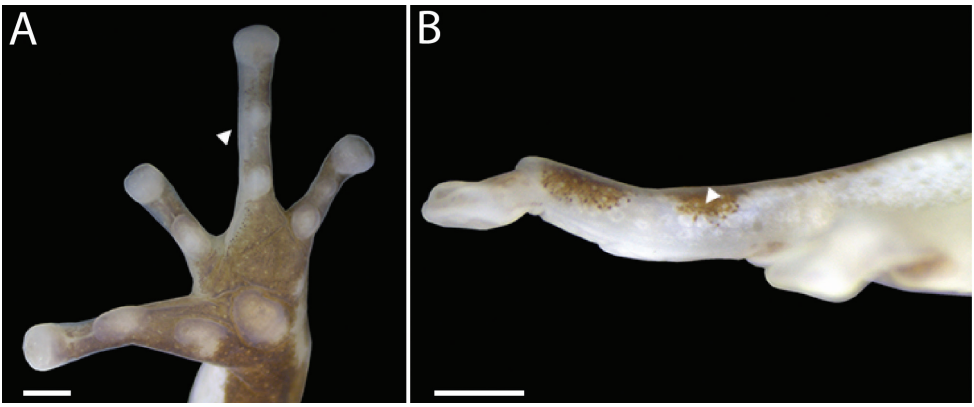

Figure 2. Right hand of *Leucostethus siapida* sp. nov. (CPZ-UV 7297, adult male) **A** hand in palmar (ventral) view (arrowhead indicates weak swelling) and **B** finger IV in pre-axial (medial) view (arrowhead indicates externally visible specialized mucous gland). Scale bars = 500 μm.

Measurements of holotype (in mm). CPZ-UV 7293 is an adult male (Fig. 1) with open vocal slits and melanized testes, SVL 22.7; FAL 5.0; HL 5.5; TL 10.2; FL 9.3; HW 7.8; HL 7.5; EL 2.9; END 2.5; IND 3.3; SL 4.0; IOD 2.4; TD 1.2.

Morphology. The following description is based on the five adult males and three adult females in the type series; measurements are reported in Table 1. Adult males 19.9–23.0 mm SVL (n = 5, $\bar{x}$ = 22.1 ± 0.56 mm); vocal slits present; swelling of finger IV barely discernible (Fig. 2); testis pigmentation variably present and absent (Table 2), forming dense brown or black reticulation when present (see also Remarks, below). Adult females 23.5–25.8 mm SVL (n = 3, $\bar{x}$ = 24.6 ± 0.67 mm), mature oocytes creamy yellow and pale brown, ca. 1.8 mm diameter; oviducts enlarged, convoluted, creamy white. Large intestine unpigmented.

Ventral and most dorsal surfaces smooth; exposed surface of shank with low, inconspicuous granules. Postrictal and cloacal tubercles absent.

Head width 33–36% of SVL and 1.0–1.2 times diagonal HL in males, 32–34% and 1.0–1.1 in females, IOD 29–36% of HW. Snout bluntly rounded in dorsal view, SL 46–58% of HL. Nares slightly flared, directed posterodorsad, EN 70–86% of EL and 57–66% of SL. Loreal region weakly concave, almost vertical. Canthus rostralis well defined, sharply rounded. Incomplete tympanic ring discernible externally along anteroventral half of tympanum. Eye length 38–48% of head length. Tympanum directed posterodorsad, TD 41–50% of EL in males, 52–53% in females. Supratympanic bulge associated with the underlying depressor musculature present. Teeth on maxillary arch present; median lingual process absent. Posterodorsal portion of tympanum concealed by m. depressor mandibulae fibers extending ventrad from origin on dorsal fasciae. Trigeminal nerve (V_3) lateral to undivided m. levator mandibulae externus.

Hand length moderate, 22–25% of SVL and 1.0–1.1 times FAL. Relative appressed finger lengths IV > II > III = V (Fig. 2). Finger II 1.1 times longer than finger III (sensu Grant et al. 2006). Fingers III and V reaching distal half of distal subarticular

tubercle of finger IV. All hand tubercles well defined and protuberant. Fingers II and III each with a single subarticular tubercle; fingers IV and V with two subarticular tubercles. Thenar tubercle elliptical, palmar tubercle elliptical or bluntly triangular. Fringes absent. Metacarpal fold absent. Discs weakly to moderately expanded, all bearing paired dorsal scutes. Carpal pad and black arm gland absent.

Tibia length 43–45% of SVL in males, 39–42% in females; FL 39–41% of SVL in males, 36–38% in females. Relative lengths of toes IV > III > V > II > I (Fig. 3). All foot tubercles well defined and protuberant. Toes I and II with one subarticular tubercle each, toes III and V with two, and toe IV with three tubercles. Webbing absent between toes I–II and IV–V; rudimentary webbing present between toes II–IV, giving formula II 2–3.5 III 3–4 IV. Fringes absent. Metatarsal fold absent. Tarsal keel well defined, short, strongly curved, tubercle-like, not extending from metatarsal tubercle, lying one-third of tarsal length from inner metatarsal tubercle. Discs bearing paired dorsal scutes; disc I weakly expanded, discs II, II, and V moderately expanded, disc IV greatly expanded. Distal thigh musculature with m. semitendinosus passing dorsad (ranid type), tendon of insertion bound to inner surface of mm. gracilis complex by secondary binding tendon.

Coloration in preservative. Dorsal coloration brown with dark brown blotches (Fig. 4). Pale dorsolateral stripes absent. Eyelid dark brown, head and snout dorsally the same color as dorsum.

Dorsal surface of thigh and shank and outer (exposed) surface of foot light brown with dark brown cross bands and blotches. Anterior surface of the thigh with prominent dark brown longitudinal stripe, delimited dorsally by narrow white line extending from groin and fading distally. Thigh ventrally immaculate. Most specimens with posterior thigh bearing elongate, tapered, pale sickle-shaped paracloacal stripe extending along proximal half to entire length of thigh, bordered dorsally by brown stripe extending along posterior shank and ventrally by solid or diffuse pale brown stripe; USNM 313839 lacking pale paracloacal marks, posterior thigh suffused with pale brown and diffuse dark brown blotches (Fig. 5). Ventral surface of thigh and concealed surfaces of shank and foot creamy white, free of melanophores. Plantar surfaces brown; contact surfaces of tubercles creamy white and gray. Webbing between toes III–IV creamy white, free of melanophores.

Dorsal surface of arm proximally pale, distally becoming pale brown with variably expressed dark-brown blotches to fingers IV and V, except USNM 313839 with entire dorsal surface of arm and fingers IV and V suffused with brown and irregular small dark brown spots. Anterior and posterior surfaces of upper arm with well-defined dark brown longitudinal stripes. Dark pigmentation on posterior surface extending distad to wrap around ventral and outer surface of elbow along posterior forearm and finger II. Anterior surfaces of forearm and dorsal surfaces of fingers II and III creamy white. Palmar surfaces pale brown; contact surfaces of tubercles creamy white.

Flank solid dark brown, divided diagonally by well-defined creamy white oblique lateral stripe from groin to posterior corner of orbit (i.e. not extending around canthus rostralis), except USNM 313839 with diffuse pale spotting below oblique lateral stripe

Figure 3. Right foot of *Leucostethus siapida* sp. nov. in life (adult male CPZ-UV 7293). Scale bar: 2 mm.

and darker oblique lateral stripe. Oblique lateral stripe continuous, except left stripe of CPZ-UV 7294 with single narrow break at mid-length. Ventrolateral stripe (see Coloration in life, below) indistinguishable from immaculate venter (e.g. CPZ-UV 5014) or evidenced solely by sparse melanophores along ventral edge (e.g. CPZ-UV 7294), extending anteriad above arm insertion, below tympanum, and below eye to tip of snout, on head delimited ventrally by suffusion of sparse melanophores terminating beneath naris (i.e. upper lip at tip of snout creamy white, lacking melanophores). Dark brown of flank extending anteriad over tympanum to posterior edge of orbit and continuing over loreal region and around snout (encompassing nares) to form dark brown face mask.

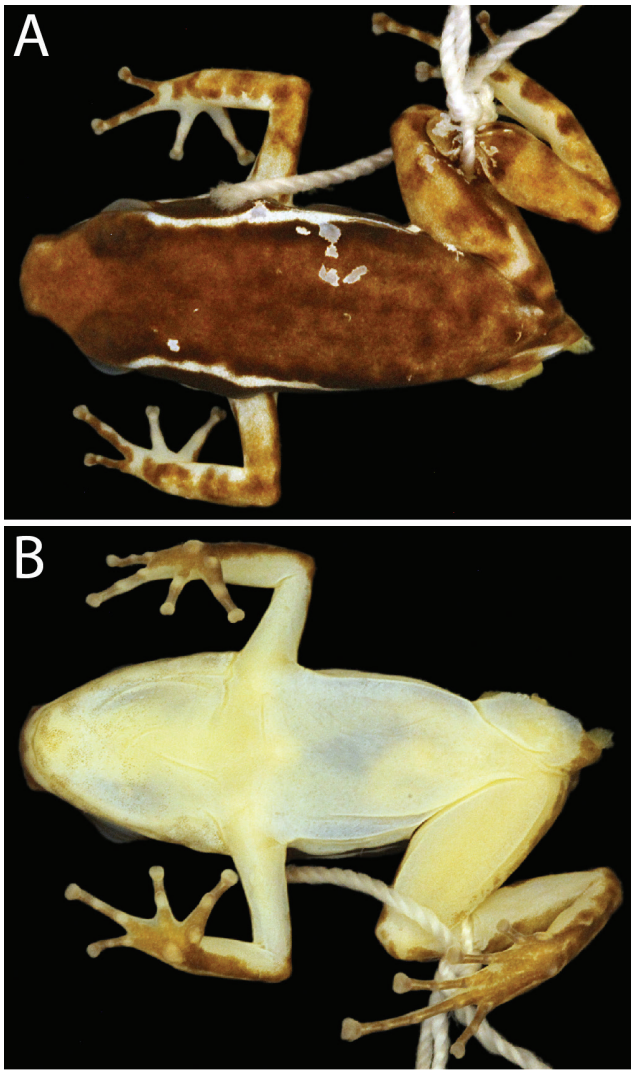

Figure 4. Preserved holotype (adult male CPZ-UV 7293, 22.7 mm SVL) of *Leucostethus siapida* sp. nov. in **A** dorsal and **B** ventral views.

Throat, chest, and belly creamy white, at most bearing faintly stippled spotting or reticulation on throat and along ventral edge of ventrolateral stripe.

Coloration in life. Dorsum brown with blackish-brown blotches (Fig. 1). Dorsal surface of snout paler than dorsum, bearing diffuse creamy white spots suffused with brown. Flanks blackish-brown with creamy white to pale yellow oblique lateral stripe with faint suffusion of melanophores anteriorly (Fig. 1). Loreal region and tip of snout blackish-brown; area beneath tympanum, eye, and loreal region creamy white to pale yellow, delimited ventrally by diffuse suffusion of black. Venter silvery white. Throat with, at most, faintly stippled spotting or reticulation (Fig. 6). Ventrolateral stripe

Figure 5. Dorsal view of *Leucostethus siapida* sp. nov. paratype USNM 313893 (adult female, 23.5 mm SVL).

wavy, creamy white to pale yellow, differing from silvery white of venter, diffuse along ventral edge (Fig. 7). Dorsal surface of upper arm near insertion creamy white to pale yellow. Axilla, groin, posteroventral thigh, and concealed shank suffused with orange. Pale paracloacal marks conspicuous creamy white to inconspicuous pale brown. Ventral surfaces of thighs, ventral surface of upper arm and concealed surface of forearm translucent creamy pink, unpigmented. Posteroventral surface of proximal portion of thighs with few (< 10) to many (> 30) miniscule white spots, present in both sexes (Fig. 8). Iris pale gold with black speckles; pupil ring pale gold, complete.

Advertisement call. On 26 May 2016, we recorded one complete call emitted by the holotype (CPZ-UV 7293; 22.7 mm SVL; Suppl. material 1: Audio S1, extracted

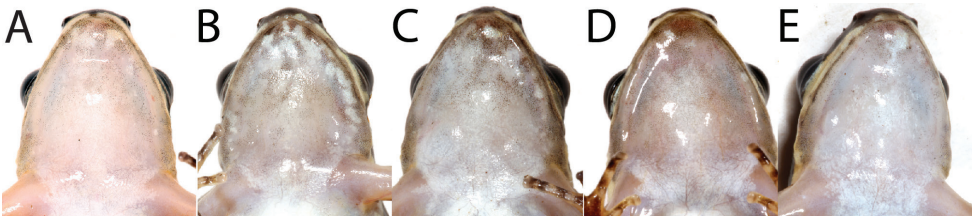

Figure 6. Variation in throat coloration of adult male *Leucostethus siapida* sp. nov. in life **A** CPZ-UV 7293 (holotype) **B** CPZ-UV 7295 **C** CPZ-UV 5013 **D** CPZ-UV 5014 **E** CPZ-UV 7297.

Figure 7. Ventrolateral view of *Leucostethus siapida* sp. nov. paratype CPZ-UV 7294 (25.8 mm SVL) in life showing difference between creamy white ventrolateral stripe and silvery white venter.

from Suppl. material 4: Video S1) at ca. 11:30 h and two complete calls emitted by paratype CPZ-UV 7295 (19.9 mm SVL) at 15:45 h (call 1, Suppl. material 2: Audio S2) and 15:47 h (call 2, Suppl. material 3: Audio S3), respectively. Ambient temperature for all three calls was 26.2 °C. Notes are shown in Figure 9 and values for standard temporal and spectral variables are reported in Table 3. Notes are extensively amplitude-modulated throughout the three calls, resulting in highly irregular envelopes. Early notes are either pulsatile or comprise a single pulse, while subsequent notes become more structured, comprising 2–4 often irregularly shaped pulses. As expected, given their different body sizes, the fundamental and dominant frequencies

Figure 8. Posteroventral view of *Leucostethus siapida* sp. nov. thigh showing miniscule white spots (examples indicated by arrows; CPZ-UV 7296; 24.5 mm SVL).

are lower for the holotype (ca. 2160 Hz and 4300 Hz, respectively) than the paratype (ca. 2370 Hz and 4750 Hz, respectively); the note repetition rate of the holotype is also faster (last 20 notes emitted at 292.8 notes/minute by the holotype, 285.8 and 285.1 notes/minute by the paratype). Notes are frequency modulated, with the dominant frequency ascending approximately 150–200 Hz in the first 10 notes and 400–500 Hz in later notes (e.g. 3840 Hz to 4330 Hz in the holotype, 4210 Hz to 4670 Hz in CPZ-UV 7295; call 2, Suppl. material 3: Audio S3). In addition to the fundamental and dominant frequencies, 3–8 harmonics are evident in most notes.

Etymology. The specific epithet, *siapida* (*sia*, 'arrow'* or 'wild cane'; *siapida*, 'people of the arrow' or 'people of the wild cane'; Harms 1989; Barreña Agirrebeitia and Pérez-Caurel 2017), used as a noun in apposition, is a word in the Emberá Eperará Siapidará dialect and the name of the indigenous group located in the southern Chocó region of Colombia, specifically the modern Departments of Cauca, Nariño, and Valle del Cauca. The Siapida have visited Gorgona Island (*Thida* in Eperará Siapidará) for centuries or more and were almost certainly the first humans to encounter this species of frog.

* *Sia* is translated as the Spanish *flecha*, which can refer to either 'arrow' or 'dart' but is usually translated as 'arrow.' As noted by Myers and Daly (1976: 180; see also Myers et al. 1978), this is mildly misleading in some contexts, given that modern English usage consistently distinguishes between arrows (used with bows) and darts.

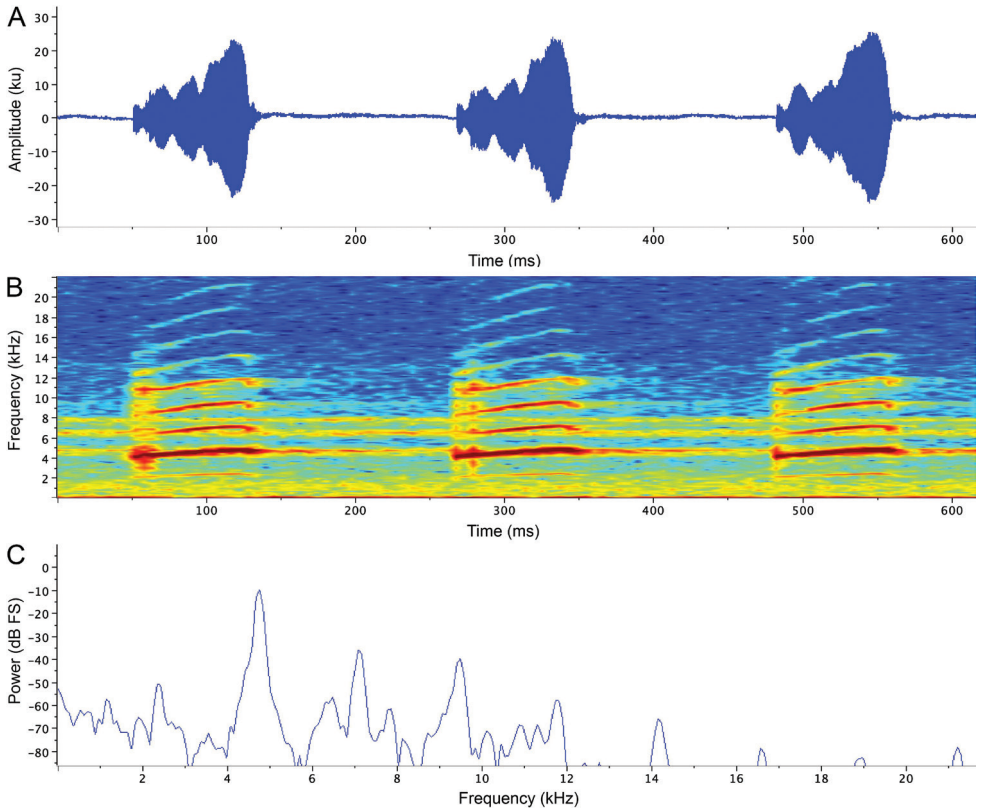

Figure 9. Advertisement call of *Leucostethus siapida* sp. nov. paratype CPZ-UV 7295 (19.9 mm SVL, 26.2°C ambient temperature; Suppl. material 2: Audio S2) **A** oscillogram and **B** audiospectrogram of three notes near the end of an 88-note call **C** power spectrum (spectrogram slice) at maximum amplitude of first note in **A** showing fundamental (2370 Hz) and dominant (4750 Hz) frequencies and harmonics (7120 Hz, 9490 Hz, 11820 Hz, 14190 Hz, 16610 Hz, 18970 Hz, and 21220 Hz). See text for analytical parameters.

Distribution and natural history. Individuals were active during the day in and on leaf litter, low vegetation, and low objects on the forest floor (e.g. rocks, fallen sticks and logs, coconut shells; Figs 1, 10) independent from streams (i.e. >> 3 m from a stream). The holotype was filmed and photographed vocalizing while fully exposed on a large fallen leaf in a clearing (Suppl. material 4: Video S1), and other individuals were observed calling in the adjacent forest on leaf litter and low objects on the forest floor. The holotype responded to playback of his own vocalization both acoustically and phonotaxically, moving ca. 2 m toward the source of the vocalization to just a few centimeters from TG's boots. Despite extensive searching and the abundance of *Epipedobates boulengeri* on the previous days without rainfall, individuals of *Leucostethus siapida* sp. nov. were only observed after ca. 6 h of heavy rain between ca. 5:00 and 11:00 h on 26 May 2016.

Remarks. The left testis of CPZ-UV 7295 is enlarged (1.4 mm diameter) and encapsulated by thick connective tissue beneath which the testis is pigmented, while the right

Figure 10. Habitat of *Leucostethus siapida* sp. nov.

testis appears to be absent. With the exception of their pigmentation, the testes of all other individuals are typical of this group (e.g. Marin et al. 2018; Vigle et al. 2020). Despite the testicular abnormality, CPZ-UV 7295 was observed and recorded vocalizing (see Fig. 9).

In life, the pale ventrolateral stripe is inconspicuous, but incontrovertibly present in all specimens. However, once pigmentation has faded in preservative, it is absent or inconspicuous in all specimens, with only a few scattered melanophores along its ventral edge remaining in some specimens to suggest a ventrolateral stripe once existed.

USNM 313839 differs in several respects from the other members of the type series and more closely resembles other trans-Andean species of *Leucostethus*, including the occurrence of diffuse pale spotting below the oblique lateral stripe and the oblique lateral stripe being extensively suffused with pale brown. Precise information on the area of the island where the specimen was collected is lacking, so it is unknown if the variation reflects highly localized geographic variation or widespread polychromatism. Nevertheless, the extent of variation that occurs among these specimens is well within that observed among conspecifics of other species (e.g. Vigle et al. 2020).

Gas-chromatography/mass spectrometry of the methanol extract of the skin of adult male paratype CPZ-UV 7297 failed to detect any alkaloids (R.A. Saporito, personal communication). Although this finding rules out the lipophilic alkaloid-based chemical defense found in many dendrobatids (e.g. Saporito et al. 2012), it is possible that tetrodotoxin or some other hydrophilic compound might be present, as reported for some species of *Colostethus* (Daly et al. 1994; Grant 2007).

Discussion

Although phylogenetic analyses strongly place *Leucostethus siapida* sp. nov. as part of the trans-Andean *Leucostethus fraterdanieli* group (the *Colostethus fraterdanieli* group of Grant et al. 2017; i.e. all species, except *L. argyrogaster* and *L. fugax*), its precise phylogenetic relationships are unclear. Grant et al. (2017) found it to be the lowland sister of the remainder of the otherwise montane trans-Andean *Leucostethus*, whose species occur from ca. 1000–2700 m elev. in the Andes and Cauca River valley. In contrast, Marin et al. (2018) and Vigle et al. (2020) found it to be nested inside the montane clade. It is unclear if this contradiction is due to differences in character evidence (e.g. inclusion of phenomic evidence by Grant et al. 2017), taxon sampling (e.g. inclusion of additional *Leucostethus* species by Marin et al. 2018 and Vigle et al. 2020), or analytical methods (DNA sequence alignment and optimality criterion). Nevertheless, there seems little reason to doubt that *L. siapida* sp. nov. is sister to *L. bilsa*, which was recently described from ca. 340 km SW in the Reserva Biológica Bilsa at 420–515 m elev., northwestern Ecuador (Vigle et al. 2020).

Vigle et al. (2020) estimated a divergence time of approximately 3 Ma for *Leucostethus bilsa* and *L. siapida* sp. nov. Given that Gorgona has only been isolated from the mainland for at most 18–20 ka, and probably considerably less (Fleming et al. 1998; Montealegre-Z et al. 2010), isolation on the island appears not to have been causally related to the speciation event, suggesting that this is a relictual population of a formerly widespread species. Moreover, given the recency of the terrestrial connection between Gorgona and the mainland, we are optimistic that mainland populations will be discovered. Indeed, given its close resemblance to species of *Silverstoneia*, it is possible that specimens misidentified as *S. nubicola* already reside in natural history collections.

Among the species of *Leucostethus*, *L. siapida* sp. nov. most resembles *L. argyrogaster* and *L. fugax* from western Amazonia at 340–870 m elev. in Ecuador and Peru. In addition to lacking dark ventral coloration, these three species share orange flash marks (reported for *L. argyrogaster* by Morales and Schulte 1993; shown for *L. fugax* by Grant et al. 2017: fig. 33B), and *L. siapida* sp. nov. and *L. argyrogaster* further share the lack of conspicuous swelling of finger IV in adult males. Despite their resemblance, phylogenetic analyses consistently place the cis-Andean species as sister taxa (for which the orange flash coloration is an apparent synapomorphy) that are far removed from *L. siapida* sp. nov.

Scoring the occurrence of swelling on finger IV of adult males is unproblematic in species that exhibit conspicuous swelling (developmental variation and preservation artifacts notwithstanding), as do most species of *Leucostethus*; however, distinguishing between absence and weak swelling is notoriously difficult (Grant et al. 2017). For example, although Grant et al. (2017) scored finger IV as unswollen in *L. siapida* sp. nov., subsequent detailed examination of external morphology indicated that it is weakly swollen, and histological analysis revealed the presence of a specialized mucous gland found exclusively in the swollen finger IV (I.R.S. Cavalcanti and TG, unpublished data). As such, extreme caution is required when employing absence versus weak swelling to diagnose similar species. For this reason, we did not distinguish between the reported absence of swelling in *L. argyrogaster* and *L. bilsa* and the weak swelling in *L. siapida* sp. nov.

A curious characteristic shared by *Leucostethus siapida* sp. nov. and its sister species *L. bilsa* is the lateral variation in testis melanization. Although ontogenetic variation in testis pigmentation is common, individual variation among adults is rare, and, prior to *L. bilsa* (Vigle et al. 2020), unilateral melanization in dendrobatoids had only been documented for *Colostethus panamansis* (Dunn, 1933) by Grant (2004). Golberg et al. (2020) found that testicular melanization and germ cell differentiation proceed in parallel in four anuran species, but the significance of intra-individual variation is unknown.

To our knowledge, the miniscule, white spots on the posteroventral surface of the thighs have not been reported previously, possibly because they are only evident in life, but they are widespread in Dendrobatoidea. Although an exhaustive review was beyond the scope of the current study, they also occur in additional species of *Leucostethus* (e.g. *L. bilsa*; Vigle et al. 2020: figs 2–5) and a least some species of the aromobatid genera *Allobates*, *Anomaloglossus*, *Aromobates*, *Mannophryne*, and *Rheobates* and the dendrobatid genera *Colostethus*, "*Colostethus*" *ruthveni*, *Epipedobates*, *Hyloxalus*, and *Silverstoneia*, and we are unaware of their occurrence in *Ectopoglossus*, *Paruwrobates*, *Phyllobates*, Dendrobatini, or potentially close relatives of Dendrobatoidea, including bufonids, hylodids, and *Thoropa*. Further study is required to determine if the presence of these spots is a synapomorphy of Dendrobatoidea with a limited number of informative losses, as available data suggest, or if their evolutionary history is more complicated.

In addition to describing the new taxon *Leucostethus siapida* sp. nov., we transferred *L. alacris*, *L. dysprosium*, and *L. yaguara* from *Colostethus* to *Leucostethus*. Vigle et al. (2020: 368) also considered the generic placement of *C. alacris* and *C. yaguara* but concluded that "placing them in the genus *Leucostethus* requires more evidence or data (e.g. molecular and/or morphological) from type series or topotypical samples." Nevertheless, it should not be overlooked that the persistence of these species in *Colostethus* for the past 15 years was not due to empirical evidence, but rather (1) their placement in *Colostethus* prior to its partitioning into multiple genera by Grant et al. (2006, 2017) and Marin et al. (2018), and (2) their overall resemblance to the species now referred to *Leucostethus*. Although referral of these species to *Leucostethus* is not based on either quantitative phylogenetic analysis or clear synapomorphies and is, therefore, more predictive than explanatory, it is not entirely unsubstantiated by morphology. All three species share with other species of *Leucostethus* the presence of a complete (i.e. groin to eye), continuous, pale oblique lateral stripe (incomplete in some specimens of *L. bilsa*). In contrast, the oblique lateral stripe is either absent (*C. thorntoni*, *C. ucumari*, and "*C.*" *ruthveni*; for phylogenetic relationships of the last species, see Grant et al. 2017), continuous but incomplete (extending from groin midway along flank in *C. furviventris*, *C. imbricolus*, *C. inguinalis*, *C. latinasus*, *C. panamansis*, and *C. pratti*), or complete but formed by a series of spots (*C. agilis*, *C. lynchi*, and *C.mertensi*).

Despite our optimism that additional populations of *Leucostethus siapida* sp. nov. will be found on the mainland, based on current knowledge, *L. siapida* is endemic to Gorgona Island. Although Gorgona Island is protected as Parque Nacional Natural (PNN) Gorgona, the fact that the only known population is confined to an island of only ca. 13 km^2 is sufficient to categorize this species as Vulnerable according to the IUCN Red List criteria (criterion D2; IUCN 2012). Nevertheless, we emphasize that this categorization should

not prevent studies of this species from being undertaken, as many of the most basic aspects of its morphology (e.g. larval morphology, ontogenetic variation) and behavioral ecology (e.g. courtship and amplexus, oviposition site, parental care) are unknown, and studies detailing its fine-scale distribution and abundance, age-sex structure, and the frequency of morphological abnormalities, such as the testicular anomaly reported herein, will be crucial for managers of PNN Gorgona to monitor and protect the species. Ultimately, the occurrence of this endemic vertebrate adds to an already lengthy list of reasons to consider Gorgona to be a crucial locality for biodiversity conservation (Giraldo et al. 2014).

Acknowledgements

We are grateful to David Andrés Velásquez-Trujillo and Andrés Felipe Gómez Fernández for assistance during fieldwork and María Ximena Zorrilla (Director of PNN Gorgona), Luis Fernando Payan, Hector Chirimia Gonzalez, and all the PNN Gorgona functionaries for both logistic support and sharing their extensive knowledge of Gorgona and its fauna and flora. We also thank Alan Giraldo and the members of the Grupo de Investigación en Ecología Animal de la Universidad del Valle for support. Adolfo Amézquita first drew our attention to the existence of a *Silverstoneia*-like species on Gorgona, and Marvin Anganoy, Isabela Cavalcanti, Julián Faivovich, Rachel Monetesinos, Marco Rada, and Geven Rodríguez shared their knowledge and insights on anuran morphology and systematics. Ralph Saporito tested the new species for the presence of skin alkaloids. The article benefitted from critical reviews by Luis Coloma and an anonymous reviewer. Hector Chirimia Gonzalez was extremely helpful in choosing the specific epithet for the new species. Kevin de Queiroz, Steve Gotte, Roy McDiarmid, and Addison Wynn authorized and enabled examination of specimens at USNM. Permission to collect in PNN Gorgona was granted by Parques Nacionales Naturales de Colombia (No. 010 de 2016). Funding was provided by the São Paulo Research Foundation (FAPESP Procs. 2012/10000-5, 2018/15425-0), the Brazilian National Council for Scientific and Technological Development (CNPq Proc. 306823/2017-9), and the Fundación Univalle.

References

Ayala SC, Williams EE (1988) New or problematic *Anolis* from Colombia. 6. Two fuscoauratoid anoles from the Pacific lowlands, *A. maculiventris* Boulenger, 1898 and *A. medemi*, a new species from Gorgona Island. Breviora 490: 1–16.

Baena-Bejarano N, Heads S (2015) Three new species of the genus *Ripipteryx* from Colombia (Orthoptera, Ripipterygidae). ZooKeys 502: 129–143. https://doi.org/10.3897/zookeys.502.8871

Barbour T (1905) Reptilia and Amphibia. In: Bangs O, Brown Jr WW, Thayer JE, Barbour T (1905) The Vertebrata of Gorgona Island, Colombia. Bulletin of the Museum of Comparative Zoology at Harvard College 46: 87–102.

Barreña Agirrebeitia A, Pérez Caurel M (2017) La revitalización de la lengua embera en Colombia: de la oralidad a la escritura. Onomázein: 58–76. https://doi.org/10.7764/onomazein.amerindias.03

Daly JW, Gusovsky F, Myers CW, Yotsu-Yamashita M, Yasumot T (1994) First occurrence of tetrodotoxin in a dendrobatid frog (*Colostethus inguinalis*), with further reports for the bufonid genus *Atelopus*. Toxicon 32: 279–285. https://doi.org/10.1016/0041-0101(94)90081-7

Dunn ER (1933) Amphibians and reptiles from El Valle de Anton, Panama. Occasional Papers of the Boston Society of Natural History 8: 65–79.

Fabrezi M, Alberch P (1996) The carpal elements of anurans. Herpetologica 52: 188–204.

Fernández F, Guerrero RJ (2008) *Technomyrmex* (Formicidae: Dolichoderinae) in the New World: synopsis and description of a new species. Revista Colombiana de Entomología 34: 110–115.

Fernández L, Schaefer SA (2005) New *Trichomycterus* (Siluriformes: Trichomycteridae) from an Offshore Island of Colombia. Copeia 2005: 68–76. https://doi.org/10.1643/CI-04-177R1

Fleming K, Johnston P, Zwartz D, Yokoyama Y, Lambeck K, Chappell J (1998) Refining the eustatic sea-level curve since the Last Glacial Maximum using far- and intermediate-field sites. Earth and Planetary Science Letters 163: 327–342. https://doi.org/10.1016/S0012-821X(98)00198-8

García Aldrete AN, González O, Sarria F (2011) Three new species of *Loneura* (Psocodea: 'Psocoptera': Ptiloneuridae) from Gorgona Island, Cauca, Colombia, with a new infrageneric classification. Zootaxa 3050: 55–62. https://doi.org/10.11646/zootaxa.3050.1.3

Giraldo A (2012) Geomorfología e hidroclimatología de la isla Gorgona. In: Giraldo A, Valencia B (Eds) Isla Gorgona: Paraíso de Biodiversidad y Ciencia. Universidad del Valle, Programa Editorial, Cali, 17–23.

Giraldo A, Valencia B [Eds] (2012) Isla Gorgona: Paraíso de Biodiversidad y Ciencia. Universidad del Valle, Programa Editorial, Cali, 221 pp.

Giraldo A, Diazgranados MC, Gutiérrez-Landázuri CF (2014) Isla Gorgona, enclave estratégico para los esfuerzos de conservación en el Pacífico Oriental Tropical. Revista de Biología Tropical 62: 1–12. https://doi.org/10.15517/rbt.v62i0.15975

Glynn PW, von Prahl H, Guhl F (1982) Coral reefs of Gorgona Island, Colombia, with special reference to corallivores and their influence on community structure and reef development. Anales Del Instituto de Investigaciones Marinas de Punta Betín 12: 185–214. https://doi.org/10.25268/bimc.invemar.1982.12.0.502

Goldberg J, Valverde BSL, Franco-Belussi L (2020) Testicular melanization in anuran species: ontogeny and sexual maturity. Amphibia-Reptilia 41: 75–86. https://doi.org/10.1163/15685381-20191206

Grant T (2004) On the identities of *Colostethus inguinalis* (Cope, 1868) and *C. panamensis* (Dunn, 1933), with comments on *C. latinasus* (Cope, 1863) (Anura: Dendrobatidae). American Museum Novitates 3444: 1–24. https://doi.org/10.1206/0003-0082(2004)444<0001:OTIOCI>2.0.CO;2

Grant T (2007) A new, toxic species of *Colostethus* (Anura: Dendrobatidae) from the Cordillera Central of Colombia. Zootaxa 1555: 39–51. https://doi.org/10.11646/zootaxa.1555.1.3

Grant T, Castro F (1998) The cloud forest *Colostethus* (Anura, Dendrobatidae) of a region of the Cordillera Occidental of Colombia. Journal of Herpetology 32: 378–392. https://doi.org/10.2307/1565452

Grant T, Myers CW (2013) Review of the frog genus *Silverstoneia*, with descriptions of five new species from the Colombian Chocó (Dendrobatidae: Colostethinae). American Museum Novitates: 1–58. https://doi.org/10.1206/3784.2

Grant T, Frost DR, Caldwell JP, Gagliardo R, Haddad CFB, Kok PJR, Means BD, Noonan BP, Schargel WE, Wheeler WC (2006) Phylogenetic systematics of dart-poison frogs and their relatives (Anura: Athesphatanura: Dendrobatidae). Bulletin of the American Museum of Natural History 299: 1–262. https://doi.org/10.1206/0003-0090(2006)299[1:PSODFA]2.0.CO;2

Grant T, Rada M, Anganoy-Criollo M, Batista A, Dias PH, Jeckel AM, Machado DJ, Rueda-Almonacid JV (2017) Phylogenetic systematics of dart-poison frogs and their relatives revisited (Anura: Dendrobatoidea). South American Journal of Herpetology 12: S1–S90. https://doi.org/10.2994/SAJH-D-17-00017.1

Haas A (2001) Mandibular arch musculature of anuran tadpoles, with comments on homologies of amphibian jaw muscles. Journal of Morphology 247: 1–33. https://doi.org/10.1002/1097-4687(200101)247:1<1::AID-JMOR1000>3.0.CO;2-3

Harms PL (1989) Comparative Word List of Chocoan Languages. SIL Language and Culture Archives, Dallas.

IUCN (2012) IUCN Red List Categories and Criteria: Version 3.1. Second edition. Second. IUCN, Gland, Switzerland.

Köhler J, Jansen M, Rodríguez A, Kok PJR, Toledo LF, Emmrich M, Glaw F, Haddad CFB, Rödel M-O, Vences M (2017) The use of bioacoustics in anuran taxonomy: theory, terminology, methods and recommendations for best practice. Zootaxa 4251: 1–1. https://doi.org/10.11646/zootaxa.4251.1.1

Lourenço WR, Flores E (1989) Los escorpiones (Chelicerata) de Colombia. I. La fauna de la isla Gorgona. Aproximación biogeográfica. Caldasia 16: 66–70.

Manchola OFS, Obando RG, Aldrete ANG (2014) Ectopsocidae (Psocodea: 'Psocoptera') from Valle del Cauca and NNP Gorgona, Colombia. Zootaxa 3786: 523–540. https://doi.org/10.11646/zootaxa.3786.5.2

Marin CM, Molina-Zuluaga C, Restrepo A, Cano E, Daza JM (2018) A new species of *Leucostethus* (Anura: Dendrobatidae) from the eastern versant of the Central Cordillera of Colombia and the phylogenetic status of *Colostethus fraterdanieli*. Zootaxa 4461: e359. https://doi.org/10.11646/zootaxa.4464.3.3

McDiarmid RW (1994) Preparing amphibians as scientific specimens. In: Heyer WR, Donnelly MA, McDiarmid RW, Hayek L-AC, Foster MS (Eds) Measuring and Monitoring Biological Diversity: Standard Methods for Amphibians. Smithsonian Institution Press, Washington, 289–297.

Mendivil Nieto JA, García Aldrete AN, González Obando R (2017) Seven new species of *Loneura* Navás (Insecta: Psocodea:'Psocoptera': Ptiloneuridae) from Valle del Cauca, Colombia. Zootaxa 4227: 495–523. https://doi.org/10.11646/zootaxa.4227.4.2

Montealegre-Z F, Postles M (2010) Resonant sound production in *Copiphora gorgonensis* (Tettigoniidae: Copiphorini), an endemic species from Parque Nacional Natural Gorgona, Colombia. Journal of Orthoptera Research 19: 347–355. https://doi.org/10.1665/034.019.0223

Montealegre-Z F, Morris GK, Sarria-S FA, Mason AC (2011) Quality calls: phylogeny and biogeography of a new genus of neotropical katydid (Orthoptera: Tettigoniidae) with ultra pure-tone ultrasonics. Systematics and Biodiversity 9: 77–94. https://doi.org/10.1080/14772000.2011.560209

Morales VR, Schulte R (1993) Dos especies nuevas de *Colostethus* (Anura, Dendrobatidae) en las vertientes de la Cordillera Oriental del Perú y del Ecuador. Alytes 11: 97–106.

Myers CW, Daly JW (1976) Preliminary evaluation of skin toxins and vocalizations in taxonomic and evolutionary studies of poison-dart frogs (Dendrobatidae). Bulletin of the American Museum of Natural History 157: 173–262.

Myers CW, Duellman WE (1982) A new species of *Hyla* from Cerro Colorado, and other tree frog records and geographical notes from western Panama. American Museum Novitates 2752: 1–32.

Myers CW, Daly JW, Malkin B (1978) A dangerously toxic new frog (*Phyllobates*) used by Emberá Indians of western Colombia, with discussion of blowgun fabrication and dart poisoning. Bulletin of the American Museum of Natural History 161: 307–366.

Passos P, Mueses-Cisneros JJ, Lynch JD, Fernandes R (2009) Pacific lowland snakes of the genus *Atractus* (Serpentes: Dipsadidae), with description of three new species. Zootaxa 2293: 1–34. https://doi.org/10.11646/zootaxa.2293.1.1

Phillips JG, Burton SE, Womack MM, Pulver E, Nicholson KE (2019) Biogeography, systematics, and ecomorphology of Pacific Island anoles. Diversity 11: e141. https://doi.org/10.3390/d11090141

Rivero JA, Serna MA (1986) Dos nuevas especies de *Colostethus* (Amphibia, Dendrobatidae). Caldasia 15: 525–531.

Rivero JA, Granados Diaz H (1989) Nuevos *Colostethus* (Amphibia, Dendrobatidae) del Departamento de Cauca, Colombia. Caribbean Journal of Science 25: 148–152.

Rivero JA, Serna MA (1991) Tres nuevas especies de *Colostethus* (Anphibia [sic], Dendrobatidae) de Colombia. Trianea 4: 481–495.

Rivero JA, Serna MA (2000) Nuevos *Colostethus* (Amphibia, Dendrobatidae) del Departamento de Antioquia, Colombia, con la descripción del renacuajo de *Colostethus fraterdanieli*. Revista de Ecología Latinoamericana 2: 45–58.

Sarria-S F, González O, García Aldrete AN (2014) Psocoptera (Insecta: Psocodea) from the National Natural Park Gorgona, Cauca, Colombia. Revista de Biología Tropical 62: 243–256. https://doi.org/10.15517/rbt.v62i0.16337

Saporito RA, Donnelly MA, Spande TF, Garraffo HM (2012) A review of chemical ecology in poison frogs. Chemoecology 22: 159–168. https://doi.org/10.1007/s00049-011-0088-0

Savage JM, Heyer WR (1967) Variation and distribution in the tree-frog genus *Phyllomedusa* in Costa Rica, Central America. Beiträge zur Neotropischen Fauna 5: 111–131. https://doi.org/10.1080/01650526709360400

Savage JM, Heyer WR (1997) Digital webbing formulae for anurans: A refinement. Herpetological Review 28: 131–131.

Serrano L, Ferrari L, López M, Maria C, Jaramillo C (2011) An integrative geologic, geochronologic and geochemical study of Gorgona Island, Colombia: Implications for the forma-

tion of the Caribbean Large Igneous Province. Earth and Planetary Science Letters 309: 324–336. https://doi.org/10.1016/j.epsl.2011.07.011

Vásquez-Vélez AI (2014) Estructura y diversidad de la vegetación del Parque Nacional Natural de la Isla Gorgona, Colombia. Revista de Biología Tropical 62: 1–13. https://doi.org/10.15517/rbt.v62i0.15976

Vigle GO, Coloma LA, Santos JC, Hernandez-Nieto S, Ortega-Andrade HM, Paluh DJ, Read M (2020) A new species of Leucostethus (Anura: Dendrobatidae) from the Cordillera Mache-Chindul in northwestern Ecuador, with comments on similar *Colostethus* and *Hyloxalus*. Zootaxa 4896: 342–372. https://doi.org/10.11646/zootaxa.4896.3.2

Supplementary material 1

Audio S1

Author: Taran Grant

Data type: WAV file

Explanation note: Advertisement call of adult male holotype of *Leucostethus siapida* sp. nov. (CPZ-UV 7293, 22.7 mm SVL; 26.2°C ambient temperature). Audio extracted from Video S1.

Link: https://doi.org/10.3897/zookeys.1057.67621.suppl1

Supplementary material 2

Audio S2

Author: Taran Grant

Data type: WAV file

Explanation note: Advertisement call 1 of adult male paratype of *Leucostethus siapida* sp. nov. (CPZ-UV 7295, 19.9 mm SVL; 26.2°C ambient temperature).

Link: https://doi.org/10.3897/zookeys.1057.67621.suppl2

Supplementary material 3

Audio S3
Author: Taran Grant
Data type: WAV file
Explanation note: Advertisement call 2 of adult male paratype of *Leucostethus siapida* sp. nov. (CPZ-UV 7295, 19.9 mm SVL; 26.2 °C ambient temperature).

Link: https://doi.org/10.3897/zookeys.1057.67621.suppl3

Supplementary material 4

Video S1
Author: Taran Grant
Data type: MOV file
Explanation note: Adult male holotype of *Leucostethus siapida* sp. nov. vocalizing in situ (CPZ-UV 7293, 22.7 mm SVL).

Link: https://doi.org/10.3897/zookeys.1057.67621.suppl4